

FINITE ELEMENT MODELLING AND SIMULATION OF DRYING  
ISOTROPIC AND ANISOTROPIC FOOD SAMPLES

A THESIS SUBMITTED TO  
THE GRADUATE SCHOOL OF NATURAL AND APPLIED SCIENCES  
OF  
MIDDLE EAST TECHNICAL UNIVERSITY

BY

MELTEM SOYDAN KARABACAK

IN PARTIAL FULFILLMENT OF THE REQUIREMENTS  
FOR  
THE DEGREE OF DOCTOR OF PHILOSOPHY  
IN  
FOOD ENGINEERING

FEBRUARY 2013



Approval of the thesis:

**FINITE ELEMENT MODELLING AND SIMULATION OF DRYING  
ISOTROPIC AND ANISOTROPIC FOOD SAMPLES**

submitted by **MELTEM SOYDAN KARABACAK** in partial fulfillment of the requirements for the degree of **Doctor of Philosophy in Food Engineering Department, Middle East Technical University** by,

Prof. Dr. Canan Özgen  
Dean, Graduate School of **Natural and Applied Sciences** \_\_\_\_\_

Prof. Dr. Alev Bayındırlı  
Head of Department, **Food Engineering** \_\_\_\_\_

Assist. Prof. Dr. Deniz Çekmeceliöglu  
Supervisor, **Food Engineering Dept., METU** \_\_\_\_\_

Prof. Dr. Ali Esin  
Co-Supervisor, **Food Engineering Dept., METU** \_\_\_\_\_

**Examining Committee Members:**

Prof. Dr. Ferhunde Us  
Food Engineering Dept., Hacettepe University \_\_\_\_\_

Assist. Prof. Dr. Deniz Çekmeceliöglu  
Food Engineering Dept., METU \_\_\_\_\_

Prof. Dr. Serpil Şahin  
Food Engineering Dept., METU \_\_\_\_\_

Assoc. Prof. Dr. Behiç Mert  
Food Engineering Dept., METU \_\_\_\_\_

Assist. Prof. Dr. İlkay Şensoy  
Food Engineering Dept., METU \_\_\_\_\_

**Date:** \_\_\_\_\_

**I hereby declare that all information in this document has been obtained and presented in accordance with academic rules and ethical conduct. I also declare that, as required by these rules and conduct, I have fully cited and referenced all material and results that are not original to this work.**

Name, Last name: MELTEM SOYDAN KARABACAK

Signature :



## ABSTRACT

### FINITE ELEMENT MODELLING AND SIMULATION OF DRYING ISOTROPIC AND ANISOTROPIC FOOD SAMPLES

Soydan Karabacak, Meltem  
Ph.D., Department of Food Engineering  
Supervisor: Assist. Prof. Dr. Deniz Çekmeceliöğlü  
Co-Supervisor: Prof. Dr. Ali Esin

February 2013, 147 pages

The aim of this study was to investigate drying characteristics (temperature gradient, rate of drying and temperature change, drying time, diffusivity values, shrinkage) of isotropic and anisotropic foods by observing the changes in temperatures at four different locations and moisture contents and to build an appropriate model for simulation of temperature and moisture distribution using finite element method. The lean meat samples (anisotropic) with three fiber configurations ( $v$ ; flow normal to fiber, drying along the fiber,  $h_1$ : flow normal to fiber,  $h_2$ ; flow along to fiber) and minced meat (isotropic) were dried at two different temperatures (48°C, 70°C) and three different velocities (0.5, 1.0, 1.7 m/s) of air. Rate of temperature change was found as  $h_2 > v > h_1$  while rate of drying was observed as  $h_2 \approx v > h_1$  minced. The order of temperature gradient through the lean meat samples was  $v < h_2 < h_1$ . Minced meat showed 1.0-4.4°C higher temperature values but 2.3-6.2% lower moisture loss than the lean meat in all fiber configurations. A model based on nonlinear coupled heat and mass transfer considering evaporation due to change in overall moisture content through the sample was found more appropriate than the model considering evaporation loss only at the surface. The diffusion coefficients for lean and minced meat were expressed as a function of temperature and moisture content. At 70°C air temperature, shrinkage should be included in the model. As a result, finite element modelling considering both anisotropic thermal conductivity and diffusivity definitions showed good agreement with experimental data and represented anisotropy effect successfully.

**Keywords:** Finite Element Modeling, simulation, isotropic food, anisotropic food, meat drying

ÖZ

SONLU ELEMANLAR YÖNTEMİ  
İLE  
YÖNE DEĞİŞMEYEN VE YÖNE BAĞIMLI BESİN ÖRNEKLERİNİN  
KURUTULMASININ MODELLENMESİ VE SİMÜLASYONU

Soydan Karabacak, Meltem  
Doktora, Gıda Mühendisliği Bölümü  
Tez Yöneticisi: Yrd. Doç. Dr. Deniz Çekmecelioğlu  
Ortak Tez Yöneticisi: Prof. Dr. Ali Esin

Şubat 2013, 147 pages

Bu çalışmada temel amaçlar; yöne bağımlı ve yönden bağımsız besin örneklerinin nem ve dört farklı konumundaki sıcaklık değişimlerini gözlemleyerek kurutma davranışlarını (sıcaklık farkı, kurutma ve sıcaklık değişimi hızı, kurutma zamanı, difüzyon katsayıları, büzülme) incelemek ve sonlu elemanlar yöntemi ile sıcaklık ve nem dağılımının simülasyonu için uygun bir model geliştirmektir. Yöne bağımlı özellikte ürünü temsilen üç farklı lif yönünde ( $v$ ; hava akış yönüne dik kurumaya paralel lifler,  $h_1$ ; hava akış yönüne dik lifler,  $h_2$ ; hava akış yönünde lifler) hazırlanan nuar ile yönden bağımsız özellikte ürünü temsilen kıyma iki farklı sıcaklıkta ( $48^\circ\text{C}$ ,  $70^\circ\text{C}$ ) ve üç farklı hava akış hızında (0.5, 1.0, 1.7 m/s) tepsili kurutucuda kurutulmuştur. Sıcaklık değişim hızı kıyma  $h_2 > v > h_1$  şeklinde bulunurken kuruma hızı sıralaması  $h_2 \approx v > h_1 > \text{kıyma}$  şeklinde gözlenmiştir. Nuar örneklerindeki lokasyonlar arası sıcaklık farkı sırası  $v < h_2 < h_1$  şeklindedir. Kıymada et örneklerine kıyasla  $1.0-4.4^\circ\text{C}$  daha yüksek sıcaklık değerleri ancak  $2.3-6.2\%$  daha düşük nem kaybı gözlenmiştir. Tüm örnekteki nem değişimine bağlı olarak buharlaşmayı ele alan, doğrusal olmayan ısı ve kütle aktarım eşitliklerine dayalı modelin sadece yüzeyde buharlaşmayı ele alan modele göre daha uygun olduğu saptanmıştır. Et ve kıyma örnekleri için sıcaklık ve nemin bir fonksiyonu olan difüzyon katsayıları hesaplanmıştır. Yüksek kurutma sıcaklıklarında ( $70^\circ\text{C}$ ), büzülmenin de difüzyon katsayısı hesaplamalarına dahil edilmesi gerektiği bulunmuştur. Yöne bağımlı ısı iletkenliği ve difüzyon katsayısı denklemleri kullanılarak oluşturulan sonlu elemanlar modeli deneysel verilerle uyum göstermiş ve başarılı bir şekilde yöne bağımlılığı temsil etmiştir.

**Anahtar Sözcükler:** Sonlu Elemanlar Yöntemi, simülasyon, yöne bağımlı besin örneği, yönden bağımsız besin örneği, et kurutma

## ACKNOWLEDGMENTS

I would like to express my gratitude to all those who gave me the possibility to complete this thesis. I am deeply indebted to my supervisor Assist. Prof. Dr. Deniz Çekmeceliolu whose guidance and valuable support helped and motivated me in all the time of research. I would like to thank him also for providing me a different point of view.

I am grateful to my co-supervisor Prof. Dr. Ali Esin for his stimulating suggestions, generating solutions, guidance and encouragement throughout the research.

I extent my sincere appreciation to all members of thesis monitoring committee, Prof. Dr. Ferhunde Us and Prof. Dr. Serpil Şahin for their guidance and helpful comments from the beginning of thesis work.

I warmly thank to my office mates at TUBITAK for their support, also Serkan Üçer, Melike Oğuz Alper, Dr. H. Mecit Öztop and Dr. Betül Söyler for their friendship and stimulating suggestions.

Finally, I would like to express my special thanks to my husband, Özgür Karabacak, my parents Sabriye Soydan and Şükrü Soydan and upcoming member of our family for their valuable support, endless love, motivation and tolerance. They never left me alone at difficult times of my life. I would also like to thank Elife Ö. Karabacak, Perihan Karabacak and Yaşar Karabacak for their support and understanding.

## TABLE OF CONTENTS

ABSTRACT.....	v
ÖZ .....	vi
ACKNOWLEDGMENTS.....	vii
TABLE OF CONTENTS.....	viii
LIST OF TABLES.....	x
LIST OF FIGURES.....	xii
LIST OF SYMBOLS AND ABBREVIATIONS .....	xx
CHAPTERS	
1. INTRODUCTION .....	1
1.1. Drying and Drying Methods .....	1
1.1.1. Stages of Drying.....	1
1.1.2. Physical Effects of Drying .....	2
1.1.3. Mechanisms of Water Transport During Drying.....	3
1.1.4. Meat Drying.....	4
1.2. Isotropic and Anisotropic Foods .....	5
1.2.1. Effect of Cellular Structure of Food on Drying.....	7
1.2.1.1. Effect of Pretreatments on Cellular Structure During Drying.....	9
1.3. Finite Element Modeling (FEM).....	11
1.3.1. Applications in Food Processing.....	13
1.3.1.1. Heating.....	14
1.3.1.2. Cooling & Freezing.....	17
1.3.1.3. Other Processes.....	18
1.3.2. FEM in Drying.....	19
1.4. Aim of the Study .....	22
2. MATERIAL AND METHODS.....	25
2.1. Materials .....	25
2.2. Parameters .....	25
2.3. Experimental Methods.....	26
2.3.1. Experimental Setup .....	26
2.3.2. Sample Preparation.....	28
2.3.3. Temperature Measurement .....	28
2.3.4. Moisture Content Measurement .....	28
2.3.5. Equilibrium Moisture Content Measurement.....	28
2.3.6. Properties of Air.....	29
2.3.7. Shrinkage Measurement .....	29
2.4. Model Construction.....	29
2.5. Comparison.....	32
3. EXPERIMENTAL RESULTS AND DISCUSSION.....	33
3.1. Temperature Distribution.....	33
3.2. Effect of Air Temperature on Temperature of Samples.....	36
3.3. Effect of Air Flow Rate on Temperature of Samples .....	38
3.4. Effect of Fiber Direction on Temperature of Samples .....	41
3.5. Temperature Comparison for Minced Meat vs. Fiber Configuration.....	42
3.6. Effect of Air Temperature and Flow Rate on Moisture Content of Samples.....	45
3.7. Effect of Fiber Direction and Structure on Moisture Content of Samples .....	47
3.8. Calculation of Equilibrium Moisture Content and Diffusion Coefficient .....	49
3.9. Shrinkage.....	51
3.10. Monitoring Properties of Air.....	51
4. MODEL RESULTS AND DISCUSSION-1 .....	53
4.1. Model Results .....	53
4.1.1. Prediction of Temperature and Comparison of Models .....	53

4.1.2. Prediction of Moisture Content .....	69
4.2. Effect of Flow Rate on Predicted Temperature and Moisture Content of Samples ...	72
4.3. Effect of Fiber Direction and Structure on Predicted Temperature and Moisture Content .....	75
5. MODEL RESULTS AND DISCUSSION-2 .....	79
5.1. Redefinition of Diffusion Coefficient.....	79
5.2. Model Construction.....	81
5.3. Prediction of Temperature .....	81
5.4. Prediction of Moisture Content .....	89
5.5. Effect of Shrinkage.....	91
5.6. Fiber Direction Effect on Predicted Moisture Content and Temperature.....	95
6. CONCLUSION AND RECOMMENDATIONS.....	99
REFERENCES.....	101
APPENDICES	
A. Properties of Food Material .....	113
B. Equilibrium Moisture Content Values.....	117
C. COMSOL Finite Element Modeling Software Windows .....	119
D. Results of FEM using Model 1 .....	129
E. Nonlinear Fitting Statements in Mathcad Software Programme .....	137
F. Diffusivity Values at Different Probe Locations .....	143
CURRICULUM VITAE.....	145

## LIST OF TABLES

### Tables

<b>Table 1.1.</b>	Thermal conductivity of cow and pig muscles .....	5
<b>Table 1.2.</b>	Diffusivity ( $D_{\text{eff}}$ ) and activation energy ( $E_a$ ) values for drying of green beans .....	6
<b>Table 1.3.</b>	Some studies using of the Finite-Element Method in Food-Processing....	14
<b>Table 2.1.</b>	Parameters used in drying experiments .....	25
<b>Table 2.2.</b>	Values of control unit switches .....	26
<b>Table 2.3.</b>	Anisotropic thermal conductivity values used in the model .....	31
<b>Table 3.1.</b>	Drying conditions used in experiments .....	33
<b>Table 3.2.</b>	Temperature readings at four locations on four different meat samples at the end of experiment (270 min) .....	34
<b>Table 3.3a.</b>	First order kinetics model parameters for temperature change at the center (AT1) during drying of different meat samples.....	37
<b>Table 3.3b.</b>	First order kinetics model parameters for temperature change at the surface (BT2) during drying of different meat samples.....	38
<b>Table 3.4.</b>	Average maximum temperature difference and temperature difference in x direction for different meat samples at four drying conditions.....	39
<b>Table 3.5.</b>	Model parameters for rate of drying ( $R^2 > 0.99$ ) .....	47
<b>Table 3.6.</b>	Drying times to decrease moisture content to 20% (wet base) .....	47
<b>Table 3.7.</b>	Diffusion coefficient values of meat samples at different drying conditions by using different models .....	50
<b>Table 3.8.</b>	Shrinkage percent at different drying conditions .....	51
<b>Table 4.1.</b>	RMSE; root mean square error for predicted vs. experimental temperature of meat samples during drying at different conditions.....	60
<b>Table 4.2.</b>	Experimental and predicted moisture content % at the end of drying (270 min).....	69
<b>Table 4.3.</b>	RMSE; root mean square error of predicted moisture content (dry base) of meat samples at different drying conditions ( $R^2 > 0.99$ in all cases).....	70
<b>Table 5.1.</b>	Diffusivity equations of lean meat with three fiber configurations.....	80
<b>Table 5.2.</b>	Anisotropic diffusivity values used in the model .....	81
<b>Table 5.3.</b>	RMSE; root mean square error of predicted temperature of meat samples during drying at different conditions .....	89
<b>Table 5.4.</b>	RMSE; root mean square error of predicted moisture content (dry base) of meat samples at different drying conditions ( $R^2 > 0.99$ in all cases)....	91
<b>Table 5.5.</b>	Diffusivity equations of lean meat with three fiber configurations.....	91

<b>Table 5.6.</b>	RMSE; root mean square error of predicted moisture content (dry base) of meat samples during drying at 70°C 0.5 m/s ( $R^2 > 0.99$ in all cases).....	93
<b>Table 5.7.</b>	RMSE; root mean square error of predicted temperature of meat samples during drying at 70°C 0.5 m/s .....	95
<b>Table A.1.</b>	Properties of Food Material .....	113
<b>Table A.2.</b>	Empirical curve-fitting parameters for Equation (a.7) in Table A.1.....	114
<b>Table A.3.</b>	Parameters and Precision of the Equation (a.9) in Table A.1 for Different Foods .....	114
<b>Table A.4.</b>	Parameters of Arrhenius equation (d.2) in Table A.1.....	115
<b>Table A.5.</b>	Composition of Meat Samples .....	115
<b>Table B.1.</b>	Equilibrium moisture content values calculated from nonlinear regression of experimental results.....	117
<b>Table F.1.</b>	Diffusivity values based on equation (5.3) for lean meat with h1 fiber configuration at the temperatures of AT1 and BT2 locations.....	143

## LIST OF FIGURES

### Figures

<b>Figure 1.1.</b>	Periods observed during drying .....	2
<b>Figure 1.2.</b>	Representation of Knudsen flow .....	3
<b>Figure 1.3.</b>	Some examples to dried traditional dried meats; Biltong, Jerky, Pastrami starting from left .....	4
<b>Figure 1.4.</b>	Schematic showing the cell membrane structure at (a) temperatures below 52°C (low temperatures); (b) temperatures above 52°C (high temperatures).....	7
<b>Figure 1.5.</b>	Schematic view for three different types of pores that can be present in a porous material .....	8
<b>Figure 1.6.</b>	SEM micrographs of banana slices dried at different temperatures .....	8
<b>Figure 1.7.</b>	SEM micrographs of parenchyma tissue from fresh and treated strawberries with a 65 Brix sucrose solution at 50 C. (a) Fresh control, (b) OD, (c) OD-OH and (d) Vi-OH. IS: intercellular space. CR: cell rupture. CW: cell wall .....	9
<b>Figure 1.8.</b>	SEM micrographs of fresh and rehydrated red pepper samples with and without pretreatment dried at different temperatures .....	10
<b>Figure 1.9.</b>	Scanning electron micrograph of fresh and dried apple (Fuji) .....	10
<b>Figure 1.10.</b>	Finite element schemes for one-dimensional problems .....	11
<b>Figure 1.11.</b>	Finite element schemes for two-dimensional problems. (a) Nine-point finite element. (b) Five-point finite element .....	12
<b>Figure 1.12.</b>	Finite element scheme for three-dimensional problems. (a) Nine-point finite element. (b) Five-point finite element .....	12
<b>Figure 1.13</b>	Representation of mesh involving quadrilateral elements augmented at the bottom and up surfaces: (a) cross section of a meat patty with (b) a symmetric half discretized into 180 elements (in parenthesis) and 209 nodes. All dimensions in mm. ....	16
<b>Figure 1.14.</b>	Example of output results, referred to numerical simulation of 900 s of heating of luncheon roll emulsion in RF oven at 200 W. Distribution of the E-field modulus within the sample (above figure), Distribution of the relative dielectric loss factor, within the sample (below figure) .....	17
<b>Figure 1.15.</b>	Discretization of food and air domains into triangular finite elements (detail of the mesh ) .....	21
<b>Figure 2.1.</b>	Fiber configurations in lean meat samples .....	25
<b>Figure 2.2a.</b>	Configuration of dryer .....	26
<b>Figure 2.2b.</b>	Laboratory scale tray dryer.....	27
<b>Figure 2.3</b>	Thermocouple locations on sample .....	28
<b>Figure 2.4.</b>	Illustration of model system. BC; Boundary Condition .....	30



<b>Figure 2.5.</b>	Mesh configuration of the model system .....	32
<b>Figure 3.1.</b>	Thermocouple locations on sample .....	33
<b>Figure 3.2a.</b>	Temperature distribution of lean meat with air flow normal to fiber (h1)...	35
<b>Figure 3.2b.</b>	Temperature distribution of lean meat with air flow normal to fiber; drying along the fiber (h2) .....	35
<b>Figure 3.2c.</b>	Temperature distribution of lean meat with air flow along the fiber (v).....	36
<b>Figure 3.2d.</b>	Temperature distribution of minced meat .....	36
<b>Figure 3.3a.</b>	Temperature change at different points of lean meat with <b>h1</b> fiber configuration during drying at $48\pm 1^\circ\text{C}$ but different velocities.....	39
<b>Figure 3.3b.</b>	Temperature change at different points of lean meat with <b>h2</b> fiber configuration during drying at $48\pm 1^\circ\text{C}$ but different velocities .....	40
<b>Figure 3.3c.</b>	Temperature change at different points of lean meat with <b>v</b> fiber configuration during drying at $48\pm 1^\circ\text{C}$ but different velocities.....	40
<b>Figure 3.3d.</b>	Temperature change at different points of <b>minced</b> meat during drying at $48\pm 1^\circ\text{C}$ but different velocities .....	41
<b>Figure 3.4.</b>	Temperature distribution of samples with three different fiber configurations; h1: flow normal to fibers, h2: flow along the fibers and v: flow normal to fibers .....	42
<b>Figure 3.5a.</b>	Temperature change at different points for different meat samples dried at $48\pm 1^\circ\text{C}$ and 0.5 m/s .....	43
<b>Figure 3.5b.</b>	Temperature change at different points for different meat samples dried at $48\pm 1^\circ\text{C}$ and 1.0 m/s .....	43
<b>Figure 3.5c.</b>	Temperature change at different points for different meat samples dried at $48\pm 1^\circ\text{C}$ and 1.7 m/s .....	44
<b>Figure 3.5d.</b>	Temperature change at different points for different meat samples dried at $70\pm 1^\circ\text{C}$ and 0.5 m/s .....	44
<b>Figure 3.6a.</b>	Change in moisture content (dry base) with respect to drying time during drying of meat samples at four different drying condition.....	46
<b>Figure 3.6b.</b>	Drying rate change with respect to moisture content (dry base) .....	46
<b>Figure 3.6c.</b>	Exponential change in moisture content (dry base) with respect to drying time, fiber direction and structure .....	47
<b>Figure 3.7a.</b>	Change in moisture content (dry base) with respect to drying time, fiber direction and structure .....	48
<b>Figure 3.7b.</b>	Change in drying rate with respect to moisture content (dry base), fiber direction and structure .....	49
<b>Figure 3.8.</b>	Temperature and relative humidity of air through drying of minced meat..	52
<b>Figure 3.9.</b>	Temperature and relative humidity of air through drying of lean meat with h2 fiber configuration .....	52
<b>Figure 4.1a.</b>	2-D Temperature distribution (x-y direction) in lean meat sample with h2 configuration during drying at $48\pm 1^\circ\text{C}$ 0.5 m/s at drying time of 18000 s (300 min), according to <b>model 1</b> .....	54

<b>Figure 4.1b.</b>	2-D Temperature distribution (x-y direction) in lean meat sample with h2 configuration during drying at $48\pm 1^\circ\text{C}$ 0.5 m/s at drying time of 18000 s (300 min), according to <b>model 2</b> .....	54
<b>Figure 4.2a.</b>	2-D moisture content distribution (x-y direction) in lean meat sample with h2 configuration during drying $48\pm 1^\circ\text{C}$ 0.5 m/s at drying time of 18000 s (300 min), according to <b>model 1</b> .....	55
<b>Figure 4.2b.</b>	2-D moisture content distribution (x-y direction) in lean meat sample with h2 configuration during drying at $48\pm 1^\circ\text{C}$ 0.5 m/s at drying time of 18000 s (300 min), according to <b>model 2</b> .....	55
<b>Figure 4.3a.</b>	Predicted temperature change at four different locations (AT1, AT2, BT1, BT2) in minced meat during drying at $48\pm 1^\circ\text{C}$ 1.0 m/s by using <b>model 1</b> .....	56
<b>Figure 4.3b.</b>	Predicted temperature change at four different locations (AT1, AT2, BT1, BT2) in minced meat during drying at $48\pm 1^\circ\text{C}$ 1.0 m/s by using <b>model 2</b> .....	57
<b>Figure 4.4.a1.</b>	Temperature change at four different locations (AT1, AT2, BT1, BT2) in lean meat with flow normal to fibers ( <b>h1</b> ) with respect to drying time during drying at $48\pm 1^\circ\text{C}$ 0.5 m/s by using <b>model 1</b> (coupled heat & mass)	58
<b>Figure 4.4.a2.</b>	Temperature change at four different locations (AT1, AT2, BT1, BT2) in lean meat with flow normal to fibers ( <b>h1</b> ) with respect to drying time during drying at $48\pm 1^\circ\text{C}$ 0.5 m/s by using <b>model 2</b> (coupled heat & mass)	58
<b>Figure 4.4.a3.</b>	Temperature change at four different locations (AT1, AT2, BT1, BT2) in lean meat with flow normal to fibers ( <b>h1</b> ) with respect to drying time during drying at $48\pm 1^\circ\text{C}$ 0.5 m/s as a result of <b>uncoupled</b> heat transfer equation .....	59
<b>Figure 4.4.a4.</b>	Temperature change at four different locations (AT1, AT2, BT1, BT2) in lean meat with flow normal to fibers ( <b>h1</b> ) during drying at $48\pm 1^\circ\text{C}$ 0.5 m/s by using model 1 boundary conditions after wet bulb temperature was reached.....	59
<b>Figure 4.5a.</b>	Temperature change at four different locations (AT1, AT2, BT1, BT2) in lean meat with flow normal to fibers ( <b>h1</b> ) with respect to drying time during drying at $70\pm 1^\circ\text{C}$ 0.5 m/s by using model 2.....	61
<b>Figure 4.5b.</b>	Temperature change at four different locations (AT1, AT2, BT1, BT2) in lean meat with flow normal to fibers ( <b>h1</b> ) with respect to drying time during drying at $48\pm 1^\circ\text{C}$ 1.0 m/s by using model 2.....	61
<b>Figure 4.5c.</b>	Temperature change at four different locations (AT1, AT2, BT1, BT2) in lean meat with flow normal to fibers ( <b>h1</b> ) with respect to drying time during drying at $48\pm 1^\circ\text{C}$ 1.7 m/s by using model 2.....	62
<b>Figure 4.6a.</b>	Temperature change at four different locations (AT1, AT2, BT1, BT2) in lean meat with flow normal to fibers, drying along the fibers ( <b>v</b> ) with respect to drying time during drying at $48\pm 1^\circ\text{C}$ 0.5 m/s by using model 2..	62
<b>Figure 4.6b.</b>	Temperature change at four different locations (AT1, AT2, BT1, BT2) in lean meat with flow normal to fibers, drying along the fibers ( <b>v</b> ) with respect to drying time during drying at $70\pm 1^\circ\text{C}$ 0.5 m/s by using model 2..	63
<b>Figure 4.6c.</b>	Temperature change at four different locations (AT1, AT2, BT1, BT2) in lean meat with flow normal to fibers, drying along the fibers ( <b>v</b> ) with respect to drying time during drying at $48\pm 1^\circ\text{C}$ 1.0 m/s by using model 2..	63

<b>Figure 4.6d.</b>	Temperature change at four different locations (AT1, AT2, BT1, BT2) in lean meat with flow normal to fibers, drying along the fibers ( <b>v</b> ) with respect to drying time during drying at $48\pm 1^{\circ}\text{C}$ 1.7 m/s by using model 2..	64
<b>Figure 4.7a.</b>	Temperature change at four different locations (AT1, AT2, BT1, BT2) in lean meat with flow along to fibers ( <b>h2</b> ) with respect to drying time during drying at $48\pm 1^{\circ}\text{C}$ 0.5 m/s by using model 2.....	64
<b>Figure 4.7b.</b>	Temperature change at four different locations (AT1, AT2, BT1, BT2) in lean meat with flow along to fibers ( <b>h2</b> ) with respect to drying time during drying at $70\pm 1^{\circ}\text{C}$ 0.5 m/s by using model 2.....	65
<b>Figure 4.7c.</b>	Temperature change at four different locations (AT1, AT2, BT1, BT2) in lean meat with flow along to fibers ( <b>h2</b> ) with respect to drying time during drying at $48\pm 1^{\circ}\text{C}$ 1.0 m/s by using model 2.....	65
<b>Figure 4.7d.</b>	Temperature change at four different locations (AT1, AT2, BT1, BT2) in lean meat with flow along to fibers ( <b>h2</b> ) with respect to drying time during drying at $48\pm 1^{\circ}\text{C}$ 1.7 m/s by using model 2.....	66
<b>Figure 4.8a.</b>	Temperature change at four different locations (AT1, AT2, BT1, BT2) in <b>minced</b> meat with respect to drying time at $48\pm 1^{\circ}\text{C}$ 0.5 m/s by using model 2 .....	66
<b>Figure 4.8b.</b>	Temperature change at four different locations (AT1, AT2, BT1, BT2) in <b>minced</b> meat with respect to drying time at $70\pm 1^{\circ}\text{C}$ 0.5 m/s by using model 2 .....	67
<b>Figure 4.8c.</b>	Temperature change at four different locations (AT1, AT2, BT1, BT2) in <b>minced</b> meat with respect to drying time at $48\pm 1^{\circ}\text{C}$ 1.0 m/s by using model 2 .....	67
<b>Figure 4.8d.</b>	Temperature change at four different locations (AT1, AT2, BT1, BT2) in <b>minced</b> meat with respect to drying time at $48\pm 1^{\circ}\text{C}$ 1.7 m/s by using model 2 .....	68
<b>Figure 4.9.</b>	Temperature change at four different locations (AT1, AT2, BT1, BT2) in lean meat with flow along to fibers ( <b>h2</b> ) with respect to drying time during drying at $70\pm 1^{\circ}\text{C}$ 0.5 m/s by using model 2 with no convection at left side of sample .....	68
<b>Figure 4.10.</b>	Moisture content change in lean meat with flow normal to fibers ( <b>h1</b> ) with respect to drying time .....	70
<b>Figure 4.11.</b>	Moisture content change in lean meat with flow along to fibers ( <b>h2</b> ) with respect to drying time .....	71
<b>Figure 4.12.</b>	Moisture content change in lean meat with flow normal to fibers, drying along the fibers ( <b>v</b> ) with respect to drying time.....	71
<b>Figure 4.13.</b>	Moisture content change in <b>minced</b> meat with respect to drying time.....	72
<b>Figure 4.14.</b>	Change in predicted and experimental moisture content in the research of Aversa <i>et. al.</i> (2007) .....	72
<b>Figure 4.15.</b>	Predicted temperature change at four different locations in lean meat with flow normal to fibers ( <b>h1</b> ) with respect to drying time (results of model 2)	73
<b>Figure 4.16.</b>	Predicted temperature change at the surface (BT2) in lean meat with flow normal to fibers, drying along the fibers ( <b>v</b> ) with respect to drying time....	74
<b>Figure 4.17.</b>	Change in predicted moisture content in lean meat with flow normal to fibers, drying along the fibers ( <b>h2</b> ) with respect to drying time.....	74

<b>Figure 4.18.</b>	Predicted temperature change at four different locations with respect to drying time during drying at $48\pm 1^{\circ}\text{C}$ 0.5 m/s by using model 2.....	75
<b>Figure 4.19.</b>	Predicted temperature change at four different locations with respect to drying time during drying at $70\pm 1^{\circ}\text{C}$ 0.5 m/s by using model 2.....	76
<b>Figure 4.20.</b>	Predicted temperature change at four different locations with respect to drying time during drying at $48\pm 1^{\circ}\text{C}$ 1.0 m/s by using model 2.....	76
<b>Figure 4.21.</b>	Predicted temperature change at four different locations with respect to drying time during drying at $48\pm 1^{\circ}\text{C}$ 1.7 m/s by using model 2.....	77
<b>Figure 4.22.</b>	Predicted moisture content change with respect to drying time.....	77
<b>Figure 5.1.</b>	Moisture content change in lean meat with flow normal to fibers ( <b>h1</b> ) with respect to drying time during drying at $48\pm 1^{\circ}\text{C}$ 0.5 m/s.....	79
<b>Figure 5.2.</b>	Change in temperature and moisture content of lean meat with flow normal to fibers ( <b>h1</b> ) with respect to drying time during drying at $48\pm 1^{\circ}\text{C}$ and 0.5 m/s. ....	81
<b>Figure 5.3.</b>	Temperature change in lean meat with flow normal to fibers ( <b>h1</b> ) with respect to drying time during drying at $48\pm 1^{\circ}\text{C}$ 0.5 m/s.....	82
<b>Figure 5.4a.</b>	Temperature change at four different locations (AT1, AT2, BT1, BT2) in lean meat with flow normal to fibers ( <b>h1</b> ) with respect to drying time during drying at $48\pm 1^{\circ}\text{C}$ 0.5 m/s .....	83
<b>Figure 5.4b.</b>	Temperature change at four different locations (AT1, AT2, BT1, BT2) in lean meat with flow normal to fibers ( <b>h1</b> ) with respect to drying time during drying at $70\pm 1^{\circ}\text{C}$ 0.5 m/s .....	83
<b>Figure 5.4c.</b>	Temperature change at four different locations (AT1, AT2, BT1, BT2) in lean meat with flow normal to fibers ( <b>h1</b> ) with respect to drying time during drying at $48\pm 1^{\circ}\text{C}$ 1.0 m/s.....	84
<b>Figure 5.4d.</b>	Temperature change at four different locations (AT1, AT2, BT1, BT2) in lean meat with flow normal to fibers ( <b>h1</b> ) with respect to drying time during drying at $48\pm 1^{\circ}\text{C}$ 1.7 m/s .....	84
<b>Figure 5.5a.</b>	Temperature change at four different locations (AT1, AT2, BT1, BT2) in lean meat with flow along to fibers ( <b>h2</b> ) with respect to drying time during drying at $48\pm 1^{\circ}\text{C}$ 0.5 m/s .....	85
<b>Figure 5.5b.</b>	Temperature change at four different locations (AT1, AT2, BT1, BT2) in lean meat with flow along to fibers ( <b>h2</b> ) with respect to drying time during drying at $70\pm 1^{\circ}\text{C}$ 0.5 m/s .....	85
<b>Figure 5.5c.</b>	Temperature change at four different locations (AT1, AT2, BT1, BT2) in lean meat with flow along to fibers ( <b>h2</b> ) with respect to drying time during drying at $48\pm 1^{\circ}\text{C}$ 1.0 m/s .....	86
<b>Figure 5.5d.</b>	Temperature change at four different locations (AT1, AT2, BT1, BT2) in lean meat with flow along to fibers ( <b>h2</b> ) with respect to drying time during drying at $48\pm 1^{\circ}\text{C}$ 1.7 m/s .....	86
<b>Figure 5.6a.</b>	Temperature change at four different locations (AT1, AT2, BT1, BT2) in lean meat with flow normal to fibers, drying along the fibers ( <b>v</b> ) with respect to drying time during drying at $48\pm 1^{\circ}\text{C}$ 0.5 m/s.....	87
<b>Figure 5.6b.</b>	Temperature change at four different locations (AT1, AT2, BT1, BT2) in lean meat with flow normal to fibers, drying along the fibers ( <b>v</b> ) with respect to drying time during drying at $70\pm 1^{\circ}\text{C}$ 0.5 m/s.....	87

<b>Figure 5.6c.</b>	Temperature change at four different locations (AT1, AT2, BT1, BT2) in lean meat with flow normal to fibers, drying along the fibers ( <b>v</b> ) with respect to drying time during drying at $48\pm 1^\circ\text{C}$ 1.0 m/s.....	88
<b>Figure 5.6d.</b>	Temperature change at four different locations (AT1, AT2, BT1, BT2) in lean meat with flow normal to fibers, drying along the fibers ( <b>v</b> ) with respect to drying time during drying at $48\pm 1^\circ\text{C}$ 1.7 m/s.....	88
<b>Figure 5.7.</b>	Moisture content change in lean meat with flow normal to fibers ( <b>h1</b> ) with respect to drying time. ....	89
<b>Figure 5.8.</b>	Moisture content change in lean meat with flow along to fibers ( <b>h2</b> ) with respect to drying time .....	90
<b>Figure 5.9.</b>	Moisture content change in lean meat with flow normal to fibers, drying along the fibers ( <b>v</b> ) with respect to drying time	90
<b>Figure 5.10.</b>	Moisture content change in lean meat with flow normal to fibers ( <b>h1</b> ) with respect to drying time during drying at $70\pm 1^\circ\text{C}$ and 0.5 m/s after inclusion of shrinkage .....	92
<b>Figure 5.11.</b>	Moisture content change in lean meat with flow along to fibers ( <b>h2</b> ) with respect to drying time during drying at $70\pm 1^\circ\text{C}$ and 0.5 m/s after inclusion of shrinkage .....	92
<b>Figure 5.12.</b>	Moisture content change in lean meat with flow normal to fibers, drying along the fibers ( <b>v</b> ) with respect to drying time during drying at $70\pm 1^\circ\text{C}$ and 0.5 m/s after inclusion of shrinkage.....	93
<b>Figure 5.13.</b>	Temperature change at four different locations (AT1, AT2, BT1, BT2) in lean meat with flow normal to fibers ( <b>h1</b> ) with respect to drying time during drying at $70\pm 1^\circ\text{C}$ , 0.5 m/s after inclusion of shrinkage.....	94
<b>Figure 5.14.</b>	Temperature change at four different locations (AT1, AT2, BT1, BT2) in lean meat with flow along to fibers ( <b>h2</b> ) with respect to drying time during drying at $70\pm 1^\circ\text{C}$ , 0.5 m/s after inclusion of shrinkage.....	94
<b>Figure 5.15.</b>	Temperature change at four different locations (AT1, AT2, BT1, BT2) in lean meat with flow normal to fibers, drying along the fibers ( <b>v</b> ) with respect to drying time during drying at $70\pm 1^\circ\text{C}$ , 0.5 m/s after inclusion of shrinkage .....	95
<b>Figure 5.16.</b>	Predicted moisture content change with respect to drying time.....	96
<b>Figure 5.17.</b>	Predicted temperature change at four different locations with respect to drying time during drying at $48\pm 1^\circ\text{C}$ , 0.5 m/s .....	97
<b>Figure 5.18.</b>	Predicted temperature change at four different locations with respect to drying time during drying at $70\pm 1^\circ\text{C}$ , 0.5 m/s .....	97
<b>Figure 5.19.</b>	Predicted temperature change at four different locations with respect to drying time during drying at $48\pm 1^\circ\text{C}$ , 1.0 m/s .....	98
<b>Figure 5.20.</b>	Predicted temperature change at four different locations with respect to drying time during drying at $48\pm 1^\circ\text{C}$ 1.7 m/s .....	98
<b>Figure C.1.</b>	Selection of application mode as transient for time dependent system....	119
<b>Figure C.2.</b>	Drawing of sample .....	119
<b>Figure C.3.</b>	Mesh definition in order to have augmented mesh around boundary 1,3,4	120
<b>Figure C.4.</b>	Constants window .....	120

<b>Figure C.5.</b>	Functions defined for air properties .....	121
<b>Figure C.6.</b>	Subdomain expressions .....	121
<b>Figure C.7.</b>	Boundary expressions .....	122
<b>Figure C.8.</b>	Subdomain integration variable definition in order to calculate average moisture concentration with respect to time (24%; dry weight percentage found experimentally) .....	122
<b>Figure C.9.</b>	Subdomain settings for heat transfer (Q is heat loss due to evaporation for model 2 defined in materials and methods chapter) .....	123
<b>Figure C.10.</b>	Initial temperature of sample .....	123
<b>Figure C.11.</b>	Boundary settings for heat transfer for boundaries 1,3,4 defined Figure 2.4.....	124
<b>Figure C.12.</b>	Boundary settings for heat transfer for boundary 2 defined Figure 2.4.....	124
<b>Figure C.13.</b>	Subdomain settings for mass transfer .....	125
<b>Figure C.14.</b>	Initial water concentration of sample .....	125
<b>Figure C.15.</b>	Boundary settings for mass transfer at boundaries 1,3,4 defined Figure 2.4.....	126
<b>Figure C.16.</b>	Boundary setting for mass transfer at boundary 2 defined Figure 2.4.....	126
<b>Figure C.17.</b>	Domain plot parameter selection after solving the model in order to observe average concentration at the subdomain .....	127
<b>Figure C.18.</b>	Cross sectional plot parameter selection after solving the model in order to observe temperature values at the probe locations.....	127
<b>Figure D.1a.</b>	Temperature change at four different locations (AT1, AT2, BT1, BT2) in lean meat with flow normal to fibers ( <b>h1</b> ) with respect to drying time during drying at $70\pm 1^{\circ}\text{C}$ 0.5 m/s by using model 1.....	129
<b>Figure D.1b.</b>	Temperature change at four different locations (AT1, AT2, BT1, BT2) in lean meat with flow normal to fibers ( <b>h1</b> ) with respect to drying time during drying at $48\pm 1^{\circ}\text{C}$ 1.0 m/s by using model 1.....	129
<b>Figure D.1c.</b>	Temperature change at four different locations (AT1, AT2, BT1, BT2) in lean meat with flow normal to fibers ( <b>h1</b> ) with respect to drying time during drying at $48\pm 1^{\circ}\text{C}$ 1.7 m/s by using model 1.....	130
<b>Figure D.2a.</b>	Temperature change at four different locations (AT1, AT2, BT1, BT2) in lean meat with flow normal to fibers, drying along the fibers ( <b>v</b> ) with respect to drying time during drying at $48\pm 1^{\circ}\text{C}$ 0.5 m/s by using model 1..	130
<b>Figure D.2b.</b>	Temperature change at four different locations (AT1, AT2, BT1, BT2) in lean meat with flow normal to fibers, drying along the fibers ( <b>v</b> ) with respect to drying time during drying at $70\pm 1^{\circ}\text{C}$ 0.5 m/s by using model 1..	131
<b>Figure D.2c.</b>	Temperature change at four different locations (AT1, AT2, BT1, BT2) in lean meat with flow normal to fibers, drying along the fibers ( <b>v</b> ) with respect to drying time during drying at $48\pm 1^{\circ}\text{C}$ 1.0 m/s by using model 1..	131

<b>Figure D.2d.</b>	Temperature change at four different locations (AT1, AT2, BT1, BT2) in lean meat with flow normal to fibers, drying along the fibers ( <b>v</b> ) with respect to drying time during drying at $48\pm 1^\circ\text{C}$ 1.7 m/s by using model 1..	132
<b>Figure D.3a.</b>	Temperature change at four different locations (AT1, AT2, BT1, BT2) in lean meat with flow along to fibers ( <b>h2</b> ) with respect to drying time during drying at $48\pm 1^\circ\text{C}$ 0.5 m/s by using model 2.....	132
<b>Figure D.3b.</b>	Temperature change at four different locations (AT1, AT2, BT1, BT2) in lean meat with flow along to fibers ( <b>h2</b> ) with respect to drying time during drying at $70\pm 1^\circ\text{C}$ 0.5 m/s by using model 1.....	133
<b>Figure D.3c.</b>	Temperature change at four different locations (AT1, AT2, BT1, BT2) in lean meat with flow along to fibers ( <b>h2</b> ) with respect to drying time during drying at $48\pm 1^\circ\text{C}$ 1.0 m/s by using model 1.....	133
<b>Figure D.3d.</b>	Temperature change at four different locations (AT1, AT2, BT1, BT2) in lean meat with flow along to fibers ( <b>h2</b> ) with respect to drying time during drying at $48\pm 1^\circ\text{C}$ 1.7 m/s by using model 1.....	134
<b>Figure D.4a.</b>	Temperature change at four different locations (AT1, AT2, BT1, BT2) in <b>minced</b> meat with respect to drying time at $48\pm 1^\circ\text{C}$ 0.5 m/s by using model 1 .....	134
<b>Figure D.4b.</b>	Temperature change at four different locations (AT1, AT2, BT1, BT2) in <b>minced</b> meat with respect to drying time at $70\pm 1^\circ\text{C}$ 0.5 m/s by using model 1 .....	135
<b>Figure D.4c.</b>	Temperature change at four different locations (AT1, AT2, BT1, BT2) in <b>minced</b> meat with respect to drying time at $48\pm 1^\circ\text{C}$ 1.0 m/s by using model 1 .....	135
<b>Figure D.4d.</b>	Temperature change at four different locations (AT1, AT2, BT1, BT2) in <b>minced</b> meat with respect to drying time at $48\pm 1^\circ\text{C}$ 1.7 m/s by using model 1 .....	136

## LIST OF SYMBOLS AND ABBREVIATIONS

AT1	midpoint of sample (center)
AT2	2/3 of length from center
BC	boundary condition
bds	bone dry solid
BT1	mid point at the bottom surface (insulated)
BT2	-2/3 of length from center on the surface exposed to air
C	concentration of water (kg/m <sup>3</sup> )
CHO	Carbohydrate
C <sub>p</sub>	heat capacity (J/kg.K)
D	Diffusion coefficient (m <sup>2</sup> /s)
D <sub>a,w</sub>	Diffusion coefficient of water in air (m <sup>2</sup> /s)
D <sub>eff</sub>	effective diffusivity (m <sup>2</sup> /s)
ds	dry solid
E <sub>a</sub>	activation energy (kJ/mol)
ext	external
FEM	Finite Element Modelling/Method
h	heat transfer coefficient (W/m <sup>2</sup> .K)
h1	flow normal to fiber
h2	flow along the fiber
k	thermal conductivity (W/m.K)
k <sub>T</sub>	rate constant of temperature change (min <sup>-1</sup> )
k <sub>c</sub>	Mass transfer coefficient (m/s)
k <sub>m</sub>	Rate constant for change in moisture content (g/gbds.min)
l	liquid
L	length of diffusion pathway (m)
L <sub>c</sub>	characteristic length
Le	Lewis number
Nu	Nusselt number
pa	parallel
Pr	Prandtl number
pro, p	protein
q <sub>v</sub>	evaporative heat loss (W/m <sup>2</sup> for model 1 and W/m <sup>3</sup> for model 2)
R <sup>2</sup>	coefficient of determination
Re	Reynolds number
RMSE	Root Mean Square Error
s	substrate/solid
Sc	Schmidt number
se	series
SEE	Standart Error of Estimate
Sh	Sherwood number
T	Temperature (°C, K)
t	time (min, sec)
T <sub>0</sub>	initial temperature (K)
T <sub>f</sub>	film temperature (K)
T <sub>m</sub>	maximum temperature of sample at an infinite drying time with respect to initial temperature
v	flow normal to fiber, drying along the fiber
v	vapor
w	water
X	moisture content (dry base) (g/g bds)
X*	dimensionless moisture content



$X_{eq}, m_e$	equilibrium moisture content (g/g bds)
$X_i$	initial moisture content (dry base) (g/g bds)
$\lambda$	latent heat of evaporation (J/kg)
$\rho$	density (kg/m <sup>3</sup> )
f	fat
a	air
$T_{fr}$	freezing temperature in Table A.1
RH	Relative Humidity
Tu	turbulence intensity of free air stream (%) in Table A.1



## CHAPTER 1

### INTRODUCTION

#### 1.1 Drying and Drying Methods

Drying is a coupled heat and mass transfer process based on removal of water from solid or semi-solid foods. Water is also an important parameter for food deterioration since many spoilage microorganisms, pathogens and deteriorating enzymes need water to be active. Thus, for centuries people have used numerous techniques to remove water from food in order to prolong shelf life, generate good flavour and aroma. Additionally, from economical point of view, drying minimizes storage and transportation costs while eases handling by reducing size, weight and the risk of microbial contamination of food. Although nowadays meat can be preserved by freezing, refrigeration and thermal processing, some traditional meat products (fermented sausages, dry-cured hams, pastrami, jerky etc.) in which drying constitutes the main process are still produced worldwide in large quantities as they have a unique and popular flavour (Arnau *et al.*, 2007).

Drying processes can be classified according to continuity of drying medium and the material to be dried. Batch drying occurs when material is placed into a dryer for a specified period of time and held until reaching desired moisture content while in continuous drying, drying medium and the material contact each other throughout the dryer, and the dried material exits from one end of the dryer (Geankoplis, 1993). If material is held constant in the dryer and the drying medium flows through the dryer, the process is called semi-batch drying.

Source of energy varies with respect to drying method. In a widely used air drying, *convective* drying occurs by passing heated air over food materials (e.g. herbs, sliced fruits) at atmospheric pressure to remove the moisture like in tray and spray dryers. *Conductive* drying is employed in drum dryers by direct contact of material to the heated walls of dryer, especially applied when the material is too wet or thin (e.g. starch, instant mashed potatoe, fruit and vegetable pulp, baby food) (Keey, 1992; Geankoplis, 1993). A limiting factor for this type is the potential food degradation or case hardening since much higher temperatures are applied than in convective drying. Electromagnetic *radiation* is another source of energy as used in infrared drying, generally applied for surface drying since penetration depth is short (Keey, 1992). Advantages of infrared are less time required and less damage to the dried material (e.g. nuts, grains, eggs, onion) (Chakraborty *et al.*, 2010). In *dielectric* drying, material is placed in electrical field oscillating very rapidly causing heat generation within the material, especially in liquid part since dielectric constants of liquid are much higher than solids (e.g. post bake drying of biscuits, preheating of dough, diced apples, potatoe). In freeze drying, moisture is removed from frozen material by sublimation (e.g. ice-cream, instant coffee, fruits, bacon) (Keey, 1992; Geankoplis, 1993).

##### 1.1.1. Stages of Drying

The driving force responsible for moisture-transport is a combination of diffusion due to moisture gradient and difference of vapor-pressure due to temperature gradient. Rate of drying changes with controlling mechanisms, being internal or external. Drying occurs theoretically in two stages, constant rate period and one or more falling rate periods (Figure 1.1). Before drying starts, there is an adaptation period in which surface of the material to be dried is heated or cooled down to wet bulb temperature of air. Then, at wet bulb temperature, constant rate period starts. During constant rate drying, moisture migration from interior to the surface is fast enough to maintain saturation at the surface which behaves as free-water so that the evaporation rate remains constant. External conditions such as temperature difference between the surface of material and air, flow rate of air,

external heat and mass transfer coefficients control the rate of drying during constant rate period. Jason (1958) showed that when velocity of air was higher than 1 m/s, external resistances became negligible. However, Farid and Kizilel (2009) reported that in general, external resistances would play a significant role in air drying.

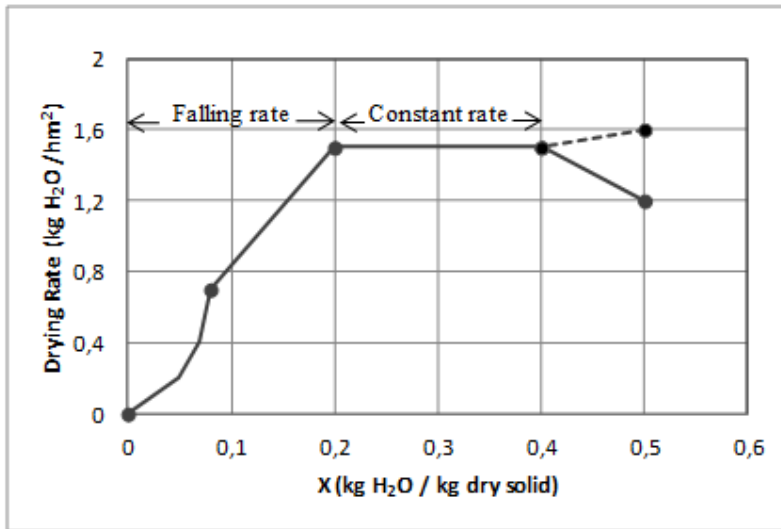


**Figure 1.1.** Periods observed during drying (Geankoplis, 1993)

Once the moisture transfer from interior is not enough to make the surface saturated, falling rate starts. Moisture content of material at the end of constant rate is defined as critical moisture content. Researches showed that critical moisture contents of many food systems are very close to initial moisture content which indicates negligible importance of constant rate period in many foods (Srikiatden and Roberts, 2007; Chirife and Cachero, 1970; Vaccarezza *et al.*, 1974a; Alzamora and Chirife, 1980). In general, constant rate period is either too short or not present in food systems since most of the water molecules are present as bound water within the cells or in intracellular space. Thus, drying mainly occurs in falling rate period (Madamba, 1996; Ayensu, 2004; Srikiatden and Roberts, 2007; Saravacos and Charm, 1962; Chirife J., 1971).

Falling rate period is controlled by internal transport since there is no more free water layer on the surface and the rate of evaporation from surface is faster than the moisture migration from interior (Keey, 1992). Surface starts to dry and temperature increases as evaporation from the surface decreases. In the first falling rate period, rate of drying decreases as the moisture content of material decreases due to internal resistance for moisture transfer and less heat flux resulting from less temperature difference between surface and drying medium. Moisture transfer to the surface might occur as liquid water or vapor from the interior side of the material. The temperature in interior sites does not exceed significantly the wet bulb temperature. When partial pressure of water throughout the material is less than the saturation level, the second falling rate period starts. At this stage, the temperature difference between air and material surface is so small that heat flux from air to the material is also very low (Geankoplis, 1993).

### 1.1.2. Physical Effects of Drying

Drying might also change the porosity of materials. Studies show that some food materials (e.g. apples) develop significant porosity during drying even if they are nonporous at the beginning (Srikiatden and Roberts, 2007; Lozano *et al.*, 1983; Zogzas, 1994; Krokid and Maroulis, 1997). Rizvi (2005), Srikiatden and Roberts (2007) reported that “in a highly porous material or when

significant porosity is developed, mass transfer occurs mainly in the vapor phase and all evaporation occurs from interior of the material” during falling rate period. However in order to supply heat for vaporization in the interior sites, heat has to be conducted through the sample which have low thermal conductivity. Thus, drying rate is very slow at this stage. Most of the food materials (apple, kiwi, carrot, etc.) show this second falling rate period (Chirife, 1983; Karel and Lund, 2003). When vapor pressure of material becomes equal to the partial vapor pressure of drying medium, drying stops. The moisture content at this stage is called equilibrium moisture content. It can be seen that water binding and porous structure of materials affect moisture transfer significantly (Srikiatden and Roberts, 2007).

### 1.1.3. Mechanisms of Water Transport During Drying

Moisture migration can take place by various ways according to passage of water through food and driving force such as molecular diffusion (liquid and/or vapor transport due to moisture concentration differences), capillary flow (liquid movement through capillaries), surface diffusion (liquid movement due to diffusion of moisture to the pore-surface and moving along the surface), thermal diffusion (vapor movement due to temperature differences), hydrostatic flow (water and vapor movement due to total pressure differences), or Knudsen flow etc. (Ayensu, 2004; Madamba, 1996).

Baini and Langrish (2008) tried to find out the type and mechanism of drying in fruits which has not been defined completely yet, by using banana as a model food. They used Knudsen diffusion which is based on pore size distribution for pore sizes between 2 nm and 50 nm in their model. Knudsen diffusion is based on an approach that the mean free path of water molecules within the pores are so large that they collide with the pore wall more frequently than with each other and they jump one adsorption site to another (Figure 1.2). In this study, Knudsen number for bananas was found very large meaning that water molecules hit the pore walls very intensely causing surface diffusion to be the fundamental mechanism in moisture transport. Researchers suggested that surface diffusion could be represented by Fickian diffusion even though pore size distribution changed during drying since surface diffusion was still the dominating mechanism. They also measured diffusivity by using different approaches including temperature and moisture dependency. It was found that moisture content had more significant effect than temperature and other components (sugar content) on moisture diffusivity during drying of banana (Baini and Langrish, 2008).

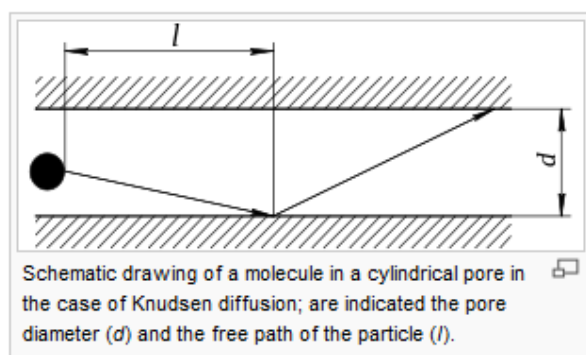


**Figure 1.2.** Representation of Knudsen flow

Betoret *et al.* (2007) studied the drying mechanism of apple when vacuum impregnation, osmotic dehydration and air drying were applied simultaneously. In vacuum impregnation, pressure

gradient and deformation-relaxation mechanism gave rise to transport of extracellular liquid water and soluble solids to external phase (hydrodynamic flow). In osmotic dehydration, water activity gradient caused water transport from intracellular to extracellular liquid then to external phase and soluble solid transport in reverse direction. The same water transport mechanism as in osmotic dehydration was observed in air drying (Betoret *et al.*, 2007).

#### 1.1.4. Meat Drying

Drying of meat is practised either to produce meat product with unique flavor such as dry-cured hams, pastrami, jerky, Bresaola (Italy), Biltong (southern Africa), Oodka (Somalia), Kuivaliha (Finland), Qwanta (Ethiopia), Kilishi (Nigeria) etc. (Figure 1.3) or complementary/aroma ingredient for foods such as instant soup, baby food, pet food etc. (Heinz and Hautzinger, 2007).

Jerky is raw meat or fish which is salted first, sometimes smoked and then dried. It is one of the popular North American dried meat products and it relies on conventional drying methods. Since 1996, beef jerky has been preferred by astronauts for space flight due to its light weight and high level of nutrition (The beef jerky blog, <http://www.thebeefjerkyblog.com/so-jerky-is-as-jerky-does/>).

The production process of pastrami is complicated and takes several weeks. The main process steps are two phase salting, washing, air drying, pressing, drying, pressing, covering with a thick layer of paste called cemen and final drying (Aktas *et al.*, 2005; Heinz and Hautzinger, 2007).



**Figure 1.3.** Some examples to dried traditional dried meats; Biltong, Jerky, Pastrami starting from left

Meat is a fibrous food composed of myofibrils and pH, ionic strength, osmotic pressure, the muscle state (in rigor mortis or in the relaxation state) and even the usage of starter cultures, affect the space between myofibrils (Castro-Giráldez *et al.*, 2010; Aktas *et al.*, 2005). Castro-Giráldez and coworkers studied the effect of salting on pork meat and stated that salting process might cause shrinkage or swelling according to concentration of salt solution since proteins constituting myofibrils have electrostatic charge. Commercial starter cultures was also found to be effective in degradation of myofibrillar proteins especially myosin during pastrami production (Aktas *et al.*, 2005).

The traditional dehydration methods used for meat are sun drying, solar drying and air drying (e.g. tunnel drying) (Heinz and Hautzinger, 2007). As drying is the major preservation method used for meat products like jerky and pastrami, it is necessary to understand the drying behavior of meat to optimize the process. Thiagarajan and co-workers (2006) studied drying characteristics of beef jerky in forced air thin layer drying. They found that relative humidity and airflow rate had significant effect on drying characteristics of beef jerky. The higher air flow rate and lower relative

humidity favored the drying process. Physical properties such as water activity, color and shrinkage were also affected by relative humidity and air flow rate. Lee & Kang (2003) also investigated the influence of temperature (50, 60, and 70°C) and moisture content (18, 21, and 24%) on the quality of jerky products using ostrich meat. They found that drying temperature had significant influence on protein solubility while change in moisture content did not affect protein solubility when samples were dried at the same temperature. Finally, the jerky product dried at 60°C, with 24% w.b. moisture content was found to have the best overall acceptability.

## 1.2 Isotropic and Anisotropic Foods

'Isotropy' or 'isotropic' means that the material displays no change in physical properties in all directions. 'Anisotropy' or 'anisotropic' (nonisotropic) means that the material displays different values of a physical property in different directions. (Bourne, 2002; <http://www.texturetechnologies.com/Bourne-Isotropic-Anisotropic.html>)

Some foods are isotropic whereas other foods are anisotropic. For isotropic foods (gels, potato flesh, liquid foods like milk) properties are not a function of direction while for an anisotropic food properties such as elasticity, conductivity and diffusivity depend on direction due to pores, fibrous nature or structural differences throughout the sample. Some examples to anisotropic foods are (Bourne, 2002):

- Meat and other fibrous foods: Cutting across the fibers will give a different texture than cutting between the fibers.
- Cooked lasagna: Appears to be softer when cut parallel to the direction of extrusion than perpendicular.
- Some cheeses: For example, Tilsit cheese constituting lentil-shaped holes requires a higher force to compress when the long axis of the holes lie parallel to the compressing platen than when the short axis is parallel to the platen.
- Surimi: It has a flaky structure. A lower force is required to compress or cut surimi when the flakes are parallel to the blade than perpendicular.

Meat is a fibrous anisotropic food as stated above. Meat tissue is formed by a network of muscular fibers surrounded by connective tissue. Fibers contain specialized contractile organelles, the myofibrils (Castro-Giráldez *et al.*, 2010). The amount of contraction or relaxation of myofibrils with respect to stresses like temperature, moisture loss or pH etc. depends on direction of these fibers to the stresses.

Studies showed that thermal conductivity value measured changes according to direction of heat flow, which indicates anisotropy (Table 1.1, Table A.2)

**Table 1.1.** Thermal conductivity of cow and pig muscles (Hill *et al.*, 1967; Bhattacharya A, Mahajan R. L., 2003)

		<b>k (W m<sup>-1</sup> K<sup>-1</sup>)</b>	<b>T (°C)</b>
<b>Cow</b>	Across fibers	0.467	36.0
	Along fibers	0.434	32.0
<b>Pig</b>	Across fibers	0.530	44.8
	Along fibers	0.485	42.9

Even though many unprocessed foods are anisotropic, generally effective properties like effective diffusivity in which dependency to the axes of food are not considered, were used in models, since it is difficult to solve models by using anisotropic properties.

For many properties, component approach can be applied to find an approximate value of a property, since the compositions of many foods and properties of these components (water, fat, carbohydrate (CHO), protein, ash) are present in literature.

For example, for thermal conductivity (W/m.K)(Choi and Okos 1986; Şahin & Şumnu, 2006);

$$k_{\text{water}} = 0.57109 + 1.7625 \cdot 10^{-3}T - 6.7036 \cdot 10^{-6}T^2 \quad (1.1)$$

$$k_{\text{CHO}} = 0.20141 + 1.3874 \cdot 10^{-3}T - 4.3312 \cdot 10^{-6}T^2 \quad (1.2)$$

$$k_{\text{protein}} = 0.17881 + 1.1958 \cdot 10^{-3}T - 2.7178 \cdot 10^{-6}T^2 \quad (1.3)$$

$$k_{\text{fat}} = 0.18071 - 2.7604 \cdot 10^{-3}T - 1.7749 \cdot 10^{-7}T^2 \quad (1.4)$$

$$k_{\text{ash}} = 0.32961 + 1.4011 \cdot 10^{-3}T - 2.9069 \cdot 10^{-6}T^2 \quad (1.5)$$

$$k_{\text{ice}} = 2.2196 - 6.2489 \cdot 10^{-3}T + 1.0454 \cdot 10^{-4}T^2 \quad (1.6)$$

For heat capacity (kJ/kg.K);

$$C_p = 4.180 \cdot X_{\text{water}} + 1.711 \cdot X_{\text{protein}} + 1.928 \cdot X_{\text{fat}} + 1.547 \cdot X_{\text{CHO}} + 0.908 \cdot X_{\text{ash}} \quad (1.7)$$

(Choi and Okos, 1986, Stroschine, 2000)

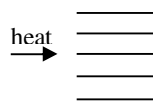
X denotes mass fractions on wet basis. Other equations are presented in Appendix A.

In order to find the overall thermal conductivity, parallel, series or Krischer models can be used according to structure of material (Şahin & Şumnu, 2006):

Paralel:

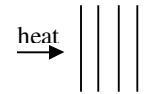
$$k_{pa} = \sum_{i=1}^n k_i \cdot X_i^v$$

$$X_i^v = \frac{\frac{x_i^w}{\rho_i}}{\sum_{i=0}^n \left( \frac{x_i^w}{\rho_i} \right)}$$



Series:

$$1/k_{se} = \sum_{i=1}^n \frac{x_i^v}{k_i}$$



v represents volume fraction, w represents mass fraction.

Rosello *et al.* (1997) also showed moisture diffusivity change with direction (Table 1.2.) and confirmed the hypothesis of anisotropic mass transfer during green bean drying. This was suggested to be resulted from no mass transfer resistance due to skin in axial direction while there was such resistance in radial direction together with internal resistance (Rosello *et al.*, 1997).

**Table 1.2.** Diffusivity ( $D_{\text{eff}}$ ) and activation energy (Ea) values for drying of green beans (Rosello *et al.*; 1997)

Model	$D_{\text{eff}}$ (m <sup>2</sup> /s)	T (°C)	Ea (kJ/mol)
Model without shrinkage, radial direction	$1.6 \times 10^{-10}$	60	43.0
Model with shrinkage, radial direction	$1.5 \times 10^{-10}$	60	43.5
Model without shrinkage, axial direction	$1.3 \times 10^{-9}$	60	22.0
Model with shrinkage, axial direction	$1.2 \times 10^{-9}$	60	24.8

Thermal properties of foods can be directly measured by experiments. However, these values become only valid for a given condition. Thus, researchers tried to find more generalized definitions for thermal properties based on food compositions or as a function of temperature or moisture content of food material. Among those thermal properties, thermal conductivity and moisture diffusivity are the most important factors determining the accuracy of model predictions (Farid and Kizilel, 2009). A considerable attention should be paid to select suitable correlation equations for a given case. Several empirical equations used in models to represent physical and thermal properties of food samples are summarized in Appendix A. None of these equations consider anisotropy except Equation (a.7) in Table A.1. All reflect bulk effective properties. Taking



constant or variant property with respect to moisture or temperature of sample is also highly important for model accuracy.

### 1.2.1 Effect of Cellular Structure of Food on Drying

Tissue structure and composition of foods appreciably affect the thermal and physical properties (e.g. water diffusion coefficient) during air drying (Fito *et al.*, 2001). Water transport in a cellular tissue depends on the pathway that water follows through food, which in turn depends on temperature. The resistance to moisture migration depends on the structure (capillary pressure; permeability of cells, fiber configuration, pore size and distribution, connection of pores with each other and also with external fluid), composition of food and type of moisture-material binding (chemical, physical or mechanical). In order to understand the mechanism lying under moisture migration, numerous studies have been conducted on moisture pathway through food during drying and some of them are described below.

Water in the cells should pass first through cell membrane, then cell wall to reach the intercellular and finally the extracellular matrix. The main driving force for this flow is the difference in water potential between media. Cell membranes are intact at low temperatures, however higher temperatures result in rupture of cell membrane and water flows through intercellular space and the lacunae created by the dead cells (Halder *et al.*, 2000) (Figure 1.4).

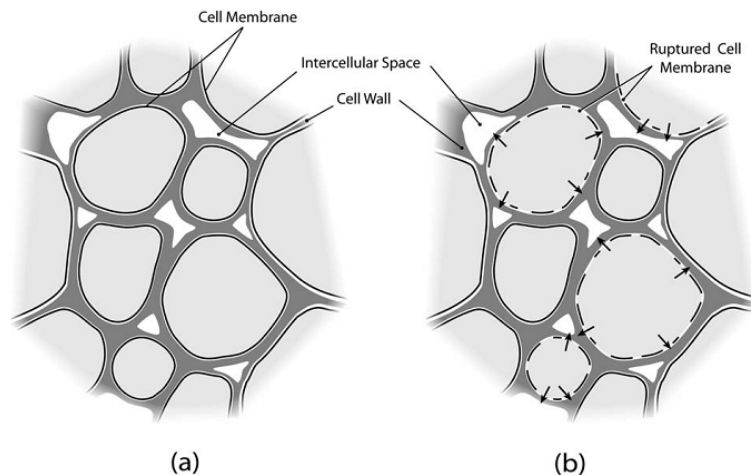


**Figure 1.4.** Schematic showing the cell membrane structure at (a) temperatures below 52°C (low temperatures); (b) temperatures above 52°C (high temperatures) (Halder *et al.*, 2010)

The potato slices left in ambient air at atmospheric pressure lost ~80% of their water over 5 days. However, with pressure-driven flow up to 1.5 MPa at 100% relative humidity, only 2% of total water can be driven out (Halder *et al.*, 2000). Halder *et al.* (2000) defined the possible reasons for this as “(1) the rest of the water (98%) is not present in the capillaries; (2) the capillary pressure (which is negative or attractive) is higher than the applied pressure and therefore more water cannot flow out of the pores; (3) the water is present in the blind pores (Figure 1.5)” or in the cells. However, researchers stressed that at least 70% of the water is intracellular in meat (Honikel and Hamm, 1994) and vegetables (Nobel, 2009; Asquith *et al.*, 2007) at room temperature, not in capillaries or pores.

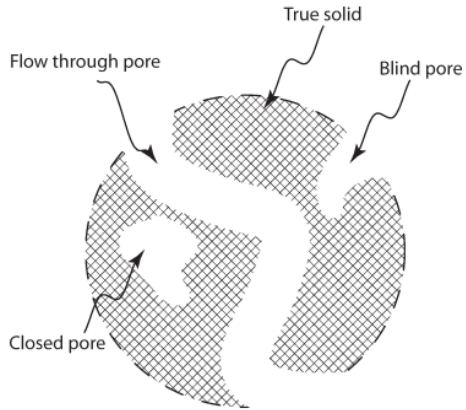


**Figure 1.5.** Schematic view for three different types of pores that can be present in a porous material (Halder *et al.*, 2010)

Halder *et al.* (2000) also showed that ~95% of the water is intracellular in potato tissue at lower temperatures, and this water becomes extracellular at temperatures above 52°C due to rupture of cell membrane. Thus, drying at higher temperatures results in higher moisture diffusivities. Similar results were also observed in several studies (Vega-Galvez *et al.*, 2008; Bondaruk *et al.*, 2007, Thuwapanichayanan *et al.*, 2011) (Figure 1.6).

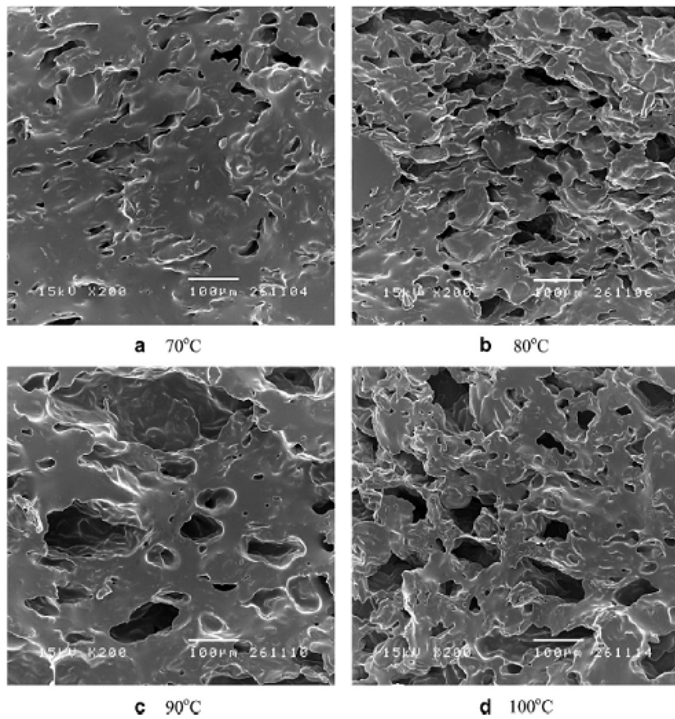


**Figure 1.6.** SEM micrographs of banana slices dried at different temperatures (Thuwapanichayanan *et al.*, 2011)

Combination of different drying techniques can have impact on final product. Moreno *et al.* (2012) studied the presence of the synergistic effect of osmotic dehydration (OD), ohmic heating (OH) and vacuum impingement (VI) on drying of strawberries. They showed the highest water removal with OD-OH treatment at 50°C, while the largest solid uptake with VI-OH at 50°C. The osmotic dehydration caused plasmolysis and in turn collapse of the cell (Figure 1.7).

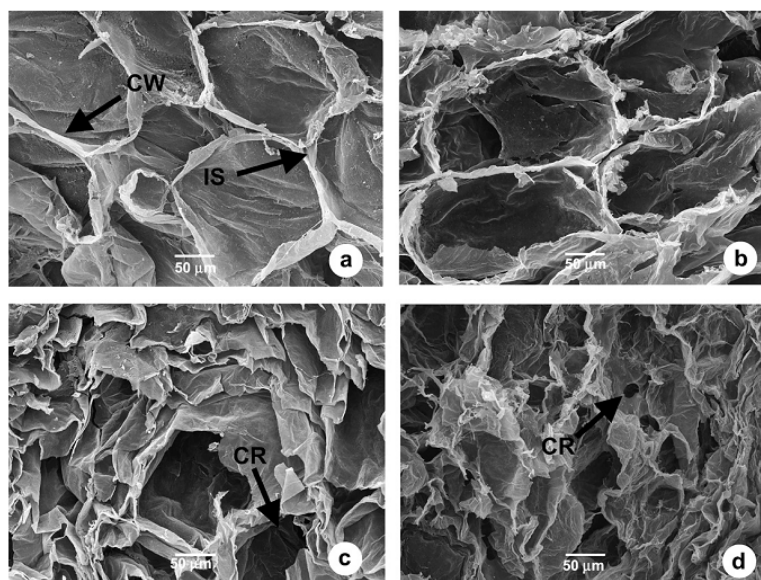


**Figure 1.7.** SEM micrographs of parenchyma tissue from fresh and treated strawberries with a 65 Brix sucrose solution at 50 C. (a) Fresh control, (b) OD, (c) OD-OH and (d) Vi-OH. IS: intercellular space. CR: cell rupture. CW: cell wall (Moreno *et al.*, 2012)

Anisotropy also affects the way that food sample shrink. The stresses due to temperature and moisture gradients within the product lead to non-uniform shrinkage according to microstructure of food. When these stresses exceed the force binding the cells, crack formation occurs, which in turn change again micro and macrostructure of the sample (Wang and Brennan, 1995; Xiao and Gao, 2012).

#### 1.2.1.1. Effect of Pretreatments on Cellular Structure During Drying

Some pretreatments applied prior to drying might alter the effect of drying on cellular structure. For example, immersing the food in a solution containing NaCl, CaCl<sub>2</sub>, Na<sub>2</sub>S<sub>2</sub>O<sub>5</sub> has been found to reduce the amount of damage given to cell structure as reported by Vega-Galvez *et al.* (2008) (Figure 1.8). Moreover, Xiao *et al.* (2009) showed that citric acid pretreatment prior to air impingement drying of sweet potato has enlarged the pores and resulted in formation of starch granules on the surface, which made diffusion of moisture easier (Xiao and Gao, 2012). Drying of carrot slices in ethano-modified supercritical carbon dioxide also gave rise to pore formation and enlargement, decreasing the process time compared to regular air drying (Brown *et al.*, 2008). Deng & Zhao (2008a and b) reported that osmoconcentration pretreatment caused calcium penetration, collapse of cell wall and structure deformation due to surface tension and pressure difference inside and outside the cells (Figure 1.9).

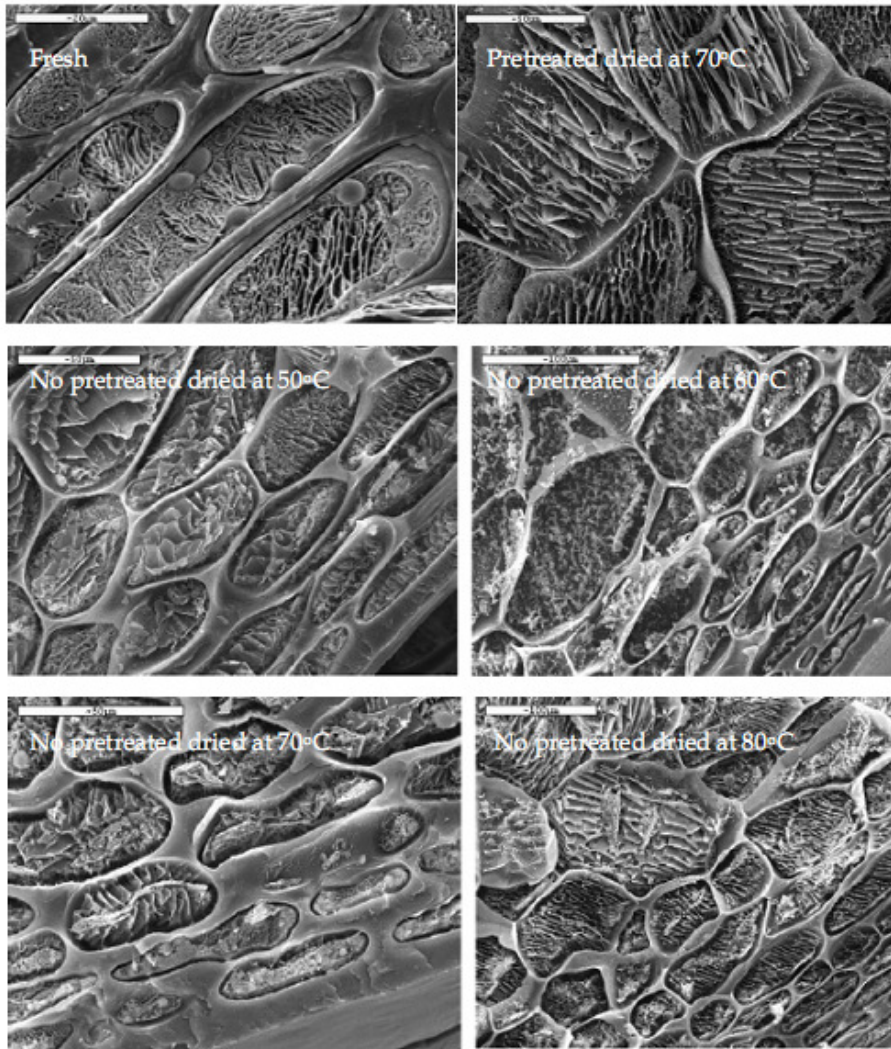


**Figure 1.8.** SEM micrographs of fresh and rehydrated red pepper samples with and without pretreatment dried at different temperatures (Vega-Gálvez *et al.*, 2008)

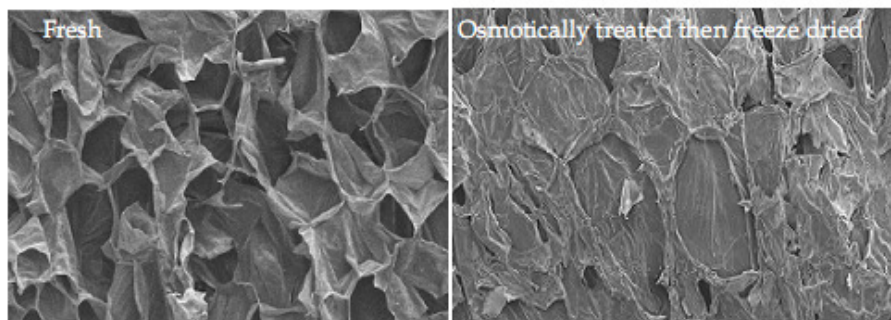


**Figure 1.9.** Scanning electron micrograph of fresh and dried apple (Fuji) (Deng & Zhao, 2008 a and b)

### 1.3 Finite Element Modeling (FEM)

Numerical modeling is an efficient and powerful tool for simulation of real systems. For simple cases, differential equations can be solved analytically. However, under complex conditions, it becomes difficult, in some cases impossible to solve a model by analytical methods.

Numerical methods can give information for a broad range of conditions within a short time whereas traditional experiments give results under specific conditions, and but a number of experiments should be done in order to make a generalization, which is inconvenient due to cost and time limitations. However, the experimental approach is inevitable for validating the models. Once proved experimentally, the model can be used for varying conditions.

Of these numerical methods, finite difference, finite element, finite volume and mesh free methods are widely used. Since the invention of the finite element method (FEM) in the 1950s, FEM has become the most popular and widely used method in engineering computations. FEM divides the matrix into discrete elements, called **discretization**. The network of these individual elements is called **mesh**. Sample discretizations for one, two and three dimensional systems are shown in Figure 1.10 - 1.12. The interpolation functions are then built upon the mesh, which ensures the compatibility of the interpolation (Li & Liu, 2002).

The advantages and disadvantages of FEM over FDM (Finite Difference Method) are summarized by Puri & Anantheswaran (1993) and Wang & Sun (2003) as below:

Advantages:

1. Spatial variation of material properties can be handled easier.
2. Irregular shapes can be modeled with greater accuracy.
3. The method gives better agreement to non-linear problems.
4. Element sizes can be easily varied.
5. Spatial interpolation is much more meaningful.
6. Mixed-boundary-value problems are easier to handle.

Disadvantages:

1. The element equations are usually much more complex compared to the grid-point equations of the FDM.
2. The method can take longer CPU time and larger memory storage space, as compared to FDM since it is numerically more intensive.

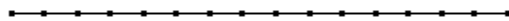


**Figure 1.10.** Finite element schemes for one-dimensional problems

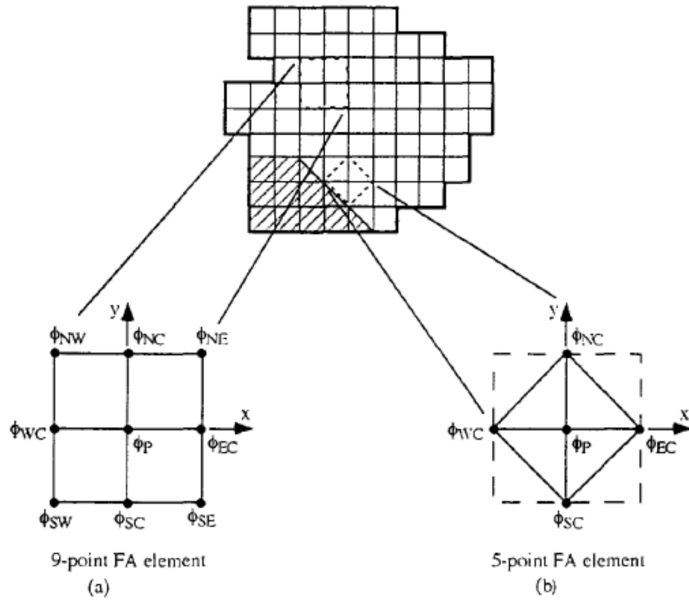


**Figure 1.11.** Finite element schemes for two-dimensional problems. (a) Nine-point finite element. (b) Five-point finite element. (Lin *et al.*, 1997)

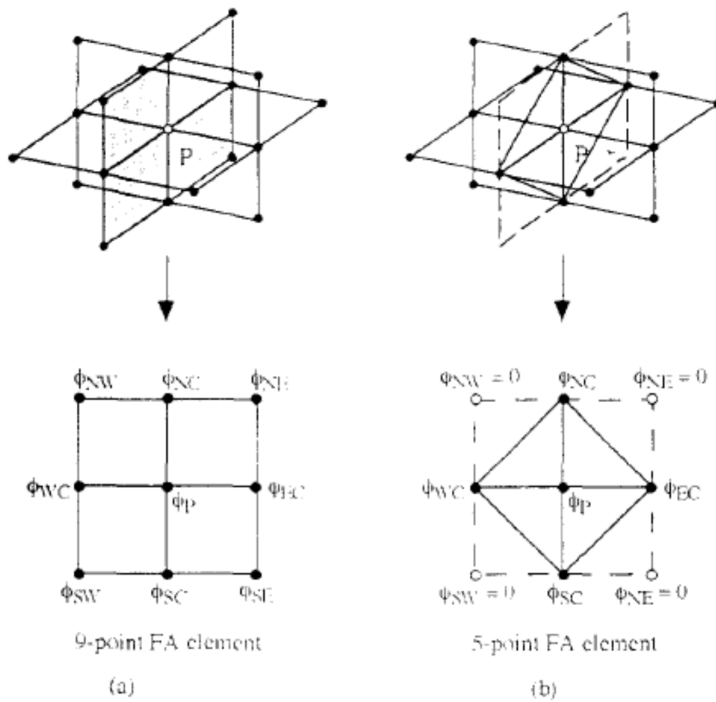


**Figure 1.12.** Finite element scheme for three-dimensional problems. (a) Nine-point finite element. (b) Five-point finite element. (Lin *et al.*, 1997)

FEM can be used in electromagnetics, nanotechnology, civil engineering (stress-strain, deformation calculation etc.), tissue engineering, biomechanics, orthopedics, simulation of total heart function, surgery, acoustic scattering, electrostatics of materials, the areas of which are hard to represent and solve by analytical methods.

Preliminary steps of finite element formulation are given below for solution of the time dependent differential equation below;

$$\frac{\partial u}{\partial t} = \frac{\partial^2 u}{\partial x^2} \quad u \text{ is a dependent variable such as temperature or concentration.}$$

Approximate solution is defined as;

$$U(t, x) = \sum \phi_i(x) U_i(t)$$

$$\frac{\partial U}{\partial t} = \sum \phi_i \frac{\partial U_i}{\partial t} \quad \text{and} \quad \frac{\partial U}{\partial x} = \sum \frac{d\phi_i}{dx} U_i$$

$\phi$  is the base function defined according to dimensions of domain and element type like rectangular, triangular etc., i and j represents nodes in an element;

$$\int_0^1 \left( \frac{\partial u}{\partial t} - \frac{\partial^2 u}{\partial x^2} \right) \phi_j dx = 0 \quad \text{apply integration by parts for } \frac{\partial^2 u}{\partial x^2} \phi_j$$

$$\int_0^1 \frac{\partial u}{\partial t} \phi_j dx - \frac{\partial u}{\partial x} \phi_j \Big|_0^1 + \int_0^1 \frac{\partial u}{\partial x} \frac{d\phi_j}{dx} dx = 0$$

$$\left[ \sum \int_0^1 \phi_i \phi_j dx \right] \frac{\partial U_i}{\partial t} - \frac{\partial U}{\partial x} \phi_j \Big|_0^1 + \left[ \sum \int_0^1 \frac{d\phi_i}{dx} \frac{d\phi_j}{dx} dx \right] U_i = 0$$

$$\int_0^1 \begin{bmatrix} \phi_1 \phi_1 & \phi_2 \phi_1 & \dots \\ \phi_2 \phi_1 & \phi_2 \phi_2 & \dots \\ \vdots & \vdots & \dots \\ \phi_n \phi_1 & \phi_2 \phi_{n+1} & \dots \end{bmatrix} dx \begin{bmatrix} \dot{U}_1 \\ \dot{U}_2 \\ \dots \\ \dot{U}_n \end{bmatrix} + \int_0^1 \begin{bmatrix} \phi_{1,x} \phi_{1,x} & \phi_{2,x} \phi_{1,x} & \dots \\ \phi_{2,x} \phi_{1,x} & \phi_{2,x} \phi_{2,x} & \dots \\ \vdots & \vdots & \dots \\ \phi_{n,x} \phi_{1,x} & \phi_{2,x} \phi_{n+1,x} & \dots \end{bmatrix} dx \begin{bmatrix} U_1 \\ U_2 \\ \dots \\ U_n \end{bmatrix}$$

$$= \frac{\partial U}{\partial x}(1) \begin{bmatrix} \phi_1(1) \\ \phi_2(1) \\ \dots \\ \phi_n(1) \end{bmatrix} - \frac{\partial U}{\partial x}(0) \begin{bmatrix} \phi_1(0) \\ \phi_2(0) \\ \dots \\ \phi_n(0) \end{bmatrix}$$

$$\dot{U}_1 \rightarrow \frac{\partial U_1}{\partial t} \quad \phi_{1,x} \rightarrow \frac{d\phi_1}{dx} \quad n \text{ is the number of nodes in mesh.}$$

Then boundary conditions applied and Crank-Nicolson approximation can be used for solution.

According to type of material, variables, processes and what is desired to model (temperature, moisture distribution, strain-stress...etc), proper modeling system should be selected. In many food systems, FEM forms satisfactory models in comparison to the experimental data if there is no formation of considerable discontinuity through the domain, which is not desired in most of the cases.

### 1.3.1 Applications in Food Processing

Modeling provides information to describe, analyze and optimize the process while decreasing the requirement for experimentation for every changing parameter. Among the numerical methods, the finite element method (FEM) is an efficient tool especially for irregular geometries, complex boundary conditions and heterogeneous materials, which are difficult to solve analytically. FEM enables theoretical prediction of transient food temperature, moisture, internal chamber pressure in vacuum cooling, effect of acoustic properties on ultrasound process, release of latent heat, sudden changes in thermal conductivity during freezing, behavior of microwaved food, potency for crack formation during noodle production, migration of additives from food package and others.

FEM is useful for estimating the thermal behavior of foods under complex conditions such as variation in initial temperature, non-linear and anisotropic thermal & physical properties, irregular-shaped bodies and time dependent boundary conditions (Puri & Anantheswaran, 1993; Wang & Sun, 2003). Summary of FEM studies are given in Table 1.3.

**Table 1.3.** Some studies using of the Finite-Element Method in Food-Processing (Puri & Anantheswaran, 1993)

Processes	Food	Model	Time dep.*	References
Drying	Corn kernels	2-D Heat	✓	Gustafson & Segerlind, 1977
	Bulk Barley	3-D Heat	✓	Alagasundaram <i>et al.</i> , 1990
	Soybean kernels	1-D Heat & Mass	✓	Upadhyaya <i>et al.</i> , 1989
Drying and thermal stress	Soybean & barley kernels	Axi Heat, Mass and Elasticity	✓	Haghighi <i>et al.</i> , 1988a, b, 1990)
Moisture transfer in mixtures	Raisin, peanuts, almonds, banana	2-D Mass	✓	Hong <i>et al.</i> , 1986
Dehulling	Black-eye peas	Axi Mass	✓	Chhinnan & Bakshi (1984)
Cooling	Broccoli	2-D Heat	✓	Jiang <i>et al.</i> , 1987
	Tomato	2-D Heat	✓	Pan & Bhowmik, 1991
Freezing	Lamb&Beef Carcasses	2-D Heat	✓	Comini <i>et al.</i> , 1974
	Ground beef	2-D Heat	✓	Purwadaria & Heldman, 1980
Sterilization	Fluid Foods	2-D Heat		McCarthy & Merson, 1989
Pasteurization	Beer	Axi Heat	✓	Engelman & Sani, 1983
Canning	Mushroom	3-D Heat & Mass	✓	Sastry, 1986
Agartine degradation	Mushroom	3-D Heat & Mass	✓	Sastry <i>et al.</i> , 1985
Microwave heating	Potato	Axi Heat	✓	Chen <i>et al.</i> , 1996
Mechanical Damage Analysis	Fruits and Vegetables	Axi Elasticity and Viscoelasticity	✓	Rumsey & Fridley, 1977
	Fruits	Axi Elasticity		Gustafson <i>et al.</i> , 1977a, b
Cell damage	Biological tissue	Axi Elasticity		Cardenas-Weber <i>et al.</i> , 1989, 1991

### 1.3.1.1. Heating

Heating and cooling are common processes which improve quality and safety and extend shelf life of food products. Modeling of these processes has been studied for a long time. Gustafson *et al.* (1977, 1979) modeled the influence of heating and cooling on stresses in non-homogeneous regions (endosperm and germ) of the corn kernel by finite-element method considering two-dimensional



time-dependent heat-conduction equation. The material properties were assumed to be independent of temperature and moisture content. Shrinkage of kernels due to moisture migration was considered negligible. However, the validation of the model with experimental data was not included.

Momentum, continuity, and energy equations in axisymmetric coordinates were solved using the finite-element software FIDAP to describe pasteurization of beer in a bottle by Engelman (1982). The penalty-function approach for approximate solution of continuity equation was applied in order to reduce the computation time. Nine-node, isoparametric quadrilateral elements were used for the velocity and temperature fields, while linear triangular elements were used for pressure.

Naveh *et al.* (1983a, b, c) studied overshooting of temperature in cans and jars when the steam-off condition prevailed and estimated the sterility of cream style corn in a jar and meat. Two-dimensional transient heat-conduction equation was solved considering axisymmetric coordinates and constant temperature and convective type boundary conditions using linear and quadratic rectangular and triangular elements. This model provided heating for different size of jars and effectiveness of sterilization process.

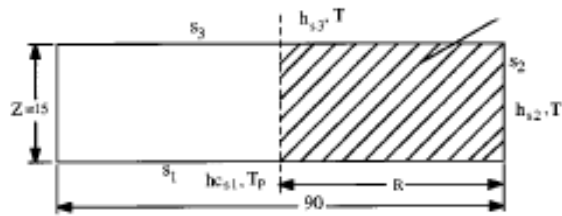
Temperature distribution of model foods in axisymmetric coordinates during microwave heating was determined by Lin *et al.* (1989) solving the transient heat-conduction equation. Microwave-heat absorption was included in the model as a heat-source term. Rectangular and cylindrical shaped model foods were used. In general, the model was favorable with experimental data but the predicted temperatures at the center in the cylindrical shaped model foods were not compatible with experimental values. This was suggested due to the incomplete description of microwave propagation within cylindrical shaped foods. The results showed that thermal diffusivity, dielectric properties, power output of microwave significantly affected temperature distribution within the food.

Chen *et al.* (1990) solved axisymmetric heat-conduction equation to describe heating characteristics of potato in cylindrical shape using Lambert's law. Heat-generation equation was added to model to describe microwave interaction. The results of FEM were in good agreement with experimental values.

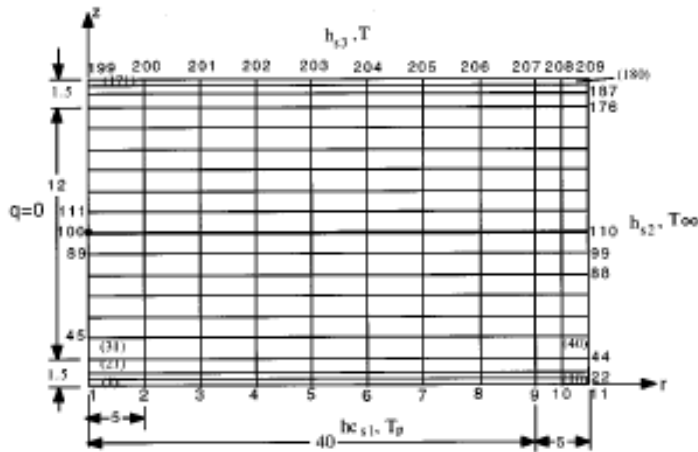
Kumar *et al.* (1990) have used FEM to find temperature distribution and cold-spot within the upright metal can heated in a steam retort. In order to refine mesh, trial-and-error technique was used. Steady state voltage distribution and unsteady state temperature distribution within particulate food during ohmic heating was also modeled by FEM, using linear triangular elements (DeAlwis and Fryer, 1990).

Heat transfer in meat patties during single-sided pan-frying without and with turn-over was modeled using FEM considering moisture loss rate, cooking time, and crust formation as a functions of pan temperature and/or turn-over frequency and time (Ikediala *et al.*, 1996). The heat of reaction due to denaturation and fat melting and shrinkage/swelling of meat patty were neglected. A two-dimensional axisymmetric transient heat conduction equation involving the heat removed due to moisture loss was solved using convective boundary conditions. The symmetrical half portion of the meat patty (Figure 1.13a) was discretized into quadrilateral elements (Figure 1.13b). Crank-Nicholson scheme was applied for the simulations time stepping. Good agreement was obtained between predicted and experimental temperature values.

Geedipalli *et al.* (2007) developed a model considering coupled Maxwell's equations for electromagnetics and heat transfer equation during microwave heating of food rotating on turntable. Transient simulation of the heating process was carried out using finite element based computational software considering the rotation of the turntable by repeating the computations for discrete angular positions of the turntable. This resulted in a 37–43% increase in uniformity by using turntable for the duration of 30 s. However, it was observed that the temperature uniformity across different layers of the food was not improved by turntable. Researchers suggested that if a system which moves the food from top to bottom (and vice versa) could be built, it could potentially increase the uniformity.



(a) Schematic View of Meat Patty



(b) Meat Patty Discretization: 209 nodes x (180) elements  
● Geometric center

**Figure 1.13.** Representation of mesh involving quadrilateral elements augmented at the bottom and up surfaces: (a) cross section of a meat patty with (b) a symmetric half discretized into 180 elements (in parenthesis) and 209 nodes. All dimensions in mm (Ikediala *et al.*, 1996)

Radio-frequency (RF) heating is arisen from interaction between the electric field produced by the electrodes of a capacitor and the dipoles and ionic-charges present within a food product. Marra and co workers (2007) analyzed formation of non-uniform temperature distribution during radio-frequency heating of cylindrical meat batters, by modeling of both electromagnetic and thermal phenomena with FEM. Meat batters were selected as a model food, with dielectric and physical property data available as a function of temperature. Quasistatic electromagnetic equation coupled with the heat transfer by conduction, plus a generation term as a function of local E-field were solved using Gauss law with 256,150 domain elements (tetrahedrons). On the external surfaces of the beaker, convective heat transfer was considered as a boundary condition. FEM predictions for electrical field modulus and dielectric loss factor, which were agreed with experimental are given in Figure 1.14.

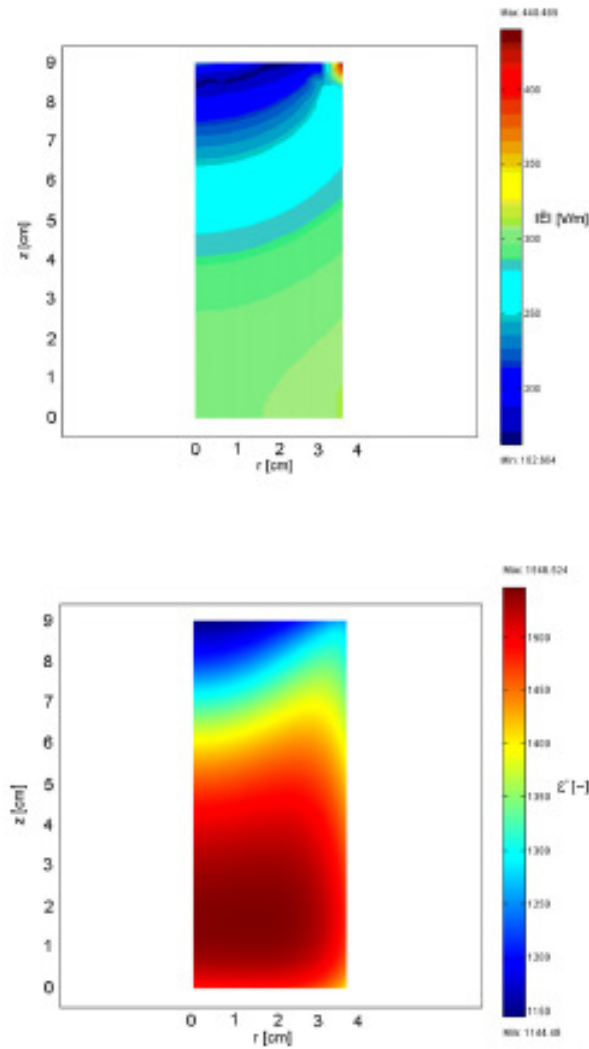


**Figure 1.14.** Example of output results, referred to numerical simulation of 900 s of heating of luncheon roll emulsion in RF oven at 200 W. Distribution of the E-field modulus within the sample (above figure), Distribution of the relative dielectric loss factor, within the sample (below figure) (Marra *et al.*, 2007)

### 1.3.1.2. Cooling & Freezing

A time-dependent axisymmetric heat-conduction equation was solved by FEM to model the stalk performance (most perishable part of broccoli) during pre-cooling of broccoli using quadrilateral elements (Polivka and Wilson, 1976). Respiration effect was included using a heat-generation term. The results showed that FEM adequately simulated the precooling process.

Simulation of temperature of apples during cooling was studied by solving one dimensional time dependent heat transfer equations with FEM using two node linear elements (Misra and Young, 1979). The main assumptions were constant drying conditions (relative humidity and temperature) and no respiration and moisture exchange between apple and ambient air. The model results were in good agreement with analytical results.

Hayakawa and Succar (1982) modelled one dimensional heat transfer and moisture loss in spherical-shaped fresh produce by FEM using Galerkin's technique. They solved heat-conduction equation including heat generation due to respiration of produce. Variable density & thermal conductivity as a function of temperature and convective boundary conditions were used. Integral of the evaporation at the surface was included to model as overall moisture loss.

Potluri (1985) studied cooling of loin carcasses and estimated surface-heat-transfer coefficients by 2-D time dependent diffusion equation of FEM and linear triangular elements. The time-dependent equations were solved using the Crank-Nicolson method. It was assumed that heat transfer was mainly by conduction. The evaporation term was introduced using modified heat-transfer coefficient. Important results obtained were that FEM could be used to predict carcass temperature and heat-transfer coefficient, which enable control of ambient temperature during cooling using simple inputs as weight and fat content of carcass.

Two-dimensional time dependent heat conduction equation with generation (respiration) was solved by ANSYS software using FEM to determine temperature distribution of tomato (Pan & Bhowmik, 1991). Good agreement was observed between predicted and experimental results of temperature and moisture loss in tomatoes. Tri Ho *et al.* (2007) used FEM to describe simultaneous O<sub>2</sub> and CO<sub>2</sub> gas transport as well as respiration in the tissue to determine O<sub>2</sub> and CO<sub>2</sub> diffusivities in pear fruit tissue.

Two dimensional temperature distribution during freezing of lamb and beef carcasses in air-blast tunnel was modeled by FEM, using variable thermal conductivity for dry and liquid parts in elliptical and trapezoidal geometries (Purwadaria and Heldman; 1980, 1982). The heat conduction equation during freezing and thawing was solved by Galerkin method in FEM formulation considering temperature dependent physical properties of material (Abdalla and Singh, 1985). Three-dimensional heat transfer equations around caverns (openings excavated in tuff at the Cappadocia Region of Turkey) for various geometries were solved by FEM in order to find their potential use for frozen food storage (Unver & Agan, 2003). It was found that energy loss due to heat transfer was three times lower in favor of underground storage cavern opened in tuff both experimentally and numerically.

### 1.3.1.3. Other Processes

Besides heating and cooling, FEM was also used to describe other processes like migration of some chemicals, mechanical damage on food products, ultrasound etc. Degradation of agaratine in canned mushrooms was modeled by solving three dimensional transient-heat-conduction and mass-diffusion equations in an irregular domain considering time-dependent convective-type boundary conditions (Sastry *et al.*, 1985). Kinetic data on the degradation of agaratine as a function of temperature was also incorporated to FEM. The model satisfactorily represented the experimental data.

Roduit *et al.* (2005) developed a diffusion model to simulate migration of additives from multilayer polymeric package during its contact with food under isothermal conditions to investigate applicability of FEM in order to avoid costly time-consuming migration tests. The packaging layers were based on five different, predefined confinement geometries (rectangular, cylindrical, spherical, truncated cone, spherical segment) describing the properties and dimensions in which food was wrapped. It was found that the modeling programme worked properly only if appropriate data describing the kinetics and thermodynamics of the migrant was considered. While diffusion coefficients in polymers were available in literature, partition coefficients of migrants between different polymers were hardly accessible, which limits the use of models.

Finite element modeling has also the potential to describe complex mechanical behavior of many food products. Liu and Scanlon, (2003) studied the mechanical change of bread crumb under compression and indentation. The crumb was discretized into quadrilateral axisymmetric continuum elements of uniform size. It was found that overall stress-strain curves of low-density bread crumb under compression and indentation were well estimated by FEM. However, the load-

displacement curves generated from spherical indenters were under-predicted, while those from cylindrical indentation were well predicted.

Mechanical damage to fruits and vegetables usually occurs during harvesting, handling, and processing. This process is another topic handled by FEM. For example, stresses during the mechanical handling of melons by robots were estimated by FEM in axisymmetric, three-dimensional coordinates using quadrilateral elements (Cardenas-Weber *et al.*, 1991). The predicted and measured data were reasonably agreed. The model showed that the loads induced by grippers had low potential to cause bruising of melons. Fruit bruising in longitudinal and transverse directions by parallel plates was also analyzed by nonlinear finite element analysis in another study (Sadriya *et al.*, 2008)

A two dimensional FEM was developed to investigate the influence of cell wall material and thickness, transducer configuration, rotation of a metallic stirrer blade and heat transfer fluid on the cell acoustic response during ultrasound process (Gachagan *et al.*, 2004). Experimentally measured pressure fields were found in good correlation with the predicted fields.

### 1.3.2 FEM in Drying

Modeling of a drying system is essential for improving process control and product quality. A proper model provides information on the shortest time of drying, optimal dimensions of the dryer, etc. It also minimizes the cost of expensive pilot scale tests while satisfactorily indicating the characteristics and safety of dried products.

For a drying process, with a small Biot number, a uniform temperature profile in foods can be assumed in simulation and the solution of a single mass transfer equation can thus be adequate to describe the process while for a drying process with a large Biot number, a coupled heat and mass transfer should be taken into account in the model. For temperature, moisture and pressure distribution during drying of a composite food system, it was shown that coupled transfer equations give good agreement with experimental data while uncoupled model produced drastically different values. (Wu & Irudayaraj, 1996, Wang & Sun, 2003).

Marchant (1976) modeled grain drying using forced air convection by FEM. Information of velocity and pressure distribution was found important for an optimal design in addition to the coupled heat and mass transfer. The variational technique was used to solve pressure drop in a two dimensional region. Quadratic triangular elements were used in a fully developed flow. Although the predicted values by Marchant (1976) had good agreement with other simulated data, the model obtained by considering three dimensional equations were found more accurate (Khompis *et al.*, 1984). The three dimensional model gave opportunity to find the pressure distribution across a plane close to the inlet having significantly higher non-uniformity than the cross-section away from the inlet.

Rumsey and Fortis (1983) simulated the pressure and flow distribution by FEM during drying of walnuts. Quadrilateral elements were used to model two dimensional steady, isotropic air flow. The predicted and experimental results showed good agreement in both high and low air velocity regions. The model was then used to improve uniformity of flow throughout the dryer by simulating different design conditions, such as reducing the angle of the false bottom, increasing static pressure under an expanded metal-screen floor. The uniformity of drying was found to be improved by these considerations.

Syarief *et al.* (1987) used FEM to determine moisture diffusivity of corn kernel as a function of kernel component analysis and moisture content. Moisture migration was assumed to be only by diffusion, not coupled with temperature and in two dimensional region. Quadrilateral elements were used in the model. In order to find the parameters in exponential equation representing diffusion coefficient, the bilinear approximation function for elements was used. The model resulted in different diffusivity values for germ and endosperm of the kernel. The diffusion

coefficient of germ was found 3.6-4.9 times higher than that of endosperms. The FEM was suggested to be an efficient tool in the determination of the diffusivity coefficient.

Air flow distribution within particulate materials during drying of grains in two and three dimensional regions was solved by ANSYS software using FEM with four node isoparametric elements for two dimensional and eight node isoparametric elements in three dimensional simulations (Talbot, 1989). Talbot's results demonstrated the effectiveness of ANSYS and FEM to represent the air flow patterns through porous media.

Alagasundaram *et al.* (1990) predicted temperature distribution of grains in a bin during drying and aeration by using non-linear, non-isotropic finite element formulation. A 3-D transient heat-conduction equation was solved using linear and quadratic hexahedron elements. The predictions by quadratic-elements were found more compatible with measured values than the linear-element predictions.

Thin film dehydration was modeled by Bowser and Wilhem (1995) by FEM. The model simultaneously considered shrinkage and one dimensional heat and mass transfer within thin films dried on a surface with convective boundary conditions. Unsteady state heat and moisture diffusion equations with convective boundary conditions were solved. Physical properties were dependent on temperature. The main difference of this study from previous ones was consideration of shrinkage in the model.

Aversa *et al.* (2007) examined the influence of some of the most important operating variables, namely velocity, humidity and temperature of air on the performance of carrot drying. They tried to increase the accuracy of modeling by the use of FEM. Although there are similar modeling studies present in literature, due to the model formulation this research deserves more attention. Bidimensional heat and moisture transfer equations considering the variable properties for both air and food as a function of local values of temperature and moisture content were solved. Later, the same research group improved their model by including air flow in their formulations (Curcio *et al.*, 2008). Simultaneous transfer of momentum, heat and mass occurring in a convective drier, where hot dry air flows under turbulent conditions around carrot slab, was studied. The mass, heat and momentum transfer equations considered in the study are shown below in equations (1.18-1.10). Two dimensional cylindrical coordinates were chosen and angular dimension were neglected. Half of the sample was considered due to symmetry (Figure. 1.15). Since physical and transport properties of both air and food are expressed in terms of the local values of temperature and/or moisture content, the system was represented by unsteady, non-linear partial differential equations (PDE) which can only be solved by means of a numerical method. Convection within the food sample was neglected, assuming low internal evaporation. The diffusion of vapor within the dehydrated material towards the food surface, was also neglected since this mechanism was suggested to be the only significant for highly porous media, whereas it can be neglected in the case of vegetables since typical void fraction values are less than 0.3 (May and Perre, 2002). The mass transfer in the product, therefore, was assumed to be only by diffusion; and heat transfer, only by conduction. Shrinkage effects were assumed to be negligible when it was less than 20%.

$$\frac{\partial C}{\partial t} + \nabla \cdot (-D_{eff} \nabla C) = 0 \quad (1.8)$$

$$\frac{\rho_s c_{ps} \partial T}{\partial t} - \nabla \cdot (-k_{eff} \nabla T) = 0 \quad (1.9)$$

The unsteady-state momentum balance was coupled to the continuity equation;

$$\frac{\rho_a \partial \varepsilon}{\partial t} + \rho_a \mathbf{u} \cdot \nabla \varepsilon = \nabla \cdot \left[ \left( \eta_a + \frac{\eta_t}{\sigma_\varepsilon} \right) (\nabla \varepsilon) \right] + \left( \frac{c_{1\varepsilon} \varepsilon}{k} \right) \left[ \eta_t P(u) - \left( \frac{2\rho_a k}{3} \right) (\nabla \cdot \mathbf{u}) \right] - \frac{c_{2\varepsilon} \rho_a \varepsilon^2}{k} \quad (1.10)$$

where  $\rho_a$  is the air density and  $\eta_a$  is its viscosity, both expressed in terms of the local values of temperature and of water content;  $P$  is the pressure within the drying chamber;  $\mathbf{u}$  is the velocity vector;  $c_{1\varepsilon}$ ,  $\sigma_\varepsilon$ ,  $c_{2\varepsilon}$  and  $c_{3\varepsilon}$  are constants whose value depends on the  $k$ - $\varepsilon$  turbulence model used (Curcio *et al.*, 2008, Verboven *et al.*, 2000). Nonlinear PDEs were solved by COMSOL

Multiphysics 3.3. Lagrange FE of order 2 was selected for all variables except from pressure for which an order of one was selected. Newton's method was used for nonlinear equations. It was found that air characteristics affected drying performance only when external resistance to mass transfer was the rate controlling step.

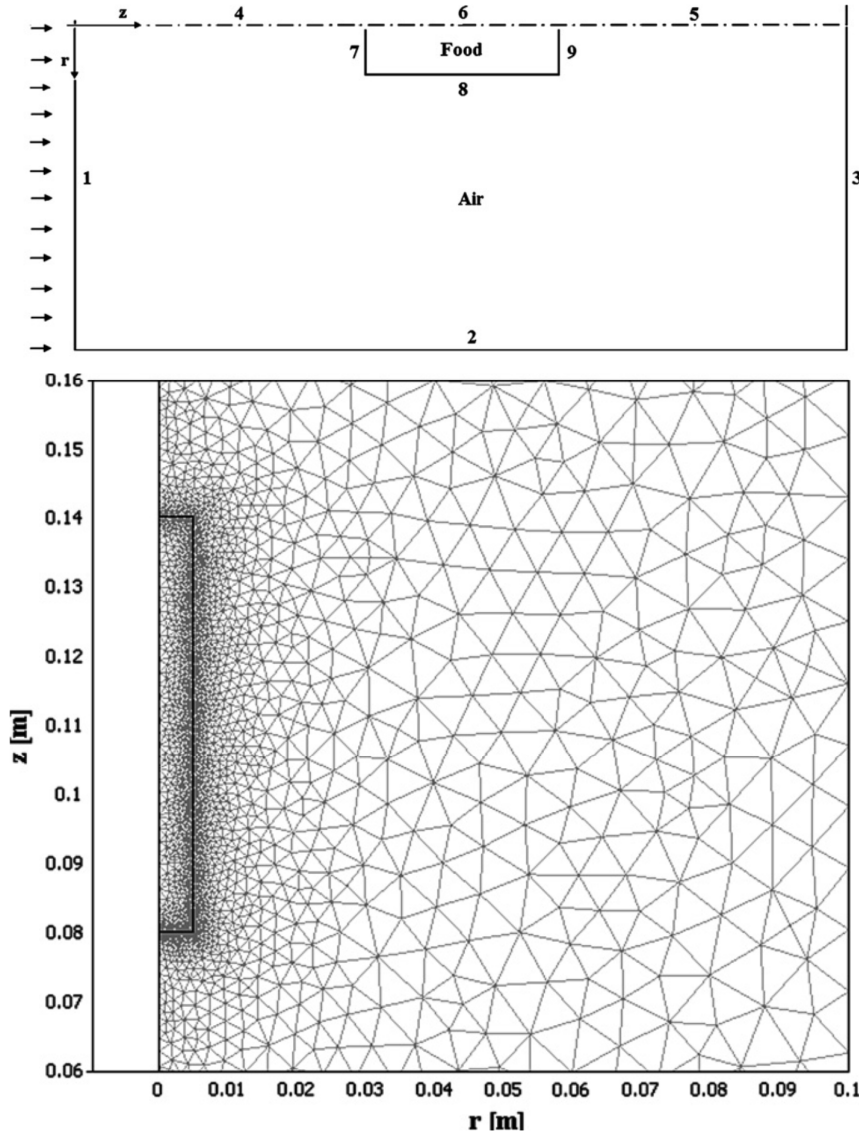


**Figure 1.15.** Discretization of food and air domains into triangular finite elements (detail of the mesh) (Curcio *et al.*, 2008)

The effect of air temperature on the performance of the drying process applied to fresh-cut vegetable slices (carrot) was also studied by De Bonis and Ruocco (2008). Two dimensional transient coupled heat and moisture transfer equations were solved by FEM. Moisture content dependent physical and thermal properties of carrot were taken from the literature (Ruiz-López *et al.*, 2004) as in the study of Aversa *et al.* (2007). Unlike studies of Aversa *et al.* (2007) and Curcio *et al.* (2008), laminar flow was prevailed during drying and the evaporation term was added to governing partial differential equations. For the food sample, the governing equations are presented

below (1.11-1.13). Discretization was similar to study of Curcio *et al.* (2008). Due to addition of evaporation term to the equation, the boundary conditions became different from Curcio *et al.* (2008).

$$\begin{array}{ll} \text{Continuity liquid water;} & \text{Continuity water vapor;} \\ \frac{\partial C_l}{\partial t} + \nabla \cdot (-D_{ls} \nabla C_l) = -K C_l & \frac{\partial C_v}{\partial t} + \nabla \cdot (-D_{vs} \nabla C_v) = K C_v \end{array} \quad (1.11) \quad (1.12)$$

$$\text{Energy;} \\ \rho_s C_p \frac{\partial T}{\partial t} - \nabla \cdot (-k_s \nabla T) = -q \quad (1.13)$$

$$\begin{array}{ll} \text{Cooling rate due to evaporation;} & \\ q = \Delta h_{vap} M_l K C_l & \end{array} \quad (1.14)$$

where K is rate of production of water vapor mass (1/s) found by minimization of error between experimental and predicted values for each experimental condition. v, l and s represent vapor, liquid and substrate.

All of these model studies show that a proper construction of partial differential equation, initial and boundary conditions, dimension setting, use of variable or constant property of material selection, element and mesh definition are important for robustness of the constructed model.

#### 1.4 Aim of the Study

Drying is a common preservation method for foods used since ancient times. With the help of drying models, it is possible to;

- ✓ find optimal set of operating conditions to improve final quality and stability of foods which can be adversely affected by high values of moisture leading to microbial spoilage and enzymatic reactions,
- ✓ analyze the behavior of industrial dryers over a wide range of process fluid dynamics conditions, material types and dimensions, within in a short time.

It is important to predict the dehydration rate, temperature distribution in the food materials during drying since both affects quality and safety of food (Farid and Kizilel, 2009). Studies showed that temperature differences though the food is significant in steam drying (Li *et al.*, 1998), freeze drying (Du *et al.*, 1997; Carn and King, 1997), air drying (Arzan and Morgan, 1967) and frying of potato chips (Farid and Chen, 1998),

Most of the unprocessed and processed food materials have anisotropic nature. Their properties vary with direction due to their nonuniform structure like in porous and fibrous foods. Drying characteristics and final textural properties of food materials are known to be changed with respect to direction of food material to air flow due to this anisotropic nature. However, generally it is difficult to consider anisotropic nature in model systems due to nonexistence of empirical equations defining anisotropic physical or thermal properties. Even if such equations are obtained; it is difficult to solve the model equations analytically since inclusion of anisotropic properties makes the model much more complicated. Thus, a more common approach is to use effective properties of materials in the model studies.

In this respect, to fulfill the gap in the literature, the aims of this research are as follows;

- to observe the effect of drying parameters (temperature and flow rate of air) and structure (fiber direction, anisotropic/isotropic nature) on temperature distribution and moisture content of meat slabs prepared from lean meat in three different fiber directions and minced meat prepared from the same lean meat as models for anisotropic and isotropic food samples, respectively. The main drying characteristics considered in the study were magnitude of temperature difference,



rate of drying and temperature change, drying time, diffusivity values and shrinkage. The results serving this aim are given in Chapter 3;

- to model both temperature and moisture distribution in the same meat samples using FEM considering anisotropic variable thermal conductivity definitions as a function of temperature, of which values were taken from literature and to observe effect of drying parameters (temperature and velocity of air) and structure (fiber direction, anisotropic/isotropic nature) on predicted temperature distribution and predicted moisture content of meat samples, and finally to make comparison with the experimental data in order to validate the model. The results serving this aim are given in Chapter 4;
- to refine the model considering both anisotropic variable thermal conductivity definitions taken from the literature and anisotropic variable diffusion coefficient values as a function of moisture content and temperature obtained from the experimental results, and finally to make comparison with the experimental data in order to find adequacy of FEM to describe drying of anisotropic and isotropic food samples. The results serving this aim are given in Chapter 5.



## CHAPTER 2

### MATERIAL AND METHODS

#### 2.1. Materials

Low fat lean meat with orderly fibrous structure from round of beef was used as a model for anisotropic food. It was cut along and against fibers with use of ultrasonic knife (Sonicblade JK-01, PRC). According to flow, three configurations were used in experiments (Figure 2.1). Double minced meat prepared from the same lean meat was used as a model for isotropic sample.

#### 2.2. Parameters

Independent and dependent parameters used in experiments are summarized in Table 2.1.

**Table 2.1.** Parameters used in drying experiments

Independent Parameters*	Dependent Parameters
Air temperature	Temperature of sample with respect to time and location
Air flow rate	Moisture content of sample with respect to time
Fiber direction to air flow	Shrinkage
Time of drying	

\*Humidity of air was not used as a parameter. It was continuously monitored to control whether there was any drastic change which might affect the experimental results.

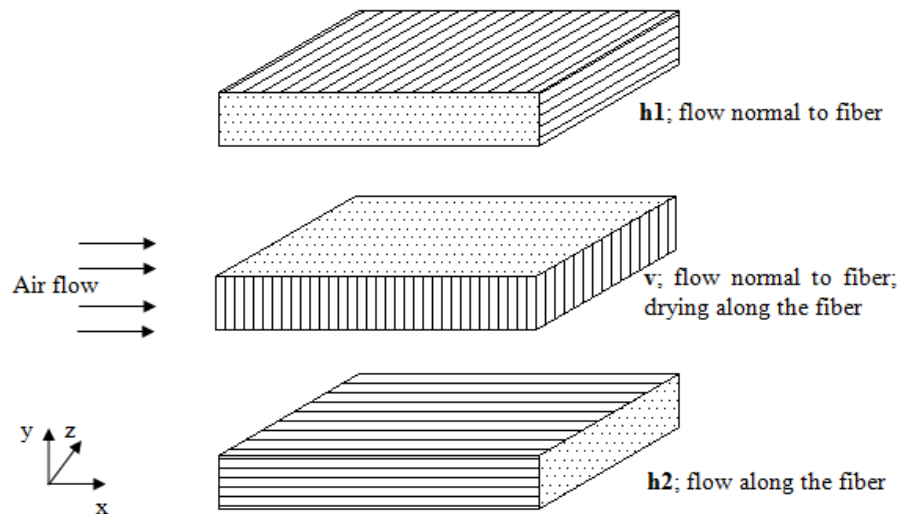


**Figure 2.1.** Fiber configurations in lean meat samples

## 2.3. Experimental Methods

### 2.3.1. Experimental Setup

Samples were dried in a laboratory scale tray dryer (1.5 X 0.28 X 0.28 m<sup>3</sup>, Armfield Limited, D.27412 England) (Figure 2.2a-b). It consists of an adjustable fan, adjustable electrical heater and sample chamber. Temperature and velocity of air were adjusted by setting knobs of fan and heater. Air flowed 1.5 m to reach sample holder unit. Hygrometer was placed just before the sampling chamber to record relative humidity and temperature of air. After setting the temperature and velocity, it was waited for temperature of inlet air to reach a constant value before placing the sample into the dryer. The approximate meaning of each knob of dryer control unit is given in Table 2.2.

**Table 2.2.** Values of control unit switches

Knobs*	Temperature (°C)				
	2	4	6	8	10
<b>Velocity</b>					
2 (0.3 m/s)	38	48	58	68	78
4 (0.7 m/s)	38	45	52	58	65
6 (1.0 m/s)	37	44	50	55	60
8 (1.3 m/s)	38	42	46	50	54
10 (1.7 m/s)	35	38	42	45	48

\*According to inlet temperature of air, indicated temperature values might change by  $\pm 5^{\circ}\text{C}$ .



**Figure 2.2a.** Configuration of dryer

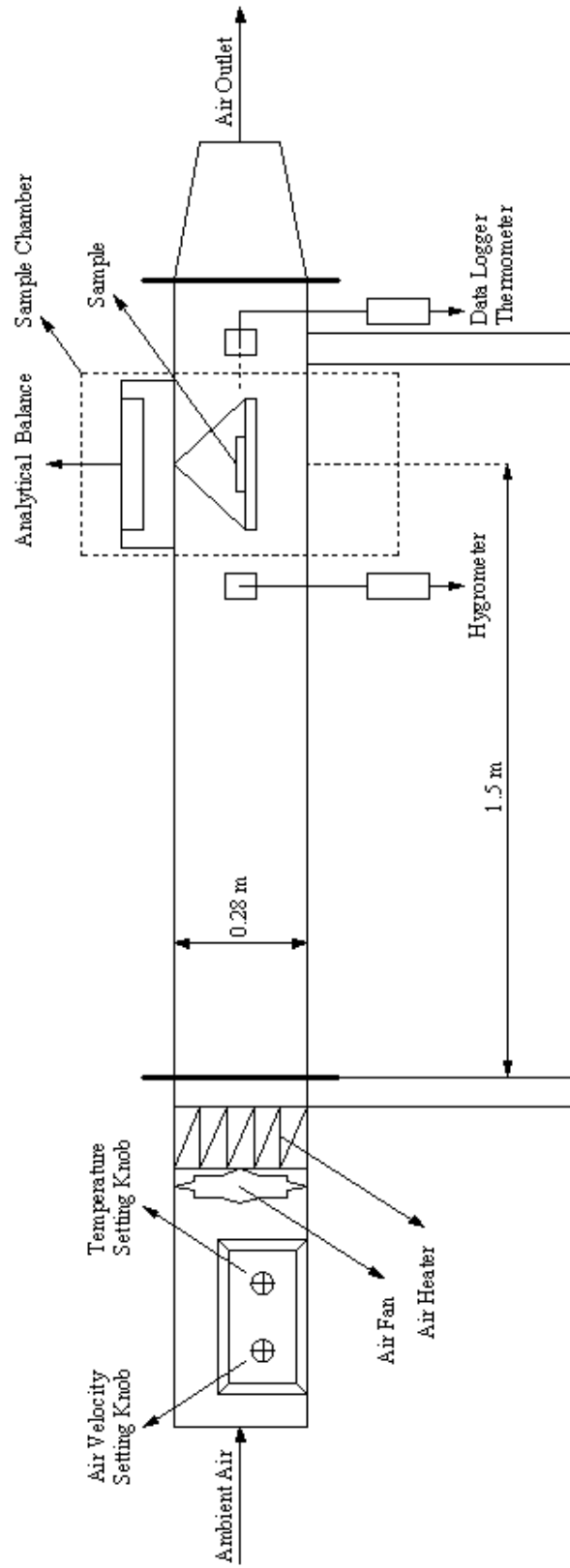


**Figure 2.2b.** Laboratory scale tray dryer

### 2.3.2. Sample Preparation

Lean meat samples were prepared by cutting the bulk lean meat along or across the fibers according to Figure 2.1 in dimensions of approximately  $6 \times 3 \times 1 \pm 0.2 \text{ cm}^3$  (length x width x thickness). For double minced meat, a mold was prepared with dimensions of 6-3-1 cm (length x width x thickness). Lean and minced meat samples were placed on a foam preventing heat and mass transfer at the bottom of sample, which was hang up in the sample chamber (Figure 2.2a-b).

### 2.3.3. Temperature Measurement

K-type thermocouples (Omega data logger thermometer/datalogger HH306A, Taiwan) attached to a data logger were used for recording temperature values at 4 different locations in the meat samples: midpoint,  $2/3$  of length from center in the middle of thickness,  $-2/3$  of length from center on the front surface, center point at the bottom surface (Figure 2.3). During drying, temperatures at those points were automatically recorded once a minute.

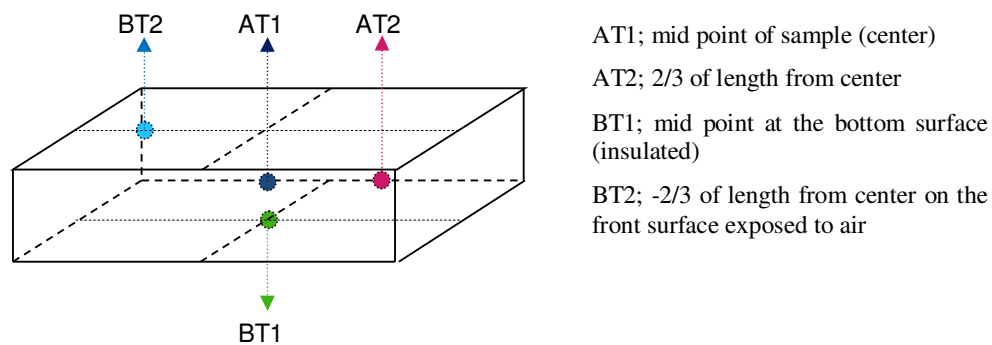


Figure 2.3. Thermocouple locations on sample

### 2.3.4. Moisture Content Measurement

Initial moisture content of samples was measured by overnight incubation of sample at  $105^\circ\text{C}$  in an oven. Weight of samples was recorded every 10 minutes during drying by an analytical balance (Radwag PS 360/C/2, Poland), to which the sample was attached via string (Figure 2.2). Before recording, the dryer was stopped for a very short time to avoid misreading due to oscillation of string and thereafter the weight was recorded. A thin insulation material (foam) was put under the balance in order to prevent transmission of heat from the dryer to the balance and lessen vibration and oscillation of string during drying.

### 2.3.5. Equilibrium Moisture Content Measurement

Equilibrium moisture content was calculated from the data of weight change during drying. First, moisture content based on bone dry solid (g/g bds) was plotted with respect to time. Two models were selected to represent moisture content change with respect to time as Henderson and Pabis (1961) (equation 2.1) and two term approach by Hendersen (1974) (equation 2.2). Exponential decay equations designated below were fitted using non linear regression tools of Sigma plot 2000 for Windows Version 6.00. The value when time goes infinity was taken as equilibrium moisture content ( $X_{eq}$ ). Henderson and Pabis (1961) model was already used for moisture content change by many researchers (Roberts and Tong, 2003; Chen X. D., 2007; Azzouz *et al.*, 2002; Zhang and Litchfield, 1991; Djendoubi *et al.*, 2009). Hendersen (1974) was also used in literature (Sharaf-Eldeen *et al.* 1980, Kaya *et al.* 2010).

$$X = X_{eq} + a'e^{-kt} \quad (2.1)$$

based on Henderson and Pabis (1961) equation below;

$$\frac{X - X_{eq}}{X_i - X_{eq}} = aexp(-kt)$$

$$X = X_{eq} + a'e^{-k_0t} + b'e^{-k_1t} \quad (2.2)$$

based on two term approach by Hendersen (1974) below;

$$\frac{X - X_{eq}}{X_i - X_{eq}} = aexp(-k_0t) + bexp(-k_1t)$$

### 2.3.6. Properties of Air

Velocity and temperature of air in the dryer was kept at desired values, by a control unit on the dryer. The velocity of air was measured by a vane type anemometer (Prova AVM-03, Taiwan). Temperature, % relative humidity and dew point of air was continuously measured and recorded by hygrometer (Comet S3121, Czech Republic) every 5 minutes. The temperature and velocity of inlet air were selected as a range of 30-75°C and 0.4-1.8 m/s (Curcio *et al.*, 2008).

### 2.3.7. Shrinkage measurement

Initial and final surface areas (after 270 minutes drying) were measured by placing sample on millimetric paper. Shrinkage ratio was then found by simple mathematical comparison. In this study, only the areas of meat samples whose surfaces were exposed to air were examined. For this examination, pixarea 1.03 software program was used to calculate the area. (ShareMe, <http://shareme.com/download/pixarea.html>)

## 2.4. Model Construction

During drying, heat is transferred from air to the surface of sample via convection and from surface to interior sides by conduction. Meanwhile, moisture is transported from interior of sample to the surfaces due to driving forces of concentration and vapor pressure difference via capillary flow through fibers or diffusion. When the surfaces of sample reach saturation and wet bulb temperature, water starts to evaporate from sample. To simulate this phenomena, 2D coupled mass and heat transfer in x-y direction represented with nonlinear partial differential equations shown below (2.3-2.5) was used and solved by finite element modeling. Insulated boundary condition at the bottom and convective boundary conditions at other surfaces of the sample were taken into account (Figure 2.4). Two different nonlinear partial differential equations were used for temperature simulation (Equation 2.4-2.5). Model 1 considered evaporation only at surface exposed to air, thus loss of heat due to evaporation was involved in the boundary conditions (Equation 2.6, 2.8, 2.9, 2.10) (Chen *et al.*, 1999; Aversa *et al.*, 2007) while loss of heat due to evaporation was involved in governing differential equation of heat transfer (Equation 2.5, 2.11) in model 2 (Srikiatden and Roberts, 2007).

$$\frac{\partial C}{\partial t} = \nabla \cdot (D_{eff} \cdot \nabla C) \quad (2.3)$$

$$\text{Model 1; } \rho C p \frac{\partial T}{\partial t} = \nabla \cdot (k \cdot \nabla T) \quad (2.4)$$

$$\text{Model 2; } \rho C p \frac{\partial T}{\partial t} = \nabla \cdot (k \cdot \nabla T) - q_v \quad (2.5)$$

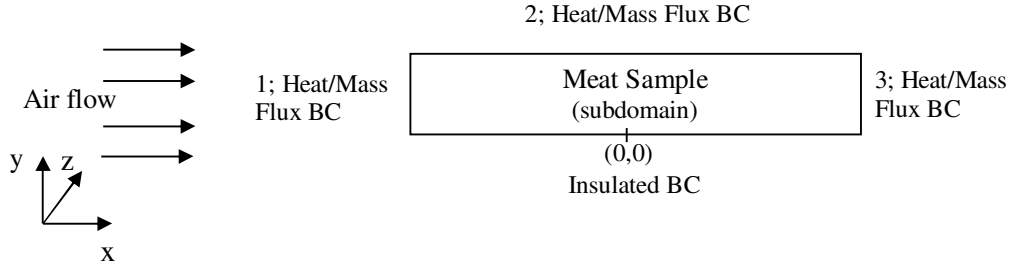


**Figure 2.4.** Illustration of model system. BC; Boundary Condition

**For Model 1:**

**Heat/Mass Flux BC:**  $k\nabla T = h \times (T_{\text{ext}} - T) - q_v$  (2.6)

$$D_{\text{eff}} \times \nabla C = k_c \times (C_{\text{bulk}} - C) \quad (2.7)$$

$$q_v = -D_{\text{eff}} \times \frac{\partial C}{\partial y} \times \lambda \quad (\text{surface 2}) \quad (2.8)$$

$$q_v = -D_{\text{eff}} \times \frac{\partial C}{\partial x} \times \lambda \quad (\text{surface 3}) \quad (2.9)$$

$$q_v = D_{\text{eff}} \times \frac{\partial C}{\partial x} \times \lambda \quad (\text{surface 1}) \quad (2.10)$$

$\lambda$ : latent heat of evaporation

**For Model 2:**

At the subdomain,  $q_v$  is identified as;

$$q_v = \lambda * \frac{\partial C}{\partial t} \quad \text{if temperature exceeds or equal wet bulb temperature.} \quad (2.11)$$

**Heat/Mass Flux BC:**  $k\nabla T = h \times (T_{\text{ext}} - T)$  (2.12)

$$D_{\text{eff}} \times \nabla C = k_c \times (C_{\text{bulk}} - C) \quad (2.13)$$

**For both models,**

**Insulated BC:**  $k\nabla T = 0$  (2.14)

$$D_{\text{eff}} \times \nabla C = 0 \quad (2.15)$$

**Assumptions:**

- Heat transfer in the product is by conduction;
- Mass transfer in the product is by diffusion;
- Change in z direction is neglected;
- Fat transport is negligible;
- The crust is as thin as that it does not hinder transport of water to the surface;
- No internal heat generation and no chemical reaction;
- Dissolved matter lost with water can be neglected in material and energy balance;
- The initial distribution of water content and temperature is uniform;
- Shrinkage during drying (less than 20 %) is negligible;
- A bidimensional rectangular domain (~6 cm of length with a thickness ranging from 1.0 to 1.2 cm) was considered;
- Air is supplied continuously to the product, and its flow is parallel to its surfaces; (Aversa *et al.*, 2007).

Variable properties of the samples with respect to dependent variables (temperature or concentration) were used. For density, an average value 1070 kg/m<sup>3</sup> was used for lean meat; 950 kg/m<sup>3</sup> was used for minced meat (Perez & Calvelo *et al.*, 1984; Proud and Lund, 1983). Perez and Calvelo (1984) showed that density did not change drastically with a moisture content (wet base) range of 0.40-0.75.



Heat capacity (Cp) was calculated according to empirical equation below (2.16) (Choi and Okos, 1986). The composition of meat samples was taken from the study of Pham and Willix (1989) and used on a wet basis;

$$Cp = 4.18 \times X_w + 1.711 \times X_{pro} + 1.928 \times X_{fat} + 1.547 \times X_{CHO} + 0.908 \times X_{ash} \quad (2.16)$$

All fractions are on wet basis (Choi and Okos, 1986).

Heat capacity equation (2.16) was converted to equation (2.17) since moisture content (c) was in kg/m<sup>3</sup> in the model;

$$Cp = 10^3 \times \left[ \left( 4.18 \times \frac{c}{\rho} \right) + \frac{(1.711 \times X_{pro} + 1.928 \times X_{fat} + 1.547 \times X_{CHO} + 0.908 \times X_{ash})}{1 - (X_{w0} - \frac{c}{\rho})} \right] \left[ \frac{J}{kg \times K} \right] \quad (2.17)$$

For diffusion coefficient of meat, Trujillo *et al.* (2005) found four different models using different assumptions. The model (2.18) selected as the most proper one by Trujillo *et al.* (2005) was used to define diffusion coefficient;

$$D = D_0 * e^{-\frac{E_a}{RT}} = 5,09 \times 10^{-6} \times e^{-\frac{23643.8}{RT}} \quad (2.18)$$

E<sub>a</sub>; kJ/mol R; 8.31434 kJ/(mol\*K)

For thermal conductivity, the equations below (2.19-2.22) were used (Pham & Willix, 1989; Equation (a.7) in Appendix Table A.1). For anisotropic nature of lean meat, relevant k values were adapted to the model as k<sub>x</sub> and k<sub>y</sub> according to fiber direction (Table 2.3).

$$k = k_f + d.(T-T_f) \quad (2.19)$$

For heat transfer perpendicular to fibers;

$$k_{\perp} = 0.421 + 0.001*(T[K]-272.1) \text{ [W/(m.K)]} \quad (2.20)$$

For heat transfer parallel to fibers;

$$k_{\parallel} = 0.450 + 0.0009*(T[K]-272.1) \text{ [W/(m.K)]} \quad (2.21)$$

$$\text{For minced meat; } k = 0.466 + 0.0011*(T[K]-272.1) \text{ [W/(m.K)]} \quad (2.22)$$

**Table 2.3.** Anisotropic thermal conductivity values used in the model

For <b>h1</b> configuration	For <b>h2</b> configuration	For <b>v</b> configuration
$k = \begin{bmatrix} k_{\perp} & 0 \\ 0 & k_{\perp} \end{bmatrix}$	$k = \begin{bmatrix} k_{\parallel} & 0 \\ 0 & k_{\perp} \end{bmatrix}$	$k = \begin{bmatrix} k_{\perp} & 0 \\ 0 & k_{\parallel} \end{bmatrix}$

Semi-empirical correlations below (2.23-2.24) for forced convection were used in order to calculate heat and mass transfer coefficients (h and k). Chilton-Colburn analogy also held (2.24b). All properties were calculated at the film temperature. Properties of air (viscosity, density, heat capacity, Prandtl Number, thermal conductivity, diffusion coefficient) with respect to temperature were entered to the model. The model then calculated the value of a property at the film temperature, which change with the sample temperature by piecewise cubic or linear interpolation and used it to calculate the values of heat and mass transfer coefficients. Moisture concentration and wet bulb temperature of air was calculated from psychrometric chart using measured values of relative humidity and dry bulb temperature (<http://www.ringbell.co.uk/info/humid.htm>).

$$Nu = \frac{h \times L_c}{k} = 0.664 \times Re^{0.5} \times Pr^{\frac{1}{3}} \quad (2.23)$$

(Geankoplis C.J., 1993; Chua K. J. et.al., 2002)

$$Sh = \frac{k_c \times L_c}{D_{eff}} = 0.664 \times Re^{0.5} \times Sc^{\frac{1}{3}} \quad (2.24a) \quad \text{or} \quad k_c = \frac{h \times Le^{\frac{2}{3}}}{\rho \times C_p} \quad (2.24b)$$

(Geankoplis C.J., 1993; Van der Smán R.G.M., 2007)

The diffusion coefficient of air was calculated by the equation below (2.25) (Bolz and Tuve, 1976; [http://www.cambridge.org/us/engineering/author/nellisandklein/downloads/examples/EXAMPLE\\_9.2-1.pdf](http://www.cambridge.org/us/engineering/author/nellisandklein/downloads/examples/EXAMPLE_9.2-1.pdf));

$$D_{a,w} = -2.775 \times 10^{-6} + 4.479 \times 10^{-8} \times T + 1.656 \times 10^{-10} \times T^2 \quad (2.25)$$

To construct the model by finite element method, COMSOL Multiphysics 3.3a with heat transfer module was used. For linear system solvers, the default solver as the Umfpack Direct Solver was used. Temperature was read with respect to time at four locations, where experimental data were taken. Average moisture content was found using integration coupling variables in the FEM in order to make comparison with experimental data. Triangular elements augmented at sides with heat flux boundary condition were used (Figure 2.5). For augmented mesh at sides with heat flux boundary condition, maximum element size was defined as  $1 \times 10^{-3}$ .

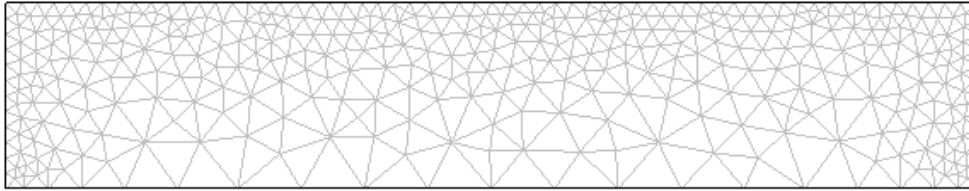


**Figure 2.5.** Mesh configuration of the model system

## 2.5. Comparison

In order to observe a difference in parameters of a sample according to drying conditions (temperature, velocity and structure effect on temperature and moisture of sample), single factor analysis of variance (ANOVA) was used with confidence level of 0.95. The adequacy of each model used for determination of diffusivity was evaluated by the coefficient of determination ( $R^2$ ) and root mean square error (RMSE) between experimental moisture loss and predicted moisture loss using the diffusion coefficient calculated. Experimental and predicted sample temperature and moisture content were also statistically compared using difference measure test with coefficient of determination ( $R^2$ ) and root mean square error (RMSE).

$$RMSE = \sqrt{\frac{1}{N} \times \sum_{i=1}^n (predicted_i - observed_i)^2} \quad (2.26)$$

## CHAPTER 3

### EXPERIMENTAL RESULTS AND DISCUSSION

#### 3.1. Temperature Distribution

At four different conditions (Table 3.1), temperatures at four different locations in the sample were measured as stated in materials and methods chapter (Chapter 2). The meanings of thermocouple abbreviations are repeated below for better understanding (Figure 3.1.).

AT1; midpoint of sample (center)

AT2; 2/3 of length from center

BT1; mid point at the bottom surface (insulated)

BT2; -2/3 of length from center on the front surface exposed to air

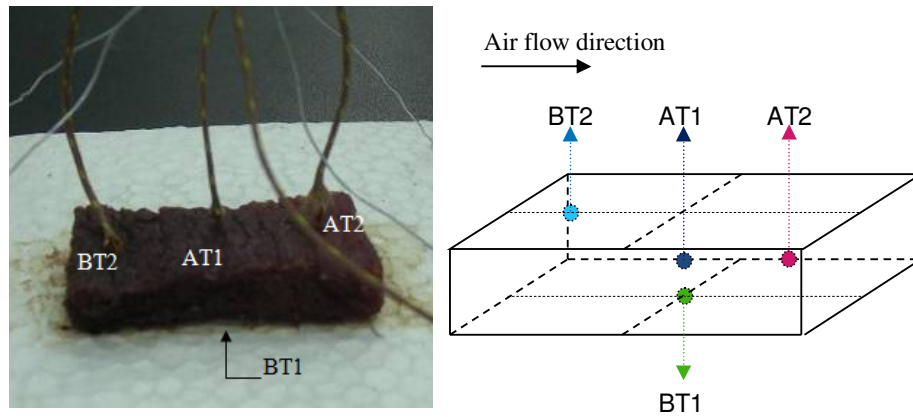


**Figure 3.1.** Thermocouple locations on sample

Temperatures at four points (AT1, AT2, BT1, BT2) on minced meat and lean meat samples at four different drying conditions (Table 3.1) are illustrated in Figures 3.2a-d.

**Table 3.1.** Drying conditions used in experiments

Abbreviations (knob positions on the dryer)	Temperature ( $^{\circ}\text{C}$ )	Drying air velocity (m/s)
v_3_T_4 *	48 $\pm$ 1	0.5
v_6_T_5	48 $\pm$ 1	1.0
v_10_T_10	48 $\pm$ 1	1.7 <sup>b</sup>
v_3_T_10	70 $\pm$ 1 <sup>a</sup>	0.5

\*v for velocity, T for temperature of air

<sup>a</sup> maximum attainable temperature in the dryer

<sup>b</sup> maximum attainable velocity in the dryer

The temperature and moisture contents of samples were average of two replicates. The results of lean meat (for any fiber configuration) and minced meat showed the same trend for temperature distribution. For all types of meat samples and in all drying conditions, the surface temperature (BT2) had higher value than the temperature at other locations (AT1, AT2 and BT1) throughout whole drying process (270 min) (Figure 3.2a-d) since the surface was directly in contact with hot air. The temperature at BT2 was in a range of 36.2-57.1°C at the end of drying (270 min) (Table 3.2) for different drying conditions. Among the four locations, temperature at a position of 2/3 of length from the center in the middle of thickness (AT2) had the lowest value (31.5-53.5°C at the end of drying) while the temperature at the midpoint (AT1, at the same thickness with AT2) had higher value (33.8-55.3°C) for all drying conditions and meat samples (Figure 3.2a-d). This showed that there was slight change in temperature with x direction (through the length) and also slightly asymmetric distribution of temperature with respect to y-axis due to flow. Such kind of slightly asymmetric temperature distribution was also represented by De Bonis M.V. and Ruocco (2008) especially at low velocity of air. Moreover, the center of bottom surface (BT1) and midpoint (AT1) showed very close temperature values confirming that there was negligible heat loss from the bottom and insulation at the bottom was achieved. It was concluded that temperature change was higher near the surfaces and slowed down considerably through interior sides of meat causing almost equal temperature at the center and midpoint of bottom surface due to internal resistances like low thermal conductivity.

During recording of weight, very little fluctuation (~0.8°C) in temperature readings at the surface (BT2) for only drying at 70°C occurred due to turning off of dryer and interruption of air flow for a very short time. After turning on the dryer, the temperature of air rapidly recovered to the original condition within 5 min, thus the effect of data acquisition for weight change on temperature was neglected.

**Table 3.2.** Temperature readings at four locations of four different meat samples at the end of drying (270 min)

Sample	Drying parameter(T ±1°C)	Sample Temperature at the end of drying			
		AT1	AT2	BT1	BT2
Lean meat _h1	48°C 0.5 m/s	33.9	31.5	33.8	36.2
	48°C 1.0 m/s	36.1	34.6	36.1	38.1
	48°C 1.7 m/s	38.3	37.4	37.9	38.9
	70°C 0.5 m/s	52.7	49.5	51.9	56.4
Lean meat _h2	48°C 0.5 m/s	36.5	34.9	36.4	38.7
	48°C 1.0 m/s	37.8	36.1	37.8	39.6
	48°C 1.7 m/s	40.5	39.8	40.7	42.3
	70°C 0.5 m/s	52.3	49.8	51.7	53.7
Lean meat _v	48°C 0.5 m/s	35.3	33.5	34.9	36.8
	48°C 1.0 m/s	37.2	35.5	37.2	38.1
	48°C 1.7 m/s	39.4	38.1	39.3	40.3
	70°C 0.5 m/s	55.3	53.6	54.9	56.5
Minced meat	48°C 0.5 m/s	38.4	35.2	37.8	39.9
	48°C 1.0 m/s	40.5	39.1	40.1	42.3
	48°C 1.7 m/s	42.3	40.8	41.7	43.2
	70°C 0.5 m/s	54.9	53.5	54.4	57.1

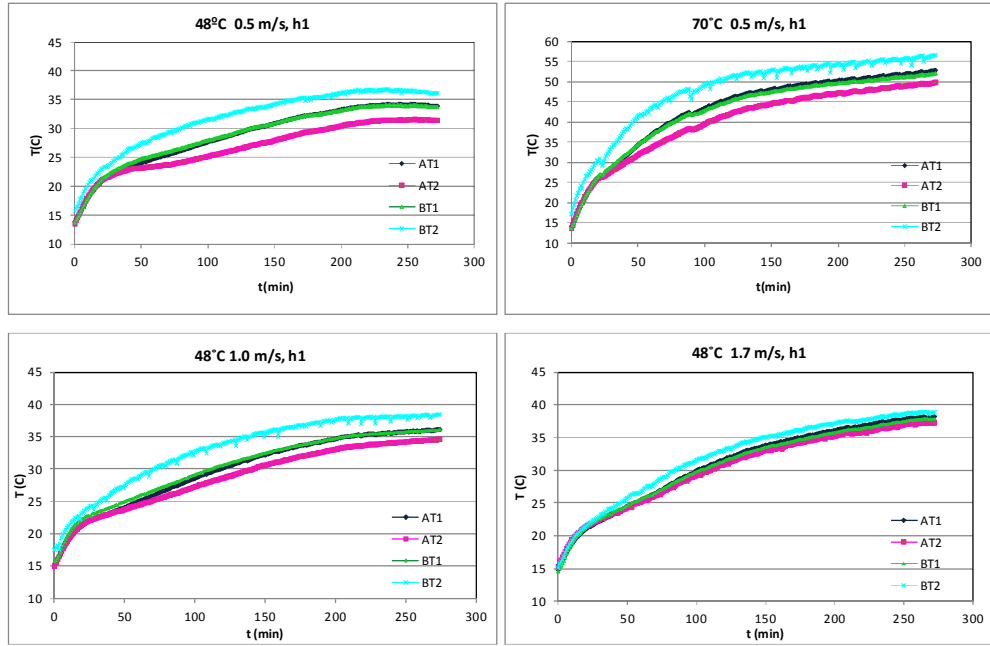


**Figure 3.2a.** Temperature distribution of lean meat with air flow normal to fiber (h1)

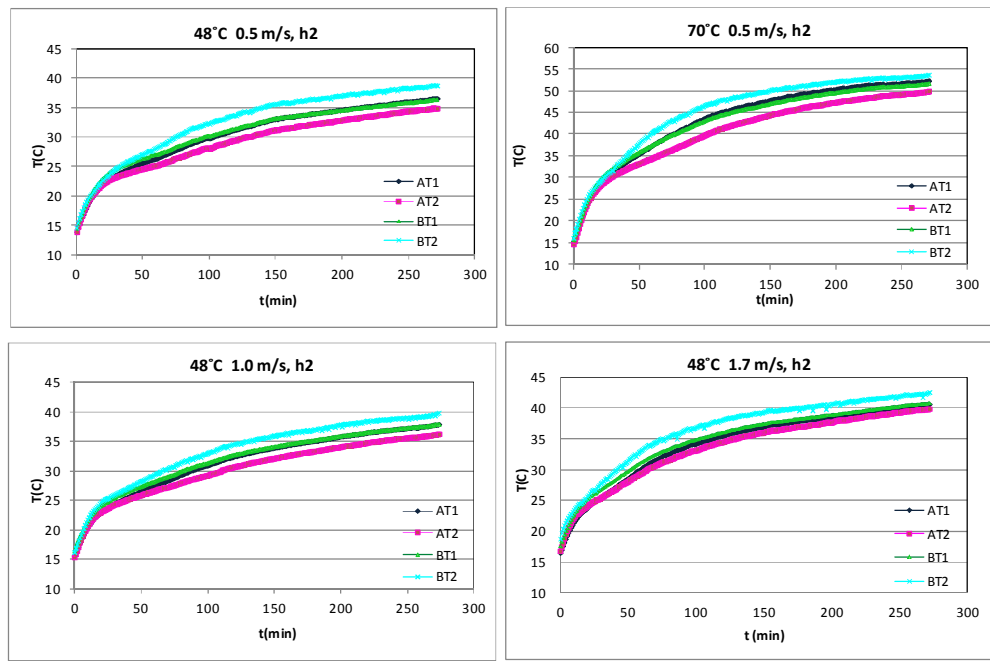


**Figure 3.2b.** Temperature distribution of lean meat with air flow normal to fiber; drying along the fiber (h2)

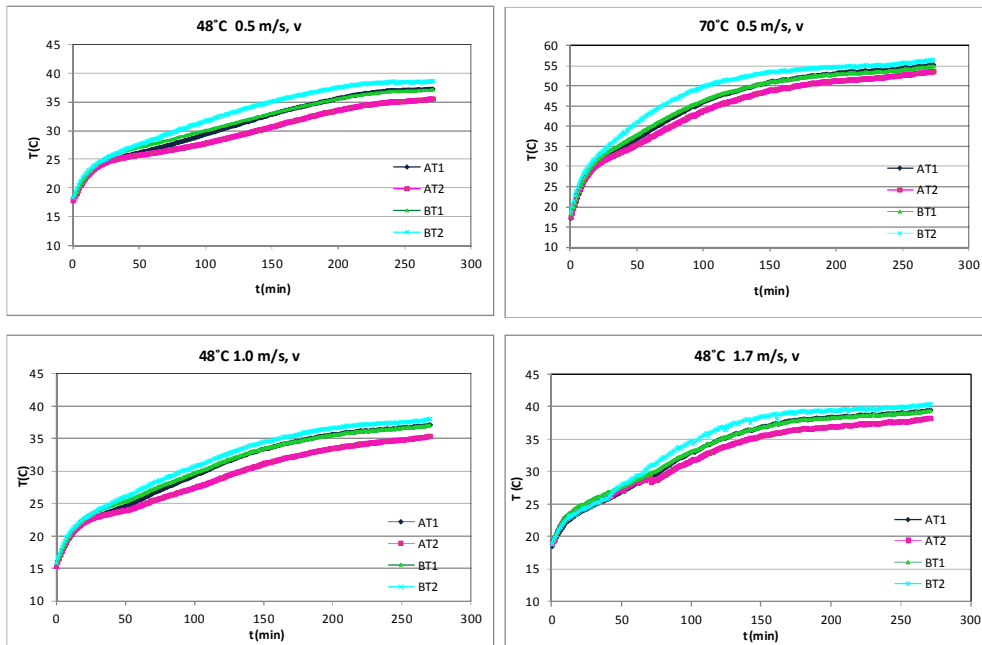


**Figure 3.2c.** Temperature distribution of lean meat with air flow along the fiber (v)

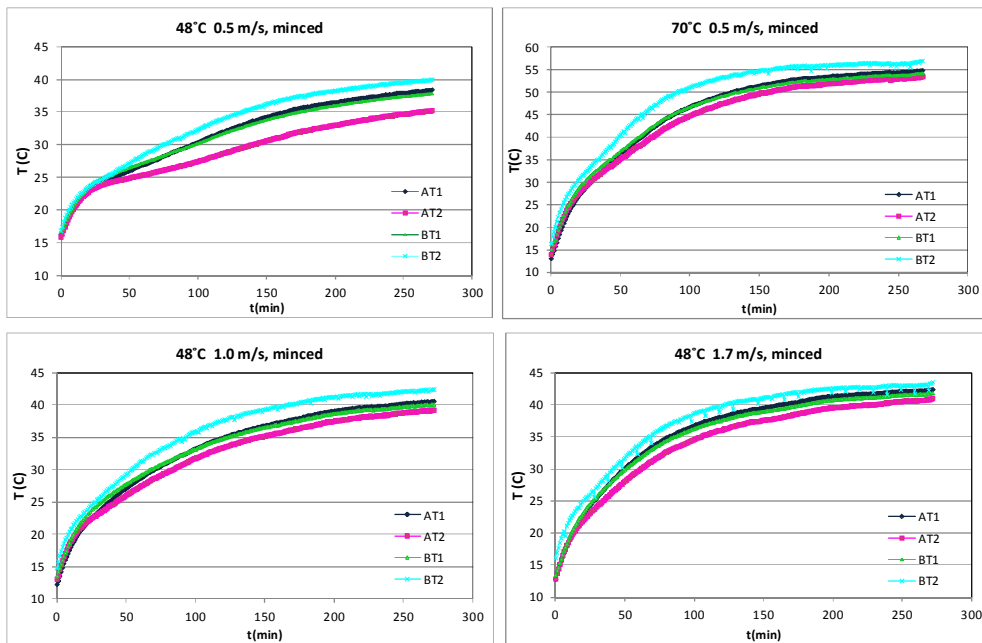


**Figure 3.2d.** Temperature distribution of minced meat

### 3.2. Effect of Air Temperature on Temperature of Samples

Air temperature is an effective parameter on sample temperature. When temperature values measured during drying at 48°C and 0.5 m/s were compared with drying at 70°C and 0.5 m/s, significantly higher temperatures were observed at drying with higher temperature in both meat

samples with three different fiber configuration and minced meat (Figure 3.2.a-d). Maximum temperatures at the surface (BT2) was 56.4, 53.7, 56.5 and 57.1°C for lean meat with h1, h2, v fiber configurations and minced meat, respectively during drying at 70°C, while these values were 36.2, 38.7, 36.8 and 39.9°C during drying at 48°C (Table 3.2).

In order to observe the effect of air temperature and other parameters (flow rate, fiber direction etc.) on temperature of samples clearly, the rate of temperature change was calculated considering first order dynamics as shown below (Cekmecelioglu and Uncu, 2012);

$$T = T_m \cdot (1 - e^{-k_T t}) \quad (3.1)$$

where T is the change in temperature (°C) with respect to initial temperature as T(t)-T<sub>0</sub>; T<sub>m</sub> is the maximum temperature of sample at an infinite drying time with respect to initial temperature; k<sub>T</sub> is the rate constant of temperature change (min<sup>-1</sup>). The constants of equation (3.1) was found by using data of both AT1 (Table 3.3a) and BT2 (Table 3.3b) locations.

Higher k<sub>T</sub> values were calculated for drying with higher air temperature meaning that the rate of temperature change was higher with higher air temperature (Table 3.3a-b). The k<sub>T</sub> values for lean meat with h1, v, h2 fiber configurations and minced meat were 0.0153, 0.0154, 0.0162 and 0.0167 min<sup>-1</sup>, respectively during drying at 70°C and 0.5 m/s while 0.0081, 0.0084, 0.014 and 0.011 min<sup>-1</sup> at 48°C and 0.5 m/s (Table 3.3a). Additionally, maximum temperature values (T<sub>m</sub>) with respect to initial temperature was also found higher (~36-41°C) at 70°C than at 48°C (~20-23°C).

**Table 3.3a.** First order kinetics model parameters for temperature change at the center (AT1) during drying of different meat samples

Drying at	Types of Meat			
	minced	h1	v	h2
<b>48°C, 0.5 m/s</b>				
T <sub>m</sub>	23.04	19.62	21.29	21.91
k <sub>T</sub>	0.011	0.0081	0.0084	0.014
R <sup>2</sup>	0.980	0.973	0.965	0.967
SEE	0.7837	0.7419	0.9155	0.9458
<b>48°C, 1.0 m/s</b>				
T <sub>m</sub>	28.10	22.37	22.91	21.65
k <sub>T</sub>	0.0147	0.0098	0.0099	0.0138
R <sup>2</sup>	0.981	0.983	0.981	0.975
SEE	0.7251	0.6952	0.7626	0.8316
<b>48°C, 1.7 m/s</b>				
T <sub>m</sub>	29.08	24.02	22.87	24.51
k <sub>T</sub>	0.0180	0.010	0.0102	0.0146
R <sup>2</sup>	0.996	0.990	0.990	0.991
SEE	0.4773	0.5954	0.5677	0.5638
<b>70°C, 0.5 m/s</b>				
T <sub>m</sub>	41.79	37.94	37.55	36.31
k <sub>T</sub>	0.0167	0.0153	0.0154	0.0162
R <sup>2</sup>	0.996	0.996	0.985	0.985
SEE	0.6563	0.6265	1.1013	1.0825

**Table 3.3b.** First order kinetics model parameters for temperature change at the surface (BT2) during drying of different meat samples

Drying at	Types of Meat			
	minced	h1	v	h2
<b>48°C, 0.5 m/s</b>				
T <sub>m</sub>	23.97	20.10	21.44	23.66
k <sub>T</sub>	0.012	0.0101	0.0107	0.0149
R <sup>2</sup>	0.987	0.990	0.976	0.981
SEE	0.6618	0.4854	0.7928	0.7743
<b>48°C, 1.0 m/s</b>				
T <sub>m</sub>	27.60	21.60	22.76	21.56
k <sub>T</sub>	0.0151	0.0121	0.0115	0.0150
R <sup>2</sup>	0.992	0.994	0.980	0.972
SEE	0.5961	0.4095	0.7815	0.8980
<b>48°C, 1.7 m/s</b>				
T <sub>m</sub>	26.99	24.70	23.04	23.97
k <sub>T</sub>	0.0178	0.0120	0.0115	0.0160
R <sup>2</sup>	0.998	0.993	0.989	0.994
SEE	0.4402	0.5125	0.6308	0.4492
<b>70°C, 0.5 m/s</b>				
T <sub>m</sub>	40.43	37.86	36.84	36.84
k <sub>T</sub>	0.0193	0.0192	0.0195	0.0185
R <sup>2</sup>	0.995	0.993	0.990	0.993
SEE	0.6951	0.7461	0.8832	0.7679

### 3.3. Effect of Air Flow Rate on Temperature of Samples

It was observed that when flow rate of air increased, temperature (T) of samples at each location (AT1, AT2, BT1, BT2) was also slightly increased (Figure 3.3a-d) for lean and minced meat samples since heat transfer coefficient, and thus heat transfer by convection increased. The k<sub>T</sub> values representing rate of temperature change increased from 0.011 to 0.0180 min<sup>-1</sup> for minced meat, from 0.0081, 0.0084, 0.014 to 0.01, 0.0102, 0.0146 min<sup>-1</sup> for h1, v, h2 configurations, respectively when velocity of air increased from 0.5 m/s to 1.7 m/s at 48°C (Table 3.3a). Maximum temperature values (T<sub>m</sub>) with respect to initial temperature were also found ~3±0.5°C higher for lean meat samples and 6°C higher for minced meat when velocity of air increased from 0.5 m/s to 1.7 m/s at 48°C.

Additionally, from temperature distribution graphs of drying at 1.7 m/s for lean meat and minced meat samples (Figure 3.2a-d), it was noticed that temperature gradient became less through the sample dried with higher air velocity (curves resembling temperature at different locations became closer with higher velocity). This was interpreted as high velocity of air resulted in more uniform temperature through the sample. The temperature differences between BT2 and AT2 giving the maximum temperature difference and between AT1 and AT2 showing the temperature change in x direction were found less with higher velocity of air for all types of meat samples (Table 3.4). The maximum temperature difference and temperature change in x direction decreased ~1-3°C and 0.7-1.5°C, respectively when velocity of air increased from 0.5 to 1.7 m/s.



**Table 3.4.** Average maximum temperature difference and temperature difference in x direction for different meat samples at four drying conditions

Drying at	Max T difference <sup>1</sup> (°C) (BT2-AT2)				$\Delta T_x$ <sup>2</sup> (°C) (AT1-AT2)			
	h1	v	h2	minced	h1	v	h2	minced
48°C, 0.5 m/s	5.1	3.2	3.5	4.2	2.1	1.5	1.4	2.6
48°C, 1.0 m/s	4.2	2.7	3.2	3.5	1.2	1.4	1.3	1.3
48°C, 1.7 m/s	1.7	1.8	2.5	3.2	0.6	0.9	0.7	1.6
70°C, 0.5 m/s	7.6	4.2	4.7	4.6	2.9	1.7	2.7	1.3

<sup>1</sup>Average of maximum temperature difference with respect to time

<sup>2</sup>Average of temperature difference in x direction with respect to time

When the effect of air temperature was compared with the effect of flow rate, it was concluded that air temperature was a more effective parameter than flow rate of air on temperature of sample since  $T_m$  and  $k_T$  values at 70°C (38.4°C, 0.016 min<sup>-1</sup> in average) was much higher than the values at all other drying conditions even at the highest velocity, 1.7 m/s (25.1°C, 0.013 min<sup>-1</sup> in average) for all samples (Table 3.3a).

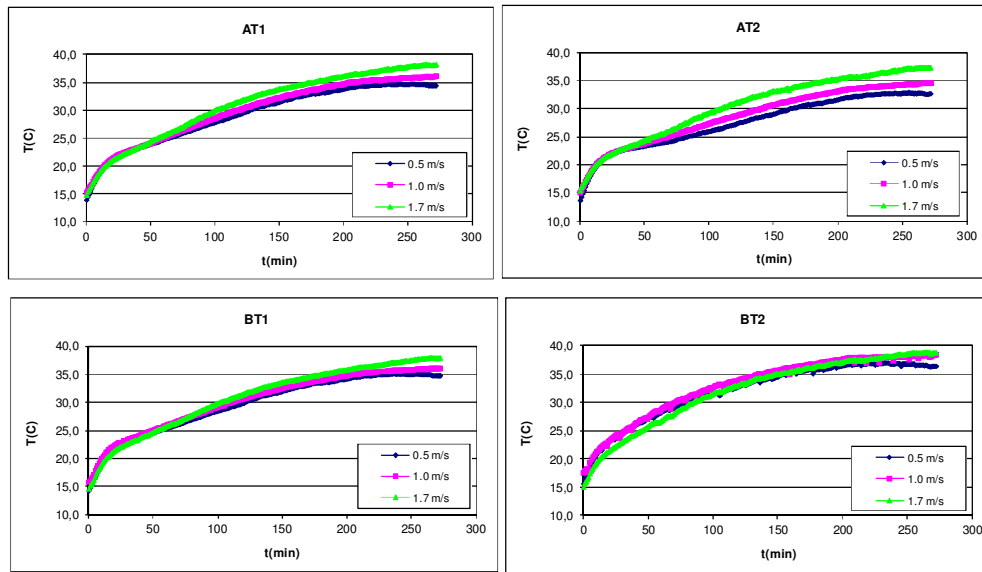


**Figure 3.3a.** Temperature change at different points of lean meat with **h1** fiber configuration during drying at 48±1°C but different velocities; (—◆—) 0.5 m/s; (—■—) 1.0 m/s; (—▲—) 1.7 m/s

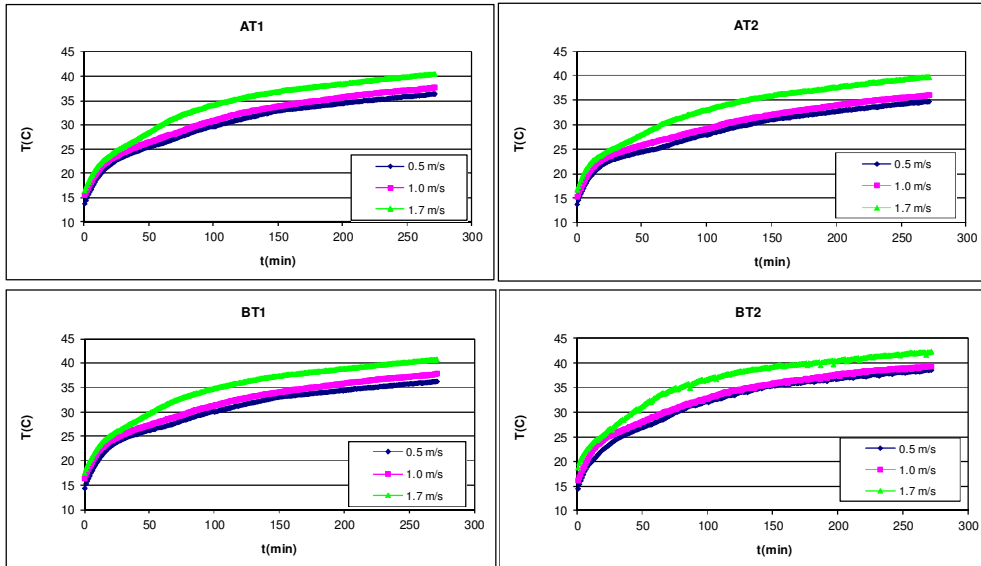


**Figure 3.3b.** Temperature change at different points of lean meat with **h2** fiber configuration during drying at  $48\pm 1^\circ\text{C}$  but different velocities; ( $\blacklozenge$ ) 0.5 m/s; ( $\blacksquare$ ) 1.0 m/s; ( $\blacktriangle$ ) 1.7 m/s

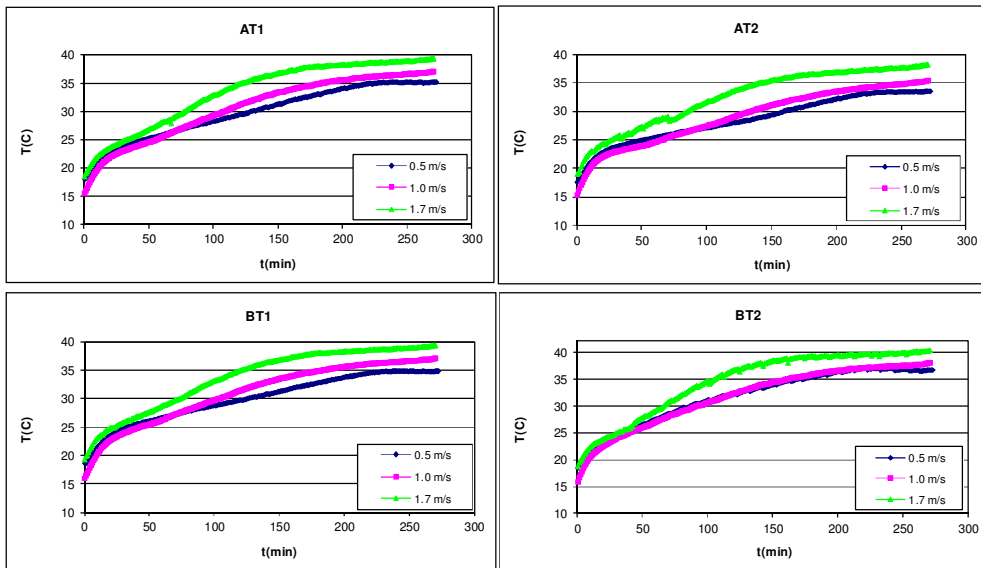


**Figure 3.3c.** Temperature change at different points of lean meat with **v** fiber configuration during drying at  $48\pm 1^\circ\text{C}$  but different velocities; ( $\blacklozenge$ ) 0.5 m/s; ( $\blacksquare$ ) 1.0 m/s; ( $\blacktriangle$ ) 1.7 m/s

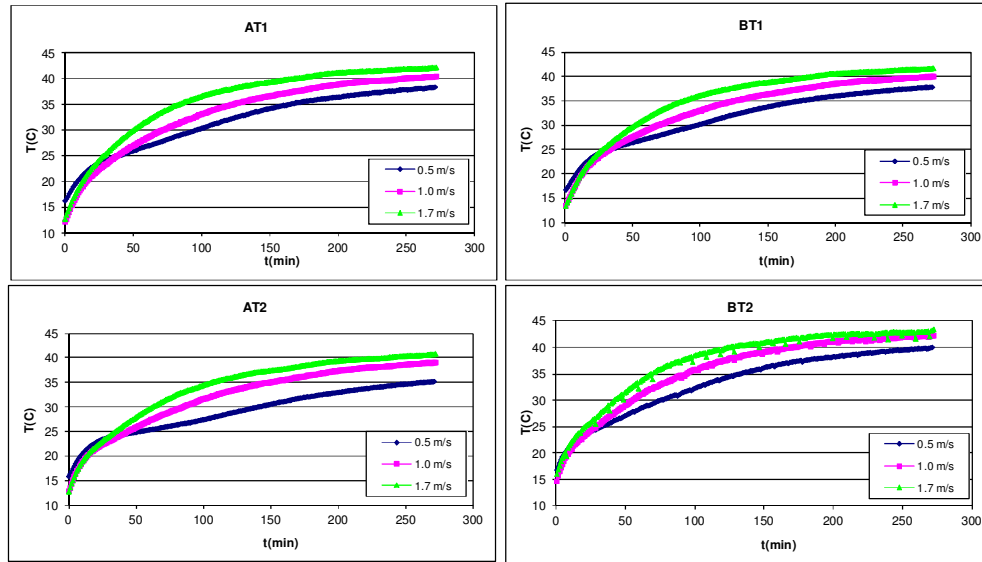


**Figure 3.3d.** Temperature change at different points of **minced** meat during drying at  $48\pm 1^\circ\text{C}$  but different velocities; ( $\blacklozenge$ ) 0.5 m/s; ( $\blacksquare$ ) 1.0 m/s; ( $\blacktriangle$ ) 1.7 m/s

### 3.4. Effect of Fiber Direction on Temperature of Samples

Drying was conducted using samples which were cut with different directions (h1: flow normal to fibers, h2: flow along the fibers and v: flow normal to fibers and drying along the fibers in Figure 2.1) in order to see whether there was fiber direction effect on temperature distribution of samples and drying rate.

The highest temperature at the surface and the lowest at AT2 location was observed in all meat samples with different fiber configurations (Figure 3.2a-d). However, the temperature difference with respect to locations was found less in v fiber condition than other fiber conditions due to probably more easily air flow through and into the sample which led to more uniform temperature within samples (Figure 3.4a-c). The lean meat samples with h2 fiber configuration also showed less temperature difference with respect to locations than the ones with h1 fiber configuration due to probably more easily flow of air through the sample. Considering the values in Table 3.4 after drying at  $48^\circ\text{C}$  vs. 0.5 m/s,  $48^\circ\text{C}$  vs. 1.0 m/s and  $70^\circ\text{C}$  vs. 0.5 m/s, lean meat with v fiber configuration showed 3.2, 2.7,  $1.8^\circ\text{C}$  differences respectively, while h2 fiber configuration showed 3.5, 3.2,  $2.5^\circ\text{C}$  and h1 showed the highest values as 5.1, 4.2,  $7.6^\circ\text{C}$ , which supported the statements above. The order of temperature gradient through the samples can be written as  $v < h2 < h1$ .

At the highest attainable flow rate of air (1.7 m/s) in the dryer, all three different fiber conditions showed very small temperature difference with respect to locations, almost uniform temperature within the samples was observed (Figure 3.4 D). Maximum temperature difference and temperature difference in x direction of lean meat samples were also found close to each other at 1.7 m/s (Table 3.4).

When rate constants ( $k_T$ ) for temperature change were compared (Table 3.3a), it was observed that  $k_{Th2} > k_{Tv} \approx k_{Th1}$  for all drying conditions, meaning that h2 fiber configuration showed faster increase in temperature than other fiber configurations. Table 3.1 also showed that in all drying conditions (except at  $70^\circ\text{C}$ ) and locations, h2 had  $\sim 1\text{-}3^\circ\text{C}$  higher temperatures than v and h1 at the end of drying; and v had  $0.5\text{-}2^\circ\text{C}$  higher temperatures than h1.

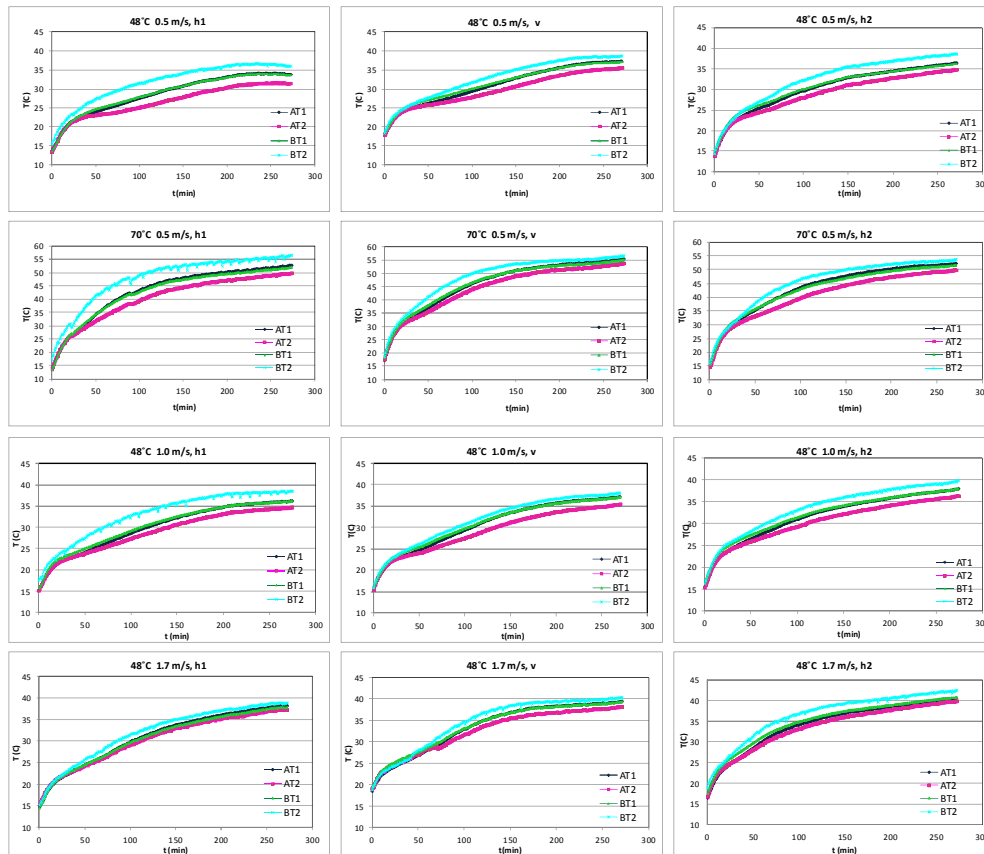


**Figure 3.4.** Temperature distribution of samples with three different fiber configurations; h1: flow normal to fibers, h2: flow along the fibers and v: flow normal to fibers.  
A:  $48 \pm 1^\circ\text{C}$ , 0.5 m/s, B:  $70 \pm 1^\circ\text{C}$ , 0.5 m/s, C:  $48 \pm 1^\circ\text{C}$  1.0 m/s, D:  $48 \pm 1^\circ\text{C}$  1.7 m/s

### 3.5. Temperature Comparison for Minced Meat vs. Fiber Configuration

Temperatures with respect to time at four locations on lean meat and minced meat samples were analyzed for each drying condition. At the end of each drying condition for each location, the temperatures of minced meat were found  $\sim 1.0\text{-}4.4^\circ\text{C}$  higher than the temperatures of lean meat samples (Figure 3.5a.-d). During drying at  $0.5\text{ m/s}$  and  $48^\circ\text{C}$ , among all meat samples, minced meat had the highest and lean meat with h1 configuration had the lowest temperatures throughout drying and the difference between the temperatures of minced and lean meat became more significant towards the end of drying (Figure 3.5a). When velocity of air increased to  $1.0\text{ m/s}$  (Figure 3.5b) and  $1.7\text{ m/s}$  (Figure 3.5c), minced meat again showed the highest and h1 configuration showed the lowest temperature throughout drying but the difference between temperature curves of samples became more distinctive with respect to low velocity condition ( $0.5\text{ m/s}$ ). It was difficult to make a comment on temperature of samples during drying at  $70^\circ\text{C}$  (Figure 3.5d) since curves seemed mostly overlapping. In general, minced meat and v fiber had on average  $\sim 2\text{-}3^\circ\text{C}$  higher temperatures than other fiber configurations at  $70^\circ\text{C}$ . However, it could be said that the structure effect on temperature of samples became less significant with higher air temperature ( $70^\circ\text{C}$ ).

From both  $k_T$  and  $T_m$  values of minced meat (Table 3.3a), it was found that in every drying condition minced meat had higher  $k_T$  and  $T_m$  values than lean meat samples. Only at  $48^\circ\text{C}$  and  $0.5\text{ m/s}$ , minced meat showed slightly less  $k_T$  value than h2 but  $1.1^\circ\text{C}$  higher  $T_m$  value.

In all lean meat samples, a bending point was observed within the first 30 minutes of drying at all locations (Figure 3.2a-c). However, minced meat showed either none or very slight bending (Figure 3.2d), and smoother temperature curves were observed in minced meat, presumably due to existence of more uniform structure. Higher  $R^2$  values also supported this finding by better fitting to first order dynamics for minced meat (Table 3.3a)

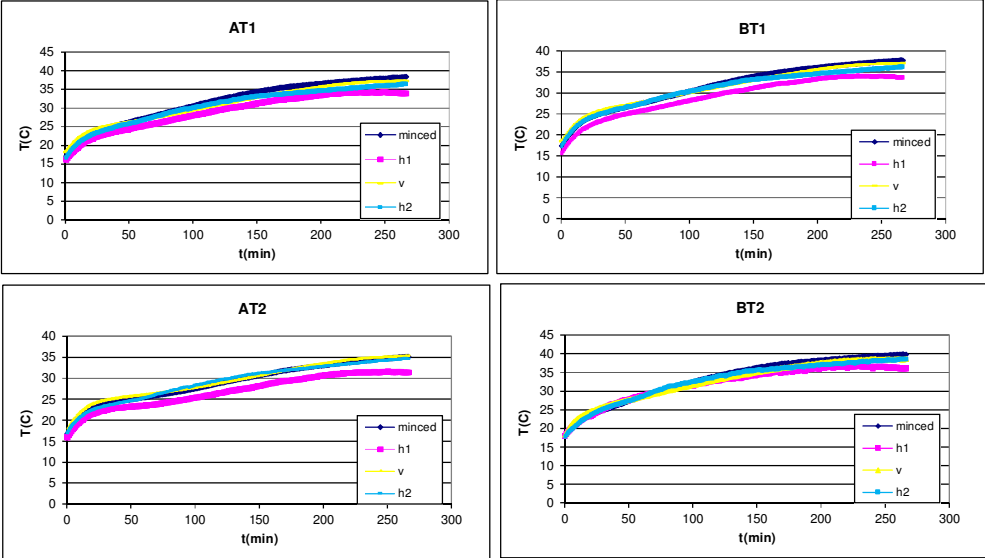


**Figure 3.5a.** Temperature change at different points for different meat samples dried at  $48\pm 1^\circ\text{C}$  and  $0.5\text{ m/s}$  (—◆—) minced; (—■—) h1; (—▲—) v; (—■—) h2

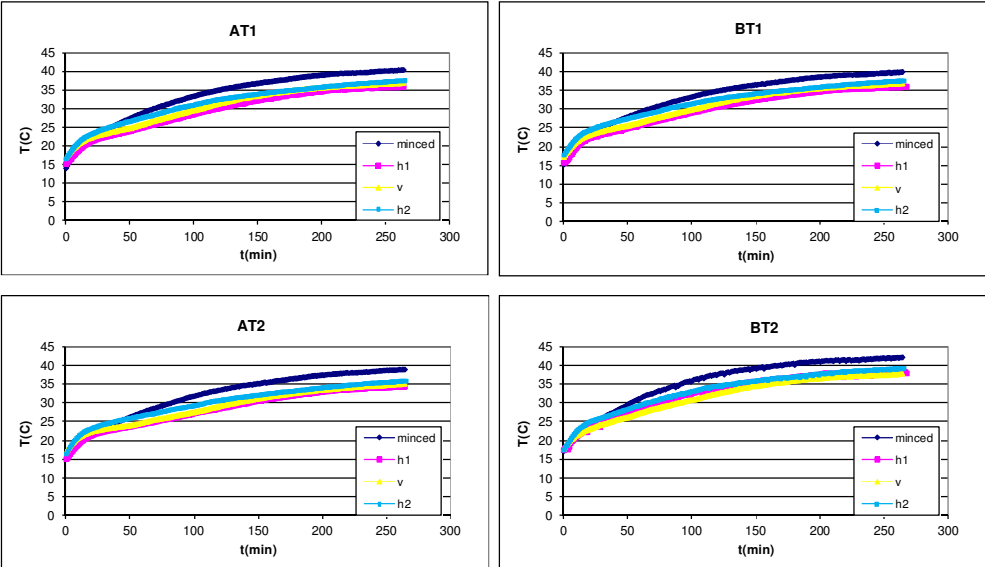


**Figure 3.5b.** Temperature change at different points for different meat samples dried at  $48\pm 1^\circ\text{C}$  and  $1.0\text{ m/s}$  (—◆—) minced; (—■—) h1; (—▲—) v; (—■—) h2

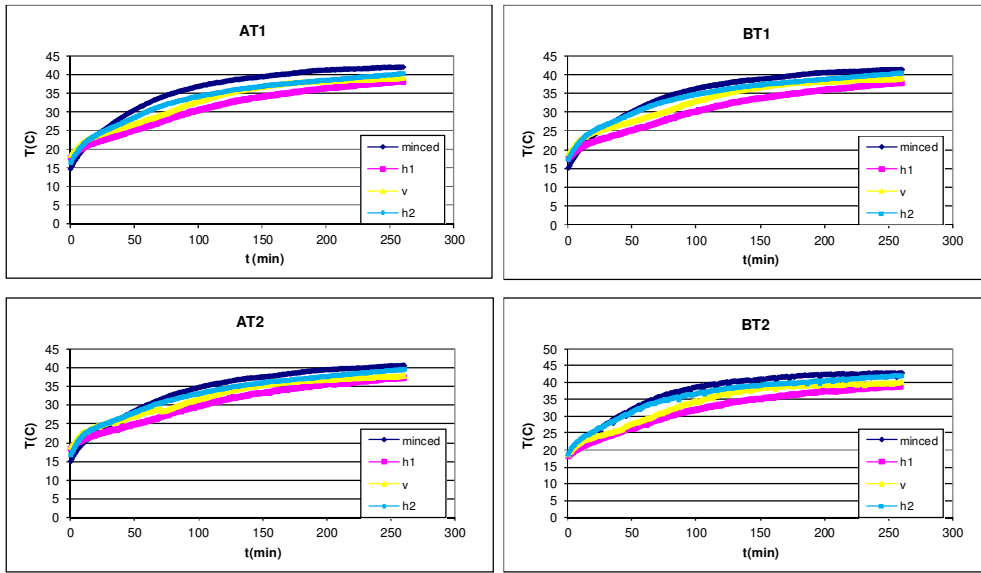


**Figure 3.5c.** Temperature change at different points for different meat samples dried at  $48\pm 1^\circ\text{C}$  and  $1.7\text{ m/s}$  (—◆—) minced; (—■—) h1; (—▲—) v; (—□—) h2

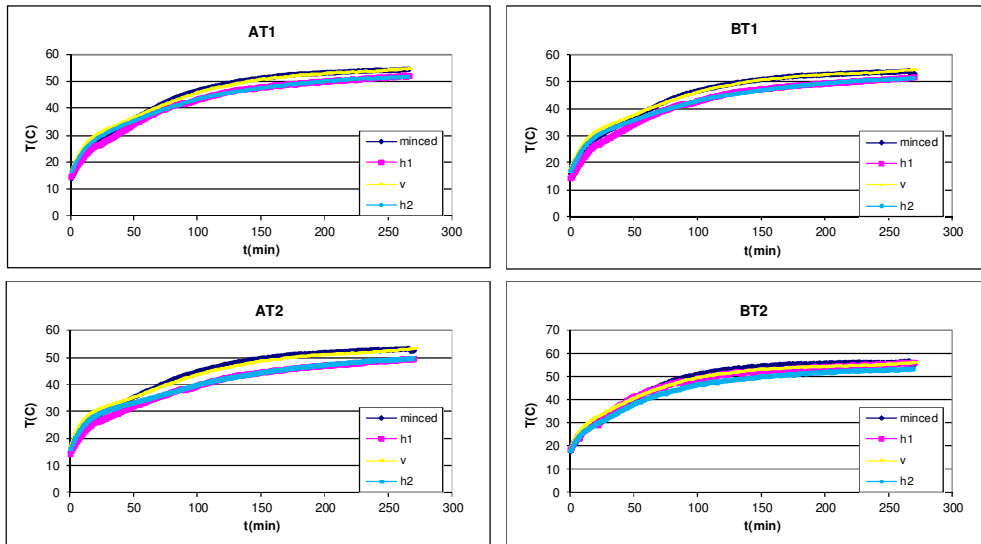


**Figure 3.5d.** Temperature change at different points for different meat samples dried at  $70\pm 1^\circ\text{C}$  and  $0.5\text{ m/s}$  (—◆—) minced; (—■—) h1; (—▲—) v; (—□—) h2

### 3.6. Effect of Air Temperature and Flow Rate on Moisture Content of Meat Samples

The weight ( $W$ ) of sample was converted to dry base moisture content as;

$$X = (W - W_{ds}) / W_{ds} \quad (\text{ds; dry solid}) \quad (3.2)$$

The dry solid percentage was used as 0.24 which was experimentally found according to section 2.3.4 and agreed with literature (Willix *et al.*, 1998). Change in average moisture content of all meat samples with respect to time was drawn for different drying conditions. Moisture content decreased exponentially with time (Figure 3.6). Initially higher moisture removal was observed then slowed down, and finally expected to reach equilibrium moisture content as in the study of Planinic *et al.* (2005).

As seen in Figures 3.6a-b, a higher moisture loss and drying rate were observed during drying at 70°C and 0.5 m/s. It was followed by drying at 48°C and 1.7 m/s and the lowest rate and moisture loss were observed at low temperature and velocity (48°C, 0.5 m/s) condition. Celen *et al.* (2010) found that air temperature increased the drying rate of mushrooms significantly but when thickness of sample increased, the effect of temperature on drying rate ceased. Other researches, who studied drying of various foods also achieved higher drying rates and lower total drying times with higher air temperature (Djendoubi *et al.*, 2009; Kashaninejad and Tabil, 2004; Kaya *et al.*, 2007a, 2007b, 2008c, 2010, Kurozawa *et al.*, 2012, Planinic *et al.*, 2005, Vega-Gálvez *et al.*, 2012; Yadollahinia and Jahangiri, 2009).

When natural logarithm of moisture content (dry base) was plotted with respect to time (Figure 3.6c), the slope of the linear regression equations gave information about the rate of drying (g/gbds.min) (Table 3.5). The rate of drying was found as 1.39, 1.68, 1.99 and 1.83  $10^{-3}$  g/gbds.min for minced meat, h1, h2 and v fiber configuration respectively during drying at 70°C and 0.5 m/s while drying at 48°C and 1.7 m/s led to lower rate of drying values as 1.26, 1.40, 1.50 and 1.51  $10^{-3}$  g/gbds.min for minced meat, h1, h2 and v fiber configuration, respectively. When drying time required to decrease moisture content from 76% to 20% (acceptable moisture % for jerky production by Lee & Kang, 2003) was calculated based on linear regression equations (Figure 3.6c), it was found that increasing velocity from 0.5 to 1.7 m/s decreased drying time by 1.2-4.2 hr (2.3 hr on average) while increasing temperature from 48°C to 70°C decreased by 3.6-6.3 hr (4.8 hr on average) for different meat samples (Table 3.6).

It could be concluded that temperature was more effective parameter than flow rate on moisture content change as in case of change in temperature of sample but increasing flow rate from 0.5 to 1.7 m/s also decreased total drying time and led to higher drying rates (increased from 1.00-1.43 to 1.39-1.83  $10^{-3}$  g /gbds.min) at the same air temperature (48°C) (Table 3.5-3.6) (Kaya *et al.*, 2010; Vega-Gálvez *et al.*, 2012; Azzouz *et al.*, 2002; Yadollahinia and Jahangiri, 2009).

In general, the constant rate period was not significant in all samples and drying conditions except for drying with the lowest flow rate (0.5 m/s) (Figure 3.6b). This agreed with the results of other studies. In general, constant rate period is either too short or not existed in food systems since most of the water molecules are present as bound water within the cells or in intracellular space. Thus, drying mainly occurs in falling rate period in food and biological materials (Madamba, 1996; Ayensu, 2004; Srikiatden and Roberts, 2007; Saravacos and Charm, 1962; Chirife J., 1971; Rosello *et al.*, 1997; Djendoubi *et al.*, 2009; Planinic *et al.*, 2005; Azzouz *et al.*, 2002).

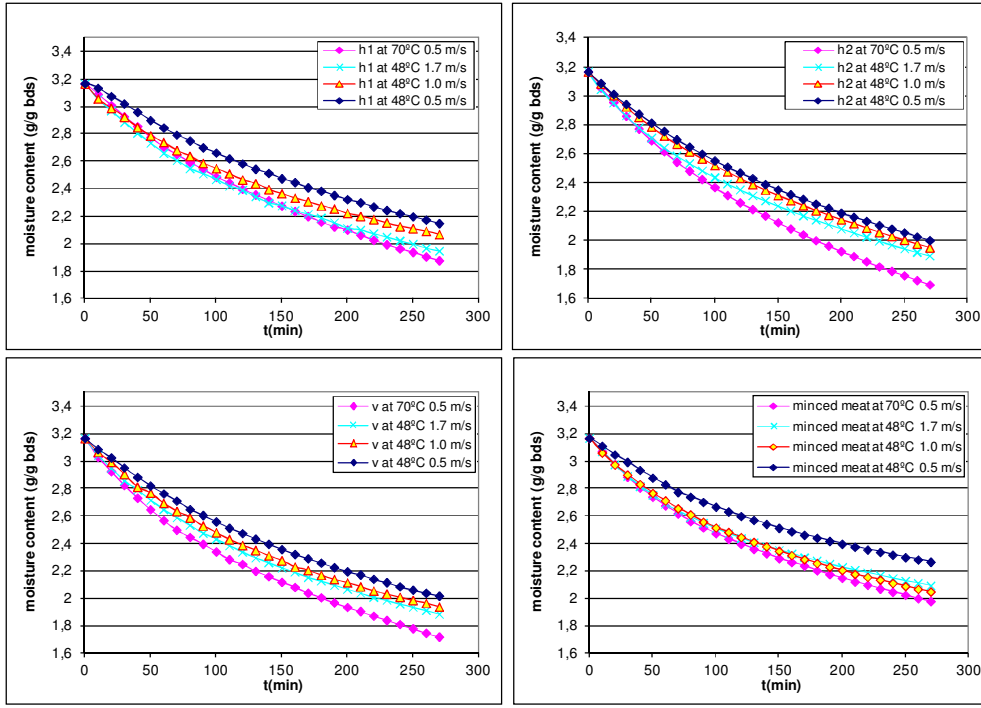


Figure 3.6a. Change in moisture content (dry base) with respect to drying time during drying of meat samples at four different drying condition

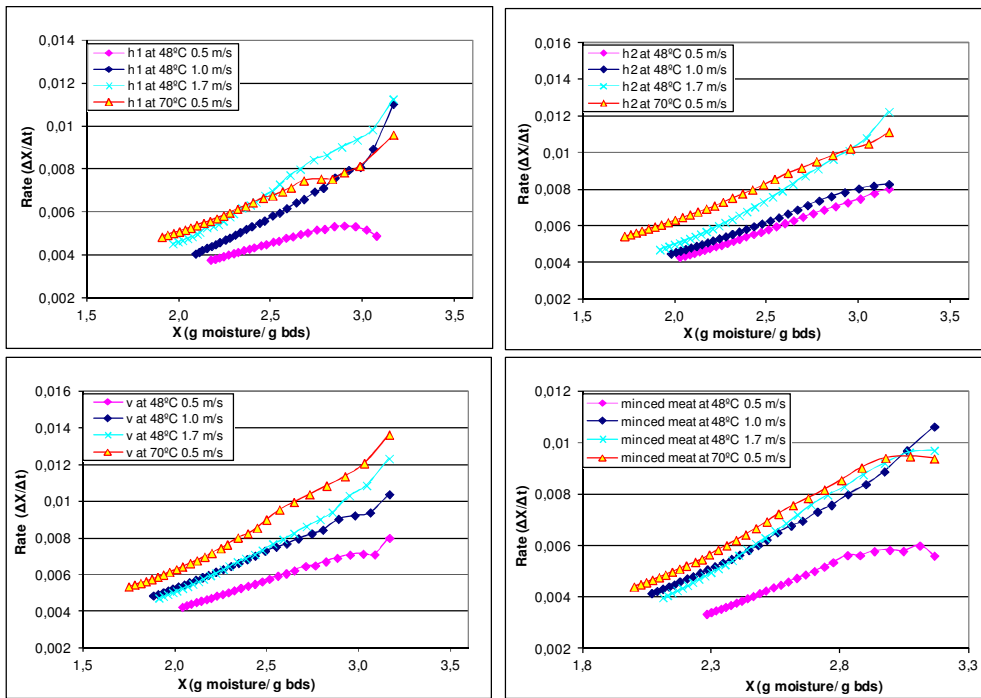
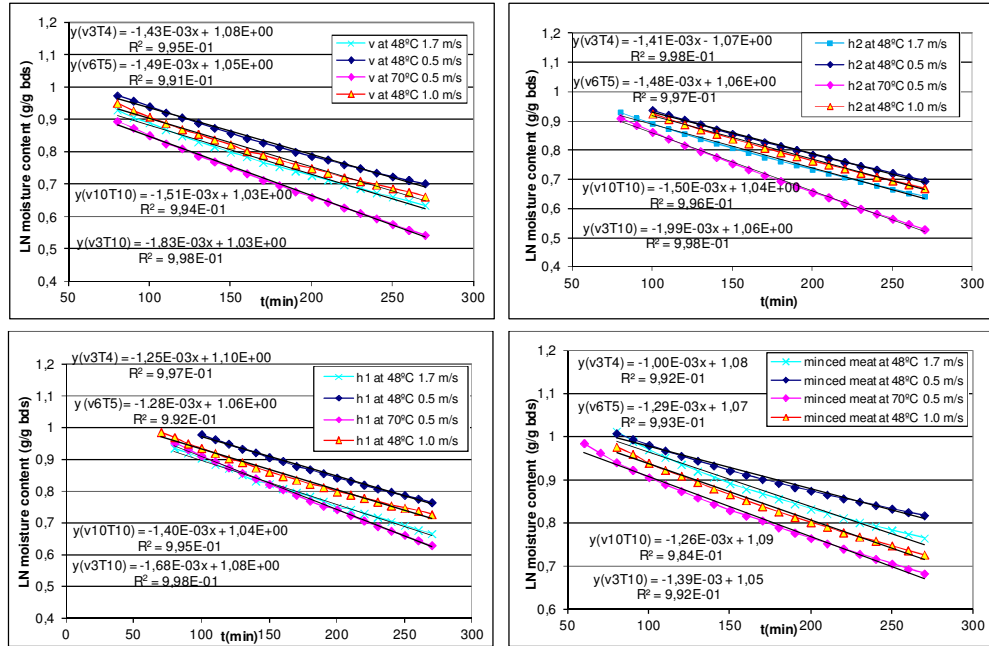


Figure 3.6b. Drying rate change with respect to moisture content (dry base).





**Figure 3.6c.** Exponential change in moisture content (dry base) with respect to drying time, fiber direction and structure.

**Table 3.5.** Model parameters for rate of drying ( $R^2 > 0.99$ )

Drying at	$k_m$ of meat samples ( $10^{-3}$ g/ g bds.min)			
	v	h2	h1	minced
48°C, 0.5 m/s	1.43	1.41	1.25	1.00
48°C, 1.0 m/s	1.49	1.48	1.28	1.29
48°C, 1.7 m/s	1.51	1.50	1.40	1.26
70°C, 0.5 m/s	1.83	1.99	1.68	1.39

\*  $k_m$  is the rate constant (g / g bds.min) for change in moisture content

**Table 3.6.** Drying times to decrease moisture content to 20% (wet base)

Drying at	Drying time (hr)			
	v	h2	h1	minced
48°C, 0.5 m/s	14.7	14.8	17.2	21.1
48°C, 1.0 m/s	13.8	14.0	16.2	16.2
48°C, 1.7 m/s	13.4	13.6	14.6	16.8
70°C, 0.5 m/s	11.1	10.4	12.6	14.8

### 3.7. Effect of Fiber Direction and Structure on Moisture Content of Samples

In order to investigate the effect of fiber direction and structure on moisture content, change in moisture content and drying rate of different meat samples at the same drying condition with respect to time was drawn (Figure 3.7a-b). Lean meat with v and h2 fiber configuration showed 3.5-5% higher moisture loss than the samples with h1 fiber configuration (Figure 3.7a) at the end of drying (270 min) at all drying conditions except for drying at 1.7 m/s. This might be due to easier

air flow leading to more efficient convection and evaporation of moisture through the sample with v and h2 fibers than h1. The result was also compatible with the study of Rosello *et al.* (2007). They found the axial diffusion coefficient to be larger than the radial one. When radial direction was accepted as perpendicular to flow and axial direction parallel to flow, then h1 was needed to have lower anisotropic diffusion coefficient since it consisted of diffusion coefficients used for perpendicular flow. At an air velocity of 1.7 m/s, drying rate of lean meat samples showed no significant difference with fiber direction (Figure 3.7b), probably due to much more easily and faster diffusion of water to air, which diminished diffusion coefficient difference with respect to flow direction.

Minced meat showed on average 2.3-6.2 % lower moisture losses than the lean meat samples with any fiber direction (Figure 3.7a) at any drying condition. This was probably resulted from diffusivity difference and more difficult moisture loss due to the destruction of fiber structure while preparing minced meat.

Rate of drying values also supported these findings (Table 3.5, Figure 3.6c). The rate constants in a descending order can be written as  $k_m(h2) \approx k_m(v) > k_m(h1) > k_m(\text{minced})$ . Drying times to decrease moisture content to 20% was also in the same order as  $t(\text{minced}) > t(h1) > t(v) \approx t(h2)$  (Table 3.6).

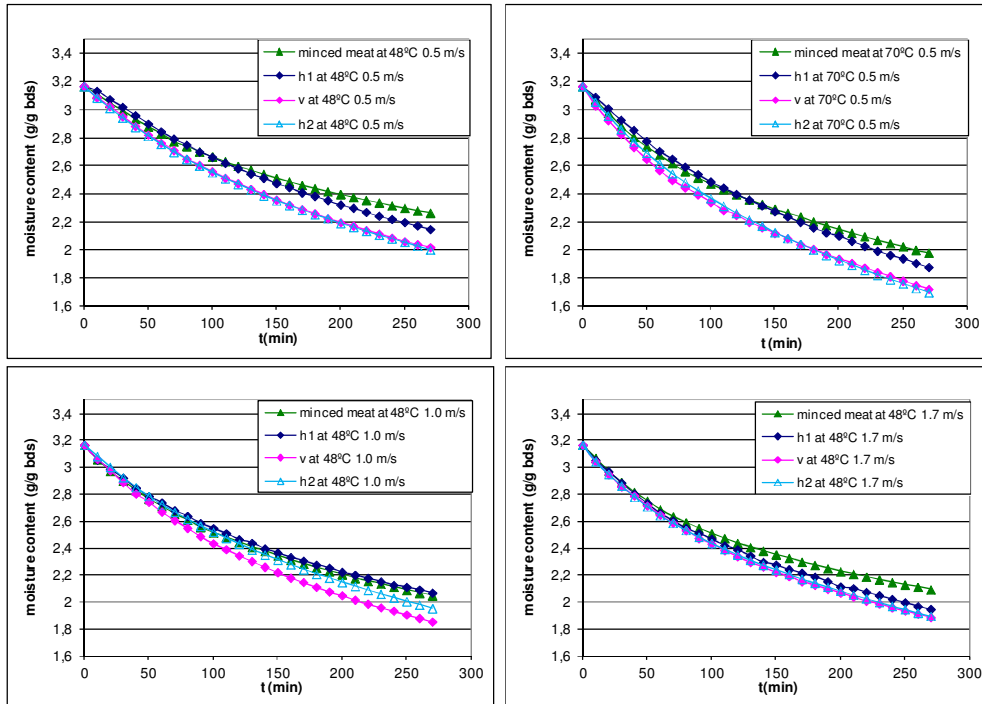


**Figure 3.7a.** Change in moisture content (dry base) with respect to drying time, fiber direction and structure

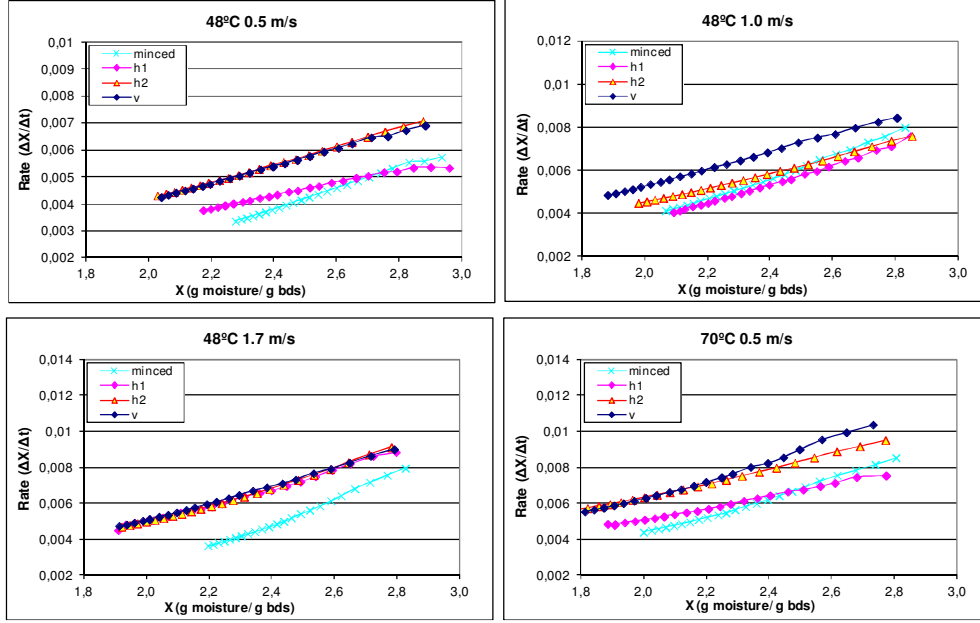


**Figure 3.7b.** Change in drying rate with respect to moisture content (dry base), fiber direction and structure

### 3.8. Calculation of Equilibrium Moisture Content and Diffusion Coefficient

Equilibrium moisture content was calculated as defined in materials and methods section 2.3.5. Exponential decay equations of the moisture removal curves (Figure 3.6a and 3.7a) designated below was found by Sigma plot 2000 for Windows Version 6.00. The result of the equations when time goes infinity was taken as equilibrium moisture content ( $X_{eq}$ ). The resulting equilibrium moisture contents are presented in appendix B (Table B.1).

$$X = X_{eq} + a'e^{-kt} \quad (3.3)$$

$$X = X_{eq} + a'e^{-k_0t} + b'e^{-k_1t} \quad (3.4)$$

For drying of an infinite slab, effective diffusion coefficient was determined by solution of Fick's second law of diffusion (Geankoplis, 1993; Crank, 1975).

$$\frac{X-X_{eq}}{X_i-X_{eq}} = \frac{8}{\pi^2} \sum_{n=0}^{\infty} \frac{1}{(2n+1)^2} \exp\left(- (2n+1)^2 \pi^2 \frac{D_{eff}}{4L^2} t\right) \quad (3.5)$$

If drying takes long time, slab thickness is small and hence dimensionless Fourier number is greater than 0.1, the series solution is simplified to its first term as;

$$\ln\left(\frac{X-X_{eq}}{X_i-X_{eq}}\right) = \ln\left(\frac{8}{\pi^2}\right) - t \cdot \left(\frac{D_{eff} \cdot \pi^2}{4L^2}\right) \quad (3.6)$$

where L is the length of diffusion pathway. Since there was diffusion at only upper side of the meat samples, the overall thickness of samples (0.01 m) was used as L. Effective diffusion coefficient was calculated from slope of a plot of  $\ln\left(\frac{X-X_{eq}}{X_i-X_{eq}}\right)$  with respect to time and the results are tabulated as model A and B in Table 3.7. To check for validity, Fourier number was calculated and found after ~60 minutes of drying and it was greater than 0.1.

Alternatively, diffusion coefficient was also calculated using Model 1 and 2 defined in the studies of Bains and Langrish (2008) and Akpinar and Dincer (2005) (Table 3.7). While applying these models, equilibrium moisture content calculated by equation (3.3) was used.

When diffusion coefficients calculated using equilibrium moisture content obtained from equation (3.3) (model A) and (3.4) (model B) were compared (Table 3.7), it was observed that equation (3.3) gave better agreement since diffusion coefficient increased with increasing air flow rate and temperature at the same flow rate as supported by other studies (Kaya *et al.*, 2010; Vega-Gálvez *et al.*, 2012). As discussed in section 3.6, fiber direction effect on moisture loss was diminished with higher velocity especially above 1 m/s. This finding was also supported by acquisition of almost the same diffusion coefficient values for lean meat samples at the highest velocity condition (1.7 m/s) in model A (Table 3.7). However, diffusion coefficients of model B showed no trend with respect to air temperature or flow rate. Thus, it was concluded that equation (3.3) was more suitable to represent moisture content change with respect to time and it could be used for calculation of equilibrium moisture content.

When compared diffusion coefficients, model A and model 1 showed close values, while model 2 calculated very different values. Literature values of diffusion coefficient were between  $5.48 \cdot 10^{-12}$  –  $1.17 \cdot 10^{-5}$  for meat and  $1 \cdot 10^{-11}$  –  $5.56 \cdot 10^{-10}$  for beef (Panagiotou *et al.*, 2004). Model 2 was significantly different than literature data. Other models produced closer diffusion coefficients ( $1.11 \cdot 10^{-9}$  –  $5.54 \cdot 10^{-9}$ ) but those were slightly larger than literature values, probably since our system was two dimensional.

**Table 3.7.** Diffusion coefficient values of meat samples at different drying conditions by using different models

Model	Sample	Diffusion coefficient* (m <sup>2</sup> /s) drying at			
		48°C 0.5 m/s	48°C 1.0 m/s	48°C 1.7 m/s	70°C 0.5 m/s
Model A by using $X_{eq}$ from Eqn 3.3 <sup>1</sup>	Lean meat_h1	2.82 E-09	3.71 E-09	4.18 E-09	3.26 E-09
	Lean meat_h2	3.27 E-09	3.41 E-09	4.23 E-09	3.62 E-09
	Lean meat_v	3.31 E-09	3.84 E-09	4.28 E-09	4.28 E-09
	Minced meat	3.88 E-09	4.31 E-09	5.54 E-09	4.60 E-09
Model B by using $X_{eq}$ from Eqn 3.4 <sup>2</sup>	Lean meat_h1	2.82 E-09	2.96 E-09	1.25 E-09	1.54 E-09
	Lean meat_h2	1.11 E-09	1.55 E-09	1.79 E-09	1.82 E-09
	Lean meat_v	1.27 E-09	1.95 E-09	2.88 E-09	1.74 E-09
	Minced meat	1.63 E-09	2.57 E-09	1.70 E-09	1.53 E-09
Model 1 <sup>3</sup>	Lean meat_h1	1.76 E-09	2.28 E-09	2.55 E-09	2.01 E-09
	Lean meat_h2	2.01 E-09	2.09 E-09	2.55 E-09	2.22 E-09
	Lean meat_v	2.04 E-09	2.35 E-09	2.58 E-09	2.60 E-09
	Minced meat	2.40 E-09	2.62 E-09	3.36 E-09	2.83 E-09
Model 2 <sup>3</sup>	Lean meat_h1	7.32 E-08	2.51 E-07	8.06 E-07	2.08 E-07
	Lean meat_h2	2.94 E-07	3.44 E-07	1.71 E-05	4.49 E-07
	Lean meat_v	2.19 E-07	4.06 E-07	4.94 E-06	1.41 E-06
	Minced meat	1.82 E-07	1.35 E-06	2.04 E-06	3.97 E-07

\*For all models,  $R^2 > 0.99$

<sup>1</sup> RMSE < 0.13

<sup>2</sup> RMSE < 0.15

<sup>3</sup> Model 1 and Model 2 were defined in Bains and Langrish (2008) and Akpinar and Dincer (2005). For model 1, RMSE < 0.014 for model 2; RMSE < 0.017

### 3.9. Shrinkage

Shrinkage was expressed as percent change in surface area of samples exposed to air after drying of 270 min. Shrinkage area was found maximum after drying at 70°C and 0.5 m/s and closely followed by drying at 1.7 m/s and 48°C for lean meat and minced meat samples (Table 3.8). The lowest area was observed at the lowest temperature and velocity (48°C, 0.5 m/s). Surface area became smaller as moisture removed. The data in Table 3.8 was average of four samples, two of them being from the same experiment. The thickness reduction was difficult to measure precisely, especially for lean meat samples due to nonuniform thickness through the sample after drying and very small values needed to be measured. It was found to be less than 10% at all drying conditions on average.

When shrinkage area was compared with respect to fiber configuration and structure of sample, a lower shrinkage area was observed in samples with flow normal to fibers (h1), due to lower moisture removal than the other two fiber configurations. Shrinkage at samples with flow along the fibers (h2) was found slightly higher than the shrinkage of the samples with flow normal the fibers, drying along the fibers (v) even though moisture removal was almost the same in both fiber configurations. It was suggested that shrinkage could be affected from moisture removal in a different proportion according to structure and fiber configuration. For minced meat, much lower values were observed than the results of lean meat samples, which agreed with moisture removal figures. Some values were excluded during averaging of shrinkage area since some individual values varied from replications for lean meat samples probably due to nonuniformity of sample or crust formation etc.

**Table 3.8.** Shrinkage percent at different drying conditions

Parameters	Shrinkage %			
	h1	v	h2	Minced meat
48±1°C 0.5 m/s	15.74	17.70	21.90	9.68
48±1°C 1.0 m/s	18.48	20.26	22.10	10.83
48±1°C 1.7 m/s	20.02	22.32	23.76	11.22
70±1°C 0.5 m/s	21.65	23.25	24.81	12.15

### 3.10. Monitoring Properties of Air

Temperature, relative humidity and dew point of inlet air were continuously monitored by a hygrometer and recorded with data logger. Two examples representing drying of minced meat and lean meat samples with h2 fiber configuration are given in Figure 3.8-3.9. Only the data after steady state was attained in the dryer (starting point of drying) was drawn in the graphs. No drastic change was observed in the properties of air during drying of any sample at any drying condition. There was only instant change when turned the dryer off for weight measurement during drying at 70°C (Figures 3.9-3.10). However, the temperature recovered at a very short time. The relative humidity was changed between ~3-7% with respect to different drying condition. These results was used to calculate moisture concentration (kg/m<sup>3</sup>) of inlet air to be used in the model studies.

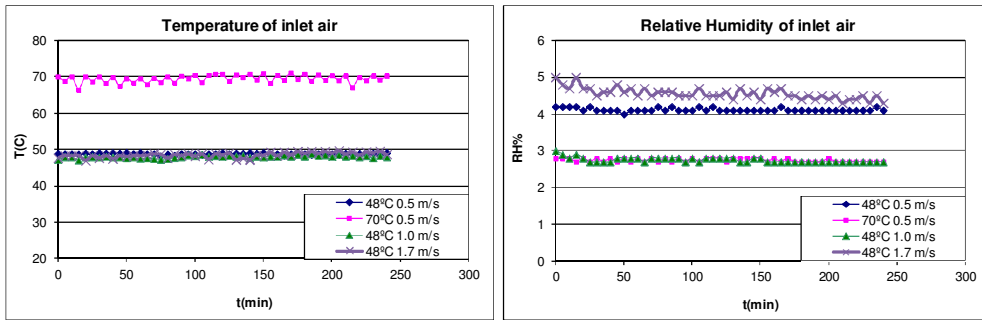


**Figure 3.8.** Temperature and relative humidity of air through drying of minced meat

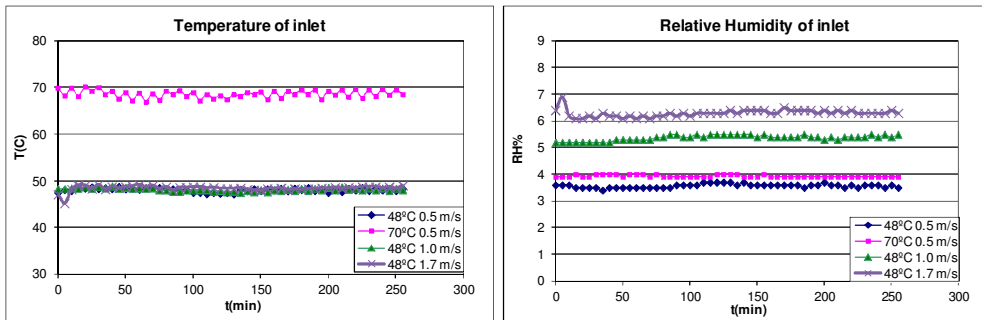


**Figure 3.9.** Temperature and relative humidity of air through drying of lean meat with h2 fiber configuration

## CHAPTER 4

### MODEL RESULTS AND DISCUSSION-1

#### 4.1. Model Results

Two dimensional, non-linear coupled heat and mass transfer equations (2.3-2.5) were solved by finite element method using COMSOL Multiphysics 3.3a with heat transfer module software. Insulated boundary condition at the bottom and convective boundary conditions at the surfaces exposed to air were used in models (Equations 2.6-2.15). For solution, 430 mesh points and 754 triangular elements were used. Model 1 was solved within 3-5 minutes, whereas model 2 was solved within 10-15 minutes by Intel ® Core™ 2Duo CPU 2.2 Ghz with 3GB Ram. FEM software windows for each entry are given in Appendix C.

##### 4.1.1. Prediction of Temperature and Moisture, Comparison of Models

The model results for temperature and moisture distribution of lean meat with h2 fiber configuration after drying of 18000 s at 48°C, 0.5 m/s are given in Figure 4.1-4.2. Other meat samples showed similar temperature and moisture distributions only with a change in maximum and minimum values according to drying conditions and sample type. Two different models showed different trend in temperature distribution. While model 1 gave convex isothermal zones from corners, model 2 gave concave zones from center of bottom (Figure 4.1a-b). Surface profile of temperature distribution in model 2 was similar to previous studies conducted with carrot slices and chicken patties (De Bonis M.V. and Ruocco, 2008; Chen *et al.*, 1999)

Moisture distribution was found to be almost the same as in both models (Figure 4.2a- b). Initial moisture content was accepted as uniform by 76%. The highest moisture removal was observed at the surfaces exposed to air. Almost all the water at the surface was removed after 18000 s, only 0.0003 % water left. However, only 2 % water was removed from bottom center. More moisture retained in the interior of meat sample as expected due to diffusional resistances.

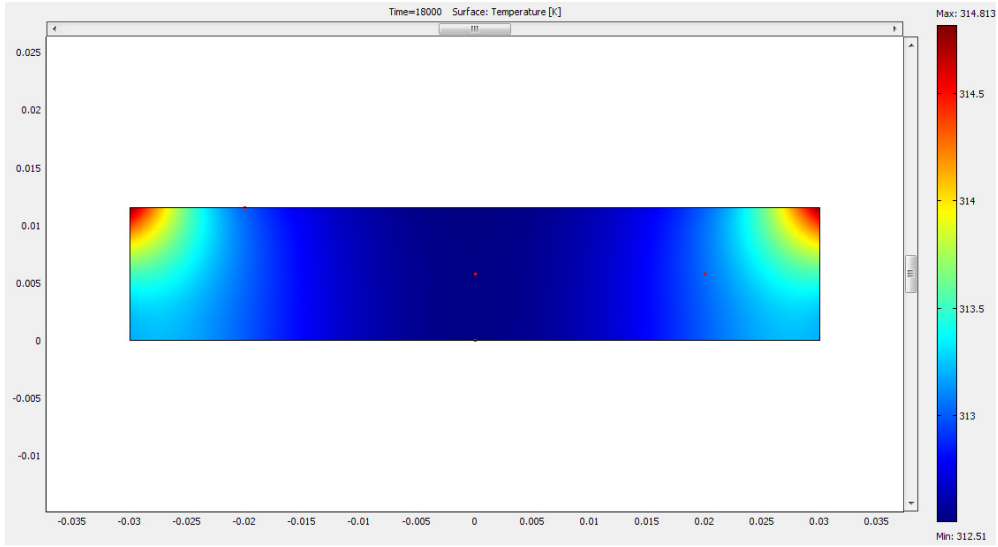


**Figure 4.1a.** 2-D Temperature distribution (x-y direction) in lean meat sample with h2 configuration during drying at  $48 \pm 1^\circ\text{C}$  0.5 m/s at drying time of 18000 s (300 min), according to **model 1**. Red dots represented thermocouple positions used in experiments.

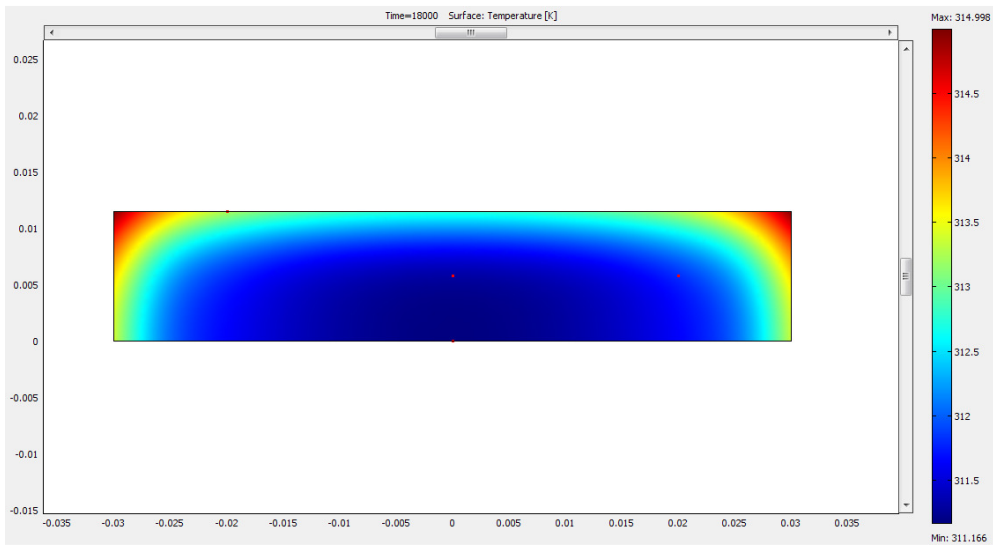


**Figure 4.1b.** 2-D Temperature distribution (x-y direction) in lean meat sample with h2 configuration during drying at  $48 \pm 1^\circ\text{C}$  0.5 m/s at drying time of 18000 s (300 min), according to **model 2**. Red dots represented thermocouple positions used in experiments.



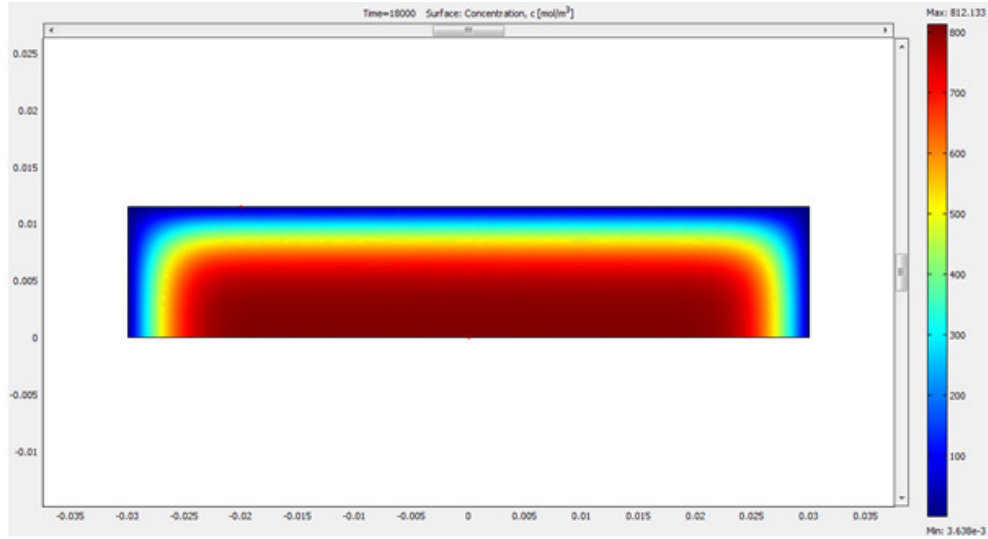


**Figure 4.2a.** 2-D moisture content distribution (x-y direction) in lean meat sample with h2 configuration during drying  $48\pm 1^\circ\text{C}$  0.5 m/s at drying time of 18000 s (300 min), according to **model 1**. Red dots represented thermocouple positions used in experiments.

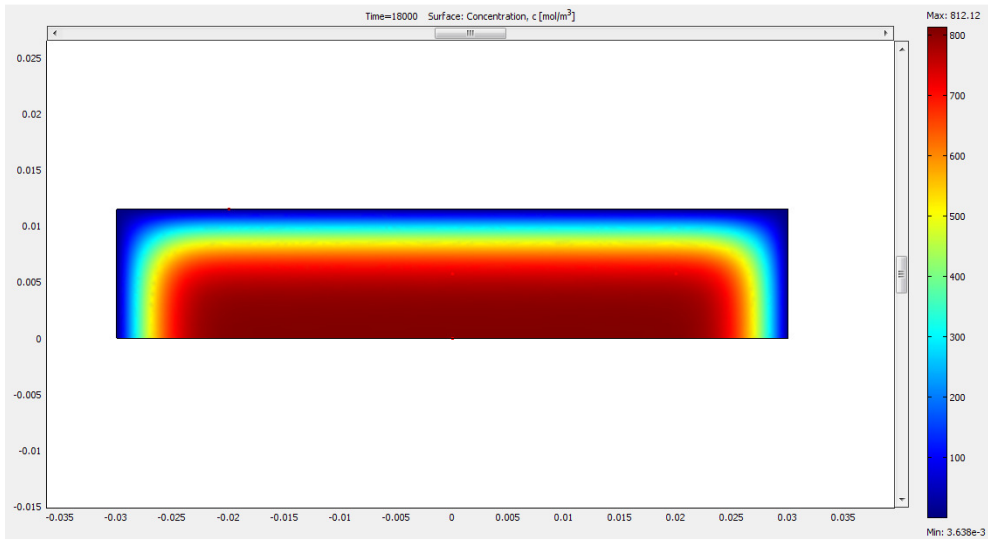


**Figure 4.2b.** 2-D moisture content distribution (x-y direction) in lean meat sample with h2 configuration during drying at  $48\pm 1^\circ\text{C}$  0.5 m/s at drying time of 18000 s (300 min), according to **model 2**. Red dots represented thermocouple positions used in experiments.

Predicted temperature values of minced meat at four locations using model 1 and model 2 were given in Figure 4.3a and 4.3b as example, other meat samples showed similar trend. Temperature at the center (AT1) and temperature at the bottom surface (BT1) showed almost equal values in both models, which was conforming experimental results. Temperature change was high at the surfaces exposed to air flow but slowed down considerably inside the meat causing almost equal temperature at the center and midpoint of bottom surface due to internal resistances like low thermal conductivity. The highest temperature was observed at the surface (BT2), being similar to

experimental results. However, model system gave higher temperature value at the location of AT2 than the temperature at the center (AT1), which was contrary to experimental results. Among four locations, experimental results showed the lowest temperature at location of AT2, which might be resulted from lower heat transfer coefficient at the right hand side of the sample due to change in velocity profile over the sample. A correction factor could be used while calculating heat transfer coefficient for the right hand side of the sample. Aversa *et. al.* (2007, 2008) and De Bonis M.V. and Ruocco (2008) also showed that slightly asymmetric temperature distribution occurred during drying of carrot slice due to flow and velocity profile around the sample. However, this asymmetric distribution of temperature became invisible with higher velocity (2.7 m/s) as in the study of De Bonis M.V. and Ruocco (2008).

The predicted temperatures in model 1 at four locations during drying experiments showed difference at the beginning of drying. However, curves indicating temperature at different locations approached each other with time and homogenized near stationary phase (Figure 4.3a). Such a case occurred in all drying conditions. However, temperature differences with respect to locations were remained the same in model 2 (Figure 4.3b), which was more compatible with experimental results (Figure 3.2).

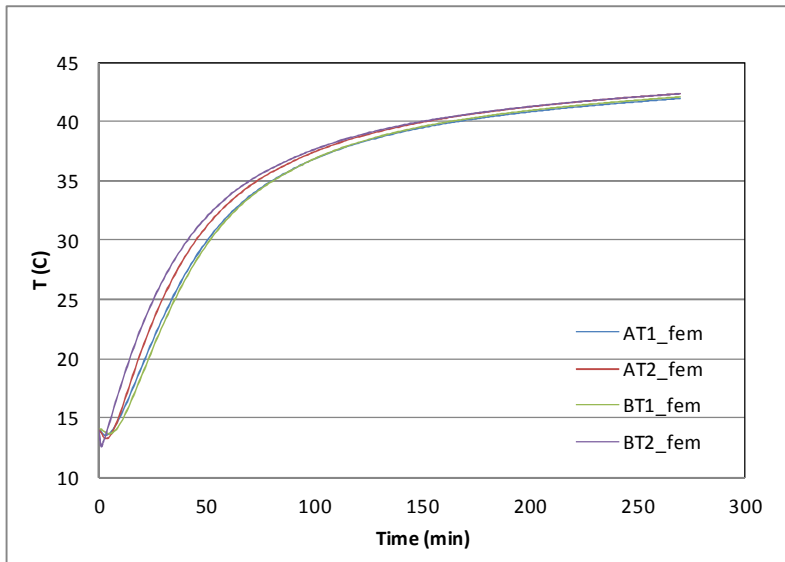


**Figure 4.3a.** Predicted temperature change at four different locations (AT1, AT2, BT1, BT2) in minced meat during drying at  $48 \pm 1^\circ\text{C}$  1.0 m/s by using **model 1**

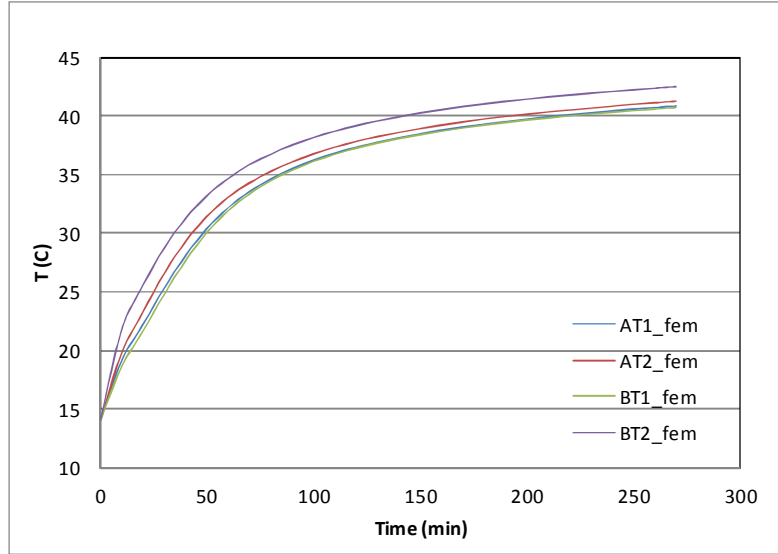


**Figure 4.3b.** Predicted temperature change at four different locations (AT1, AT2, BT1, BT2) in minced meat during drying at  $48 \pm 1^\circ\text{C}$  1.0 m/s by using **model 2**

When compared the results of uncoupled heat transfer model with coupled heat and mass transfer model represented with model 1 and 2, it was observed that model of coupled heat and mass transfer (Figure 4.4.a1-a2) gave better agreement with experimental data than the model using only heat transfer (Figure 4.4.a3) due to exclusion of evaporative heat loss in uncoupled model. The same result was also observed in the study of Chen *et. al.* (1999).

The predicted temperatures of lean meat with h1 fiber configuration at  $48^\circ\text{C}$  and 0.5 m/s using model 1 were given in Figure 4.4.a1. The predicted temperatures of other meat samples at different drying conditions were presented in Appendix D. It was observed that predicted temperatures of model 1 showed a slight decrease at the beginning of drying. At higher velocity of air, the decrease was less observable but at low velocity, low temperature condition ( $48^\circ\text{C}$ , 0.5 m/s), this temperature decrease was remarkable contrary to experimental results. Model 1 gave such a decrease as evaporation was started with initialization of process in solution. However, as the product was heated, moisture started to move to the surface. Once the surface was saturated, then drying started. In order to eliminate this decrease at the beginning in model 1, an 'if' statement was added to program -if temperature exceeded wet bulb temperature, use  $q_v = D_{eff} \times \nabla C \times \lambda s$  as boundary condition at the exposed surfaces-. Thus, this problem of temperature decrease at the beginning of drying was solved (Figure 4.4.a4). However, the computation time increased by 6 h. In model 2, again the same 'if clause' - if temperature exceeded wet bulb temperature, use  $q_v = \lambda * \frac{\partial C}{\partial t}$  - was defined for the subdomain. However, the computation time was at most 15 minutes. Model 2 was found more appropriate to simulate temperature distribution during drying of meat due to requirement of less computation time and compatible temperature distribution with literature as concave isothermal zones from center of bottom.

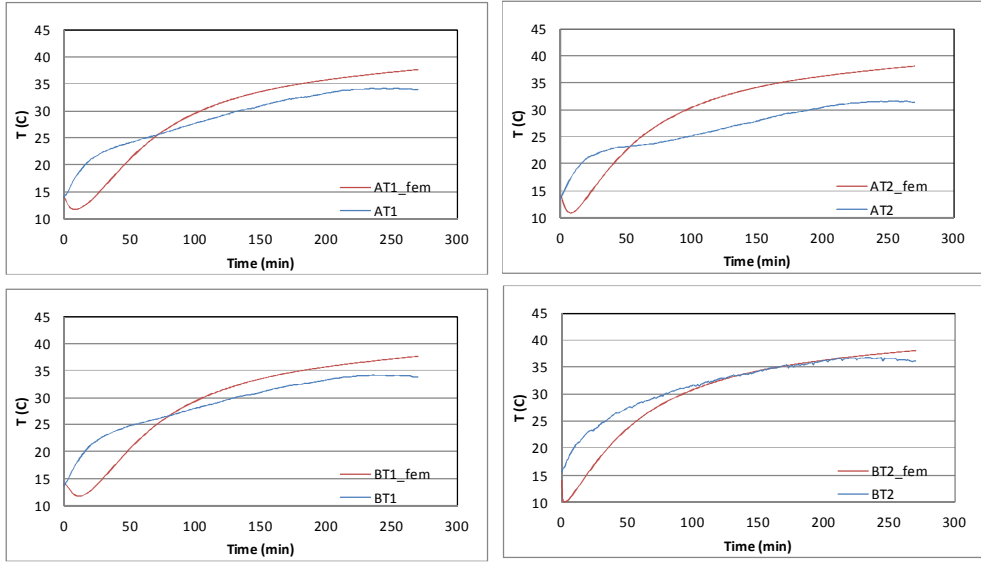


**Figure 4.4.a1.** Temperature change at four different locations (AT1, AT2, BT1, BT2) in lean meat with flow normal to fibers (**h1**) with respect to drying time during drying at  $48\pm 1^\circ\text{C}$  0.5 m/s by using **model 1** (coupled heat & mass)

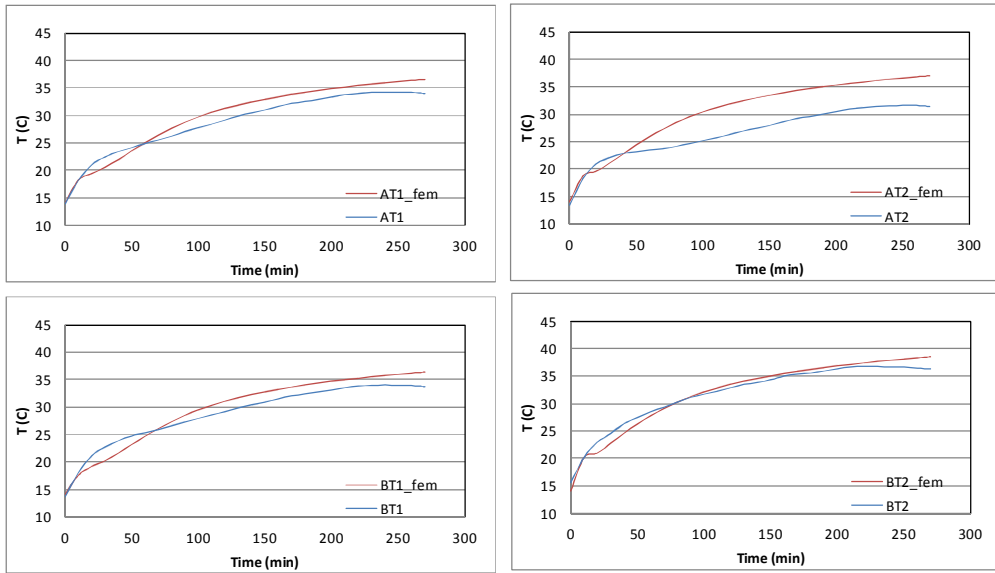


**Figure 4.4.a2.** Temperature change at four different locations (AT1, AT2, BT1, BT2) in lean meat with flow normal to fibers (**h1**) with respect to drying time during drying at  $48\pm 1^\circ\text{C}$  0.5 m/s by using **model 2** (coupled heat & mass)

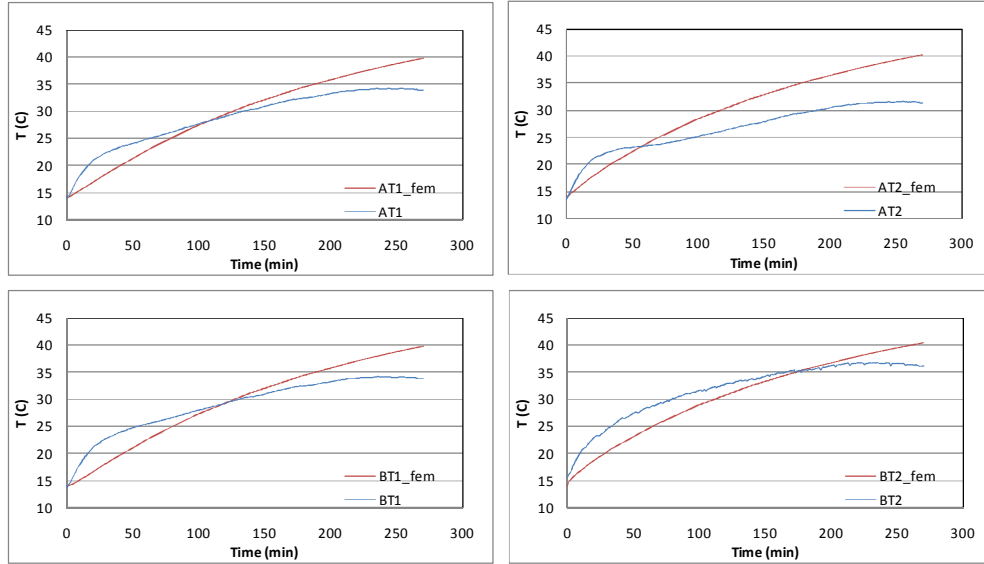


**Figure 4.4.a3.** Temperature change at four different locations (AT1, AT2, BT1, BT2) in lean meat with flow normal to fibers (**h1**) with respect to drying time during drying at  $48\pm 1^\circ\text{C}$   $0.5\text{ m/s}$  as a result of uncoupled heat transfer equation.

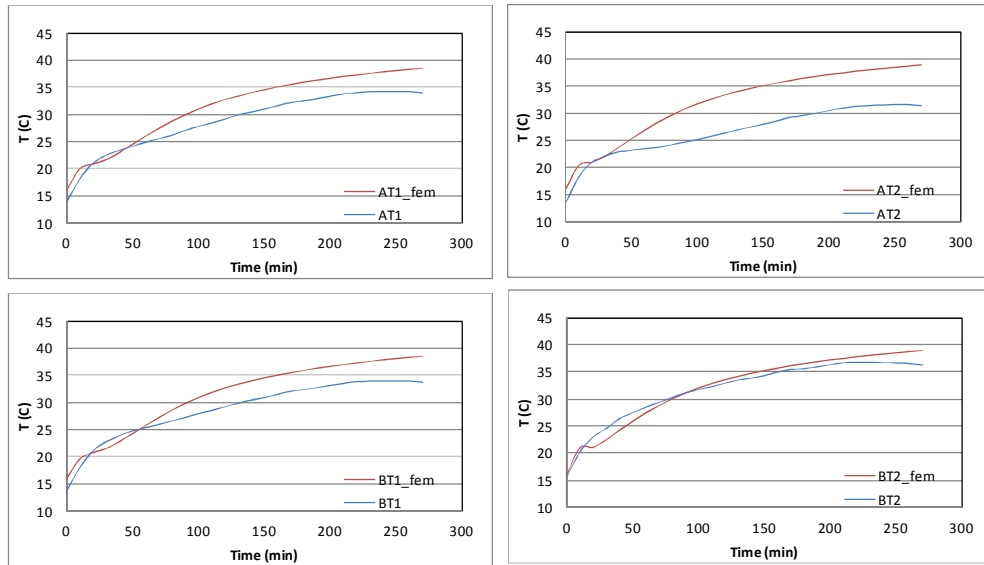


**Figure 4.4.a4.** Temperature change at four different locations (AT1, AT2, BT1, BT2) in lean meat with flow normal to fibers (**h1**) during drying at  $48\pm 1^\circ\text{C}$   $0.5\text{ m/s}$  by using model 1 boundary conditions after wet bulb temperature was reached

The predicted temperatures of model 2 were given in Figure 4.3.a2 and Figure 4.5-4.8. Model 2 showed slightly higher temperatures than experimental data in all conditions. The difference below 10% with experimental was accepted as indication of good fit in the study of Boquet *et al.* (1978). According to this information, root mean square error (RMSE) values less than  $4^\circ\text{C}$  after drying at  $48^\circ\text{C}$  and  $5.5^\circ\text{C}$  after drying at  $70^\circ\text{C}$  are in acceptable range. At the highest attainable temperature

of dryer (70°C 0.5 m/s), predicted (the legend written as fem) and experimental values were found almost equal in all types of samples (lean meat with h1, h2, v fiber configuration and minced meat) (Figure 4.5a, 4.6b, 4.7b, 4.8b). RMSE values are also less than 5.5°C (Table 4.1) and in acceptable range except for AT2 location. Linear regression results of predicted temperature versus observed showed R<sup>2</sup> (coefficient of determination) greater than 0.99 during drying at 70°C 0.5 m/s (Table 4.1). At higher velocity (48°C, 1.0 and 1.7 m/s), it seemed that the difference between predicted and experimental values became more distinguishable (Figure 4.5b-c, 4.6c-d, 4.7c-d, 4.8c-d) than low velocity condition (0.5 m/s) for lean meat samples. In general, RMSE values were still in acceptable range, less than 4°C except for AT2 but closer to the limit than drying at 0.5 m/s. Anova studies also resulted in no significant difference between observed and predicted except for the predicted AT2 values but calculated P value became also closer to confidence interval (0.05) at higher velocity of air (48°C 1.0 m/s and 1.7 m/s). Predicted values were the same as experimental at the beginning of drying but became higher at later stages in conditions with higher velocity. This was probably resulted from less moisture removal, so less heat loss due to latent heat of evaporation was observed in predicted than in experimental results which was discussed in section 4.3.

Minced meat showed better agreement with experimental values than lean meat samples for all fiber configurations (Figure 4.8a-d). Except for AT2 location, RMSE of predicted temperature of minced meat with respect to observed was less than 2.5°C in general, much lower than the acceptance limit (4°C for drying at 48°C and 5.5°C for drying at 70°C) but in lean meat samples it can be as high as 4.8°C (Table 4.1). It was seen that predicted moisture removal curves also fit the experimental results in minced meat. As a result of difference measure test, it could be said that main component of difference between predicted and observed temperature was from systematic error which meant that model could be improved for lean meat samples.

**Table 4.1.** RMSE; root mean square error for predicted vs. experimental temperature of meat samples during drying at different conditions

Sample	Drying parameter	RMSE (°C)				R <sup>2</sup>
		AT1	AT2	BT1	BT2	
Lean meat_h1	48°C 0.5 m/s	1.6	4.4	1.7	1.1	0.947-0.991
	48°C 1.0 m/s	2.6	4.3	2.2	1.7	0.934-0.970
	48°C 1.7 m/s	3.8	4.8	3.7	4.8	0.891-0.919
	70°C 0.5 m/s	1.6	5.6	1.8	1.0	0.990-0.999
Lean meat_h2	48°C 0.5 m/s	1.2	3.1	4.5	0.9	0.982-0.996
	48°C 1.0 m/s	2.9	4.7	2.6	3.2	0.951-0.977
	48°C 1.7 m/s	2.5	3.8	1.9	2.6	0.953-0.976
	70°C 0.5 m/s	2.3	6.1	2.7	3.5	0.985-0.998
Lean meat_v	48°C 0.5 m/s	1.3	2.9	1.6	1.0	0.930-0.985
	48°C 1.0 m/s	2.7	4.6	2.3	3.8	0.920-0.961
	48°C 1.7 m/s	2.7	4.0	2.4	3.7	0.922-0.940
	70°C 0.5 m/s	1.1	3.7	1.1	1.9	0.991-0.997
Minced meat	48°C 0.5 m/s	1.0	4.2	1.3	1.1	0.945-0.984
	48°C 1.0 m/s	2.0	3.7	1.8	1.9	0.958-0.979
	48°C 1.7 m/s	1.3	3.0	1.2	1.7	0.954-0.982
	70°C 0.5 m/s	2.5	4.7	2.2	2.3	0.989-0.998

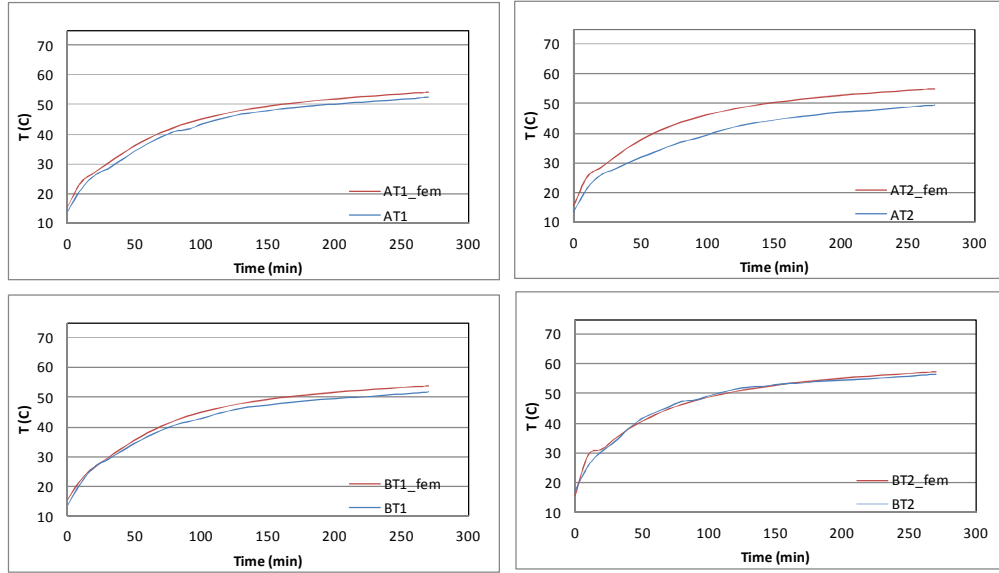


**Figure 4.5a.** Temperature change at four different locations (AT1, AT2, BT1, BT2) in lean meat with flow normal to fibers ( $h_1$ ) with respect to drying time during drying at  $70\pm 1^\circ\text{C}$  0.5 m/s by using model 2

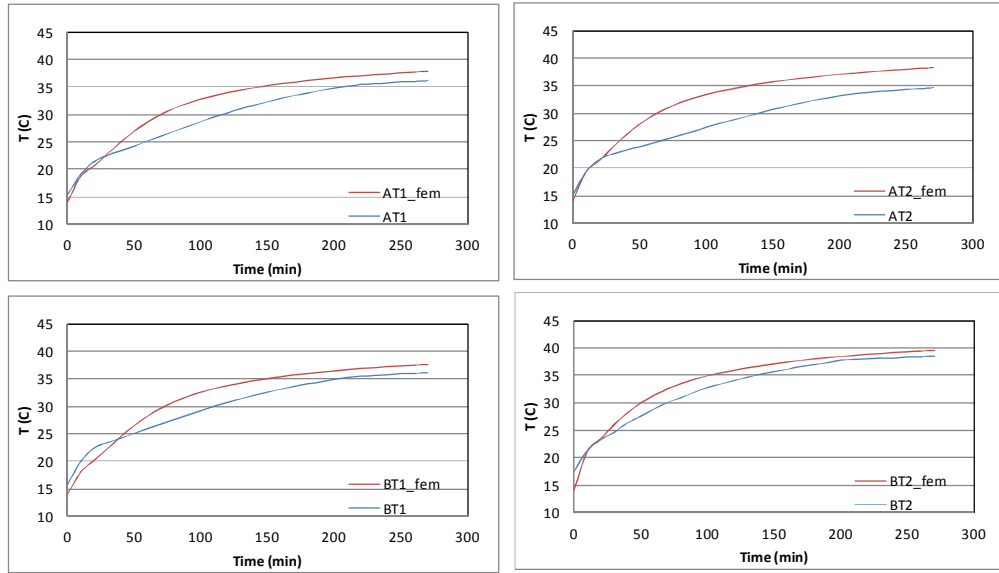


**Figure 4.5b.** Temperature change at four different locations (AT1, AT2, BT1, BT2) in lean meat with flow normal to fibers ( $h_1$ ) with respect to drying time during drying at  $48\pm 1^\circ\text{C}$  1.0 m/s by using model 2

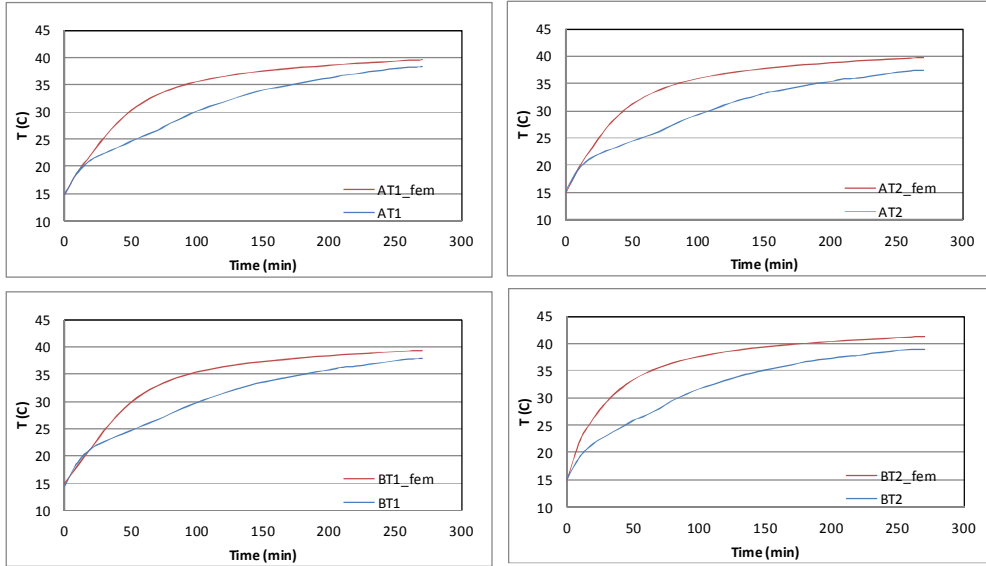


**Figure 4.5c.** Temperature change at four different locations (AT1, AT2, BT1, BT2) in lean meat with flow normal to fibers (**h1**) with respect to drying time during drying at  $48 \pm 1^\circ\text{C}$  1.7 m/s by using model 2

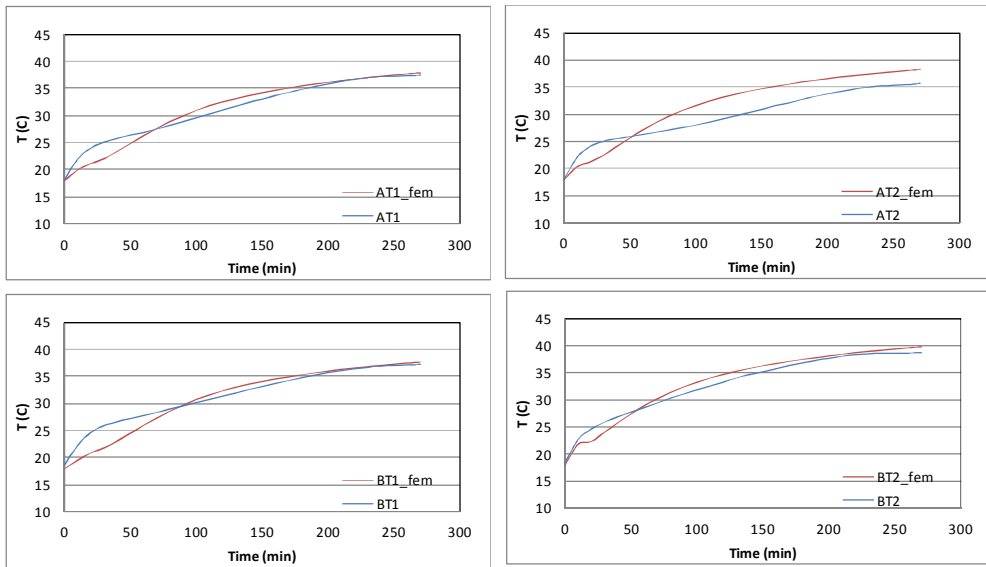


**Figure 4.6a.** Temperature change at four different locations (AT1, AT2, BT1, BT2) in lean meat with flow normal to fibers, drying along the fibers (**v**) with respect to drying time during drying at  $48 \pm 1^\circ\text{C}$  0.5 m/s by using model 2



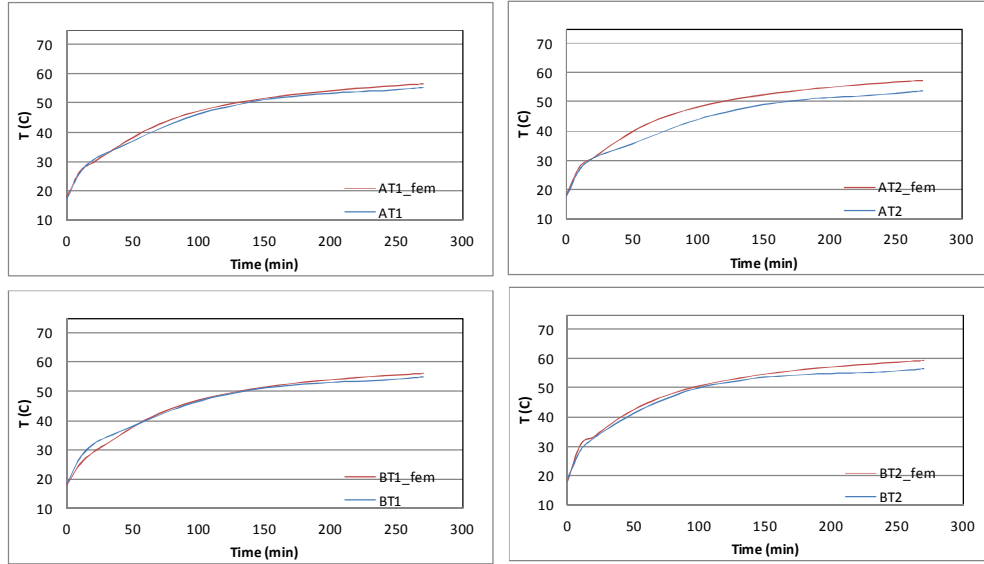


**Figure 4.6b.** Temperature change at four different locations (AT1, AT2, BT1, BT2) in lean meat with flow normal to fibers, drying along the fibers ( $v$ ) with respect to drying time during drying at  $70\pm 1^\circ\text{C}$  0.5 m/s by using model 2

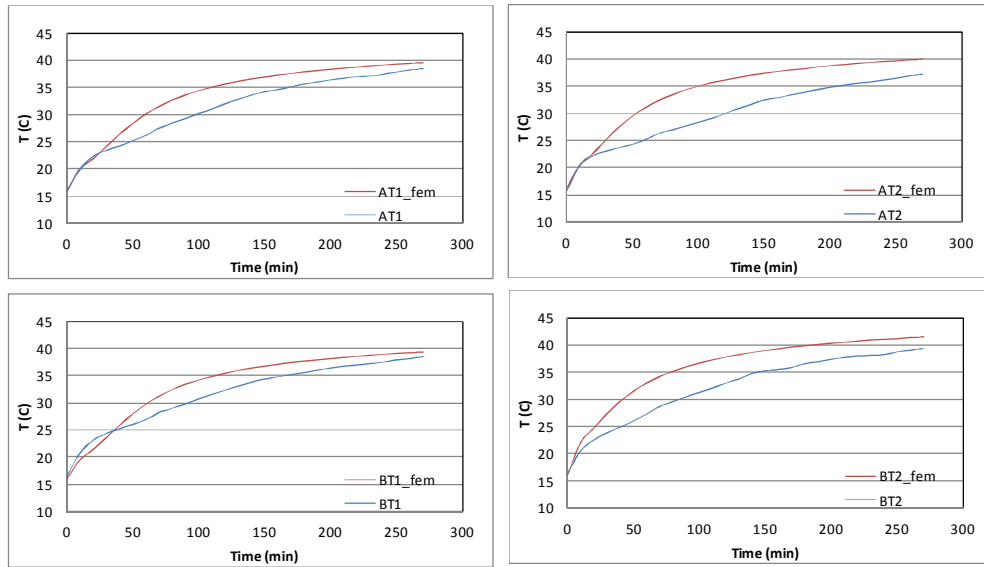


**Figure 4.6c.** Temperature change at four different locations (AT1, AT2, BT1, BT2) in lean meat with flow normal to fibers, drying along the fibers ( $v$ ) with respect to drying time during drying at  $48\pm 1^\circ\text{C}$  1.0 m/s by using model 2

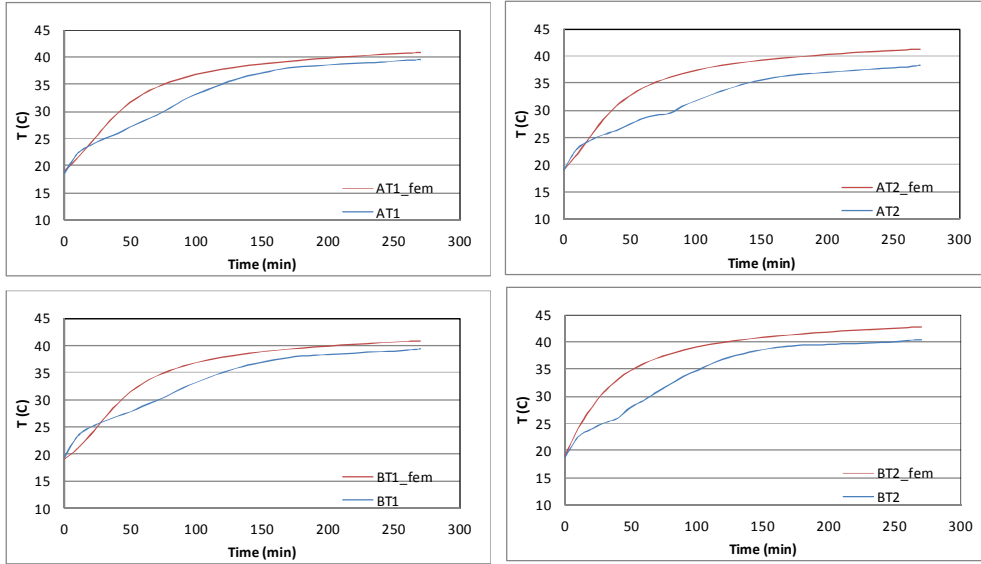


**Figure 4.6d.** Temperature change at four different locations (AT1, AT2, BT1, BT2) in lean meat with flow normal to fibers, drying along the fibers (**v**) with respect to drying time during drying at  $48 \pm 1^\circ\text{C}$  1.7 m/s by using model 2

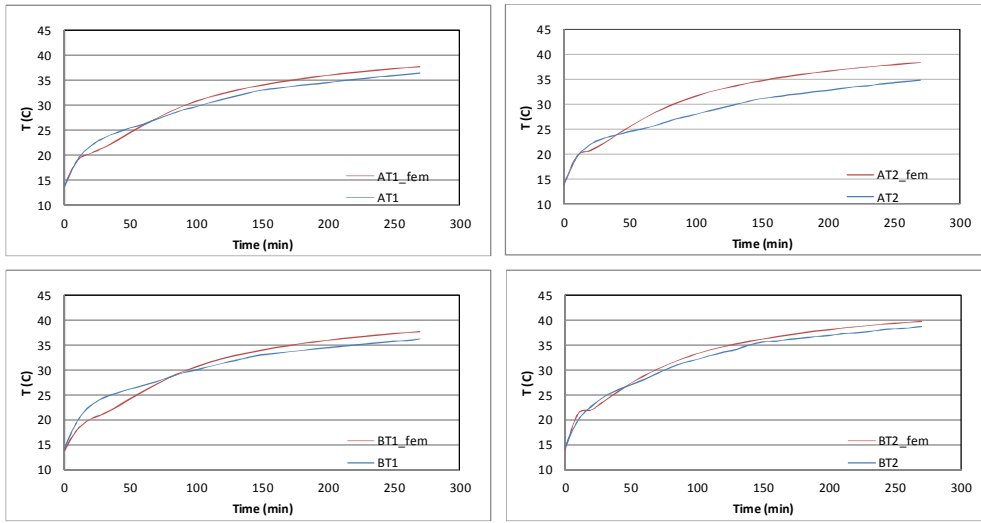


**Figure 4.7a.** Temperature change at four different locations (AT1, AT2, BT1, BT2) in lean meat with flow along to fibers (**h2**) with respect to drying time during drying at  $48 \pm 1^\circ\text{C}$  0.5 m/s by using model 2

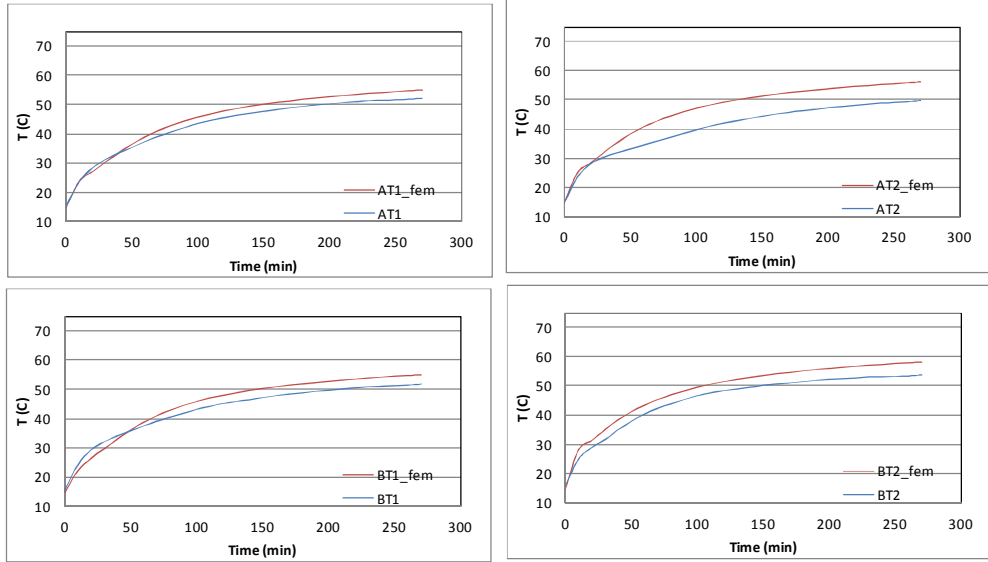


**Figure 4.7b.** Temperature change at four different locations (AT1, AT2, BT1, BT2) in lean meat with flow along to fibers (**h2**) with respect to drying time during drying at  $70\pm 1^\circ\text{C}$  0.5 m/s by using model 2

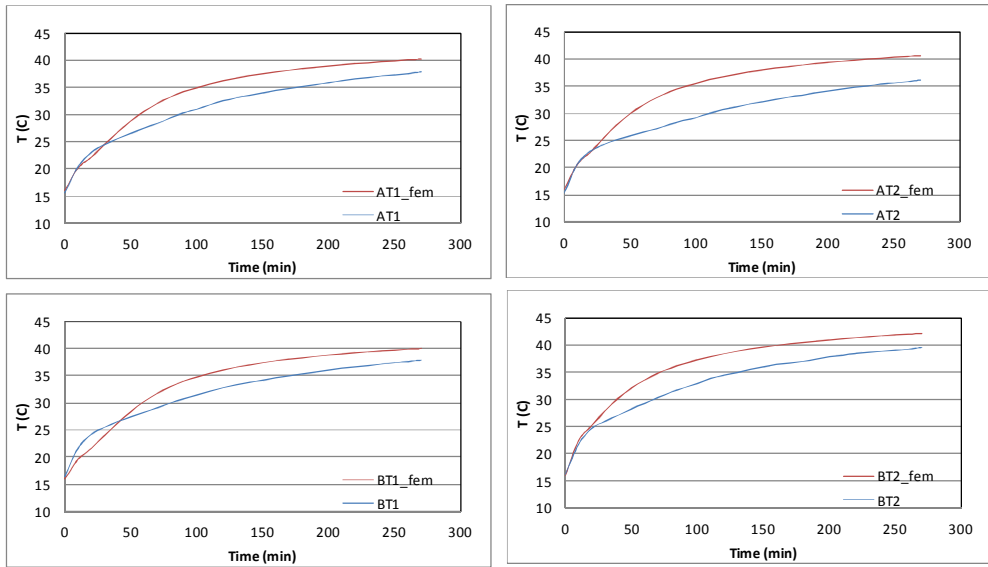


**Figure 4.7c.** Temperature change at four different locations (AT1, AT2, BT1, BT2) in lean meat with flow along to fibers (**h2**) with respect to drying time during drying at  $48\pm 1^\circ\text{C}$  1.0 m/s by using model 2

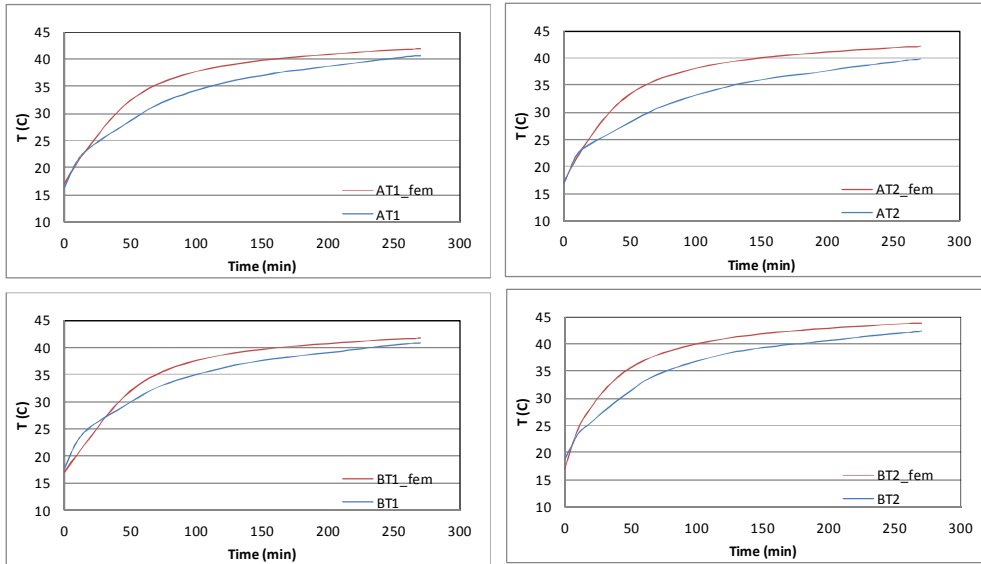


**Figure 4.7d.** Temperature change at four different locations (AT1, AT2, BT1, BT2) in lean meat with flow along to fibers (**h2**) with respect to drying time during drying at  $48 \pm 1^\circ\text{C}$  1.7 m/s by using model 2

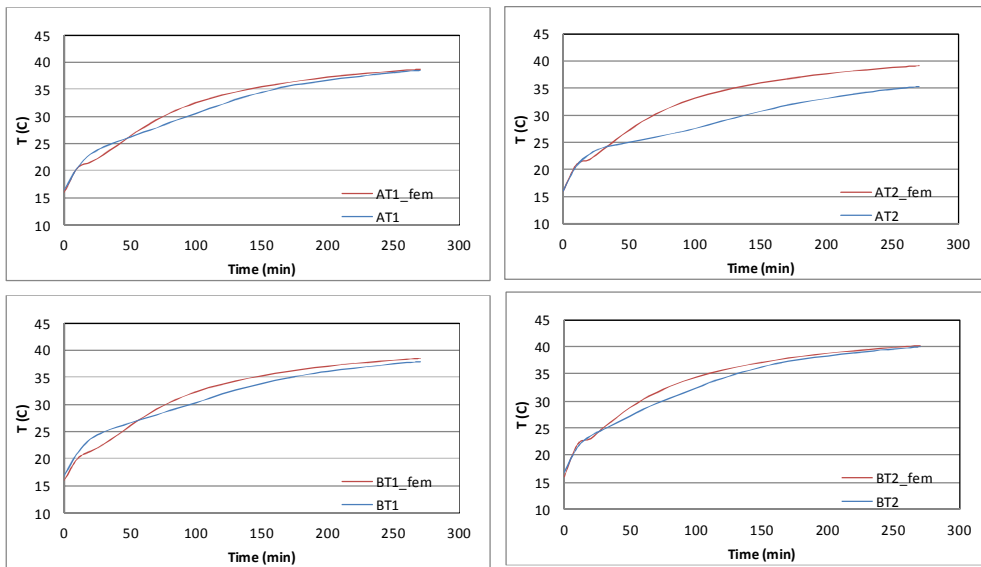


**Figure 4.8a.** Temperature change at four different locations (AT1, AT2, BT1, BT2) in minced meat with respect to drying time at  $48 \pm 1^\circ\text{C}$  0.5 m/s by using model 2

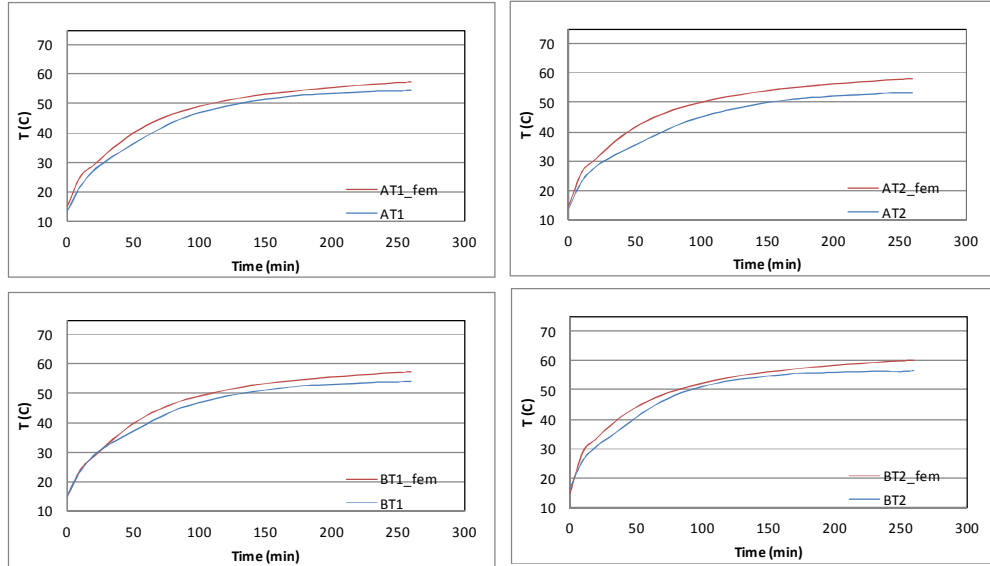


**Figure 4.8b.** Temperature change at four different locations (AT1, AT2, BT1, BT2) in **minced** meat with respect to drying time at  $70\pm 1^\circ\text{C}$  0.5 m/s by using model 2

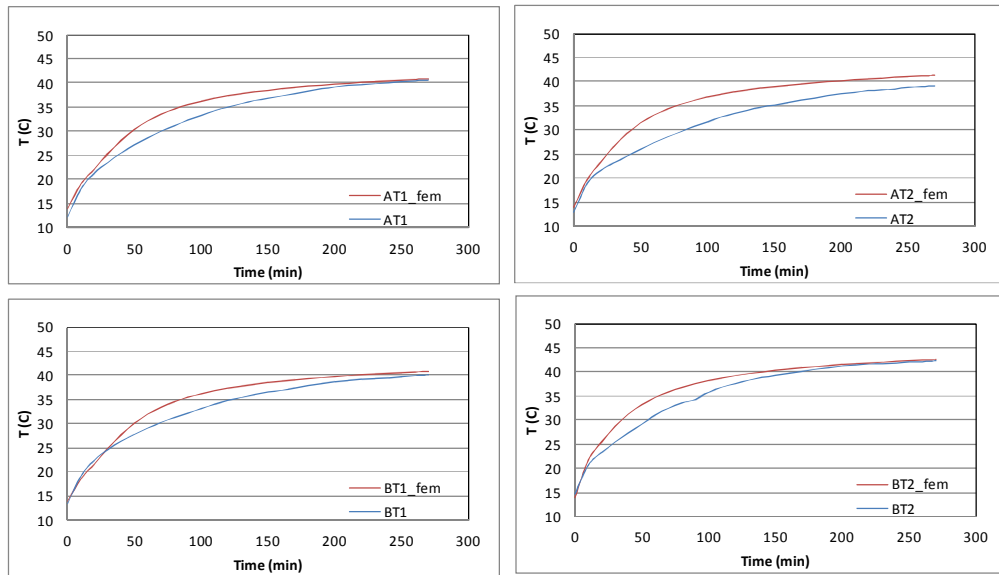


**Figure 4.8c.** Temperature change at four different locations (AT1, AT2, BT1, BT2) in **minced** meat with respect to drying time at  $48\pm 1^\circ\text{C}$  1.0 m/s by using model 2

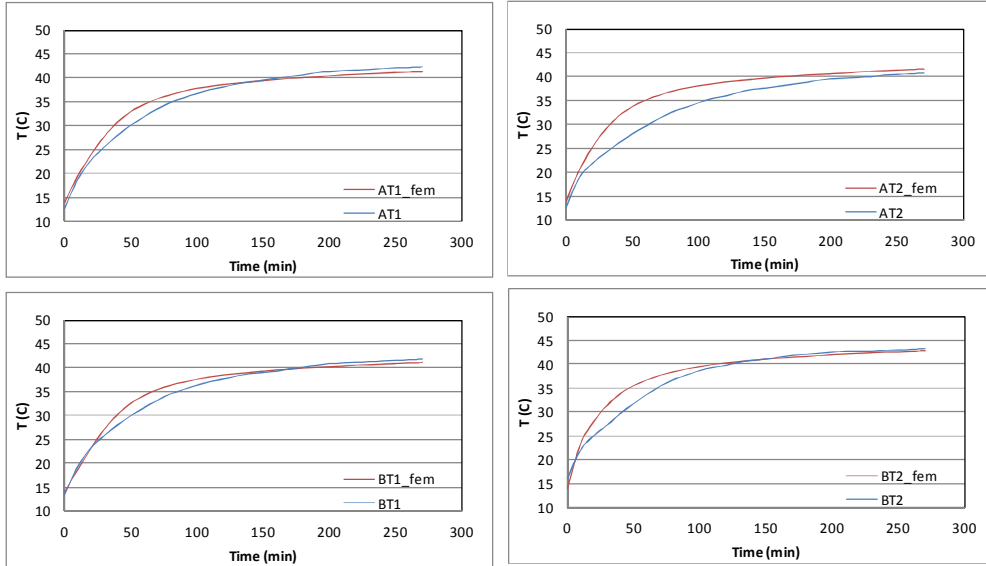


**Figure 4.8d.** Temperature change at four different locations (AT1, AT2, BT1, BT2) in minced meat with respect to drying time at  $48\pm 1^\circ\text{C}$  1.7 m/s by using model 2

Among four locations, experimental results showed the lowest temperature at location of AT2, which might be due to lower heat transfer coefficient at the right hand side of the sample due to lower velocity values at that side. However, results of model gave higher value. A correction factor could be used while calculating heat transfer coefficient at right hand side of the sample. When it was assumed that there was no heat transfer on right hand side of sample, predicted values for also AT2 agreed with experimental results (Figure 4.10).

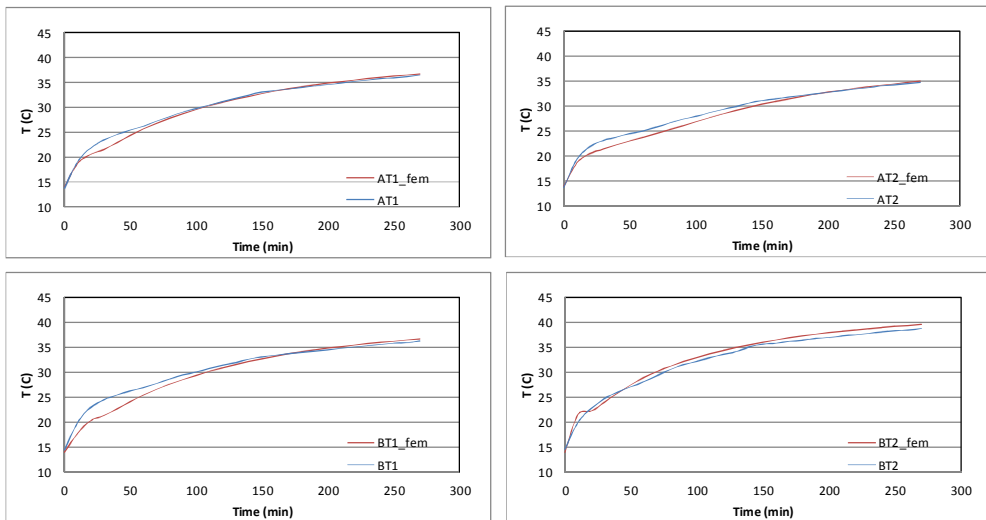


**Figure 4.9.** Temperature change at four different locations (AT1, AT2, BT1, BT2) in lean meat with flow along to fibers ( $h_2$ ) with respect to drying time during drying at  $70\pm 1^\circ\text{C}$  0.5 m/s by using model 2 with no convection at right side of sample

#### 4.1.2. Prediction of Moisture Content

Predicted and experimental moisture values at the end of 270 min drying were given in Table 4.2 and moisture content changes of different meat samples at four drying conditions tested with respect to time were given in Figure 4.10-4.13. In all drying conditions, where lean meat with different fiber configuration was used, predicted moisture content was equal (at higher velocity-1.7 m/s or high temperature-70°C condition) or slightly lower (at 48°C, 0.5 m/s) than experimental within the first hour of drying (Figure 4.10-4.13). However, at later stages moisture removal in model system was slowed down and became lower than experimental values. Initial slower moisture loss in experimental results might be due to sample heating especially at low velocity of drying air. Predicted moisture profiles was actually compatible with predicted temperature profiles since predicted temperature values were almost the same at the beginning but became higher at later stages due to less water removal. Similar results were obtained in the study of Aversa *et al.* (2007) (Figure 4.14). In the study of Curcio *et al.* (2008) who modelled coupled heat and mass transfer with flow in carrot drying, similar moisture content change was found in the model system with experimental data at 50°C while incompatibility was observed at lower drying temperatures such as 35°C.

In all cases, the difference between final predicted and experimental values were less than 10% (Table 4.2). Linear regression results of predicted moisture versus observed showed R<sup>2</sup> value greater than 0.99. Anova studies also resulted in no significant difference between observed and predicted except for drying of lean meat with v fiber configuration at 48°C, 1.0 m/s and 1.7 m/s. Root mean square error (RMSE) values in Table 4.3 indicated that lean meat samples h1 configuration showed better agreement (lower RMSE) than other configurations (h2, v) with experimental. However, the model system for minced meat showed almost the same values as experimental data (Figure 4.13) and much lower RMSE values than lean meat samples. In general, the error with experimental did not exceed 1.5% (wet base) for minced meat while it could be as large as 5% in lean meat samples. Only for drying at 48°C and 1.0 m/s, slightly higher predicted moisture content was observed than experimental in minced meat probably due to difference in structure or composition of sample. The difference between final predicted and experimental moisture values was in a range of 0-2.7% for minced meat while it was 2.5-7.9% for lean meat samples (Table 4.2). It could be concluded that predicted moisture content of minced meat was in good agreement with experimental. As a result of difference measure test, it could be said that the main component of difference between predicted and observed was from systematic error which meant that the model could be improved for lean meat samples. For this reason, different diffusion coefficients might be applied for lean meat samples in order to obtain a better agreement. Anisotropic nature might also be applied for diffusion coefficient using the same ratios as in anisotropic thermal conductivity values.

**Table 4.2.** Experimental and predicted moisture content % at the end of drying (270 min)

Drying <sup>1</sup>	h1		h2		v		minced	
	Exp. <sup>2</sup>	Pred. <sup>3</sup>	Exp.	Pred.	Exp.	Pred.	Exp.	Pred.
48°C 0.5 m/s	51.6	54.4	48.0	54.0	48.5	53.9	52.0	53.6
48°C 1.0 m/s	51.1	53.6	46.8	52.9	44.4	53.1	50.0	52.7
48°C 1.7 m/s	46.6	52.9	45.5	52.1	45.3	52.4	52.3	52.3
70°C 0.5 m/s	45.1	48.8	40.7	48.6	41.3	48.0	47.5	47.6

<sup>1</sup>initial moisture content is 76%

<sup>2</sup>Experimental

<sup>3</sup>Predicted

**Table 4.3.** RMSE; root mean square error of predicted moisture content (dry base) of meat samples at different drying conditions ( $R^2 > 0.99$  in all cases)

Sample	RMSE (g water/g bds)* drying at			
	48°C 0.5 m/s	48°C 1.0 m/s	48°C 1.7 m/s	70°C 0.5 m/s
Lean meat_h1	0.07	0.066	0.17	0.097
Lean meat_h2	0.15	0.15	0.17	0.22
Lean meat_v	0.15	0.24	0.21	0.2
Minced meat	0.057	0.11	0.028	0.032

\*In order to find RMSE as a wet base percentage, the value should be multiplied by 24 (percentage of BDS found experimentally)

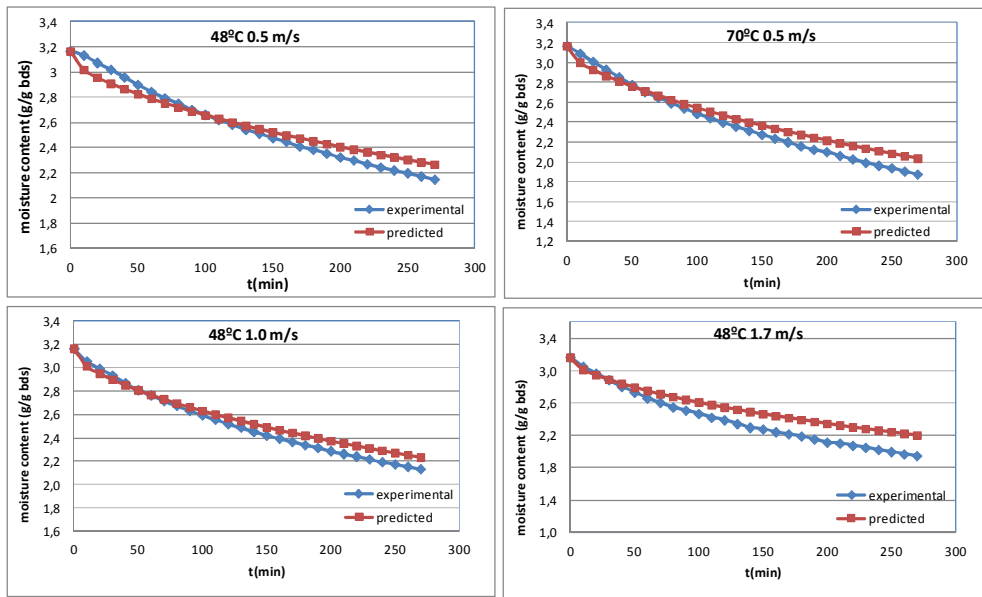


**Figure 4.10.** Moisture content change in lean meat with flow normal to fibers (**h1**) with respect to drying time



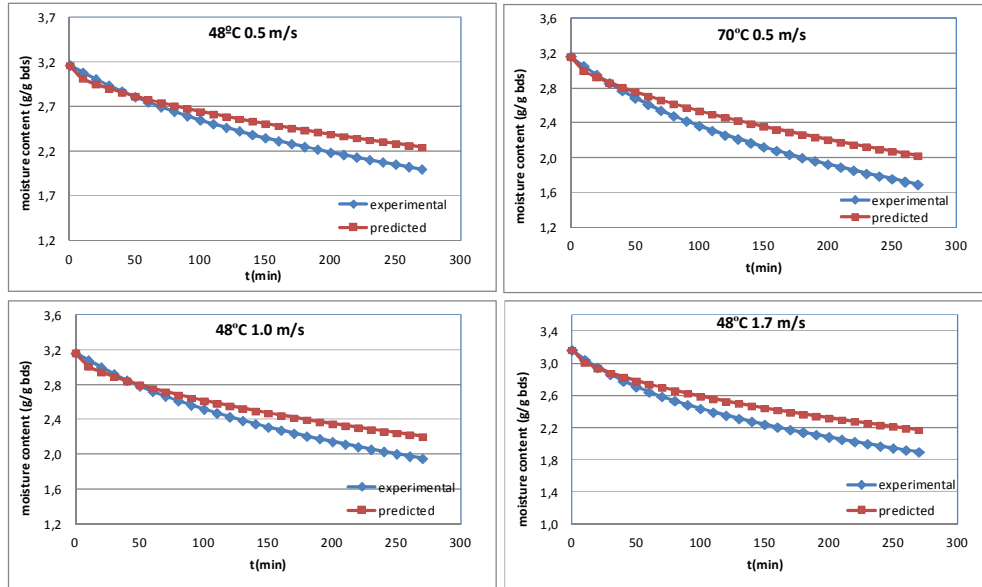


**Figure 4.11.** Moisture content change in lean meat with flow along to fibers (h2) with respect to drying time

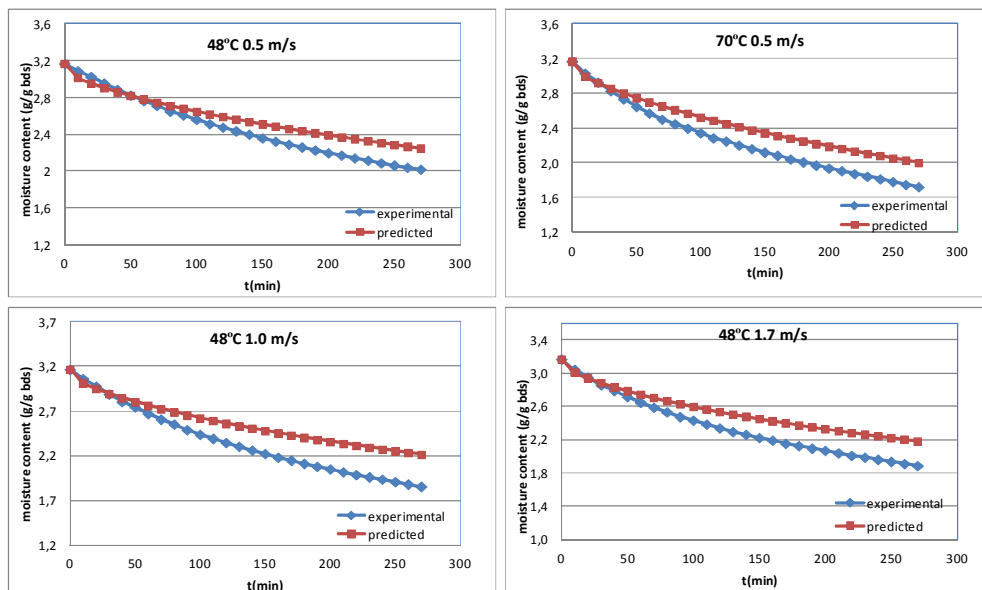


**Figure 4.12.** Moisture content change in lean meat with flow normal to fibers, drying along the fibers (v) with respect to drying time

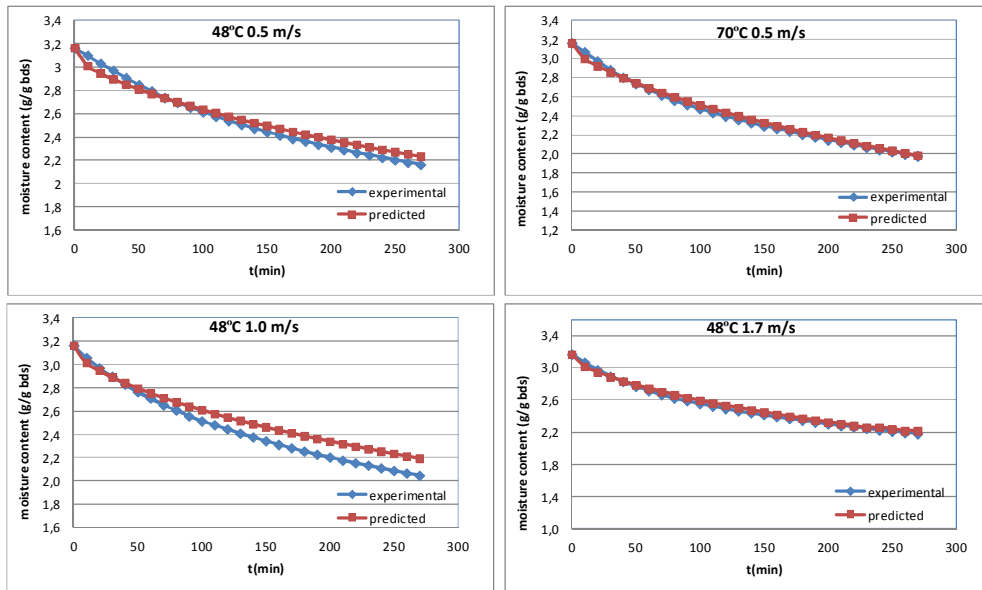


Figure 4.13. Moisture content change in minced meat with respect to drying time

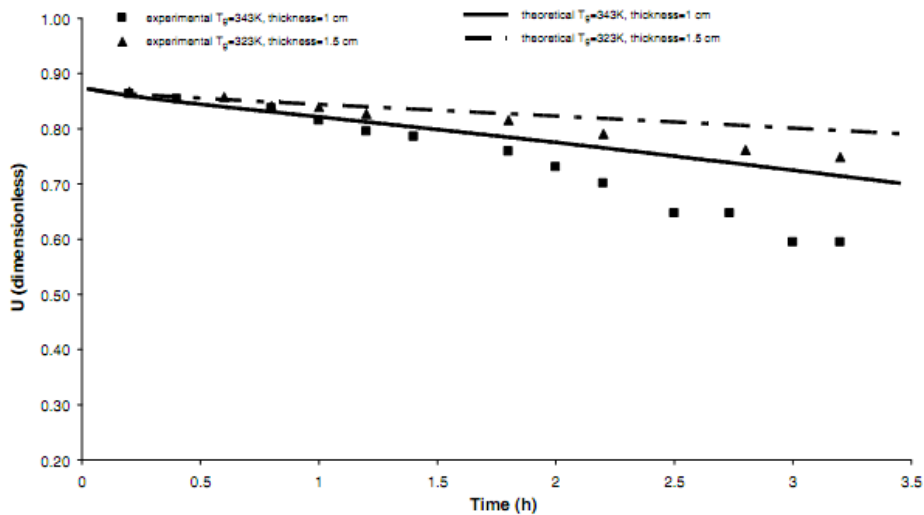
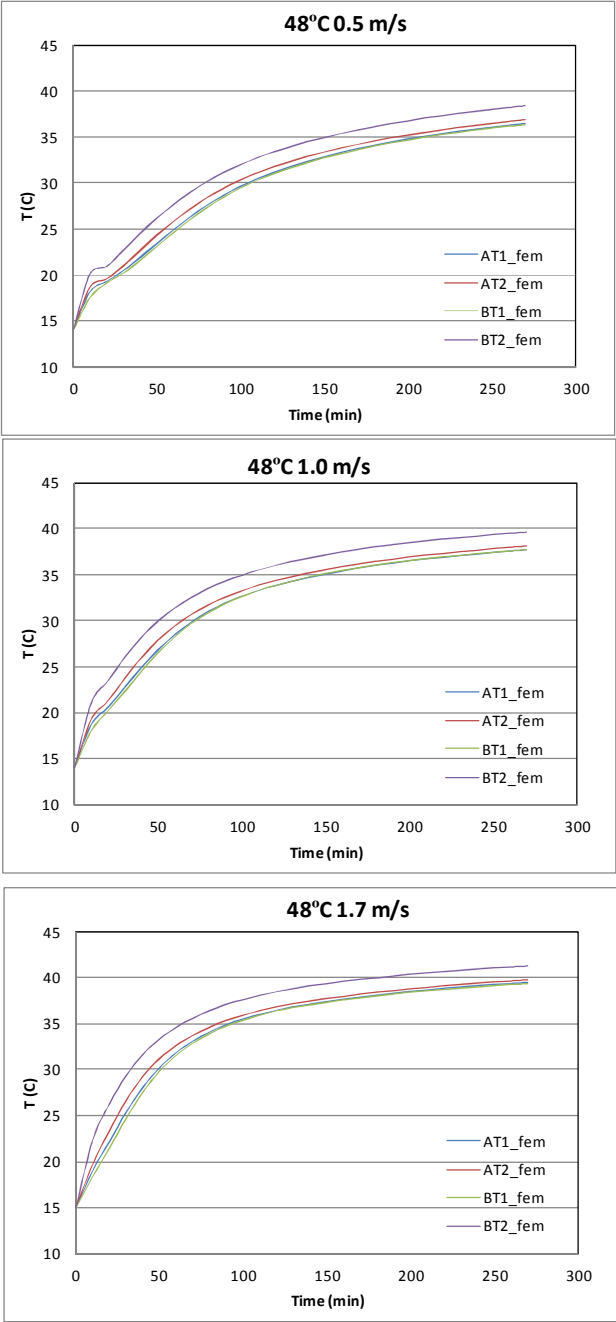


Figure 4.14. Change in predicted and experimental moisture content in the research of Aversa *et. al.* (2007)

#### 4.2. Effect of Flow Rate on Predicted Temperature and Moisture Content of Samples

The time required to reach a stationary temperature value became shorter with higher velocities of air since steeper temperature curves were observed with higher velocity (Figure 4.15-4.16). However, the temperature at stationary phase did not change drastically with higher velocities. Experimentally, it was found that temperature increased slightly with increasing air velocity under unsteady state conditions, which was also agreed with model data since until reaching stationary phase, rate of change in temperature was increasing with increasing velocity (Figure 4.16).

The change in predicted moisture content with respect to time was found to be different with different air flow rates at the same air temperature. Moisture removal in the model system was higher with increasing flow rate (Figure 4.17), compatible with experimental findings. However, temperature was more effective parameter on moisture removal than flow rate since even the highest attainable velocity in the dryer (48°C, 1.7 m/s) resulted in lower moisture loss than drying at 70°C, 0.5 m/s. This conclusion also agreed with experimental results.



**Figure 4.15.** Predicted temperature change at four different locations in lean meat with flow normal to fibers (**h1**) with respect to drying time (results of model 2)

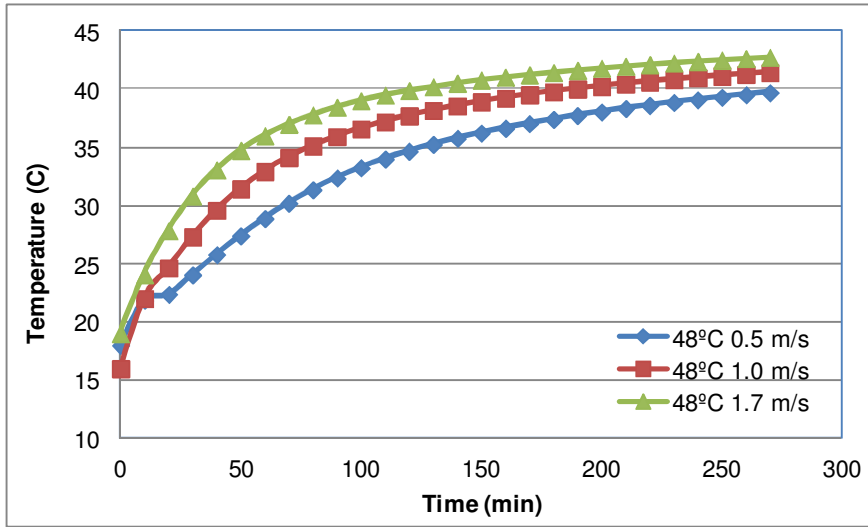


**Figure 4.16.** Predicted temperature change at the surface (BT2) in lean meat with flow normal to fibers, drying along the fibers ( $v$ ) with respect to drying time

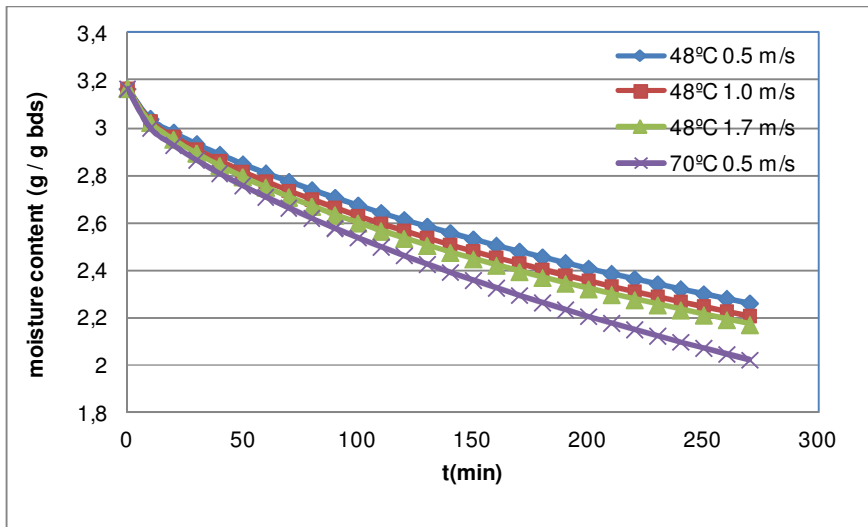


**Figure 4.17.** Change in predicted moisture content in lean meat with flow normal to fibers, drying along the fibers ( $h_2$ ) with respect to drying time

### 4.3. Effect of Fiber Direction and Structure on Predicted Temperature and Moisture Content

The predicted temperatures of different meat samples at the same drying conditions were presented in Figure 4.18-4.21. In all drying conditions, predicted temperature values of minced meat were higher than temperature of lean meat with all fiber configurations and the lowest temperature was observed in lean meat with h1 fiber configuration, which was compatible result with experimental data. Thus, it could be concluded that anisotropic representation of thermal conductivity as explained in section 2.4 (Table 2.3), was applicable to define real food systems in finite element modeling. Temperature of lean meat with h2 fiber configuration was almost the same as v configuration at low temperature and flow rate condition (48°C, 0.5 m/s). However, at 70°C, temperature of v fiber configuration was slightly higher than h2 configuration (Figure 4.19), whereas at higher velocity as 1.0 m/s (Figure 4.20) h2 started to exceed temperature of v fiber configuration and almost reached minced meat temperature at the highest velocity (1.7 m/s) (Figure 4.21).

In all drying conditions, similar moisture content change was observed in both lean meat and minced meat samples (Figure 4.22). Experimental moisture content of different meat samples at the same drying condition showed 4-7% difference at the end of 270 min (Table 4.2). However, this difference was less than 1.2% for predicted moisture content. It could be concluded that no difference was observed according to fiber configuration and structure in predicted moisture, which was not compatible with experimental. This was resulted from that the same diffusion coefficient was used in all types of samples. Even the diffusion coefficient equation taken from literature (Equation 2.18; Trujillo *et al.*, 2005) used in the model was a function of sample temperature, it was seen that diffusion coefficient did not change so much with respect to temperature within the range reached in the model even though slight change in temperature profiles were observed with different fiber configurations and isotropic samples. In order to observe anisotropy effect in moisture content change, it was suggested that different diffusion coefficients according to structure should be used in the model.

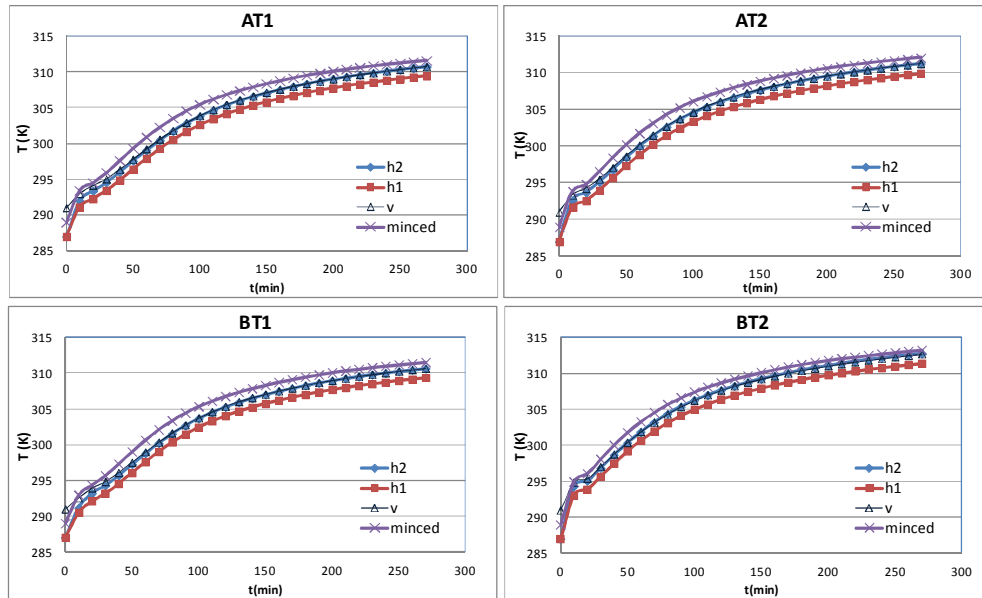


**Figure 4.18.** Predicted temperature change at four different locations with respect to drying time during drying at  $48 \pm 1^\circ\text{C}$  0.5 m/s by using model 2

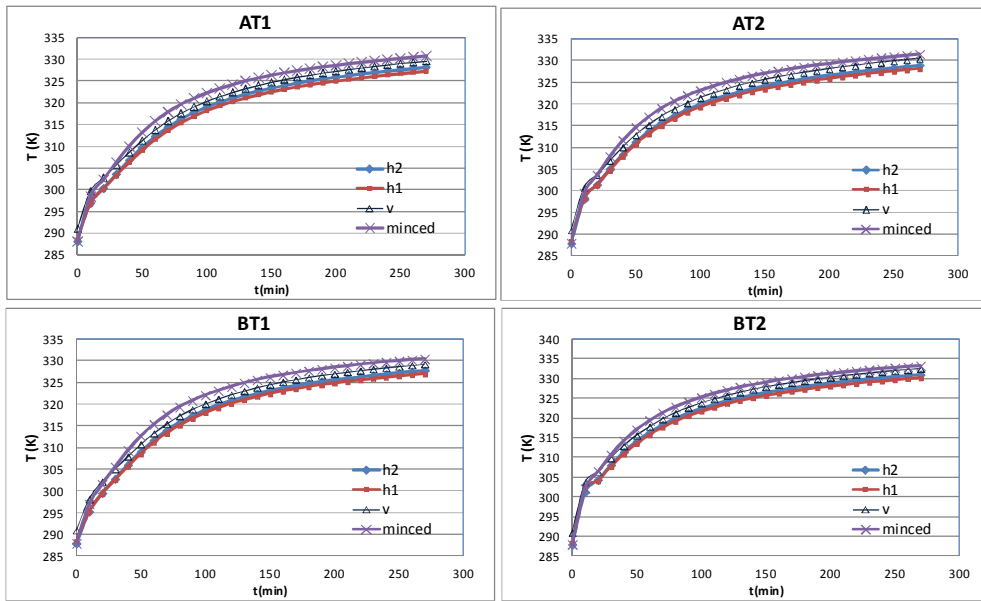


**Figure 4.19.** Predicted temperature change at four different locations with respect to drying time during drying at  $70\pm 1^\circ\text{C}$  0.5 m/s by using model 2

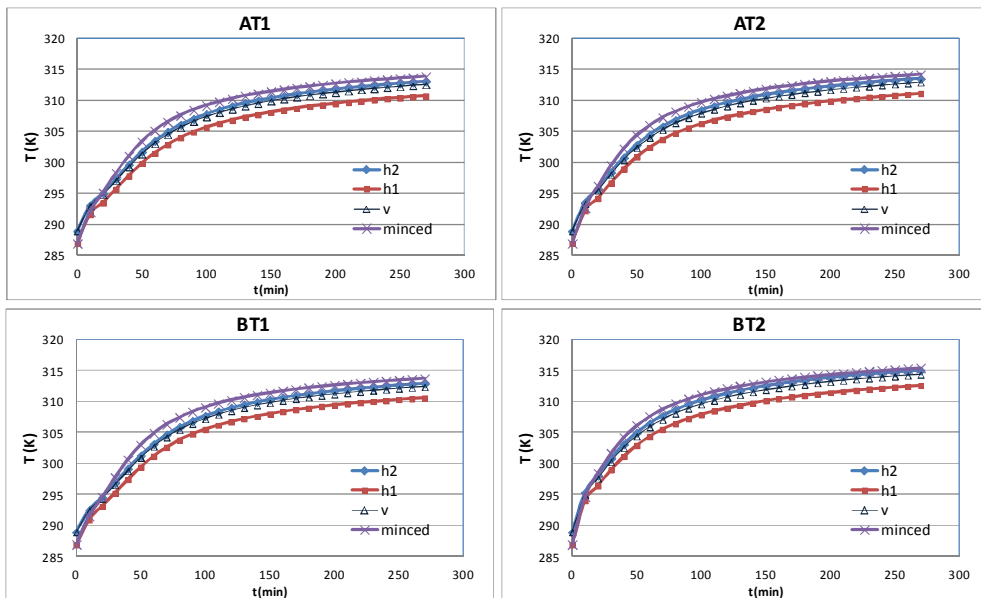


**Figure 4.20.** Predicted temperature change at four different locations with respect to drying time during drying at  $48\pm 1^\circ\text{C}$  1.0 m/s by using model 2

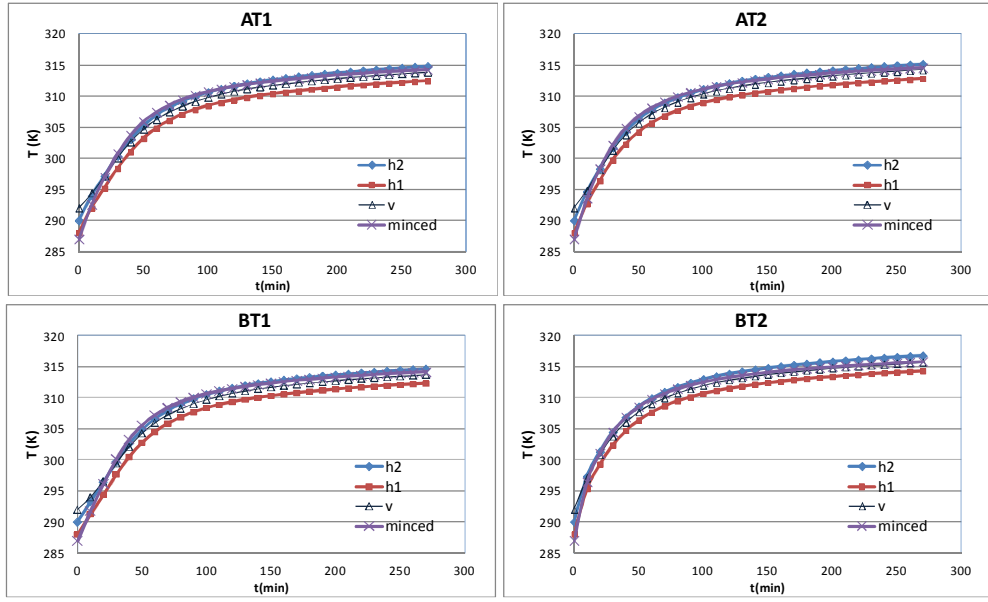


**Figure 4.21.** Predicted temperature change at four different locations with respect to drying time during drying at  $48\pm 1^\circ\text{C}$  1.7 m/s by using model 2

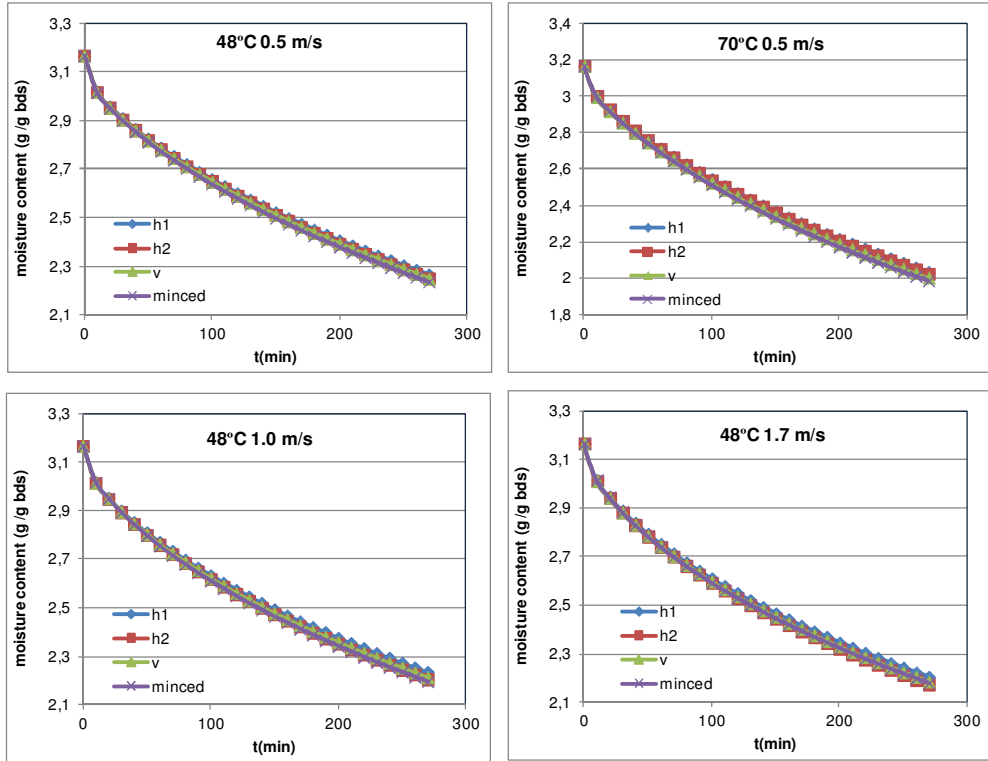


**Figure 4.22.** Predicted moisture content change with respect to drying time





## CHAPTER 5

### MODEL RESULTS AND DISCUSSION-2

#### 5.1. Redefinition of Diffusion Coefficient

Selection of most proper diffusivity is very important for all processes in which mass transfer is significant. Different approaches either experimental, analytic or numerical, were applied for calculation of diffusion coefficient (Baini and Langrish, 2008; Akpınar and Dincer, 2005; Ruiz-Lopez and Garcia-Alvarado, 2007, Ramos *et al.*, 2010). Diffusion coefficient found by equation (3.4) in chapter 3.6 based on simplified version of Fick's law for sufficiently long drying times was not enough to be used in the model studies since it did not depend on any process parameters like temperature or moisture content. This single number for diffusion coefficient could be valid only for the end of drying, not enough to model overall process as supported also in the studies of Chen (2007). When finite element model defined in material and methods chapter (section 2.4) was applied using diffusion coefficients found in section 3.8 model A (Table 3.7), the predicted moisture loss became too much and far from experimental results (Figure 5.1). The reason of this was the use of a single value for diffusion coefficient that can be only valid through the end of drying, during overall process. Actually, diffusion coefficient should be much lower at the beginning of drying than the one calculated due to low temperature of sample. Thus, diffusion coefficient was redefined as a function of temperature and/or moisture content (dry base) of sample using equations below (5.1-5.2). As well as there were different definitions of diffusion coefficient for dependence to moisture content (Azzouz *et al.*, 2002; Baini and Langrish, 2008; Ruiz-Lopez and Garcia-Alvarado, 2007), all were based on exponential dependence. Definition used by Baini and Langrish (2008) study was chosen since it was found as the most proper definition within seven different models for diffusion coefficient.

$$D_{eff} = D_0 * \exp\left(-\frac{E_a}{RT}\right) \quad (5.1)$$

$$D_{eff} = D_0 * \exp\left(-\frac{E_a}{RT}\right) (A * \exp(X) + B) \quad (5.2)$$

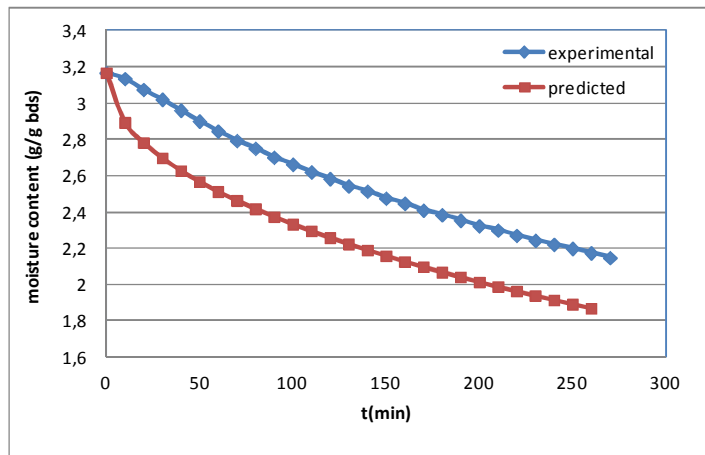


**Figure 5.1.** Moisture content change in lean meat with flow normal to fibers (h1) with respect to drying time during drying at  $48 \pm 1^\circ\text{C}$  0.5 m/s

In most of the studies consisted of diffusivity estimation based on Arrhenius type equation (5.1), sample temperature was assumed constant due to ease of handling (Hernandez *et al.*, 2000; Lewicki *et al.*, 1998; Mulet, 1994; Rosello *et al.*, 1992; Ruiz-Lopez *et al.*, 2004). Even though drying medium temperature or average temperature of sample throughout the drying by taking integral with respect to time (Trujillo *et al.*, 2005) were used in literature for T in Arrhenius equation of diffusivity, it was not totally correct approach as stated in studies of Chen (2007) and Ruiz-Lopez and Garcia-Alvarado (2007). Thus, in this study sample temperature was considered. Diffusivity definitions above (Equation 5.1, 5.2) were replaced  $D_{\text{eff}}$  in equation (3.5). Equation 3.5 was redefined as below,

$$\frac{X-X_{eq}}{X_i-X_{eq}} = \frac{8}{\pi^2} \sum_{n=0}^{\infty} \frac{1}{(2n+1)^2} \exp\left(- (2n+1)^2 \pi^2 \frac{D_0 \cdot \exp\left(-\frac{E_a}{RT}\right)}{4L^2} t\right) \quad (5.3)$$

$$\frac{X-X_{eq}}{X_i-X_{eq}} = \frac{8}{\pi^2} \sum_{n=0}^{\infty} \frac{1}{(2n+1)^2} \exp\left(- (2n+1)^2 \pi^2 \frac{D_0 \cdot \exp\left(-\frac{E_a}{RT}\right) (A \cdot \exp(X) + B)}{4L^2} t\right) \quad (5.4)$$

Unknown coefficients of equations were solved by nonlinear regression tool (MinErr) of MathCAD in a way that standard error between predicted and experimental dimensionless moisture content near zero and coefficient of determination near 1 by taking first 20 terms into consideration in equations (5.3-5.4). Example of statements written to MathCAD was presented in AppendixE. Temperature and moisture data were taken from the experimental results of drying at the highest temperature (70°C) since change in temperature and moisture were the highest at that condition. Temperature at the surface (BT2 location) was accepted as T in equations (5.1) and (5.2) again due to higher change observed with respect to time than in other locations. In other conditions noise coming from experimental data would be higher since change in temperature and moisture was much lower. Trujillo *et al.* (2005) also suggested that surface temperature could represent sample temperature. When diffusivity was calculated by using both temperature at the center and at the surface, it was observed only maximum 0.2 fold change occurred in the results (Appendix F), but standard error became 2.5 fold greater so taking temperature at the surface was more appropriate (Table F.1).

The diffusivity definitions for lean meat samples with three different fiber configurations were presented below (Table 5.1). The diffusivity values found for lean meat samples were in agreement with literature as in a range of  $1 \cdot 10^{-11}$  –  $5.56 \cdot 10^{-10}$  (Panagiotou *et al.*, 2004). Standard error was less than 0.01 and coefficient of determination was greater than 0.99 in all three fiber configurations. Since the model results using diffusivity definition found in the study of Trujillo *et al.* (2005) was in good agreement with experimental data of minced meat (figured in chapter 4), new definitions of diffusivity were not found necessary for minced meat.

**Table 5.1.** Diffusivity equations of lean meat with three fiber configurations

Diffusivity equation	Standard error	R <sup>2</sup>	Eqn.no
$D(h1) = 4.356 \cdot \exp\left(-\frac{6960}{T}\right)$	0.0041	0.998	5.5a
$D(h1) = 1.48 \cdot \exp\left(-\frac{7019}{T}\right) (0.074 \exp(X) + 2.875)$	0.0014	0.999	5.5b
$D(h2) = 1.807 \cdot \exp\left(-\frac{6568}{T}\right)$	0.0099	0.996	5.6a
$D(h2) = 1.153 \cdot \exp\left(-\frac{6902}{T}\right) (0.132 \exp(X) + 3.395)$	0.0028	0.998	5.6b
$D(v) = 0.047 \cdot \exp\left(-\frac{5369}{T}\right)$	0.01	0.995	5.7a
$D(v) = 1.141 \cdot \exp\left(-\frac{6899}{T}\right) (0.161 \exp(X) + 3.229)$	0.0094	0.995	5.7b

## 5.2. Model Construction

The model 2 defined in Chapters 2.4 and 4.1 was used in FEM studies since it produced better agreement with experimental and needed less computation time. For heat capacity, density, heat transfer coefficients and thermal conductivity, the same values/definitions as defined in section 2.4 were used. For diffusivity of lean meat, anisotropic definitions represented below (Table 5.2) were introduced to FEM in order to be able to observe anisotropy effect on moisture loss which could not be observed when only one diffusivity definition from literature (Trujillo *et al.*, 2005) for all lean meat samples and minced meat was used as stated in Chapter 4.5.

**Table 5.2.** Anisotropic diffusivity values used in the model

For <b>h1</b> configuration	For <b>h2</b> configuration	For <b>v</b> configuration
$D = \begin{bmatrix} D_{h1} & 0 \\ 0 & D_{h1} \end{bmatrix}$	$D = \begin{bmatrix} D_{h2} & 0 \\ 0 & D_{h1} \end{bmatrix}$	$D = \begin{bmatrix} D_v & 0 \\ 0 & D_{h1} \end{bmatrix}$

## 5.3. Prediction of Temperature

Diffusivity definition (Equation 5.2) as a function of both sample temperature and moisture content (dry base) gave slightly more compatible results with experimental data than diffusivity definition as a function of only sample temperature (Figure 5.2). Thus equations (5.5b-5.6b-5.7b) were used in the rest of modelling studies presented in this chapter.

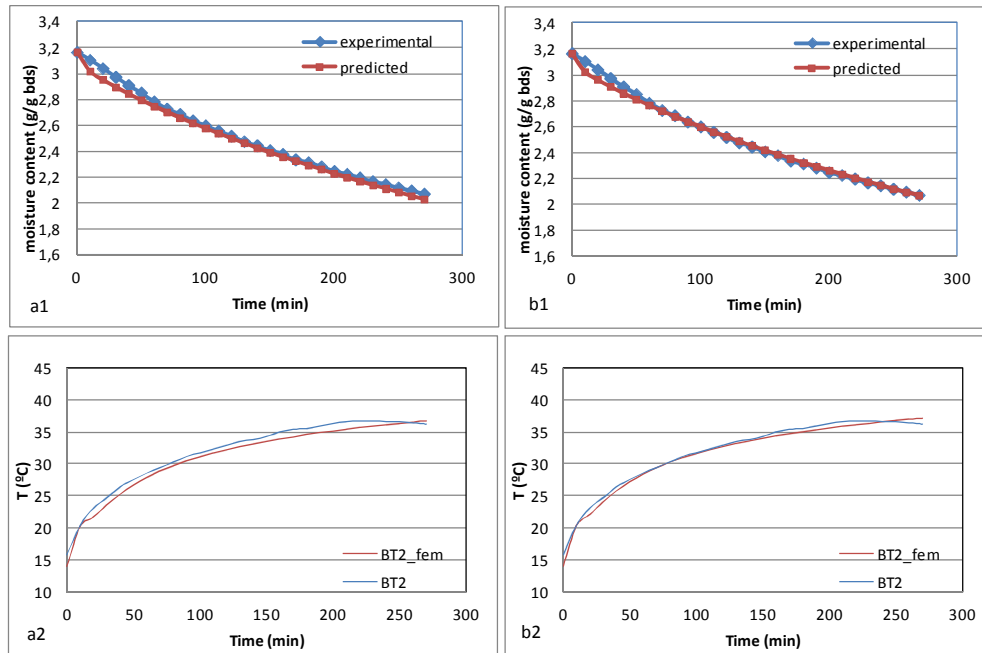


**Figure 5.2.** Change in temperature and moisture content of lean meat with flow normal to fibers (h1) with respect to time during drying at  $48 \pm 1^\circ\text{C}$  and  $0.5 \text{ m/s}$ . For a and b, equation (5.5a) and (5.5b) were used respectively.

The difference between surface temperature and other locations became larger than the results obtained using single isotropic diffusivity in chapter 4 (Figure 5.3). The predicted temperature distribution was symmetric according to (0,0) point as in Figure 4.1b. However, experimental results showed that slightly asymmetric temperature distribution probably due to lower velocity profile at the right hand side of the sample due to flow as discussed in previous chapter section 4.2. On the other hand, the difference between predicted and experimental temperature at AT2 location became lower than found in chapter 4 (Figure 5.4-5.6). When compared RMSE values of Table 4.1 with RMSE of Table 5.3 for sample temperature, averagely 1-2°C less RMSE values were observed in the model used in this chapter except for drying at 70°C. It could be said that the approach used in this chapter using anisotropic diffusivity was more compatible with the experimental.

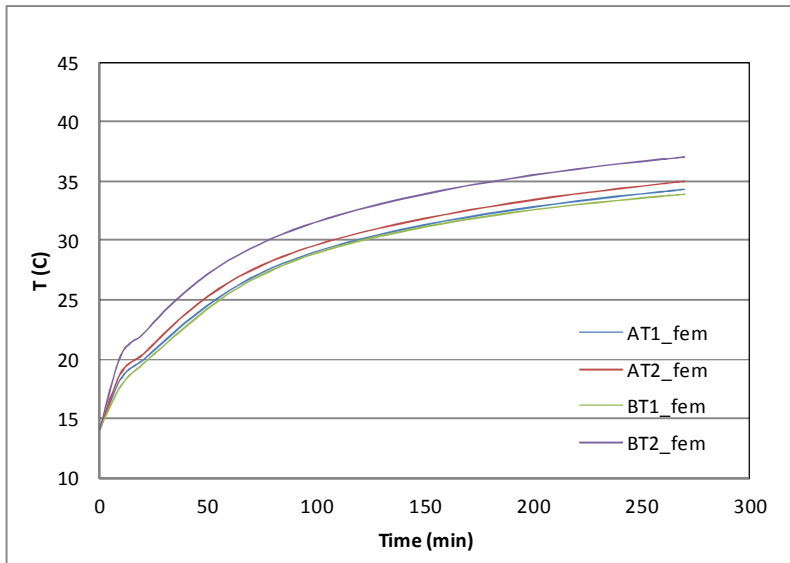


**Figure 5.3.** Temperature change in lean meat with flow normal to fibers (**h1**) with respect to drying time during drying at  $48 \pm 1^\circ\text{C}$  0.5 m/s

In general, the predicted temperature values were in good agreement with experimental results for lean meat samples in all three fiber configurations except for drying at the highest temperature (70°C) (Figure 5.4b-5.5b-5.6b). The difference between predicted and experimental became as large as 5°C at 70°C while it was around 2°C in other drying conditions (Table 5.3). At the highest attainable air temperature (70°C), the predicted temperatures were slightly lower than experimental due to higher moisture loss, thus higher heat loss due to evaporation in model (Figure 5.7-5.9). At higher velocity (1.0, 1.7 m/s), faster increase in sample temperature was observed than experimental at the beginning of drying since high velocity resulted in high heat transfer coefficient. At later stages of drying, temperature curves of predicted and experimental became closer (Figure 5.4c-d, 5.5c-d, 5.6c-d).

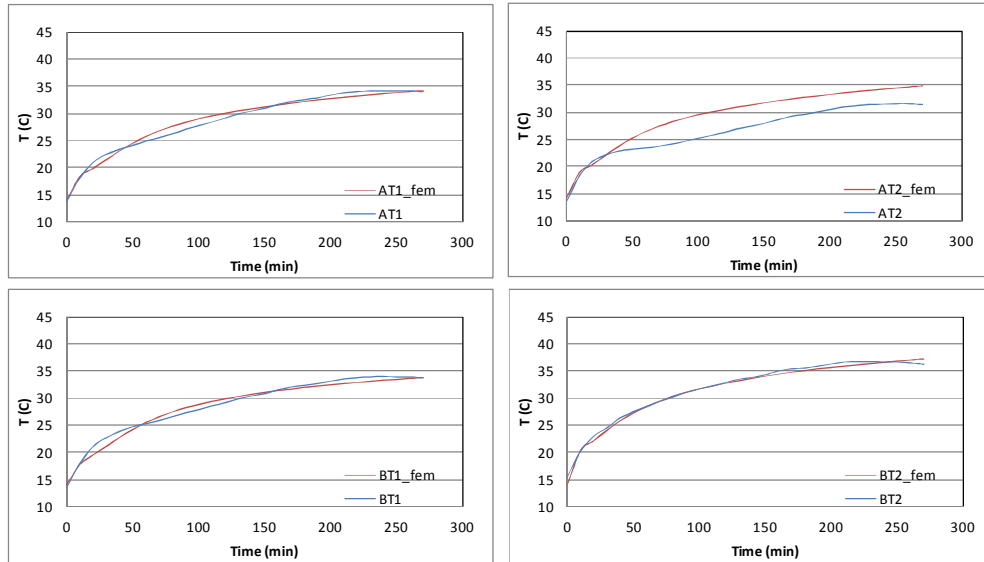


**Figure 5.4a.** Temperature change at four different locations (AT1, AT2, BT1, BT2) in lean meat with flow normal to fibers (**h1**) with respect to drying time during drying at  $48 \pm 1^\circ\text{C}$  0.5 m/s

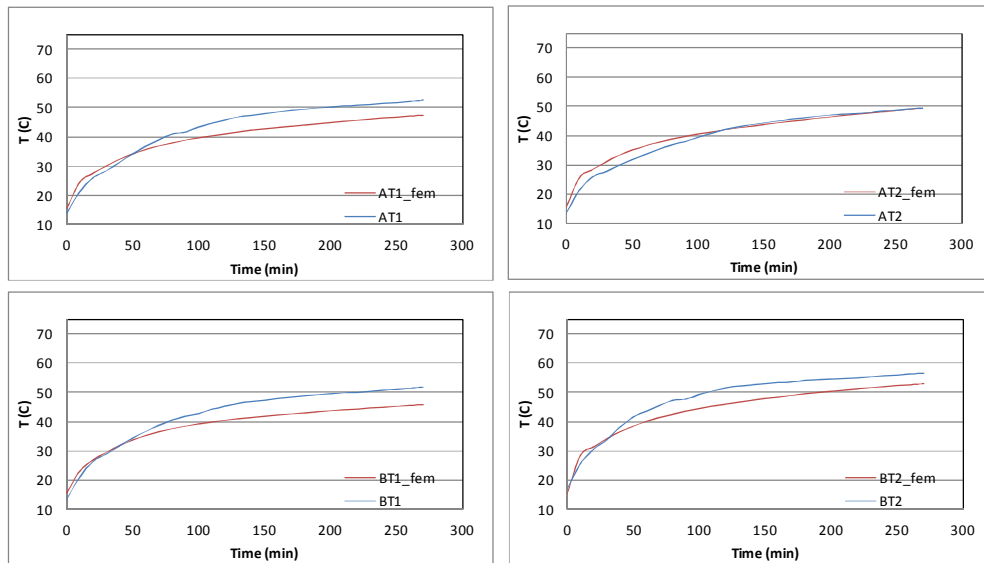


**Figure 5.4b.** Temperature change at four different locations (AT1, AT2, BT1, BT2) in lean meat with flow normal to fibers (**h1**) with respect to drying time during drying at  $70 \pm 1^\circ\text{C}$  0.5 m/s

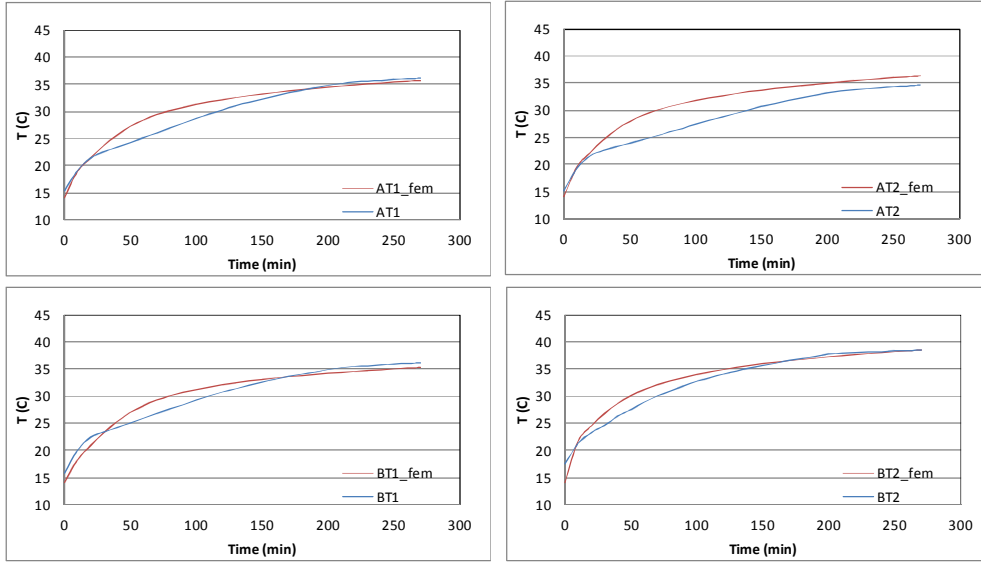


**Figure 5.4c.** Temperature change at four different locations (AT1, AT2, BT1, BT2) in lean meat with flow normal to fibers (**h1**) with respect to drying time during drying at  $48\pm 1^\circ\text{C}$  1.0 m/s

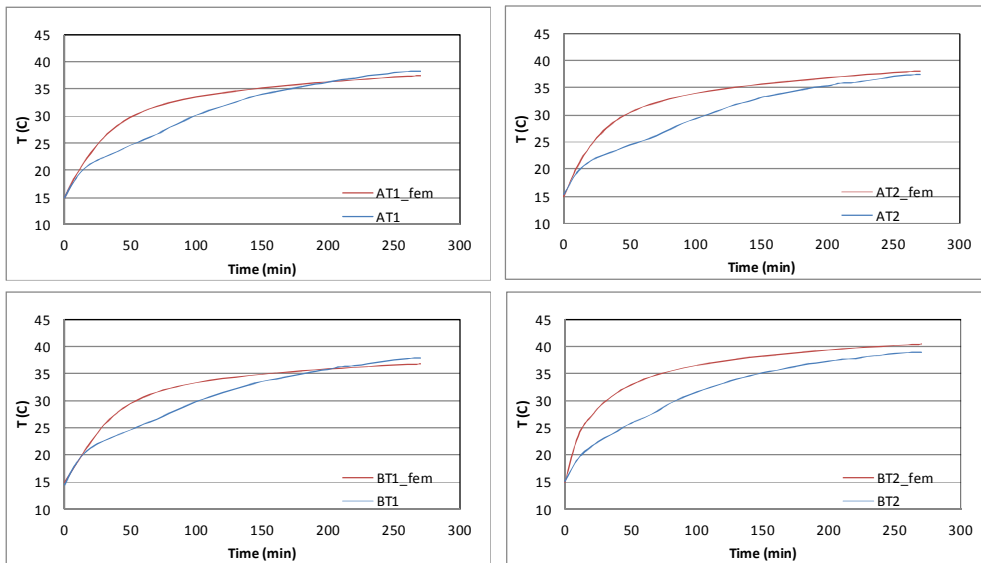


**Figure 5.4d.** Temperature change at four different locations (AT1, AT2, BT1, BT2) in lean meat with flow normal to fibers (**h1**) with respect to drying time during drying at  $48\pm 1^\circ\text{C}$  1.7 m/s

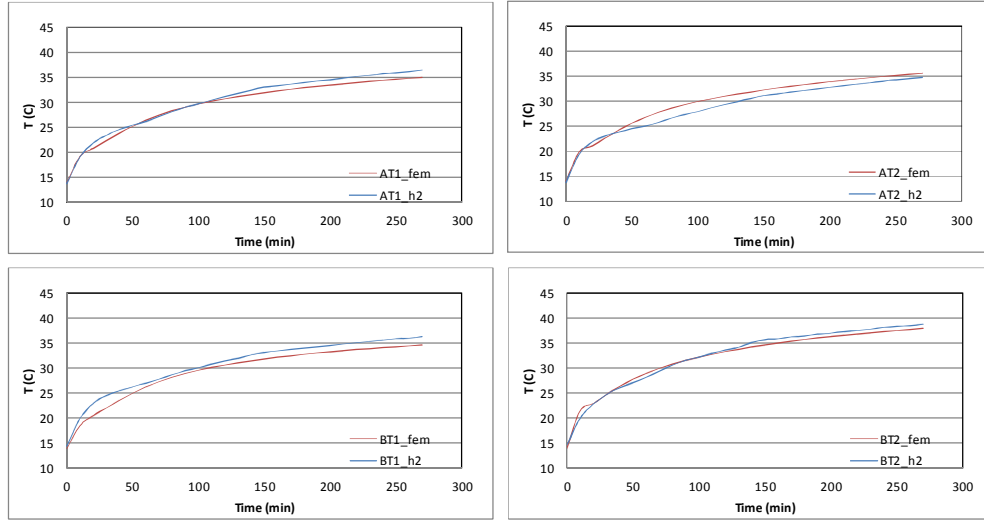


**Figure 5.5a.** Temperature change at four different locations (AT1, AT2, BT1, BT2) in lean meat with flow along to fibers (h2) with respect to drying time during drying at  $48\pm 1^\circ\text{C}$  0.5 m/s

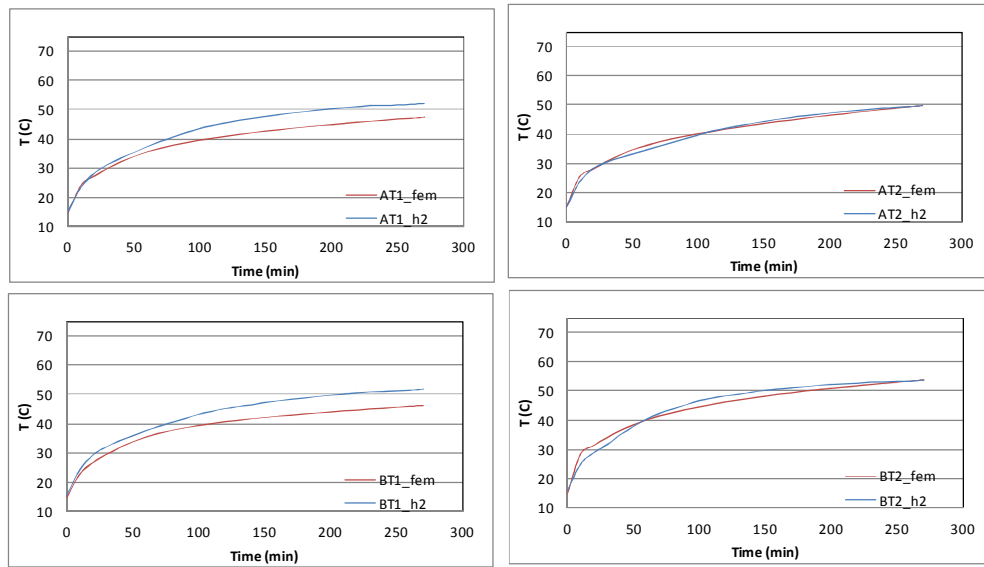


**Figure 5.5b.** Temperature change at four different locations (AT1, AT2, BT1, BT2) in lean meat with flow along to fibers (h2) with respect to drying time during drying at  $70\pm 1^\circ\text{C}$  0.5 m/s

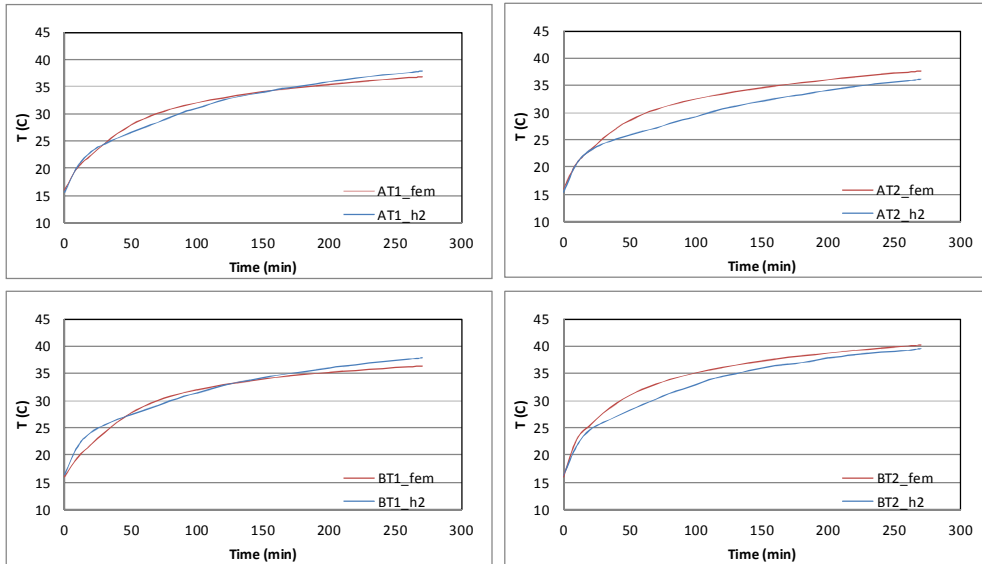


**Figure 5.5c.** Temperature change at four different locations (AT1, AT2, BT1, BT2) in lean meat with flow along to fibers (**h2**) with respect to drying time during drying at  $48\pm 1^\circ\text{C}$  1.0 m/s

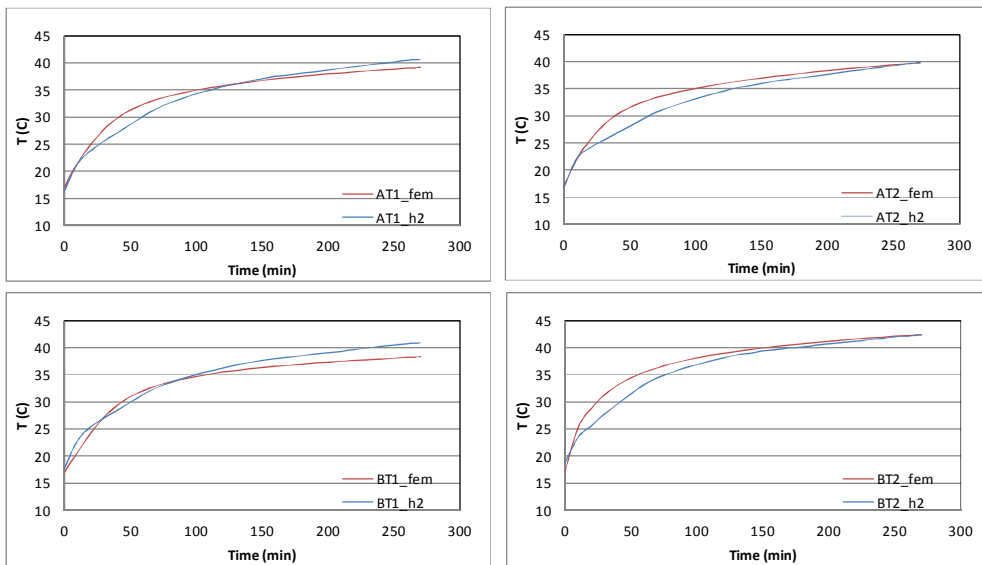


**Figure 5.5d.** Temperature change at four different locations (AT1, AT2, BT1, BT2) in lean meat with flow along to fibers (**h2**) with respect to drying time during drying at  $48\pm 1^\circ\text{C}$  1.7 m/s



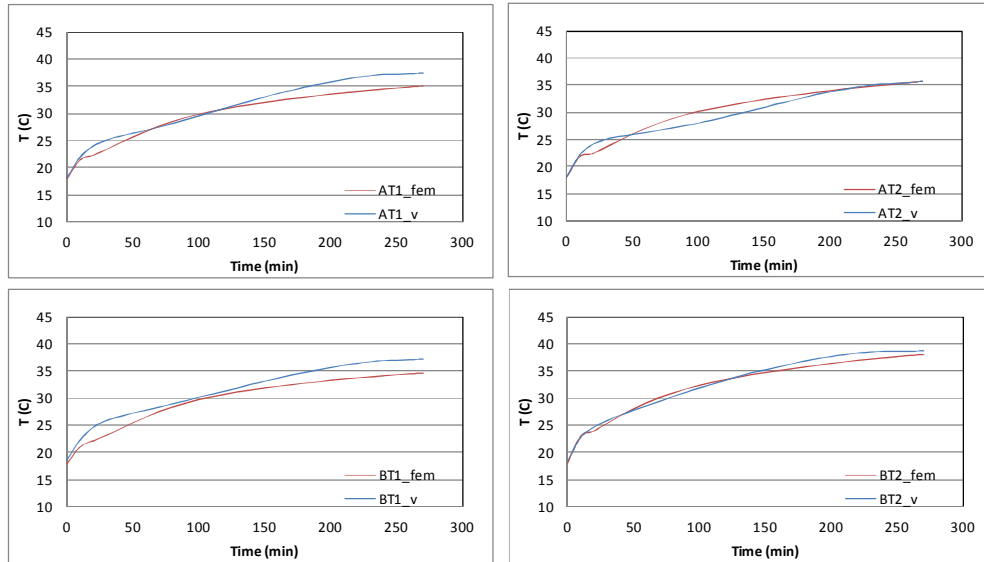


**Figure 5.6a.** Temperature change at four different locations (AT1, AT2, BT1, BT2) in lean meat with flow normal to fibers, drying along the fibers (v) with respect to drying time during drying at  $48\pm 1^\circ\text{C}$  0.5 m/s

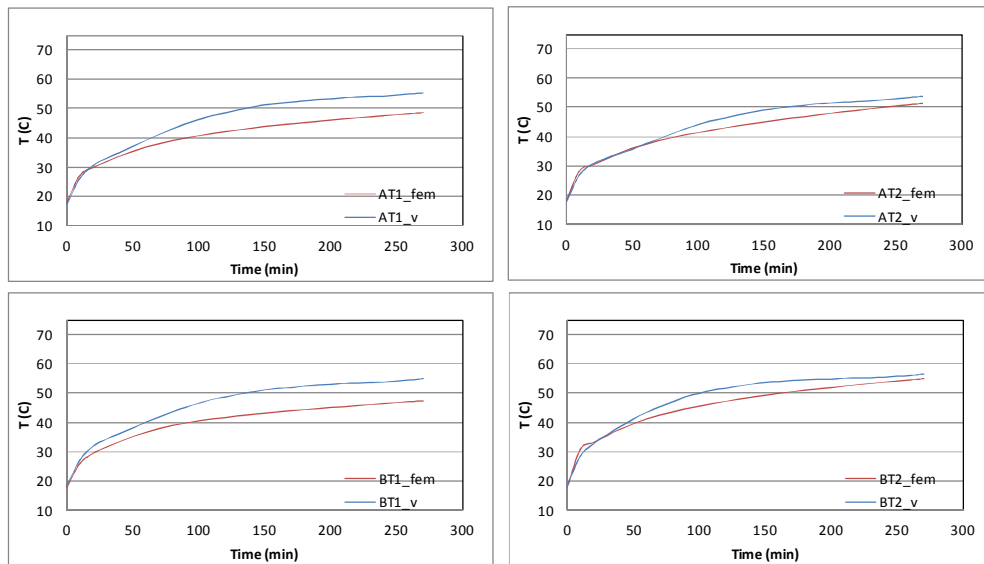


**Figure 5.6b.** Temperature change at four different locations (AT1, AT2, BT1, BT2) in lean meat with flow normal to fibers, drying along the fibers (v) with respect to drying time during drying at  $70\pm 1^\circ\text{C}$  0.5 m/s

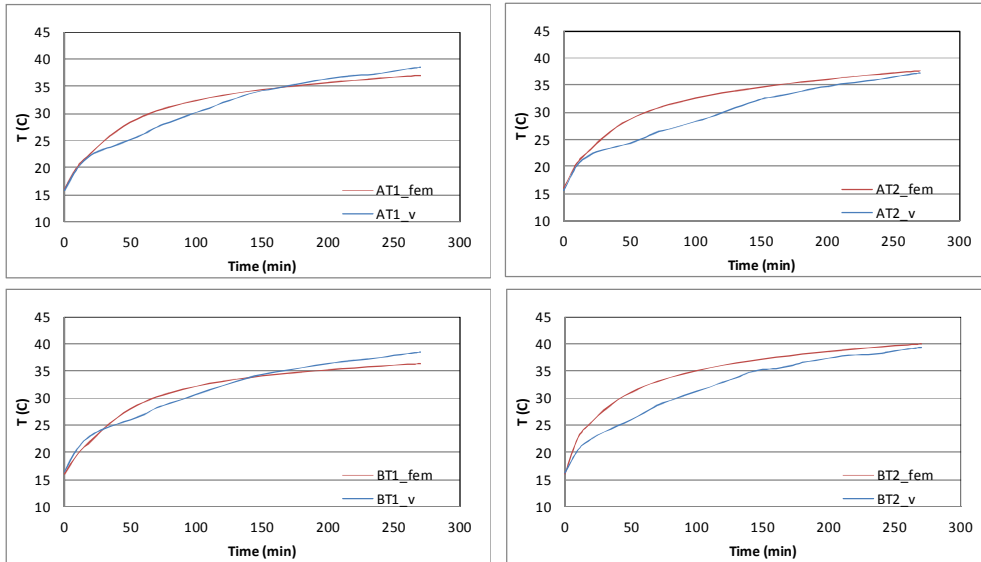


**Figure 5.6c.** Temperature change at four different locations (AT1, AT2, BT1, BT2) in lean meat with flow normal to fibers, drying along the fibers (v) with respect to drying time during drying at  $48\pm 1^\circ\text{C}$  1.0 m/s

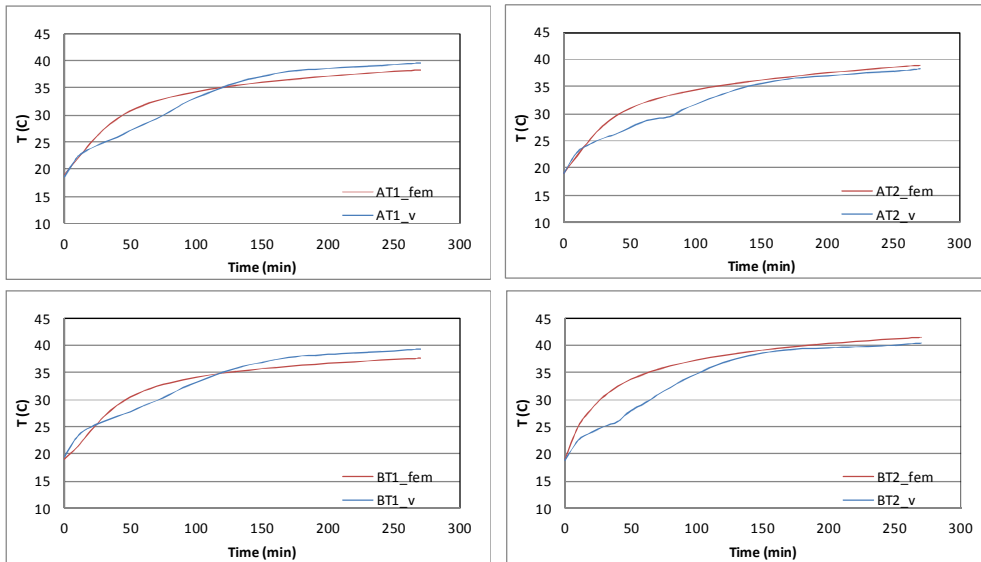


**Figure 5.6d.** Temperature change at four different locations (AT1, AT2, BT1, BT2) in lean meat with flow normal to fibers, drying along the fibers (v) with respect to drying time during drying at  $48\pm 1^\circ\text{C}$  1.7 m/s

**Table 5.3.** RMSE; root mean square error of predicted temperature of meat samples during drying at different conditions

Sample	Drying parameter	RMSE (°C)				R <sup>2</sup>
		AT1	AT2	BT1	BT2	
Lean meat _h1	48°C 0.5 m/s	0.7	3.1	0.7	0.6	0.952-0.994
	48°C 1.0 m/s	1.7	2.6	1.3	1.3	0.930-0.960
	48°C 1.7 m/s	2.6	3.3	2.4	4.2	0.900-0.910
Lean meat _h2	70°C 0.5 m/s	4.4	1.7	4.5	3.8	0.979-0.994
	48°C 0.5 m/s	0.9	1.2	1.4	0.7	0.986-0.994
	48°C 1.0 m/s	0.8	2.3	1.0	1.5	0.974-0.983
	48°C 1.7 m/s	1.2	1.5	1.4	1.5	0.966-0.974
Lean meat _v	70°C 0.5 m/s	4.0	0.9	4.3	1.5	0.981-0.994
	48°C 0.5 m/s	1.5	1.2	1.9	0.86	0.950-0.988
	48°C 1.0 m/s	1.6	2.7	1.37	2.8	0.931-0.949
	48°C 1.7 m/s	1.7	1.9	1.6	2.8	0.924-0.942
	70°C 0.5 m/s	5.6	2.8	6.5	3.0	0.976-0.992

#### 5.4. Prediction of Moisture Content

The predicted moisture content values were in good agreement with experimental results for lean meat samples in all fiber configurations except for drying at 70°C (Figure 5.7-5.9). The difference between predicted and experimental moisture content was in a range of 0.4-1.3% on wet basis (Table 5.4) which supported compatibility and were much lower than the results of previous chapter (2-5%) (Table 4.2) except for drying at 70°C. The difference at 70°C might be resulted from unnegligible shrinkage effect at high temperatures, which was discussed in next section.

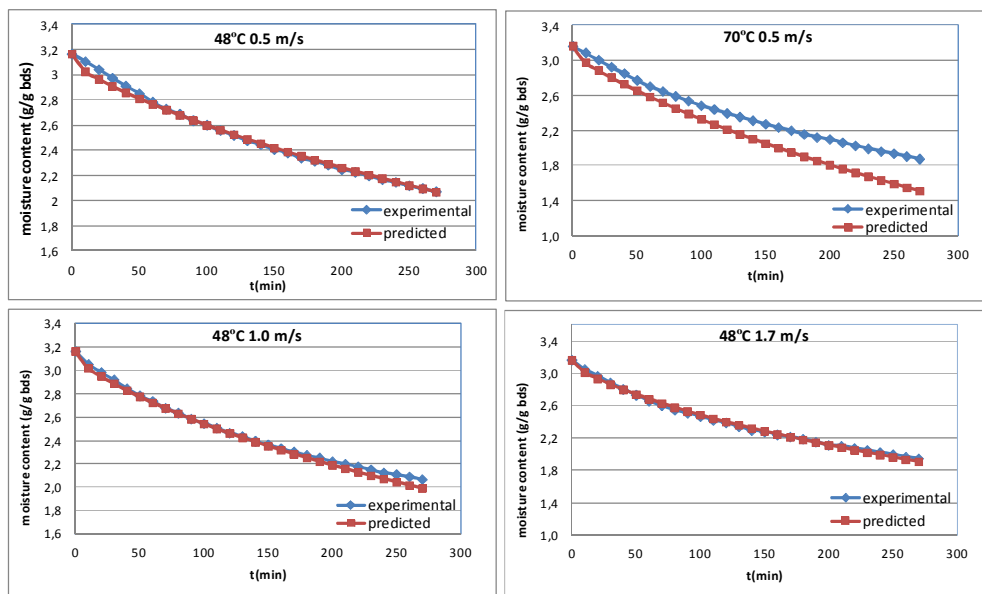


**Figure 5.7.** Moisture content change in lean meat with flow normal to fibers (h1) with respect to drying time

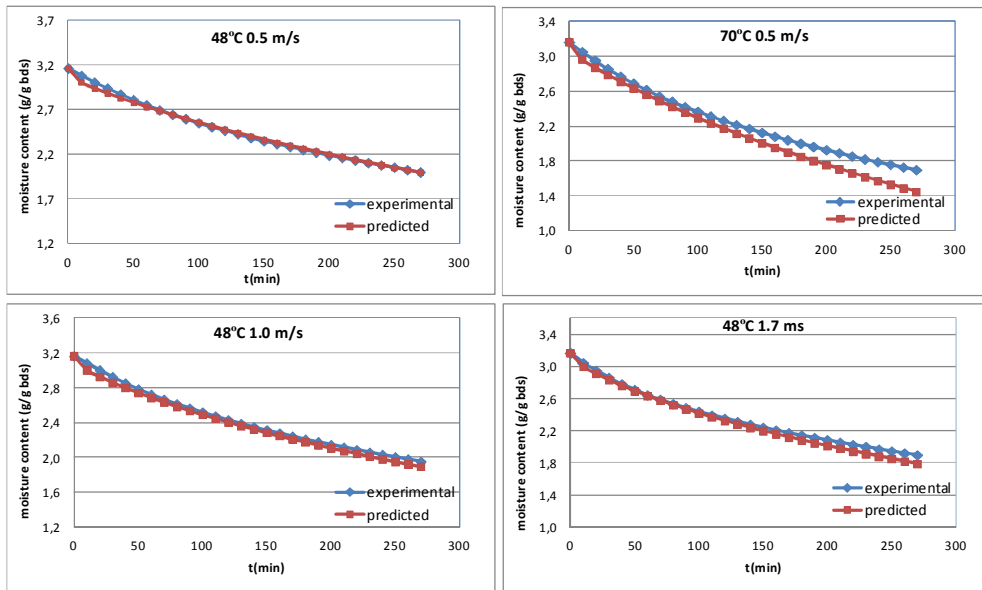


**Figure 5.8.** Moisture content change in lean meat with flow along to fibers (h2) with respect to drying time

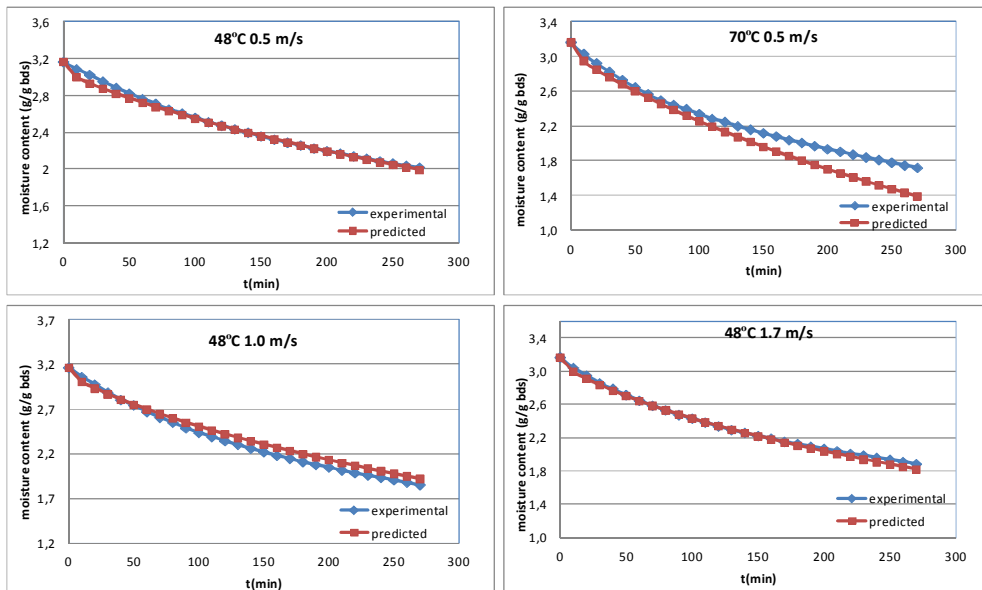


**Figure 5.9.** Moisture content change in lean meat with flow normal to fibers, drying along the fibers (v) with respect to drying time

**Table 5.4.** RMSE; root mean square error of predicted moisture content (dry base) of meat samples at different drying conditions ( $R^2 > 0.99$  in all cases)

Sample	RMSE (g water/g bds) drying at			
	48°C 0.5 m/s	48°C 1.0 m/s	48°C 1.7 m/s	70°C 0.5 m/s
Lean meat _h1	0.028	0.032	0.019	0.23
Lean meat _h2	0.025	0.042	0.056	0.14
Lean meat _v	0.035	0.053	0.029	0.18

\*In order to find RMSE as a wet base percentage, the value should be multiplied by 24 (percentage of BDS found experimentally)

### 5.5. Effect of Shrinkage

Good correlation between predicted and experimental could not be observed for drying at 70°C and 0.5 m/s. Most possible reason for that was the effect of shrinkage and change in thickness, which was neglected. Thus, shrinkage term was added to equation(5.4)and diffusion coefficients was estimated again for drying at high temperature using nonlinear fitting of equation (5.9) in MathCAD as explained in section 5.1. For shrinkage, a simple definition stated in literature (Azzouz *et al.*, 2002; Ruiz-Lopez and Garcia-Alvarado, 2007; Srikiatden and Roberts, 2007) was used (5.8).

$$L = c + d.X^* \quad (5.8)$$

At the  $t=0$ ,  $X^*$  (dimensionless moisture content) and  $L$  (thickness of slab) was equal to 1 and 0.01, respectively. So,

$$c = 0.01 - d$$

$$X^* = \frac{X - X_{eq}}{X_i - X_{eq}} = \frac{8}{\pi^2} \sum_{n=0}^{\infty} \frac{1}{(2n+1)^2} \exp\left(- (2n+1)^2 \pi^2 \frac{D_0 * \exp\left(-\frac{E_a}{RT}\right) (A \cdot \exp(X) + B)}{4(0.01 - d + d.X^*)^2} t\right) \quad (5.9)$$

The new definitions of diffusion coefficients for lean meat samples with three fiber configurations was given in equations (5.10-5.12) below considering shrinkage (Table 5.5). Again anisotropic diffusivity values were introduced to model as in Table 5.2.

**Table 5.5.** Diffusivity equations of lean meat with three fiber configurations

Diffusivity equation*	Standard error	R <sup>2</sup>	Eqn no
$D(h1) = 1.94 * \exp\left(-\frac{7153}{T}\right) (0.13 \exp(X) + 1.113)$	0.0092	0.996	5.10
$D(h2) = 1.467 * \exp\left(-\frac{6791}{T}\right) (0.115 \exp(X) + 0.343)$	0.0086	0.997	5.11
$D(v) = 0.337 * \exp\left(-\frac{6530}{T}\right) (0.286 \exp(X) + 0.1)$	0.0096	0.996	5.12

\*Shrinkage was considered.

Figures 5.10-5.12 reflected high compatibility between predicted and experimental moisture content during drying at 70°C for lean meat samples in three fiber configurations. It was observed very slight difference in h2 and v fiber configurations which might be arisen from difference in sample composition, structure or experimental conditions. The difference between predicted and

experimental moisture content was in a range of 0.5-2.4 % on wet basis (Table 5.6) which supported compatibility.

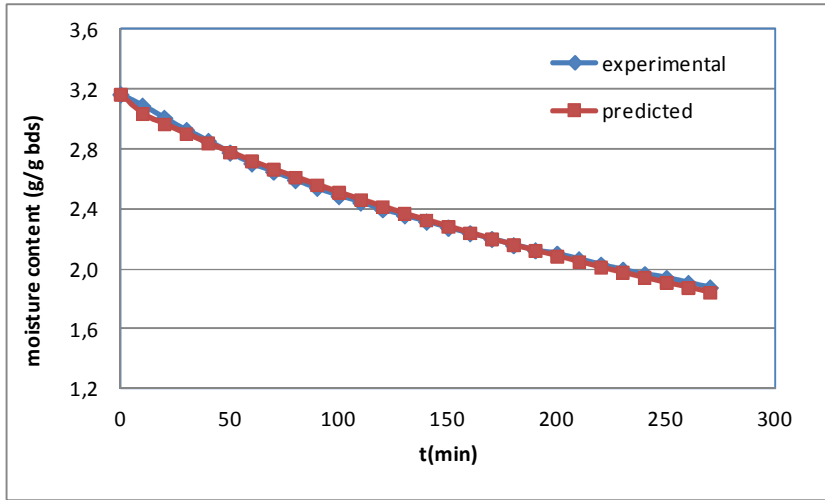


**Figure 5.10.** Moisture content change in lean meat with flow normal to fibers (**h1**) with respect to drying time during drying at  $70\pm 1^\circ\text{C}$  and 0.5 m/s after inclusion of shrinkage

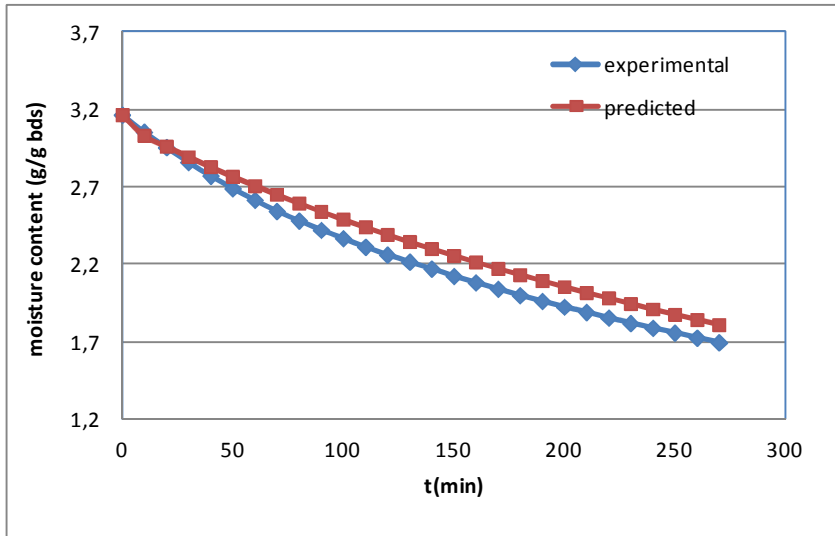


**Figure 5.11.** Moisture content change in lean meat with flow along to fibers (**h2**) with respect to drying time during drying at  $70\pm 1^\circ\text{C}$  and 0.5 m/s after inclusion of shrinkage

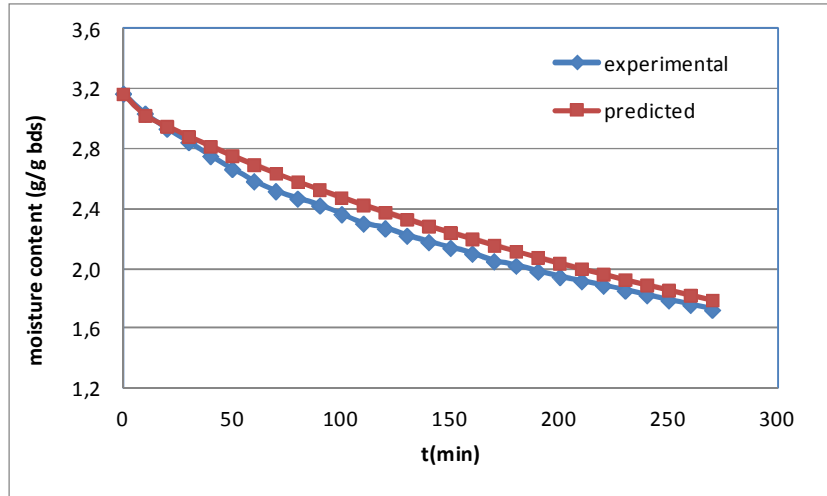


**Figure 5.12.** Moisture content change in lean meat with flow normal to fibers, drying along the fibers (v) with respect to drying time during drying at  $70\pm 1^\circ\text{C}$  and 0.5 m/s after inclusion of shrinkage

**Table 5.6.** RMSE; root mean square error of predicted moisture content (dry base) of meat samples during drying at  $70^\circ\text{C}$  0.5 m/s ( $R^2 > 0.99$  in all cases)

Sample	RMSE
Lean meat _h1	0.021
Lean meat _h2	0.10
Lean meat _v	0.089

The predicted temperature values were also in better agreement with experimental at  $70^\circ\text{C}$  after inclusion of shrinkage in diffusivity calculations (Figure 5.13-5.15). The RMSE values (Table 5.7) became  $\sim 2^\circ\text{C}$  lower than found without shrinkage (Table 5.2), which supported better compatibility. Only the temperature at AT2 showed difference as previously discussed due to slight effect of flow on velocity profile, thus on heat transfer coefficient.

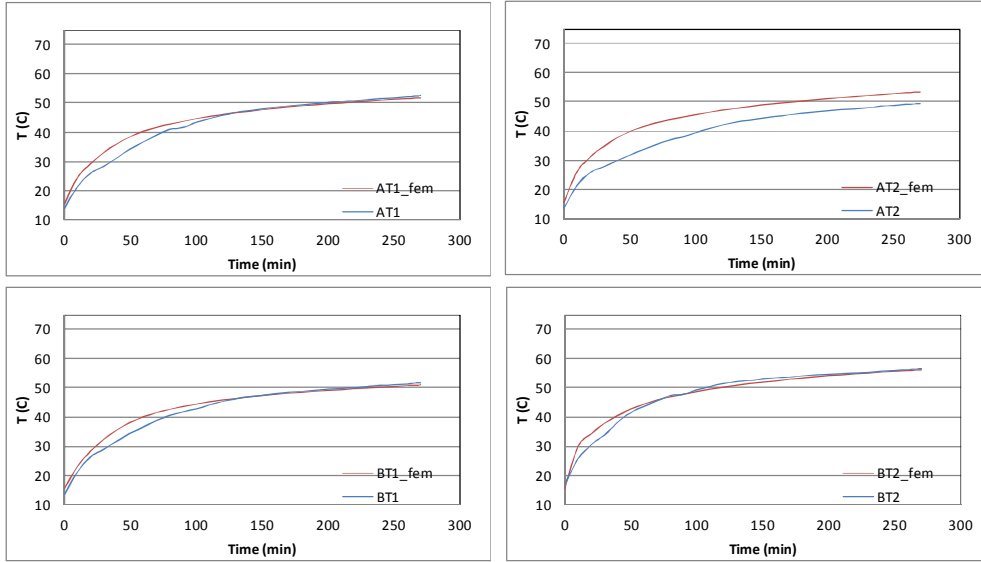


**Figure 5.13.**Temperature change at four different locations (AT1, AT2, BT1, BT2) in lean meat with flow normal to fibers (**h1**) with respect to drying time during drying at  $70\pm 1^\circ\text{C}$ , 0.5 m/s after inclusion of shrinkage

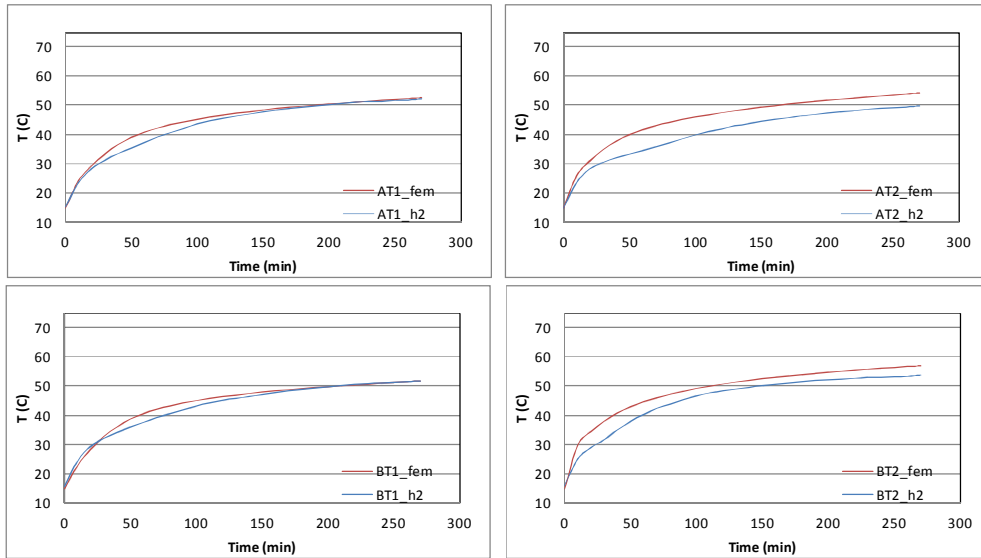


**Figure 5.14.**Temperature change at four different locations (AT1, AT2, BT1, BT2) in lean meat with flow along to fibers (**h2**) with respect to drying time during drying at  $70\pm 1^\circ\text{C}$ , 0.5 m/s after inclusion of shrinkage



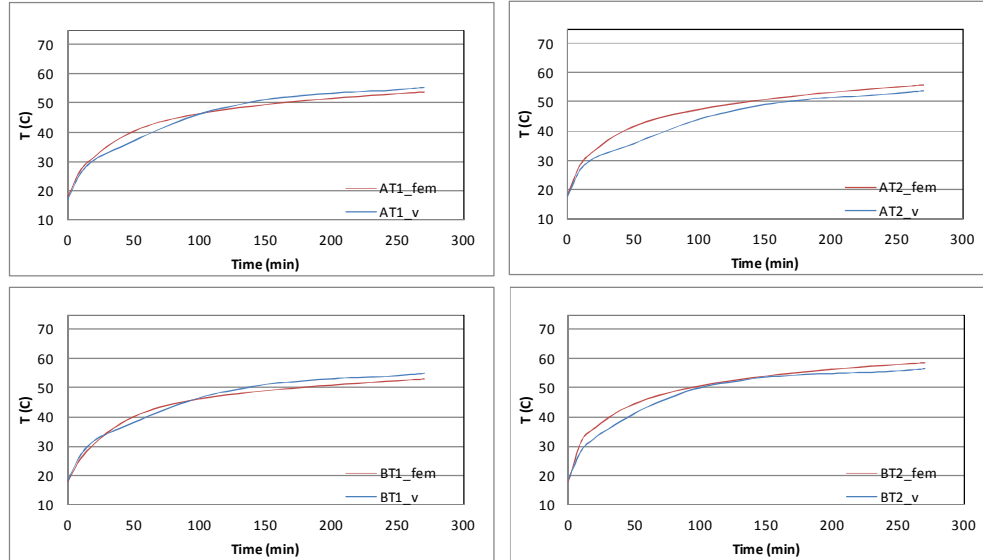


**Figure 5.15.** Temperature change at four different locations (AT1, AT2, BT1, BT2) in lean meat with flow normal to fibers, drying along the fibers (v) with respect to drying time during drying at  $70\pm 1^\circ\text{C}$ , 0.5 m/s after inclusion of shrinkage

**Table 5.7.** RMSE; root mean square error of predicted temperature of meat samples during drying at  $70^\circ\text{C}$  0.5 m/s

Sample	RMSE				R <sup>2</sup>
	AT1	AT2	BT1	BT2	
Lean meat_h1	1.9	5.1	1.6	1.5	0.973-0.987
Lean meat_h2	1.5	5.0	1.4	3.4	0.975-0.986
Lean meat_v	1.7	3.1	1.74	1.88	0.976-0.985

### 5.6. Fiber Direction Effect on Predicted Moisture Content and Temperature

In previous chapter, anisotropy effect could not be observed in predicted moisture content values when the same temperature dependent diffusivity equation from literature (2.18) was used (Figure 4.23) since temperature differences between samples could not produce enough difference in diffusion coefficients and thus moisture content of different meat samples at the same drying conditions. When anisotropic diffusivity values were used as defined in section 5.1, lower moisture loss was observed in minced meat than in lean meat samples and lean meat with h1 fiber configuration showed lower moisture loss than lean meat with other fiber configurations (h2 and v). The same result was also observed experimentally, which supported that anisotropic representation of diffusivity values was applicable to define real food systems in finite element modeling.

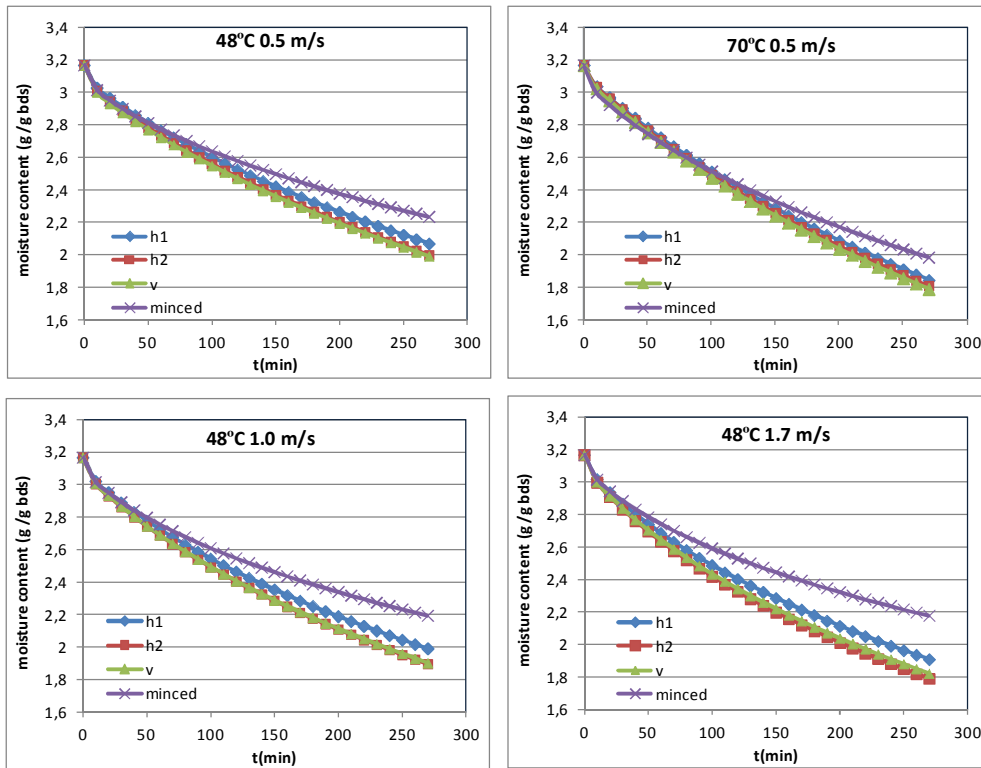


**Figure 5.16.** Predicted moisture content change with respect to drying time

In all drying conditions, the predicted temperature values of minced meat were higher than temperature of lean meat with all fiber configurations (Figure 5.17-5.20) and the lowest temperature was observed in lean meat with h1 fiber configuration, which was compatible result with experimental data. Thus, it could be concluded that anisotropic representation of thermal conductivity as explained in section of Material and Methods chapter 2.4 (Table 2.3), was applicable to define real food systems in finite element modeling.

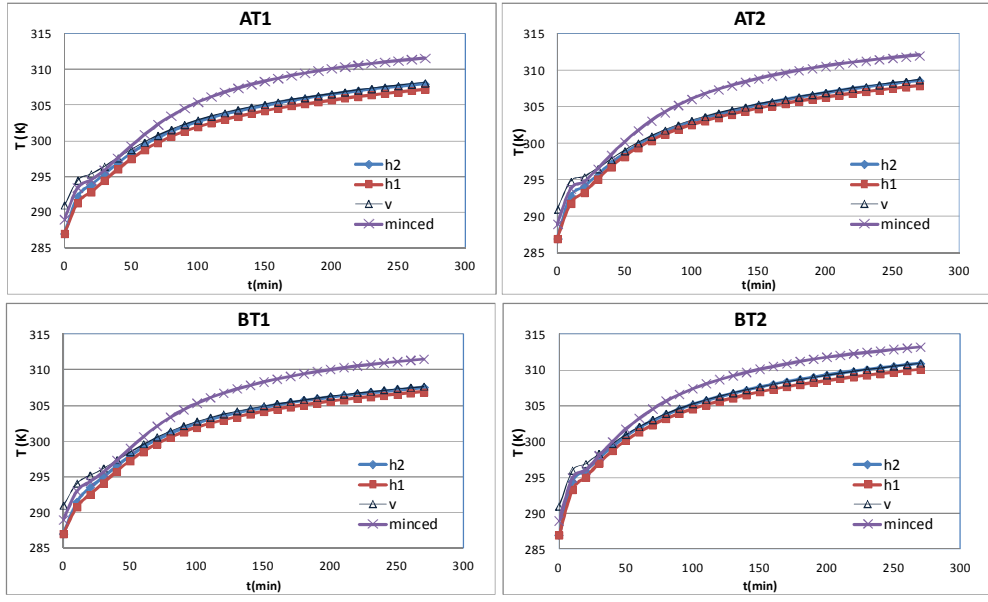


**Figure 5.17.** Predicted temperature change at four different locations with respect to drying time during drying at  $48\pm 1^\circ\text{C}$ , 0.5 m/s

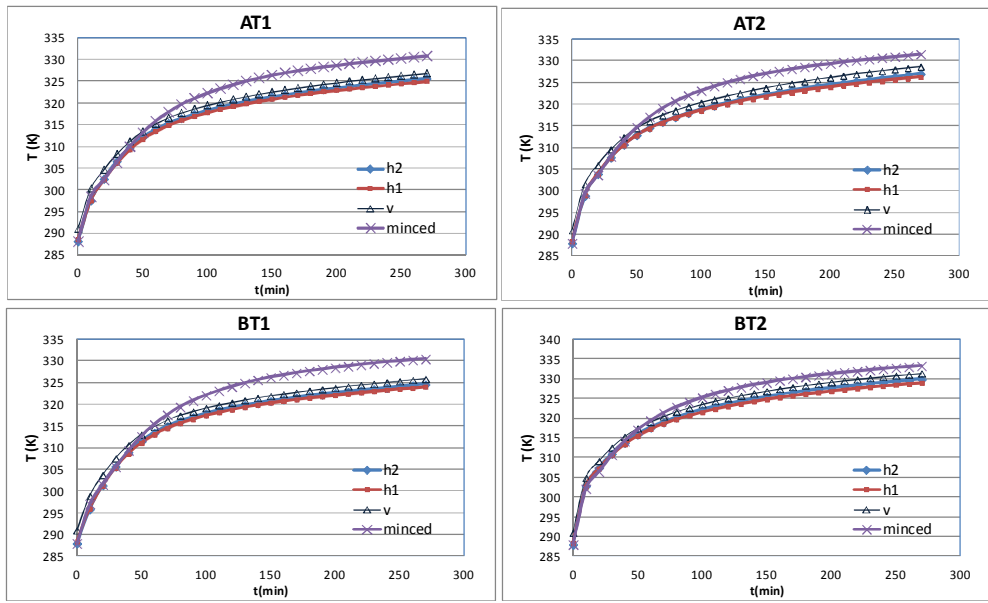


**Figure 5.18.** Predicted temperature change at four different locations with respect to drying time during drying at  $70\pm 1^\circ\text{C}$ , 0.5 m/s

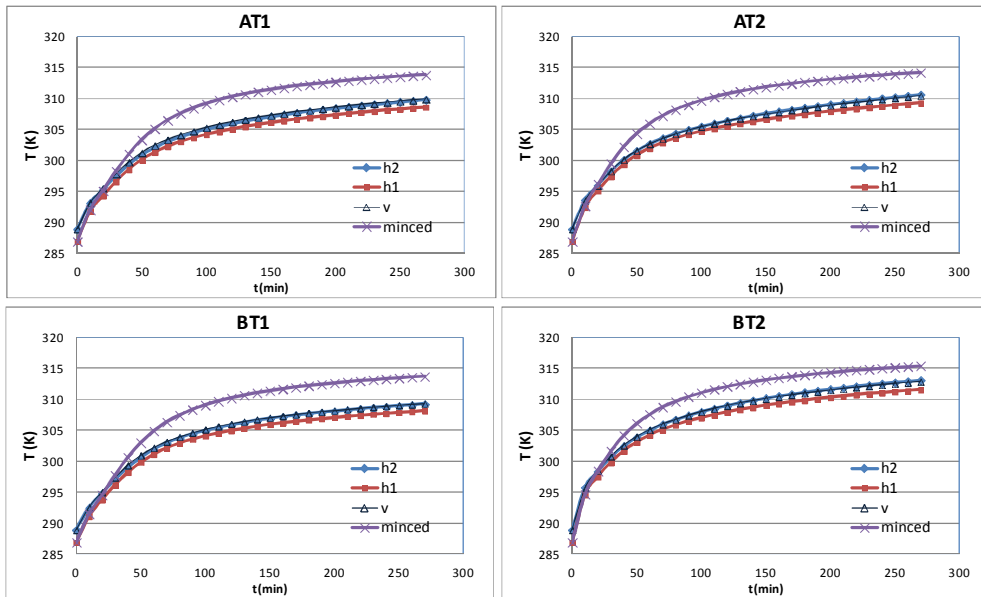


**Figure 5.19.** Predicted temperature change at four different locations with respect to drying time during drying at  $48\pm 1^\circ\text{C}$ , 1.0 m/s

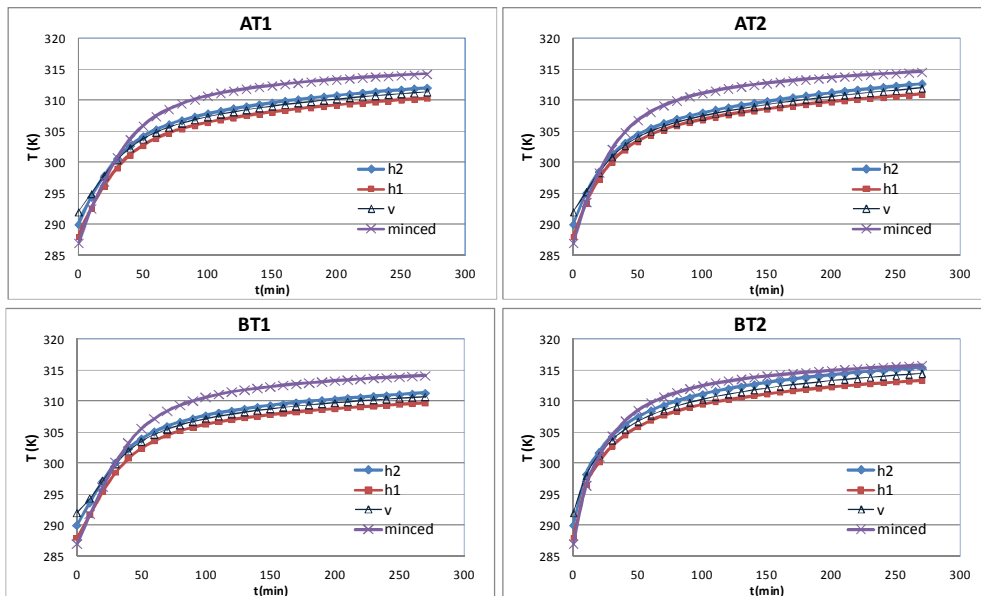


**Figure 5.20.** Predicted temperature change at four different locations with respect to drying time during drying at  $48\pm 1^\circ\text{C}$ , 1.7 m/s

## CHAPTER 6

### CONCLUSION AND RECOMMENDATIONS

In this study, there were two main purposes. First aim was to observe change in drying characteristics (degree of temperature difference, rate of drying and temperature change, drying time, diffusivity values, shrinkage) during drying of meat samples at different conditions and to investigate existence of difference arising from structure and fiber configuration of meat samples. Second aim was to model distribution of temperature and moisture content within the sample by using finite element method (FEM) and compare the solutions of FEM with experimental results and thus to observe anisotropy if exists.

In order to observe effect of structure and fiber configuration, lean meat with three fiber configurations and double minced meat were chosen as anisotropic and isotropic samples, respectively. In all drying conditions and samples, the highest temperature was observed at the surface. Temperature changed faster near surfaces while this change became slower after mid thickness. Slightly asymmetric temperature change was observed with respect to y-axis due to velocity profile around the sample. Order of temperature values was as follows  $BT2 > AT1 \approx BT1 > AT2$ . Minced meat showed either no or very slight bending in temperature curves with respect to time within 30 minutes of drying, which was significantly observed in lean meat samples, presumably due to existence of more uniform structure in minced meat.

Increase in temperature and velocity of air resulted in higher temperature and moisture loss of samples with respect to drying time but temperature was found more effective parameter than velocity. Velocity was more effective at the beginning of drying since external resistances like heat and mass transfer coefficients were rate controlling. Rate of temperature change was compared using first order dynamics equation (3.1) and rate constants ( $k_T$ ) in descending order were  $k_T(70^\circ\text{C}, 0.5 \text{ m/s}) > k_T(48^\circ\text{C}, 1.7 \text{ m/s}) > k_T(48^\circ\text{C}, 1.0 \text{ m/s}) > k_T(48^\circ\text{C}, 0.5 \text{ m/s})$ . The same order with respect to drying conditions was also observed in comparison of rate of drying. It was observed that increasing velocity from 0.5 to 1.7 m/s decreased drying time 1.2-4.2 hr while increasing temperature from 48°C to 70°C decreased 3.6-6.3 hr. Temperature difference between locations was also found to be less with higher velocity of air. When air velocity increased from 0.5 to 1.7 m/s, temperature difference between locations decreased from ~3°C to ~1°C.

In general, either no or very short constant rate was observed in all samples since most of the water was present as bound water within the samples. Short constant rate was observed only for drying at low temperature, low velocity condition (48°C, 0.5 m/s) since removal of free moisture was slower and constant rate became visible.

Anisotropy effect was observed in lean meat samples. The lean meat with flow normal to fibers but drying along the fibers ( $v$ ) showed less temperature gradient within the sample than other fiber configurations due to more easily air flow through and into the sample which led to more uniform temperature within sample. The order of temperature gradient through the lean meat samples was found as  $v < h2 < h1$ . At the highest attainable flow rate of air in the dryer, all three different fiber conditions showed very small temperature difference with respect to locations. When rate constants ( $k_T$ ) for temperature change were compared, it was observed that  $k_{T(\text{minced})} > k_{T(h2)} > k_{T(v)} \approx k_{T(h1)}$ , meaning that minced meat showed faster increase in temperature than lean meat samples while  $h2$  fiber configuration showed faster increase in temperature than other fiber configurations. Lean meat samples with  $h1$  fiber configuration showed lower temperature values and lower moisture loss than the samples with other fiber directions ( $v$  and  $h2$ ). The rates of drying in a descending order was found as  $k_m(h2) \approx k_m(v) > k_m(h1) > k_m(\text{minced})$ . Minced meat showed higher temperature due to

lower moisture loss, so far less shrinkage than lean meat samples, which might be resulted from more difficult moisture loss due to the structure of minced meat.

Equilibrium moisture content for each drying condition was found efficiently by defining simple exponential decay equation of moisture loss with respect to drying time based on moisture data attained experimentally. Diffusion coefficients were calculated by considering first term of equation (3.5) based on Fick's law. However, it was found that diffusivities found by this procedure was high and could only be valid at the end of drying and not enough to represent moisture loss at initial stages of drying. Diffusivity should be as a function of temperature or moisture content of sample in order to be able to define overall drying process.

The model based on coupled heat and mass transfer equations was first constructed by considering anisotropic thermal conductivity but the same diffusion coefficient as a function of temperature for all type of samples with two different approaches. First approach was based on heat loss due to evaporation only at the surface, second approach was based on heat loss due to change in overall moisture content through the sample. Both of them could only be valid after reaching wet bulb temperature. Second approach was found more proper since it had much shorter computation time, more compatible results with experimental data and temperature distribution in literature.

Model 2 gave similar temperature distribution with experimental data except for AT2 location probably resulted from slightly different velocity profile around the sample due to flow. Minced meat showed good agreement with experimental data for both temperature and moisture distribution, however the model needed to be refined for lean meat samples. When sought for anisotropy effect on predicted temperatures, this model produced similar results for change in temperature distribution for different types of samples with experimental data. On the other hand, no difference was observed in moisture loss with respect to drying time for lean meat and minced meat samples, which showed that use of the same diffusion coefficient was not adequate to represent anisotropy effect on moisture loss even if it was a function of sample temperature since the change in sample temperature was not large enough to cause a difference in moisture loss.

For refining of the model in order to observe anisotropy effect on moisture loss, diffusion coefficients were computed for lean meat samples as a function of temperature and both temperature & moisture content by nonlinear fitting of experimental data considering change in surface temperature at 70°C. The diffusivity as a function of both temperature and moisture content was found to be slightly more appropriate than the one as a function of only temperature. The predicted temperature and moisture content found using both anisotropic thermal conductivity and diffusion coefficient definitions showed good agreement for lean meat samples with all three fiber configurations except for drying at the highest temperature (70°C). In order to improve the model for drying at high temperatures, it was suggested that shrinkage should be introduced to diffusivity calculation. After inclusion of the shrinkage, predicted temperature and moisture content at 70°C became also compatible with the experimental values. From the aspect of anisotropy effect, it could be concluded that the model considering both anisotropic thermal conductivity and diffusion coefficient represented well the difference in temperature and moisture content according to different fiber configurations of lean meat compared to experimental results. Additionally, the model showed good agreement with experimental to represent the difference between anisotropic (lean meat) and isotropic samples (minced meat).

For further studies, shrinkage could be incorporated not only to diffusion coefficient but also to finite element model by considering moving boundaries with respect to time in order to observe better fitting with local temperature values. Secondly, coupled heat, mass and fluid dynamics equations could be solved in order to be able to observe slightly asymmetric temperature distribution within the sample.

## REFERENCES

- Abdalla, H. & Singh, R. P., 1985, Simulation of thawing foods using finite element method, *Journal of Food Process Engr.*, 7: 273-86
- Akpinar E. K., Dincer I., 2005, Moisture transfer models for slabs drying. *International Communications in Heat and Mass Transfer*, 32(1–2): 80–93
- Aktas N., Aksu M. I., Kaya M., 2005, Changes in myofibrillar proteins during processing of pastirma (Turkish dry meat product) produced with commercial starter cultures, *Food Chemistry*, 90: 649–654
- Alagasundaram, K., Jayas, D. S., White, N.D.G., Muir, W. E., 1990, Three dimensional finite element heat transfer model of temperature distribution in grain storage bins, *Tran ASAE*, 33:577-84.
- Alzamora S.M., Chirife J., 1980, Some Factors Controlling the Kinetics of Moisture Movement during Avocado Dehydration, *Journal of Food Science*, 45: 1649–1651, 1657.
- Arnau J., Serra X., Comaposada J., Gou P., Garriga M., 2007, Technologies to shorten the drying period of dry-cured meat products, *Meat Science*, 77: 81-89
- Arzan A.A., Morgan R.P., 1967, A two-region, moving boundary analysis of the drying process, *Chem. Eng. Progr. Symp. Ser.*, 63 (79): 24–33
- Asquith MH, Kirk E, Kirkland M, Morrey SM, Ormerod AP, Ralfs JD, Sharp DG, Sidebottom CM. Freezing vegetables. US Patent 7,169,426. January 30, 2007
- Aversa M., Curcio S., Calabro V., Iorio G., 2007 An analysis of the transport phenomena occurring during food drying process, *Journal of Food Engineering* 78: 922–932
- Ayensu A., 2003, Thermal convection and moisture-diffusion in thin-layer fixed-bed solar drying, *Quarterly SCIENCE VISION*, 9: 1-14 Available from [http://www.sciencevision.org.pk/BackIssues/Vol9/9.thermal\\_convection.pdf](http://www.sciencevision.org.pk/BackIssues/Vol9/9.thermal_convection.pdf) last date accessed 10.2012
- Azzouz S., Guizani A., Jomaa W., Belghith A., 2002, Moisture diffusivity and drying kinetic equation of convective drying of grapes, *Journal of Food Engineering*, 55: 323–330
- Baini R., Langrish T. A. G., 2008, An assessment of the mechanisms for diffusion in the drying of bananas, *Journal of Food Engineering* 85:201–214
- The beef jerky blog, So Jerky is as Jerky Does, <http://www.thebeefjerkyblog.com/so-jerky-is-as-jerky-does/>, last access date 05.10.2011
- Bellara S. R., McFarlane C. M., Thomas C. R., Fryer P. J., 2000, The growth of *Escherichia coli* in a food simulatant during conduction cooling: combining engineering and micro-biological modelling. *Chemical Engineering Science*, 55: 6085–6095.
- BenYoseph E., Hartel R.W., Howling D., 2000, Three-dimensional model of phase transition of thin sucrose films during drying, *Journal of Food Engineering*, 44: 13–22

- Betoret N., Andre´s A., Segui L., Fito P., 2007, Application of safes (systematic approach to food engineering systems) methodology to dehydration of apple by combined methods, *Journal of Food Engineering*, 83:186–192
- Bhattacharya A., Mahajan R. L., 2003, Temperature dependence of thermal conductivity of biological tissues, *Physiological Measurement*, 24: 769-783
- Bondaruk, J., Markowski, M., Blaszcak, W., 2007, Effect of drying conditions on the quality of vacuum-microwave dried potato cubes, *Journal of Food Engineering*, 81: 306-312
- Boquet R., Chirife J., Iglesias H.A., 1978, Equations for fitting water sorption isotherms of foods. II. Evaluation of various two parameter models, *Journal of Food Technology*, 13: 319–327
- Bourne M. C., 2002, *Food Texture and Viscosity Second Edition: Concept and Measurement*, 400 pages, Academic Press, New York
- Bowman H. F., Cravalho E. G., Woods M., 1975, Theory, measurement, and application of thermal properties of biomaterials, *Annual Review of Biophysics and Bioengineering*, 4 :43-80
- Bowser T. J., Wilhelm L. R., 1995, Modeling Simultaneous Shrinkage and Heat and Mass Transfer of a Thin, Nonporous Film During Drying, *Journal of Food Science*, 60(4):753-757
- Brown, Z.K., Fryer, P.J., Norton, I.T., Bakalis, S., Bridson, R.H., 2008, Drying of foods using supercritical carbon dioxide-Investigations with carrot, *Innovative Food Science and Emerging Technologies*, 9: 280-289.
- Cardenas-Weber M. C., Stroshine R. L., Haghighi K., Edan Y., 1989, Finite element analysis of melons handled by different robot gripper designs, ASAE Paper No. 89-1602. ASAE, St. Joseph, MI, USA
- Cardenas-Weber, M. C. Stroshine, R. L., Haghighi, K., Edan, Y., 1991, Melon material properties and finite element analysis of melon compression with application to robot gripping, *Trans ASAE*, 34:920-9.
- Carn R.M., King C.J., 1997, Modification of conventional freeze dryers to accomplish limited freeze drying, In water removal process, drying and concentration of foods and other materials, *AIChE Symp. Ser.* 124–130
- Castro-Giráldez M., Fito P.J., Fito P., 2010, Non-equilibrium thermodynamic approach to analyze the pork meat (*Longissimus dorsi*) salting process, *Journal of Food Engineering*, 99: 24–3
- Cekmecelioglu, D., Uncu, O.N., 2012, Kinetic modeling of enzymatic hydrolysis of pretreated kitchen wastes for enhancing bioethanol production, *Waste Management*
- Celen S., Kahveci K., Akyol U., Haksever A., 2010, Drying Behavior of Cultured Mushrooms, *Journal of Food Processing and Preservation*, 34: 27–42
- Chakraborty, M., Savarese, M., Harbertson, E., Harbertson, J., Ringer, K., 2010, Effect of the Novel Radiant Zone Drying Method on Anthocyanins and Phenolics of Three Blueberry Liquids, *J. Agric. Food Chem.*, 58(1): 324–330
- Chau K. V., Gaffney J. J., 1990, A finite difference model for heat and mass transfer in products with internal heat generation and transpiration, *Journal of Food Science*, 55: 484–487.
- Chavez M. S., Luna J. A., Garrote R. L., 1997, A mathematical model to describe potato chemical, NaOH) peeling. Energy and mass transfer model solution, *Journal of Food Engineering*, 32: 209–223



- Chen, D.-S.D., Singh, R. K., Haghjghi, K. & Nelson, P. E., 1990, Finite element analysis of temperature distribution in microwaved particulate foods, ASAE Paper No, 90-6602. ASAE, St. Joseph, MI, USA
- Chen X. D., 2007, Moisture Diffusivity in Food and Biological Materials, *Drying Technology*, 25: 1203–1213
- Chhinnan M. S., Bakshi A. S., 1984, Finite element analysis to model moisture transfer in rewetted California blackeye peas during drying, ASAE Paper No. 84-6516. ASAE, St. Joseph, MI, USA
- Chirife J., 1971, Diffusional Process in the Drying of Tapioca Root, *Journal of Food Science*, 36: 327–330
- Chirife J., 1983, Fundamentals of the Drying Mechanism during Air Dehydration of Foods, In *Advances in Drying*, Mujumdar A.S., Ed., Hemisphere Publishing Corp., Washington DC, 2, 73–102
- Chirife, J.; Cacherro, R.A., 1970, Through-circulation Drying of Tapioca Root, *Journal of Food Science*, 35:364–368
- Choi Y., Okos M. R., 1986, Effects of temperature and composition on the thermal properties of foods, In Le M. Maguer, P. Jelen (Eds.), *Food Engineering and Process Applications*, 1:93-101
- Chua K. J., Chou S. K., Hawlader M. N. A., Mujumdar A. S., Ho J. C., 2002, Modelling the Moisture and Temperature Distribution within an Agricultural Product undergoing Time-varying Drying Schemes, *Biosystems Engineering*, 81(1): 99-111
- Comini, G., DelGuidice, S., Lewis, R. W., Zienkiewicz, O. C., 1974, Finite element solution of non-linear heat conduction problems with special emphasis on phase changes. *Znt. J. Num. Meth. Engr.*, 8:613-24
- Coulter S., Pham Q. T., McNeil I, McPhail N. G., 1995, Geometry, cooling rates and weight losses during pig chilling, *International Journal of Refrigeration*, 18:456–464.
- Crank J., 1975, *The Mathematics of Diffusion*. (Oxford University Press, London, England)
- Curcio S., Aversa M., Calabro V., Iorio G., 2008, Simulation of food drying: FEM analysis and experimental validation, *Journal of Food Engineering*, 87: 541–553
- De Bonis M. V., Ruocco G., 2008, A generalized conjugate model for forced convection drying based on an evaporative kinetics, *Journal of Food Engineering*, 89: 232–240
- De Elvira C., Sanz P. D., Carrasco J. A., 1996, Characterising the detachment of thermal and geometric centres in a parallelepipedic frozen food subjected to a fluctuation in storage temperature, *Journal of Food Engineering*, 29: 257–268
- DeAlwis, A. A. P. & Fryer, P. J., 1990, A finite-element analysis of heat generation and transfer during ohmic heating of food, *Chemical Engineering Science*, 45: 1547-59
- Deng, Y., Zhao, Y.Y., 2008a, Effects of pulsed-vacuum and ultrasound on the osmodehydration kinetics and microstructure of apples (Fuji), *Journal of Food Engineering*, 85:84-93
- Deng, Y., Zhao, Y.Y., 2008b, Effect of pulsed vacuum and ultrasound osmopretreatments on glass transition temperature, texture, microstructure and calcium penetration of dried apples (Fuji), *LWT-Food Science and Technology*, 41:1575-1585
- Djendoubi N., Boudhriouaa N., Bonazzi C., Kechaoua N., 2009, Drying of sardine muscles: Experimental and mathematical investigations, *Food and Bioproducts Processing*, 87:115–123

- Du X.U., Xiling Q.I., Wang B., 1997, Influence of heating methods on heat and mass transfer during vacuum freeze-drying, *J. Eng. Thermophys*, 18: 612–615
- Engelman, M. S., 1982, FIDAP - a fluid dynamics analysis package, *Advances in Engineering Software*, 4:163-6
- Engelman M. S., Sani R. L., 1983, Finite element simulation of an in package pasteurization process, *Numerical Heat Transfer*, 6:41-54
- Farid M., Kizilel R., 2009, A new approach to the analysis of heat and mass transfer in drying and frying of food products, *Chemical Engineering and Processing* 48: 217–223
- Farid M.M., Chen X.D., 1998, The analysis of heat and mass transfer during frying of food using a moving boundary solution procedure, *Heat Mass Transfer* 34: 69–77
- Farkas B. E., Singh R. P., Rumsey T. R., 1996a, Modelling heat and mass transfer in immersion frying. I, model development, *Journal of Food Engineering*, 29: 211–226.
- Farkas B. E., Singh R. P., Rumsey T. R., 1996b, Modelling heat and mass transfer in immersion frying. II, model solution and verification, *Journal of Food Engineering*, 29: 227–248.
- Fasina O. O., Fleming H. P., 2001, Heat transfer characteristics of cucumbers during blanching, *Journal of Food Engineering*, 47:203–210
- Fito P., Chiralt A., Barat J. M., Andre´s A., Mart´ınez-Monzo´ J., Martinez-Navarrete N., 2001, Vacuum impregnation for development of new dehydrated products, *Journal of Food Engineering*, 49:297–302.
- Gachagan A. , McNab A., Blindt R., Patrick M., Marriot C., 2004, A high power ultrasonic array based test cell, *Ultrasonics* 42: 57–68
- Geankoplis C. J., 1993, *Transport Processes and Unit Operations*, 3<sup>rd</sup> edition, Prentice Hall International Inc., New Jersey
- Geedipalli S.S.R, Rakesh V., Datta A.K., 2007, Modeling the heating uniformity contributed by a rotating turntable in microwave ovens, *Journal of Food Engineering*, 82: 359–368
- Ghani A. G. A., Farid M. M., Chen X. D., Richards P., 1999a, Numerical simulation of natural convection heating of canned food by computational fluid dynamics, *Journal of Food Engineering*, 41:55–64
- Ghani A. G. A., Farid M. M., Chen X. D., Richards P., 1999b, An investigation of deactivation of bacteria in a canned liquid food during sterilisation using computational fluid dynamics, CFD, *Journal of Food Engineering*, 42:207–214
- Ghani A. G. A., Farid M. M., Chen X. D., Richards P., 2001, Thermal sterilisation of canned food in a 3-D pouch using computational fluid dynamics, *Journal of Food Engineering*, 48: 147–156.
- Gowda B. S., Narasimham G. S. V. L., Murthy M. V. K., 1997, Forced-air precooling of spherical foods in bulk: a parametric study, *International Heat and Fluid Flow*, 18:613–624
- Gustafson, R. J. & Segerlind, L. J., 1977, Continuum theory for gas-solid-liquid media - II: Finite element method, *Trans ASAE*, 20:1190-3, 1200
- Gustafson R. J., Mase G. E., Segerlind L. J., 1977a, Continuum theory for gas-solid-liquid media-I: Theory development, *Trans ASAE*, 20: 1186-9

- Gustafson R. J., Thompson D. R., Sokhansanj S., 1977b, Temperature and stress analysis of corn kernel using the finite element method, ASAE Paper No. 77-5514. ASAE, St. Joseph, MI, USA
- Gustafson, R. J., Thompson, D. R. & Sokhansanj, S., 1979, Temperature and stress analysis of corn kernels - finite element analysis, *Trans ASAE*: 22: 955-60
- Haghighi K., Segerlind L. J., 1988a, Modeling simultaneous heat and mass transfer in an isotropic sphere - a finite element approach, *Trans ASAE*, 31: 629-37
- Haghighi K., Segerlind L. J., 1988b, Failures of biomaterials subjected to temperature and moisture gradients using the finite element method, Parts I and II. *Trans ASAE*, 31:930-7,938-46
- Haghighi K., Irudayaraj J., Strohshine R. L., Sokhansanj S., 1990, Grain kernel drying simulation using the finite element method, *Trans ASAE*, 33:1957-65
- Halder A., Datta A. K., Spanswick R. M., 2010, Water transport in cellular tissues during thermal processing, *AIChE Journal*, 57(9): 2574-2588
- Hayakawa, K., Succar, J., 1982, Heat transfer and moisture loss from spherical fresh produce, *Journal of Food Science*, 47:596-605
- Heinz G., Hautzinger P., 2007, Meat Processing Technology For Small- To Medium- Scale Producers, Food and Agriculture Organization of The United Nations Regional Office for Asia and The Pacific, Bangkok, p.221 <http://www.fao.org/docrep/010/ai407e/AI407E18.htm>, last access date 08.11.2012
- Henderson S.M., Pabis S., 1961, Grain drying theory: I. Temperature effects on drying coefficient, *J. Agric. Eng. Res.*, 6(3): 169–174
- Henderson, S.M., 1974, Progress in developing the thin layerdrying equation. *Trans ASAE*, 17: 1167–1172
- Hernandez, J. A., Pavon, G., Garcia, M. A., 2000, Analytical solution of mass transfer equation considering shrinkage for modeling food drying kinetics, *Journal of Food Engineering*, 45: 1–10
- Hill J. E., Leitman J. D., Sunderland J. E., 1967, Thermal conductivity of various meats, *Food Technology*, 21:1143–8
- Hong Y. C., Bakshi A. S., Labuza T. P., 1986, Finite element modeling of moisture transfer during storage of mixed multicomponent dried fruits, *J. Food Sci.*, 51:554-8
- Honikel KO, Hamm R., 1994, Measurement of Water-Holding Capacity and Juiciness, Quality Attributes in Meat, Poultry and Fish Products. London: Blackie Academic and Professional Publication, p.125–161
- Hu Z. H., Sun D.-W., 2000, CFD simulation of heat and moisture transfer for predicting cooling rate and weight loss of cooked ham during air-blast chilling process, *Journal of Food Engineering*, 46:189–197
- Hu Z. H., Sun D.-W., 2001b, Predicting local surface heat transfer coefficients by different turbulentk-Emodels to simulate heat and moisture transfer during air-blast chilling, *International Journal of Refrigeration*, 24:702–717

- Hu Z. H., Sun D.-W., 2002, CFD evaluating the influence of air-flow on the thermocouple-measured temperature data during air-blast chilling, *International Journal of Refrigeration*, 25:546 – 551
- Hu, Z. H., Sun, D.-W., 2001a, Effect of fluctuation in inlet airflow temperature on CFD simulation of air-blast chilling process, *Journal of Food Engineering*, 48:311–316.
- Humidity calculator, <http://www.ringbell.co.uk/info/humid.htm>, last access date 10.12.2012
- Ikedia J. N., Correia L. R., Fenton G. A., and N. Ben-Abdallah N., 1996, Finite Element Modeling of Heat Transfer in Meat Patties During Single-sided Pan-frying, *Journal Of Food Science*, 61 (4):796-802
- Jason A.C., 1958, A Study of Evaporation and Diffusion Processes in the Drying of Fish Muscle, In *Fundamental Aspects of Dehydration of Foodstuffs*, Soc. Chem. Ind., London and MacMillan Co., New York, 103–135.
- Jiang H., Thompson D. R., Morey R. V, 1987, Finite element model of temperature distribution in broccoli stalks during forced-air processing, *Tran ASAE*, 30:1473-7
- Jung A., Fryer P. J., 1999, Optimising the quality of safe food: computational modelling of a continuous sterilisation process, *Chemical Engineering Science*, 54:717–730
- Karel M., Lund D.B., 2003, *Physical Principles of Food Preservation*, 2nd ed.; Marcel Dekker Inc., New York
- Kashaninejad M., Tabil L.G., 2004, Drying characteristics of Purslane (*Portulaca oleraceae*L.). *Drying Technology*, 22(9): 2183–2200
- Kaya A., Aydın O., Dincer I., 2006, Numerical modeling of heat and mass transfer during forced convection drying of rectangular moist objects, *International Journal of Heat and Mass Transfer*, 49:3094–3103
- Kaya A., Aydın O., Demirtas C., 2007, Drying kinetics of red delicious apple, *Biosystems Engineering*, 96(4): 517–524
- Kaya A., Aydın O., Demirtas C., Akgun, M., 2007, An experimental study on the drying kinetics of quince, *Desalination*, 212: 328–343
- Kaya A., Aydın O., Demirtas C., 2007, Concentration boundary conditions in the theoretical analysis of convective drying process. *Journal of Food Process Engineering*, 30: 564–577
- Kaya A., Aydın O., Kolaylı S., 2010, Effect of different drying conditions on the vitamin C (ascorbic acid) content of Hayward kiwifruits (*Actinidia deliciosa Planch*), *Food and Bioproducts Processing* 88:165–173
- Keey R. B., 1992, *Drying principles and practice*, 5<sup>th</sup> edition, Pergamon Press, Oxford
- Khompis, V., Segerlind, L. J. & Brook, R. C., 1984, Pressure patterns in cylindrical grain storages, ASAE Paper No. 84-3011, ASAE, St. Joseph, MI, USA
- Kurozawa L. E., Hubinger M. D., Park K.J., 2012, Glass transition phenomenon on shrinkage of papaya during convective drying, *Journal of Food Engineering* 108: 43–50
- Krokida M. K., Panagiotou N. M., Maroulis Z. B. , Saravacos G. D., 2001, Thermal Conductivity: Literature Data Compilation For Foodstuffs, *International Journal of Food Properties*, 4(1): 111-137

- Krokida M.K., Maroulis Z.B., 1997, Effect of Drying Method on Shrinkage and Porosity, *Drying Technology*, 15 (10), 2441–2458.
- Kumar, A., Bhattacharya, M. & Blaylock, J., 1990, Numerical simulation of natural convection heating of canned thick viscous liquid food products, *Journal of Food Science*, 55: 1403-11
- Lee S. W., Kang C. S., 2003, Effects of moisture content and drying temperature on the physicochemical properties of ostrich jerky, *Nahrung*, 47(5):330-333
- Lewicki, P. P., Witrowa-Rajchert, D., Nowak, D., 1998, Effect of drying mode on drying kinetics of onion, *Drying Technology*, 16 (1&2): 59–81
- Li S., Liu W. K., 2002, Meshfree and particle methods and their applications, *Appl. Mech. Rev.*, 55(1):1-34
- Li Y.B., Yagoobi J.S., Moreira R.G., Yamasaengsung R., 1998, Steam impingement drying of tortilla chips, in: *Drying '98-Proceedings of the 11th International Drying Symposium*, 1221–1228
- Lin W., Haik Y., Bernatz R., Chen C. J., 1997, Finite analytic method and its applications: a review, *Dynamics of Atmospheres and Oceans*, 27:17-33
- Lin, Y. E., Anantheswaran, R. C. & Puri, V. M., 1989, Modeling temperature distribution during microwave heating, ASAE Paper No. 89-6506, ASAE, St. Joseph, MI, USA
- Liu G. R., *Mesh Free Methods Moving beyond the Finite Element Method*, CRC Press, Singapore, 2002
- Liu Z., Scanlon M. G., 2003, Modelling Indentation of Bread Crumb by Finite Element Analysis, *Biosystems Engineering*, 85(4): 477–484
- Lozano J.E., Rotstein E., Urbicain M.J., 1983, Shrinkage, Porosity, and Bulk Density of Foodstuffs at Changing Moisture Contents, *Journal of Food Science*, 48:1497–1502, 1553
- Madamba, P. S., Griscoll, R. H., Buckle, K. A., 1996, The thin layer drying characteristics of garlic slices, *Journal of Food Engineering*, 29:75–97
- Marchant, J. A., 1976, The prediction of air flows in crop drying systems by the finite element method. *J. Agr. Engng Res*, 21:417-29
- Marra F., Lyng J., Romano V., McKenna B., 2007, Radio-frequency heating of foodstuff: Solution and validation of a mathematical model, *Journal of Food Engineering*, 79: 998–1006
- May B.K., Perre P., 2002, Importance of considering exchange surface area reduction to exhibit a constant drying flux period in food stuffs, *Journal of Food Engineering*, 54: 271–282
- McCarthy K. L., Merson R. L., 1989, A finite element method to model steam infusion heat transfer to a free falling film, *J. Food Process Engng*, 11:43-54
- Mirade P. S., Daudin J. D., 2000, Numerical study of the airflow patterns in a sausage dryer, *Drying Technology*, 18:81–97
- Mirade P. S., Picgirard L., 2001, Assessment of airflow patterns inside six industrial beef carcass chillers, *International Journal of Food Science and Technology*, 36:463–475
- Misra, R. N. & Young, J. H., 1979, Finite element approach for solution of transient heat transfer in spheres, *Trans ASAE*, 22:944-9

- Moreno J., Simpson R., Baezaa A., Morales J., Muñoz C., Sastryd S., Almonacid S., 2012, Effect of ohmic heating and vacuum impregnation on the osmodehydration kinetics and microstructure of strawberries (cv. Camarosa), *LWT-Food Science and Technology*, 45:148-154
- Mulet, A., 1994,. Drying modelling and water diffusivity in carrots and potatoes, *Journal of Food Engineering*, 22: 329–348
- Naveh, D., Kopelman, L. J., Pflug, I. J., 1983c, The finite element method in thermal processing of foods, *Journal of Food Science*, 48:1086-93
- Naveh, D., Pflug, I. J., Kopelman, I. J., 1983b, Transient cooling of conduction heating products during sterilization: sterilization values. *Journal of Food Processing & Preservation*, 7:275-86
- Nobel PS. Cells and Diffusion, *Physicochemical and Environmental Plant Physiology*, 4th ed. San Diego, CA: Elsevier, Inc., 2009:3–42
- Pan Z., Singh R. P., Rumsey T. R., 2000, Predictive modelling of contact-heating process for cooking a hamburger patty, *Journal of Food Engineering*, 46:9–19
- Pan, J. C. & Bhowmik, S. R., 1991, The finite element analysis of transient heat transfer in fresh tomatoes during cooling, *Trans ASAE*, 34:972-6
- Panagiotou N. M., Krokida M. K., Maroulis Z. B., Saravacos G. D., 2004, Moisture Diffusivity: Literature Data Compilation for Foodstuffs, *International Journal of Food Properties*, 7(2):273 -299
- Perez M. G. R., Calvelo A., 1984, Modeling the Thermal Conductivity of Cooked Meat, *Journal of Food Science*, 49:152-156
- Pham Q. T., Willix J., 1989, Thermal Conductivity of Fresh Lamb Meat, Offals and Fat in the Range - 40 to + 30°C: Measurements and Correlations, *Journal of Food Science*, 54(3):508-515
- Planinic M., Velic D., Tomas S., Bilic M., Bucic A., 2005, Modelling of drying and rehydration of carrots using Peleg's model, *Eur Food Res Technol*, 221:446–451
- Polivka, R. M. & Wilson, E. L., 1976, Finite element analysis of nonlinear heat transfer problems. User's Guide for Determination of Temperature, DOT, Department of Civil Engineering, University of California, Berkeley, CA, USA
- Potluri, P. L., 1985, Modeling temperature and surface heat transfer coefficient in beef carcass cooling using finite element technique, Ph.D. dissertation, Texas A & M University, College Station, TX, USA
- Proud L. C., Lund D. B., 1983, Thermal Properties of Beef Loaf Produced in Foodservice Systems, *Journal of Food Science*, 48:677-680
- Purwadaria J. K., Heldman, D. R., 1980, A finite element method for prediction of freezing rates in food products with anomalous shapes, ASAE Paper No. 80-6015, ASAE, St. Joseph, MI, USA
- Purwadaria, J. K., Heldman, D. R., 1982, A finite element model for prediction of freezing rates in food products with anomalous shape, *Trans ASAE*, 25:827-32
- Quang Tri Ho Q., Verlinden B. E., Verboven P., Vandewalle S., Nicolai B. M., 2007, Simultaneous measurement of oxygen and carbon dioxide diffusivities in pear fruit tissue using optical sensors, *Journal of the Science of Food and Agriculture*, 87:1858–1867

- Rahman M. S., Ched X. D., Perera C. O., 1997, An Improved Thermal Conductivity Prediction Model for Fruits and Vegetables as a Function of Temperature, Water Content and Porosity, *Journal of Food Engineering*, 31: 163-170
- Rahman, M. S., Potluri, P. L., 1991, Thermal conductivity of fresh and dried squid meat by line source probe method, *Journal of Food Science*, 56: 582-583.
- Ramallo L.A., Mascheroni R.H., 2012, Quality evaluation of pineapple fruit during drying process, *Food and bioproducts processing*, 90:275-283
- Ramos I.N., JMiranda J.M.R., Brandão Teresa R.S., Silva C.L.M., 2010, Estimation of water diffusivity parameters on grape dynamic drying, *Journal of Food Engineering*, 97: 519–525
- Rizvi S.S.H. , 2005, Thermodynamic Properties of Foods in Dehydration. In *Engineering Properties of Foods*, 3rd ed. Rao M.A., Rizvi S.S.H., Datta A.K., Eds., Marcel Dekker Inc., New York, 239–326
- Roberts J. S., Tong C. H., 2003, Drying Kinetics of Hygroscopic Porous Materials Under Isothermal Conditions and the Use of a First Order Reaction Kinetic Model for Predicting Drying, *International Journal of Food Properties*, 6 (3): 355–367
- Roduit B., Borgeat C. H., Cavin S., Fragnière C., Dudler V., 2005, Application of Finite Element Analysis (FEA) for the simulation of release of additives from multilayer polymeric packaging structures, *Food Additives and Contaminants*, 22(10): 945–955
- Rosello C., Canellas J., Simal S., Berna, A., 1992, Simple mathematical model to predict the drying rates of potatoes, *Journal of Agriculture and Food Chemistry*, 40: 2374–2378
- Rosello C., Simal S., SanJuan N., Mulet A., 1997, Nonisotropic Mass Transfer Model for Green Bean Drying, *J. Agric. Food Chem*, 45: 337–342
- Rovedo C. O., Suarez C., Viollaz P. E., 1995, Drying of foods: evaluation of a drying model, *Journal of Food Engineering*, 26:–12
- Ruiz-Lopez I.I., Cordova A.V., Rodriguez-Jimenes G.C., García-Alvarado M.A., 2004, Moisture and temperature evolution during food drying: effect of variable properties, *Journal of Food Engineering*, 63: 117–124.
- Ruiz-Lopez I.I., Garcia-Alvarado M.A., 2007, Analytical solution for food-drying kinetics considering shrinkage and variable diffusivity, *Journal of Food Engineering*, 79: 208–216
- Rumsey T. R., Fridley R. B., 1977, Analysis of viscoelastic contact stresses in agricultural products using the finite element method, *Trans ASAE*, 20:162-7,171
- Sadrnia H., Rajabipour A. Jafari A., Javadi A., Mostofi Y., Kafashan J., Dintwa E., De Baerdemaeker J., 2008, Internal bruising prediction in watermelon compression using nonlinear models, *Journal of Food Engineering*, 86: 272–280
- Sahin S., Şumnu G. S., *Physical Properties of Foods*, Springer, 2006
- Saravacos G.D., Charm S.E., 1962, A Study of the Mechanism of Fruit and Vegetable Dehydration, *Food Technology*, 16 (1): 78–81.
- Sastry, S. K., Beelman, R. B., Speroni, L. J., 1985, A three-dimensional finite element model for thermally induced changes in foods: application to degradation of agaritine in canned mushrooms. *Journal of Food Science*, 50:1293-9, 1325

- Sastry S. K., 1986, Mathematical evaluation of process schedules for aseptic processing of low-acid foods containing discrete particulates, *J. Food Sci.*, 51:1323-8.
- Sharaf-Eldeen, Y.I., Blaisdell, J.L., Hamdy, M.Y., 1980, A model for ear corn drying, *Trans. ASAE* 23(5): 1261–1265
- ShareMe, PixArea Download, <http://shareme.com/download/pixarea.html>, last access date 10.12.2011
- Spells, K. E. 1960. The thermal conductivities of some biological fluids, *Physics in Medicine and Biology* 5(2), 139-153
- Srikiatden J., Roberts J.S., 2007, Moisture Transfer In Solid Food Materials: A Review Of Mechanisms, Models, And Measurements, *International Journal of Food Properties*, 10: 739–777
- Straatsma J., Houwelingen G. V., Steenbergen A. E., De Jong P., 1999, Spray drying of food products: 1. simulation model, *Journal of Food Engineering*, 42:67–72
- Stroshine R., *Physical Properties of Agricultural Materials and Food Products*, Purdue University, USA Indiana, 2000
- Sun D., Zheng L., 2006, Vacuum cooling technology for the agri-food industry: Past, present and future, *Journal of Food Engineering*, 77:203-14
- Sweat V. E., Haugh C. G., Stadelman W. J., 1973, Thermal Conductivity of Chicken Meat at Temperatures between -75 and 20°C, *Journal of Food Science*, 38:158-160
- Syarief, A. M., Gustafson, R. J. & Morey, R. V., 1987, Moisture diffusion coefficients for yellow-dent corn components. *Trans ASAE*, 30:522-8
- Talbot, M. T., 1989, Pressure patterns established by commercial finite element package. ASAE Paper No. 89-6039. ASAE, St. Joseph, MI, USA
- Tassou S. A., Xiang, W. 1998, Modelling the environment within a wet air-cooled vegetable store, *Journal of Food Engineering*, 38: 169–187
- Thiagarajan I. V., Meda V., Panigrahi S., Shand P., 2006, Thin - Layer Drying Characteristics of Beef Jerky, *ASABE MBSK 06-214*
- Thuwapanichayanan, R., Prachayawarakorn, S., Kunwisawa, J., Soponronnarit, S., 2011, Determination of effective moisture diffusivity and assessment of quality attributes of banana slices during drying, *LWT-Food Science and Technology*, 44: 1502-1510
- Trujillo F. J., Wiangkaew C., Pham Q. T., 2007, Drying modeling and water diffusivity in beef meat, *Journal of Food Engineering* 78: 74–85
- Unver B., Agan C., 2003, Application of heat transfer analysis for frozen food storage caverns, *Tunnelling and Underground Space Technology*, 18: 7–17
- Upadhyaya, S. K., Cooke, J. R., Rand, R. H., 1985, A fluid filled spherical shell model of thermal elastic behavior of avian eggs, *J. Agr. Engng Res.*, 32: 95-109
- Upadhyaya S. K., Rumsey T. R., 1989, A finite element model for coupled equations. ASAE Paper No. 89-6578, ASAE, St. Joseph, MI, USA
- Vaccarezza L.M., Lombardi J.L., Chirife J., 1974a, Kinetics of Moisture Movement during Air Drying of Sugar Beet Root. *J. Food Technology*, 9: 317–327.



- Van der Sman R.G.M., 2007, Moisture transport during cooking of meat: An analysis based on Flory–Rehner theory, *Meat Science*, 76: 730–738
- Vega-Gálvez, A., Lemus-Mondaca, R., Bilbao-Sáinz, C., Fito, P., Andrés, A., 2008, Effect of air drying temperature on the quality of rehydrated dried red bell pepper (var. Lamuyo), *Journal of Food Engineering*, 85:42-50
- Vega-Gálvez A., Ah-Hen K., Chacana M., Vergara J.,Martínez-Monzó J., García-Segovia P., Lemus Mondaca R., Di Scala K., 2012, Effect of temperature and air velocity on drying kinetics, antioxidant capacity, total phenolic content, colour, texture and microstructure of apple (var. Granny Smith) slices, *Food Chemistry*, 132: 51–59
- Verboven P., Scheerlinck N., De Baerdemaeker J., Nicolai B.M., 2000a, Computational fluid dynamics modelling and validation of the isothermal airflow in a forced convection oven, *Journal of Food Engineering*, 43:41–53
- Verboven P., Scheerlinck N., De Baerdemaeker J., Nicolai B.M., 2000b, Computational fluid dynamics modelling and validation of the temperature distribution in a forced convection oven, *Journal of Food Engineering*, 43:61–73
- Wang L., Sun D., 2002, Modelling three-dimensional transient heat transfer of roasted meat during air blast cooling by the finite element method, *Journal of Food Engineering* 51:319–328
- Wang L., Sun D., 2003, Recent developments in numerical modelling of heating and cooling processes in the food industry - a review, *Trends in Food Science and Technology*, 14:408-423
- Wang Z. H., Chen G. H., 1999, Heat and mass transfer during low intensity convection drying, *Chemical Engineering Science*, 54:3899–3908
- Wang, N., Brennan, J.G., 1995, Changes in structure density and porosity of potato during dehydration, *Journal of Food Engineering*, 24: 61–76.
- Willix J., Harris M. B., Carson J. K., 2006, Local surface heat transfer coefficients on a model beef side, *Journal of Food Engineering* , 74: 561–567
- Willix J., Lovatt S. J., Amos N. D., 1998, Additional Thermal Conductivity Values of Foods Measured by a Guarded Hot Plate, *Journal of Food Engineering* 37: 159-174
- Wu, Y., & Irudayaraj, J., 1996, Analysis of heat, mass and pressure transfer in starch based food systems, *Journal of Food Engineering*, 29: 399–414
- Xiao H. W., Gao Z. j., 2012, The Application of Scanning Electron Microscope (SEM) to Study the Microstructure Changes in the Field of Agricultural Products Drying, *Scanning Electron Microscopy*, Dr. Viacheslav Kazmiruk (Ed.), ISBN: 978-953-51-0092-8, p213-226 InTech, Available from:<http://www.intechopen.com/books/scanning-electron-microscopy/the-application-of-scanning-electron-microscope-sem-to-study-the-microstructure-changes-in-the-field> last date access date 05.10.2012
- Xiao, H.W., Lin, H., Yao, X.D., Du, Z.L., Lou, Z., Gao, ZJ., 2009, Effects of different pretreatments on drying kinetics and quality of sweet potato bars undergoing air impingement drying, *International Journal of Food Engineering*, 5, Article 5
- Xu Y. F., Burfoot D., 1999a, Simulating the bulk storage of foodstuffs, *Journal of Food Engineering*, 39: 23–29
- Xu Y. F., Burfoot D., 1999b, Predicting condensation in bulks of foodstuffs, *Journal of Food Engineering*, 40:121–127

Yadollahinia A., Jahangiri M., 2009, Shrinkage of potato slice during drying, *Journal of Food Engineering*, 94: 52–58

Yang H.S., Kang S.W., Jeong J.Y., Chun J.Y., Joo S.T., Park G.B., Choi S.G., 2009, Optimization of Drying Temperature and Time for Pork Jerky Using Response Surface Methodology, *Food Science and Biotechnology*, 18 (4): 985-990

Zhang, Q., Litchfield, J.B., 1991, An optimization of intermittent corn drying in a laboratory scale thin layer dryer, *Drying Technology*, 9: 233–244

Ziegler G. R., Rizvi S. S. H., Acton J. C., 1987, Relationship of Water Content to Textural Characteristics, Water Activity, and Thermal Conductivity of Some Commercial Sausages, *Journal of Food Science*, 52(4):901-905

Zogzas N.P., Maroulis Z.B., 1994, Marinos-Kouris, D. Densities, Shrinkage and Porosity of Some Vegetables during Air Drying, *Drying Technology*, 12 (7): 1653–1666

APPENDIX A

PROPERTIES OF FOOD MATERIAL

Table A.1. Properties of Food Material

	Equation/data	Food Sample	Reference
<b>a. Thermal Conductivity (k)</b>			
1	$k_{\text{water}} = 0.57109 + 1.7625 \cdot 10^{-3}T - 6.7036 \cdot 10^{-6}T^2$ $k_{\text{CHO}} = 0.20141 + 1.3874 \cdot 10^{-3}T - 4.3312 \cdot 10^{-6}T^2$ $k_{\text{protein}} = 0.17881 + 1.1958 \cdot 10^{-3}T - 2.7178 \cdot 10^{-6}T^2$ $k_{\text{fat}} = 0.18071 - 2.7604 \cdot 10^{-3}T - 1.7749 \cdot 10^{-7}T^2$ $k_{\text{ash}} = 0.32961 + 1.4011 \cdot 10^{-3}T - 2.9069 \cdot 10^{-6}T^2$ $k_{\text{ice}} = 2.2196 - 6.2489 \cdot 10^{-3}T + 1.0454 \cdot 10^{-4}T^2$	General (0-90°C)	Choi and Okos, 1986; Şahin and Şumnu, 2006
2	$K = K_w X_w + K_f X_f + K_p X_p$ $K_w = 5.94 \times 10^{-1} + 9.57 \times 10^{-4}T$ $K_f = 1.79 \times 10^{-1} - 2.23 \times 10^{-4}T$ $K_p = 1.72 \times 10^{-1} + 2.81 \times 10^{-4}T$	Cooked beef (whole and ground chuck)	Baghe-Khandan M. S., Okos M. R., 1981
3	$k = a + b \cdot T + c \cdot T^2 + d \cdot T^3$	Pork and beef dripping	Willix <i>et al.</i> , 1998
4	$\left(\frac{k_c}{k_o}\right)\left(\frac{1}{1-\varepsilon_a}\right) = 1.82 - 1.66 \exp(-0.85 \frac{X_w}{X_i})$	Apple, pear, squid, beef, potato	Rahman, 1992
5	$k = 0.481 + 0.000865T$ dark meat, 0-20°C $k = 0.476 + 0.000605T$ white meat, 0-20°C $k = 1.14 - 0.0146T - 0.986 \times 10^{-4}T^2$ dark meat, -75 to -10°C $k = 1.07 + 0.0149T - 1.04 \times 10^{-4}T^2$ white meat, -75 to -10°C	White and dark chicken meat	Sweat <i>et al.</i> , 1973
6	$k = 0.056 + 0.57 \cdot X_w$	Biological materials with more than 50% moisture	Spells, 1960
7	for subfreezing range; $k = a + bT + c/T$ $k = k_f + b(T - T_f) + c\left(\frac{1}{T} - \frac{1}{T_{fr}}\right)$ $k = k_f + d(T - T_{fr})$ above freezing	Different meat samples(-40 - 30°C), parallel and perpendicular heat is applied, constants given on Table A.2	Pham & Willix, 1989
8	$k = 0.216 + 0.0024(\text{moisture}\% \text{ wetbasis})$	Salami, sausage	Ziegler <i>et al.</i> , 1987
9	$\frac{K_d}{K_o} = A - B \exp(-C \frac{X_w}{X_{w0}})$	constants given on Table A.3	Rahman, 1992
10	k values for large range of foods	general	Krokida <i>et al.</i> , 2001; Bowman <i>et al.</i> , 1975
<b>b. Heat Capacity (C<sub>p</sub>)</b>			
1	$C_p = 4.180 \cdot X_{\text{water}} + 1.711 \cdot X_{\text{protein}} + 1.928 \cdot X_{\text{fat}} + 1.547 \cdot X_{\text{CHO}} + 0.908 \cdot X_{\text{ash}}$	general	Choi and Okos, 1986

**Table A.1 (continued)**

2	$C_p = A + BT + CT^2$ constants for each component given p.140 on reference.	general	Şahin & Şumnu, 2006
<b>c. Heat Transfer Coefficient (h)</b>			
1	$h = Bi \cdot k / L_0$	Beef loaf	Proud & Lund, 1983
2	$h = 8.3u^{0.77}$ (Tu=2.5%) $h = 21u$ (Tu>20%) $h = 12.5u^{0.6}$ (for cooling)	Carcass	Willix <i>et al.</i> , 2006
3	$Nu_{fc} = 0.102 \cdot Re^{0.675} Pr^{0.333}$ 5000<Re<50000	Forced convection	Wang & Sun, 2002
<b>d. Diffusivity/Diffusion coefficient (D)</b>			
1	Diffusivity values for large range of foods	general	Panagiotou <i>et al.</i> , 2004
2	$D = D_0 e^{\left(-\frac{E_a}{RT}\right)}$	constants given on Table A.4 for beef	Trujillo <i>et al.</i> , 2007
3	$\frac{X_m - X_{eq}}{X_i - X_{eq}} = \frac{8}{\pi^2} \sum_{n=0}^{\infty} \frac{1}{(2n+1)^2} e^{-\frac{(2n+1)^2 \pi^2 Dt}{4L^2}}$	general	Trujillo <i>et al.</i> , 2007
<b>Equilibrium Moisture Content (m<sub>e</sub>)</b>			
1	$RH = \exp\left(-\frac{5222.47}{RT} \times m_e^{-1.0983}\right)$	chicken meat	Chen <i>et al.</i> , 1999

**Table A.2** Empirical curve-fitting parameters for Equation (a.7) in Table A.1 (Pham & Willix, 1989)

Material	kf W/mK	b W/mK	c W/m	d W/mK <sup>2</sup>
Group I				
Leg muscle perpendicular	0.450	-0.0063	0.69	0.0009
Leg muscle minced	0.466	-0.0043	0.71	0.0011
Hearts	0.390	-0.0046	0.71	0.0009
Hearts minced	0.407	-0.0065	0.68	0.0008
Liver	0.417	-0.0073	0.65	0.0006
Liver minced	0.425	-0.0067	0.67	0.0012
Brains	0.494	-0.0039	0.84	0.0003
Kidneys	0.507	-0.0075	0.78	0.0012
Thymus	0.497	-0.0047	0.91	0.0012
Thymus minced	0.487	-0.0053	0.85	0.0009
Group II				
Leg muscle perpendicular	0.421	-0.0037	0.67	0.0010
Group III				
Fat	0.219	-0.0003	0.05	-0.0005
Fat minced	0.212	-0.0000	0.06	-0.0004

**Table A.3** Parameters and Precision of the Equation (a.9) in Table A.1 for Different Foods (Rahman, 1992)

Material	Process	n	A	B	C	r <sup>2</sup>	SD
Apple	Air drying	15	0.155	-0.021	-3.713	0.999	1.73
Beef	Cooking	41	1.832	1.737	0.814	0.995	9.05
Pear	Air drying	15	1.120	1.166	2.368	0.999	0.89
Potato	Air drying	10	1.245	1.279	1.654	0.999	0.09
Squid	Air drying	39	1.200	1.350	1.750	0.991	9.91

n, no of data points; r<sup>2</sup>, regression coefficient; SD, mean percent deviation

**Table A.4** Parameters of Arrhenius equation (d.2) in Table A.1 (Trujillo *et al.*, 2007)

	Model A	Model B	Model Bo	Model C
Slope	-3382.212	-3023.82	-3757.256	-2964.14
Ea	-28119.71	-25140.04	-31237.83	-24643.8
Intercept	-10.70998	-11.85469	-9.970738	-12.1888
D <sub>0</sub>	2.23E-5	7.11E-6	4.67E-05	5.09E-06
Correlation coefficient (r)	0.991	0.9872	0.8617	0.9888

Model A; constant temperature, constant volume

Model B& Bo; constant volume

Model C; variable volume

**Table A.5** Composition of Meat Samples (Pham and Willix, 1989)

Material	Water	Protein	Fat	Ash
Lean meat paralel	73.6	19.9	4.7	1.1
Lean meat perpendicular	72.5	19.3	7.2	0.9
Lean meat minced	73.9	18.6	4.5	1.0



**APPENDIX B**

**EQUILIBRIUM MOISTURE CONTENT VALUES**

**Table B.1** Equilibrium moisture content values calculated from nonlinear regression of experimental results.

Sample	Drying condition	$X_{eq}$ (g/g bds) based on	
		Equation 3.3 R <sup>2</sup> >0.999 SEE<0.02	Equation 3.4 R <sup>2</sup> >0.999 SEE<0.007
Lean meat_h1	48°C 0.5 m/s	1.6594	1.6594
	48°C 1.0 m/s	1.8563	1.7087
	48°C 1.7 m/s	1.6227	7.23 10 <sup>-9</sup>
	70°C 0.5 m/s	1.4195	2.24 10 <sup>-9</sup>
Lean meat_h2	48°C 0.5 m/s	1.5915	1.32 10 <sup>-9</sup>
	48°C 1.0 m/s	1.5589	0.588
	48°C 1.7 m/s	1.649	0.772
	70°C 0.5 m/s	1.2753	1.23 10 <sup>-9</sup>
Lean meat_v	48°C 0.5 m/s	1.6099	0.316
	48°C 1.0 m/s	1.5153	0.7809
	48°C 1.7 m/s	1.6379	1.334
	70°C 0.5 m/s	1.4421	3.17 10 <sup>-9</sup>
Minced meat	48°C 0.5 m/s	2.0253	1.29
	48°C 1.0 m/s	1.7773	1.3966
	48°C 1.7 m/s	2.0889	1.28
	70°C 0.5 m/s	1.7813	0.3056

<sup>1</sup>SEE; Standard error of estimate





## APPENDIX C

### COMSOL FINITE ELEMENT MODELING SOFTWARE WINDOWS

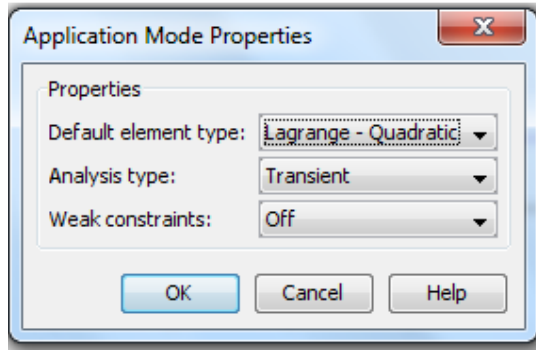


Figure C.1. Selection of application mode as transient for time dependent system

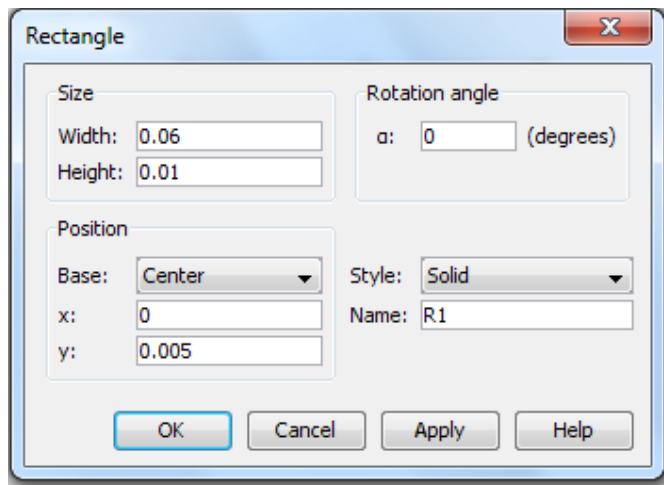


Figure C.2. Drawing of sample

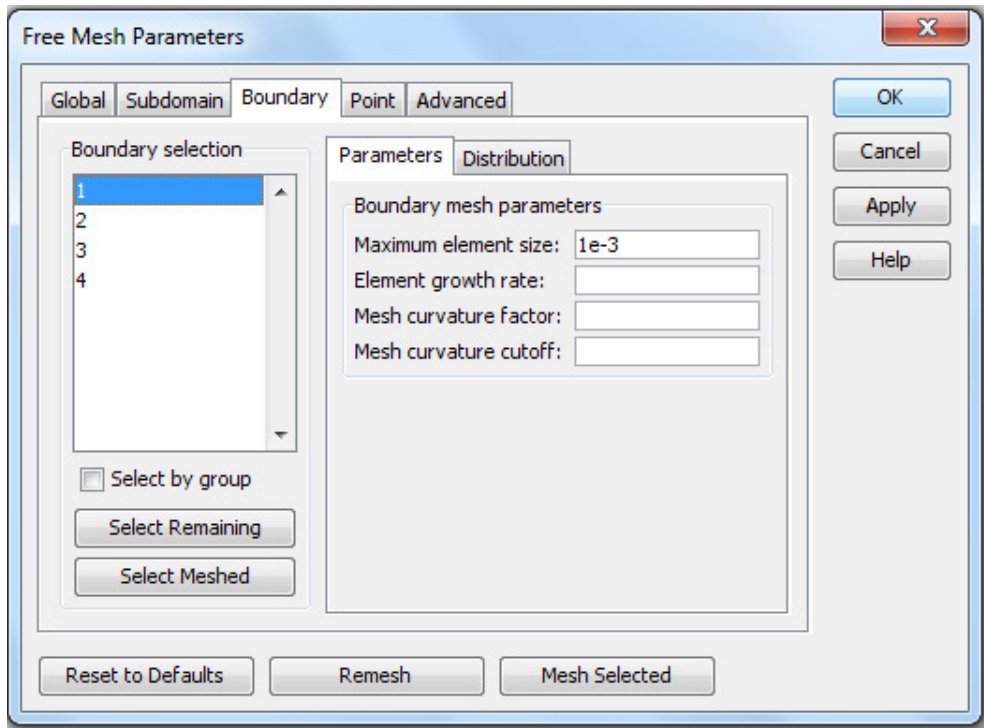


Figure C.3. Mesh definition in order to have augmented mesh around boundary 1,3,4

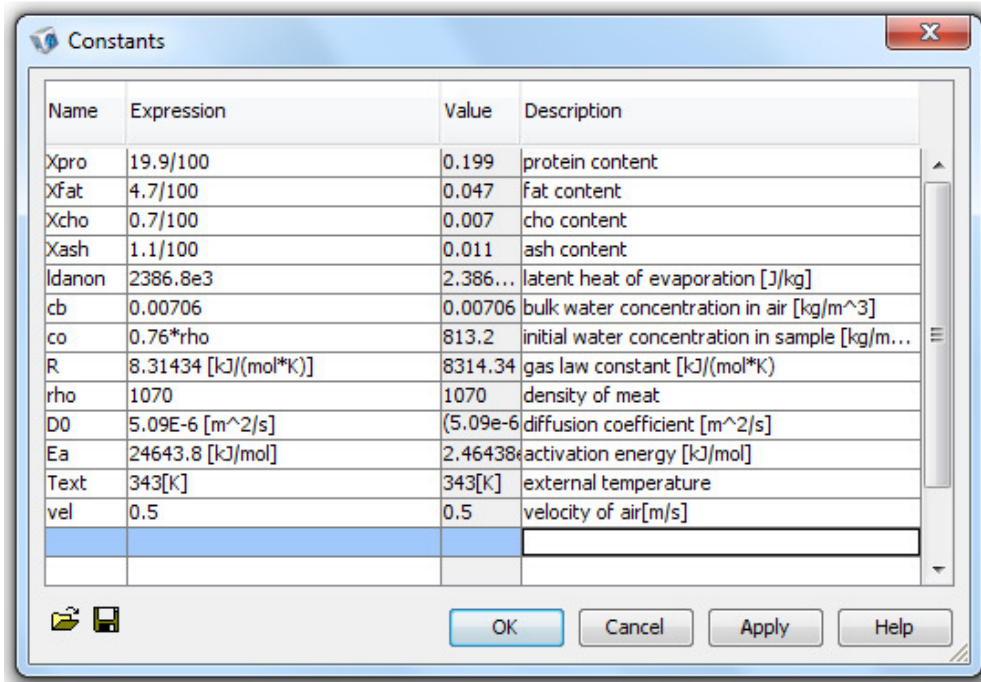


Figure C.4. Constants window

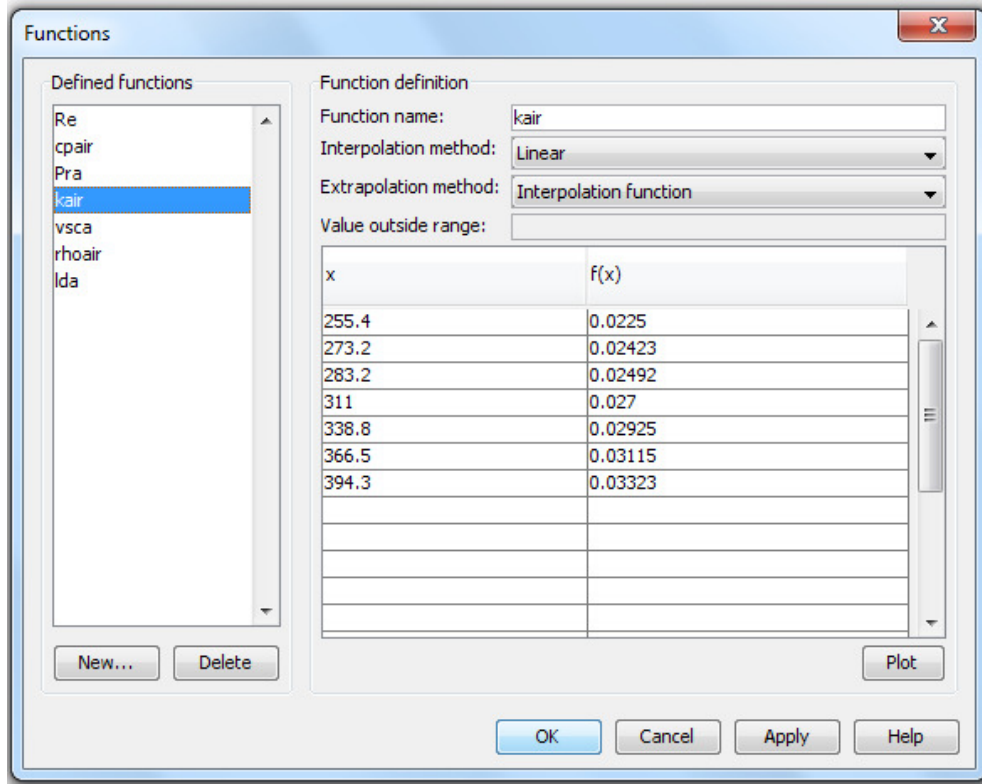


Figure C.5. Functions defined for air properties

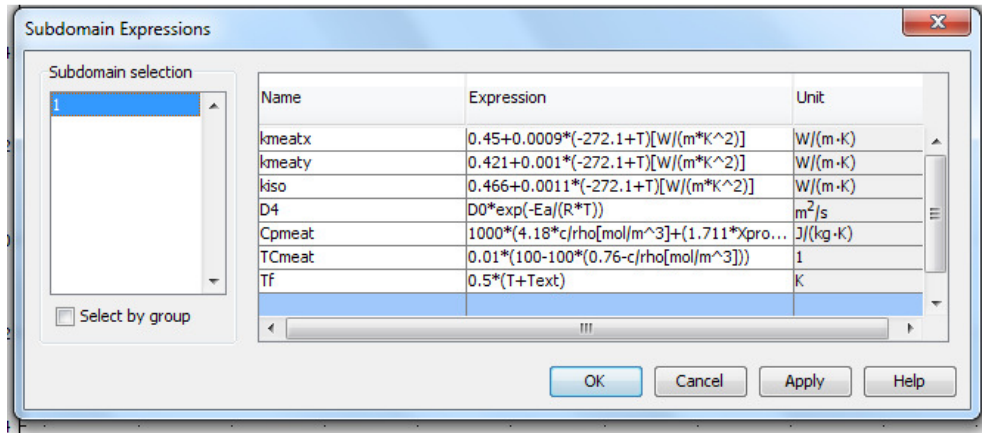


Figure C.6. Subdomain expressions

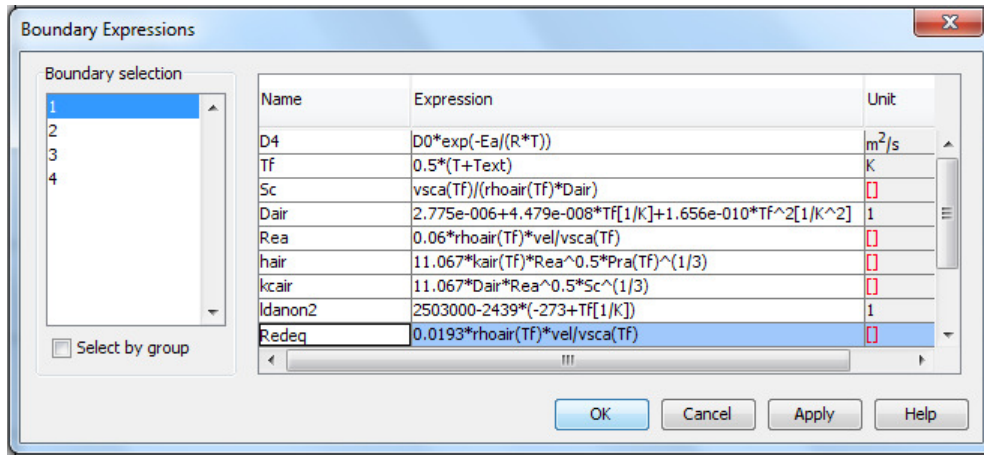


Figure C.7. Boundary expressions

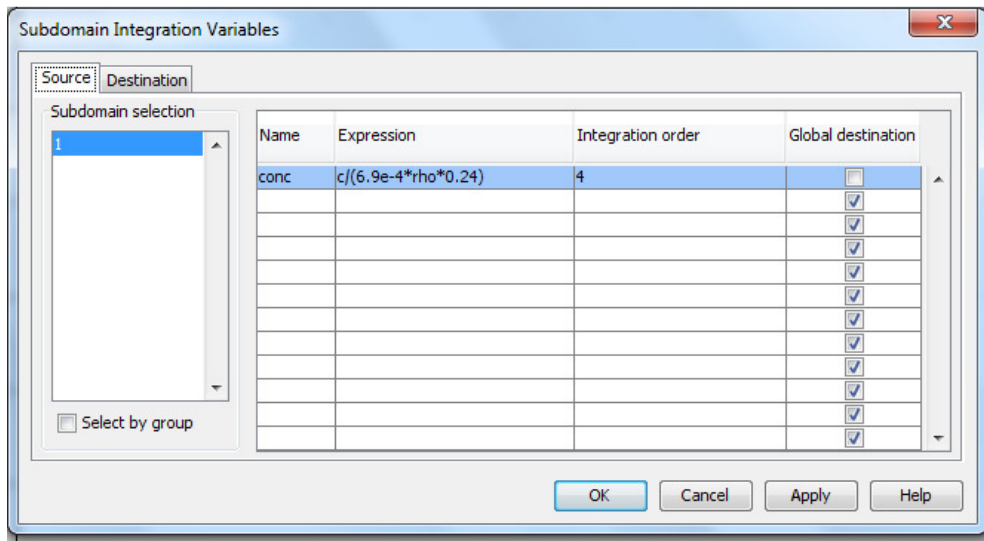
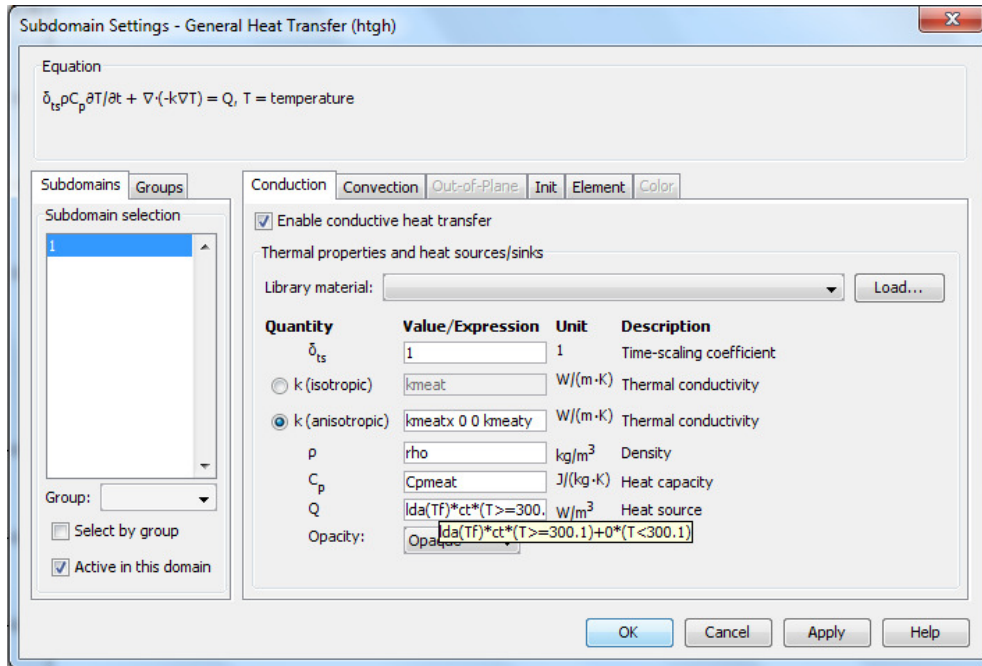
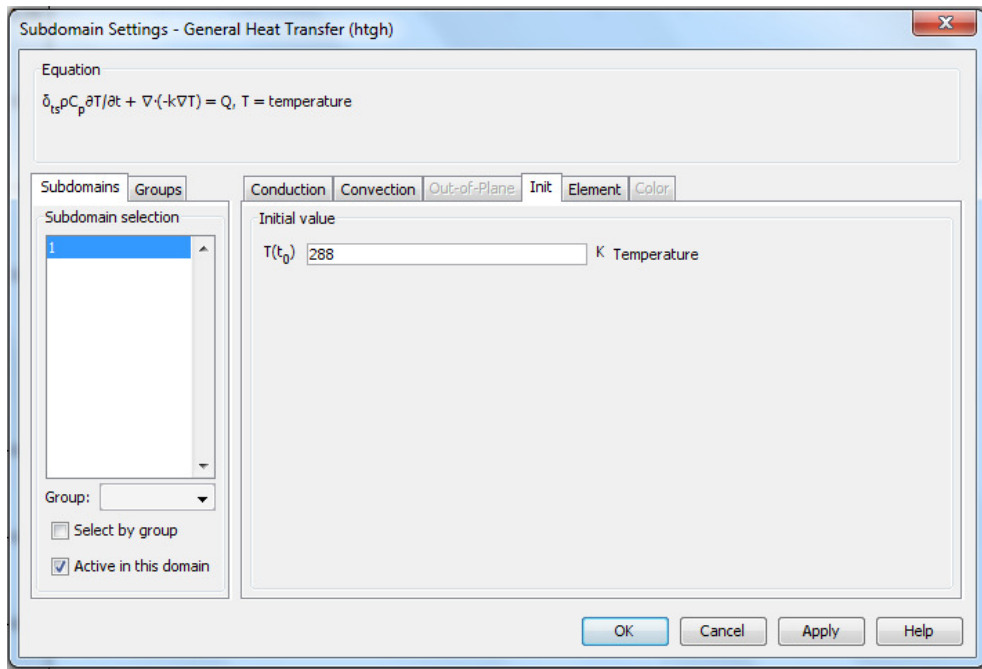


Figure C.8. Subdomain integration variable definition in order to calculate average moisture concentration with respect to time (24%; dry weight percentage found experimentally)



**Figure C.9.** Subdomain settings for heat transfer (Q is heat loss due to evaporation for model 2 defined in materials and methods chapter)



**Figure C.10.** Initial temperature of sample

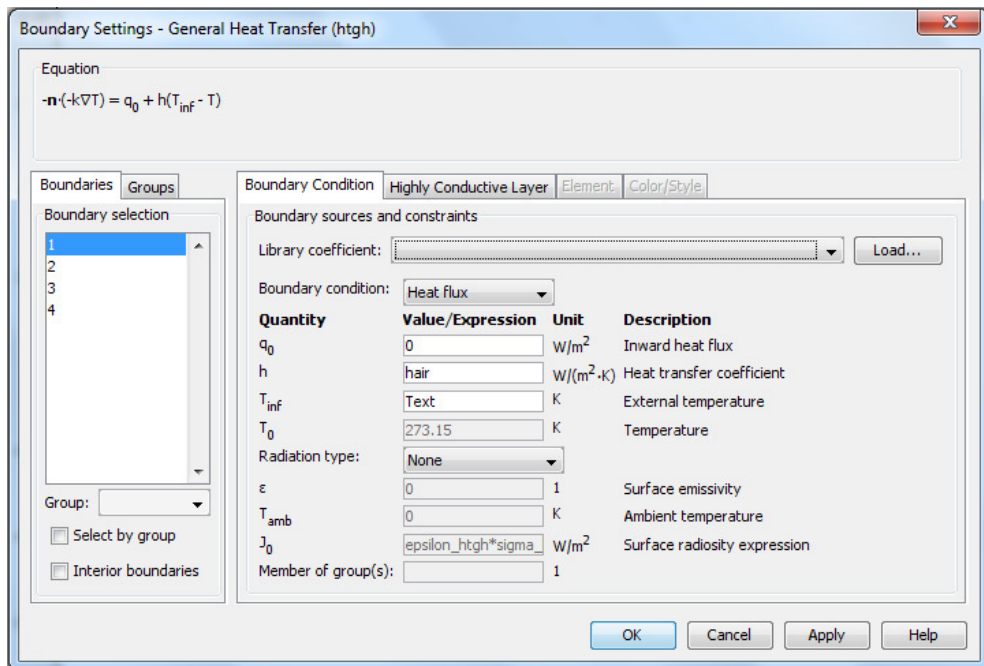


Figure C.11. Boundary settings for heat transfer for boundaries 1,3,4 defined Figure 2.4

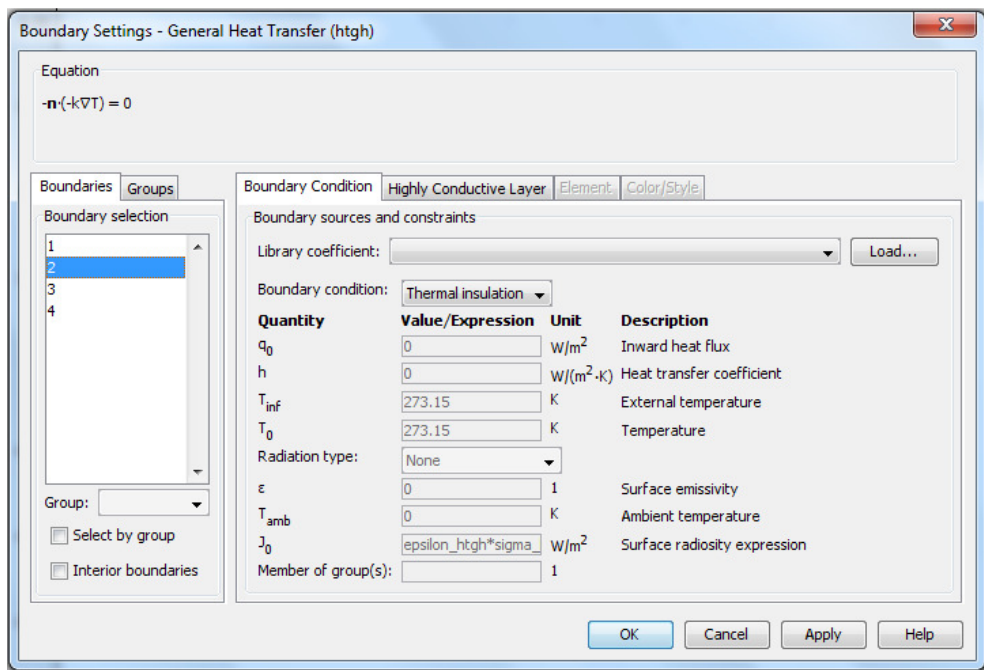


Figure C.12. Boundary settings for heat transfer for boundary 2 defined Figure 2.4

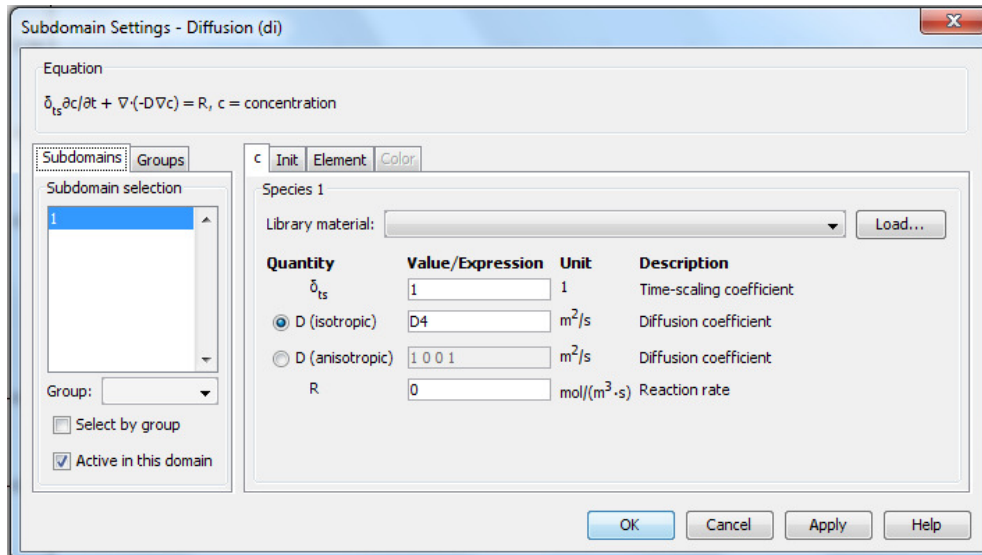


Figure C.13. Subdomain settings for mass transfer

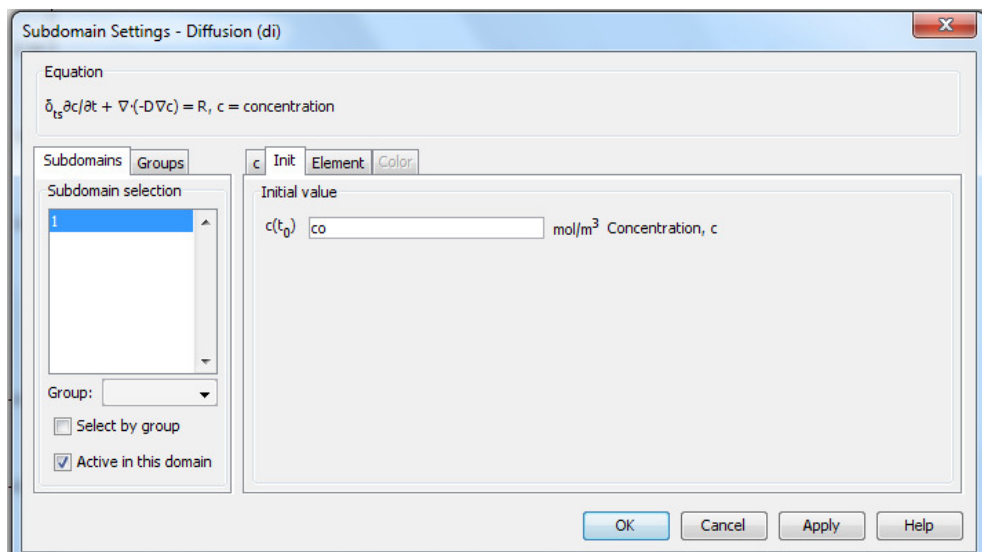


Figure C.14. Initial water concentration of sample



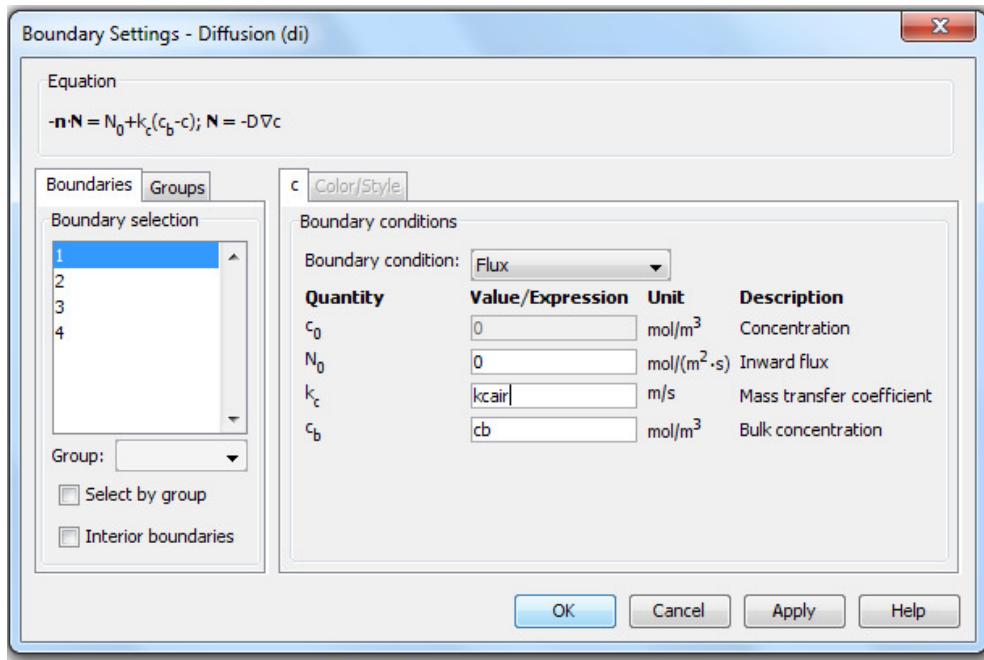


Figure C.15. Boundary settings for mass transfer at boundaries 1,3,4 defined Figure 2.4

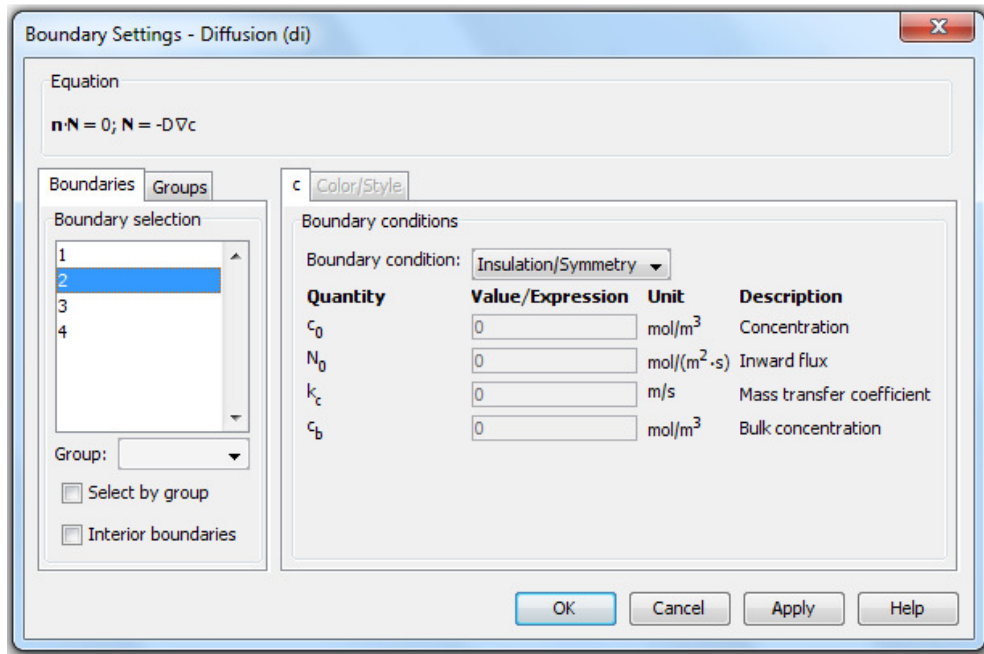
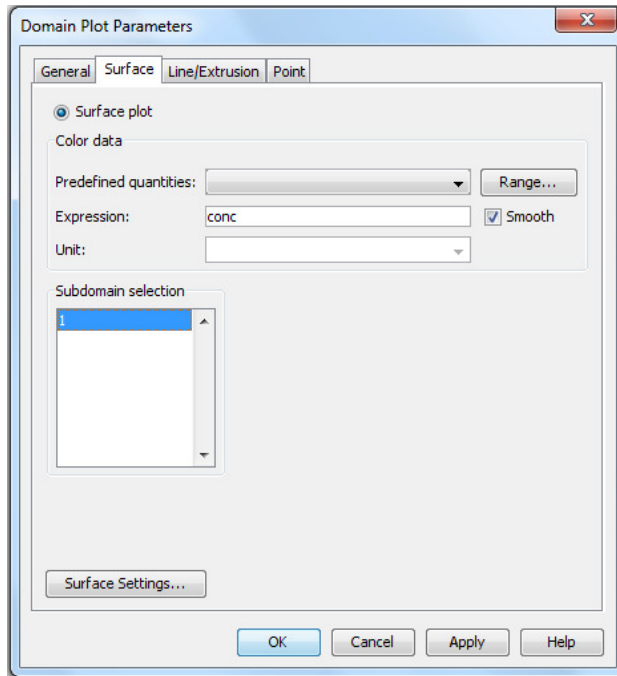
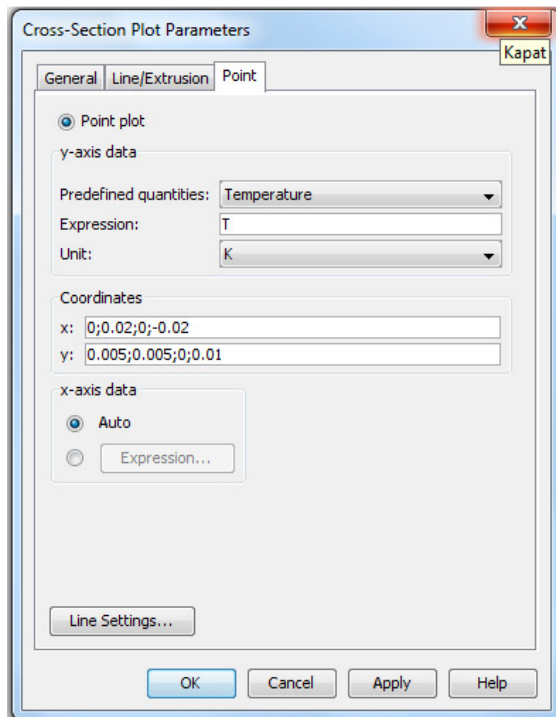


Figure C.16. Boundary setting for mass transfer at boundary 2 defined Figure 2.4





**Figure C.17.** Domain plot parameter selection after solving the model in order to observe average concentration at the subdomain



**Figure C.18.** Cross sectional plot parameter selection after solving the model in order to observe temperature values at the probe locations



## APPENDIX D

### RESULTS OF FEM USING MODEL 1

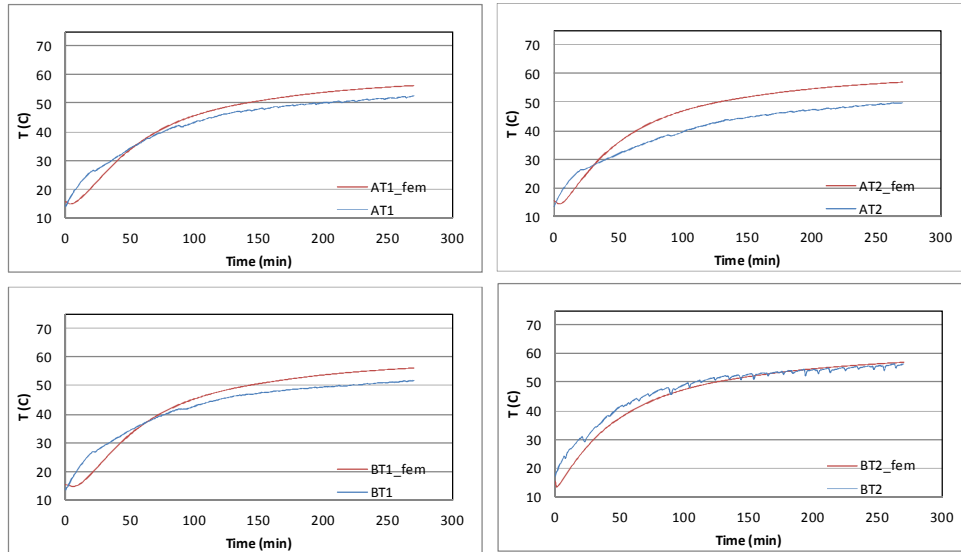


**Figure D.1a.** Temperature change at four different locations (AT1, AT2, BT1, BT2) in lean meat with flow normal to fibers (**h1**) with respect to drying time during drying at  $70\pm 1^\circ\text{C}$  0.5 m/s by using model 1

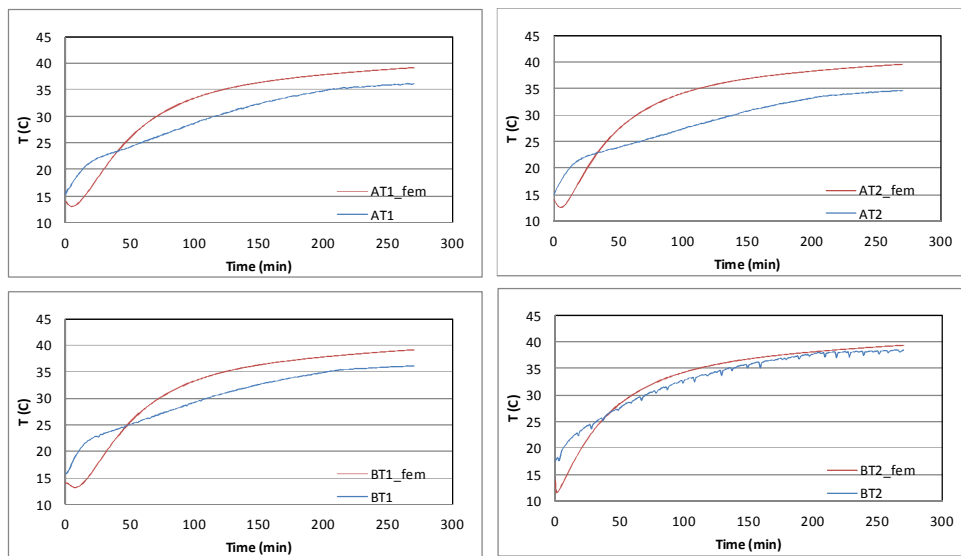


**Figure D.1b.** Temperature change at four different locations (AT1, AT2, BT1, BT2) in lean meat with flow normal to fibers (**h1**) with respect to drying time during drying at  $48\pm 1^\circ\text{C}$  1.0 m/s by using model 1

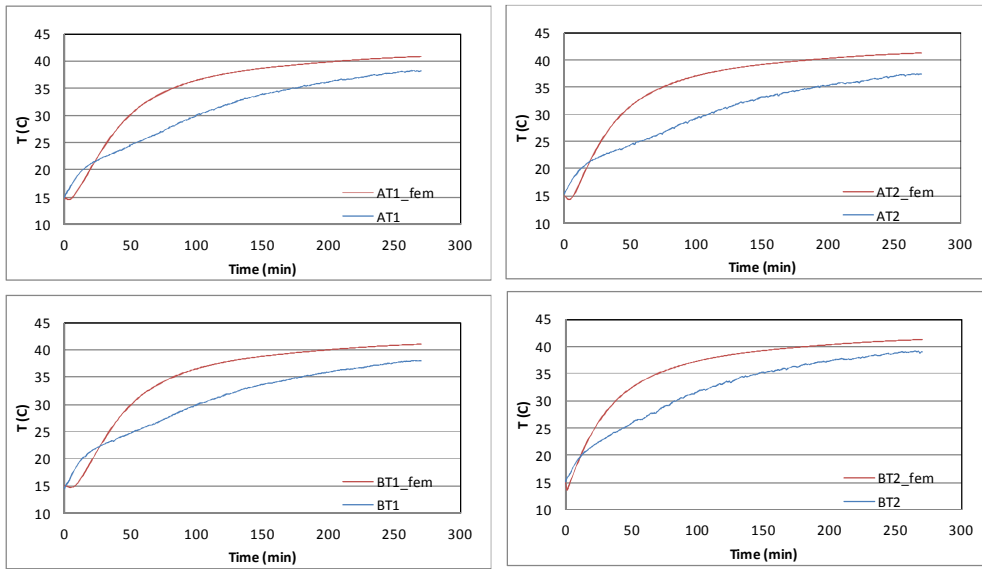


**Figure D.1c.** Temperature change at four different locations (AT1, AT2, BT1, BT2) in lean meat with flow normal to fibers (**h1**) with respect to drying time during drying at  $48\pm 1^\circ\text{C}$  1.7 m/s by using model 1

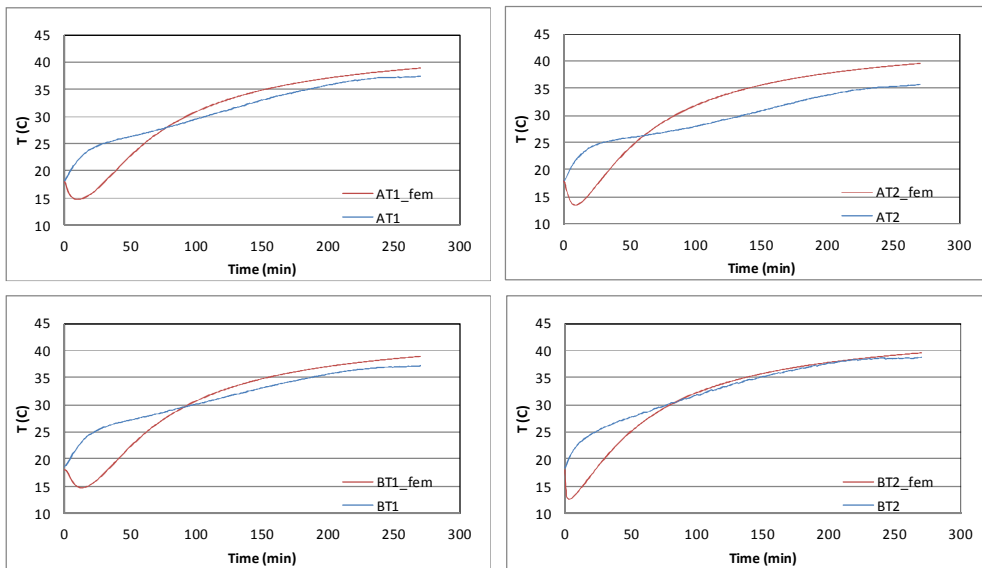


**Figure D.2a.** Temperature change at four different locations (AT1, AT2, BT1, BT2) in lean meat with flow normal to fibers, drying along the fibers (**v**) with respect to drying time during drying at  $48\pm 1^\circ\text{C}$  0.5 m/s by using model 1

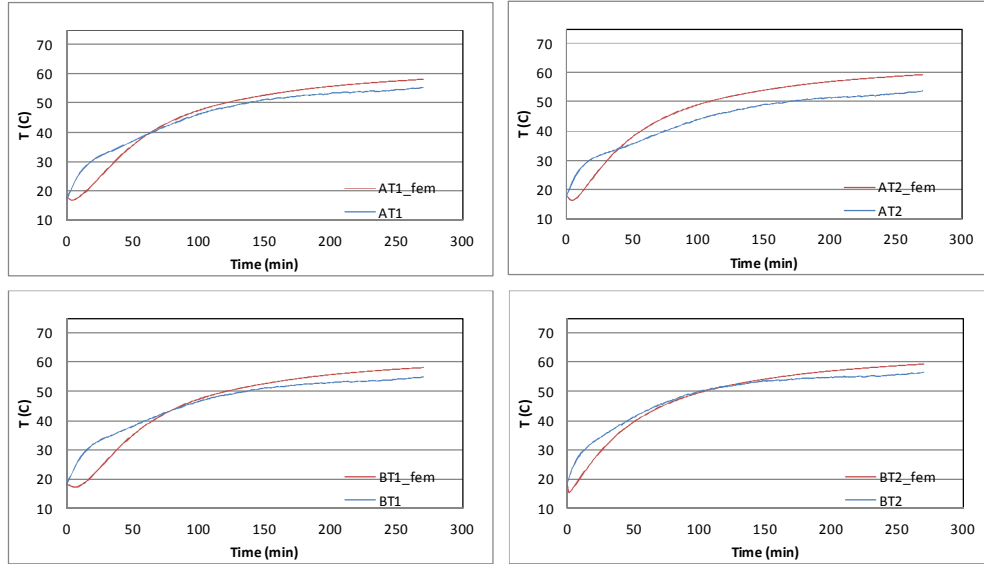


**Figure D.2b.** Temperature change at four different locations (AT1, AT2, BT1, BT2) in lean meat with flow normal to fibers, drying along the fibers ( $\nu$ ) with respect to drying time during drying at  $70\pm 1^{\circ}\text{C}$  0.5 m/s by using model 1

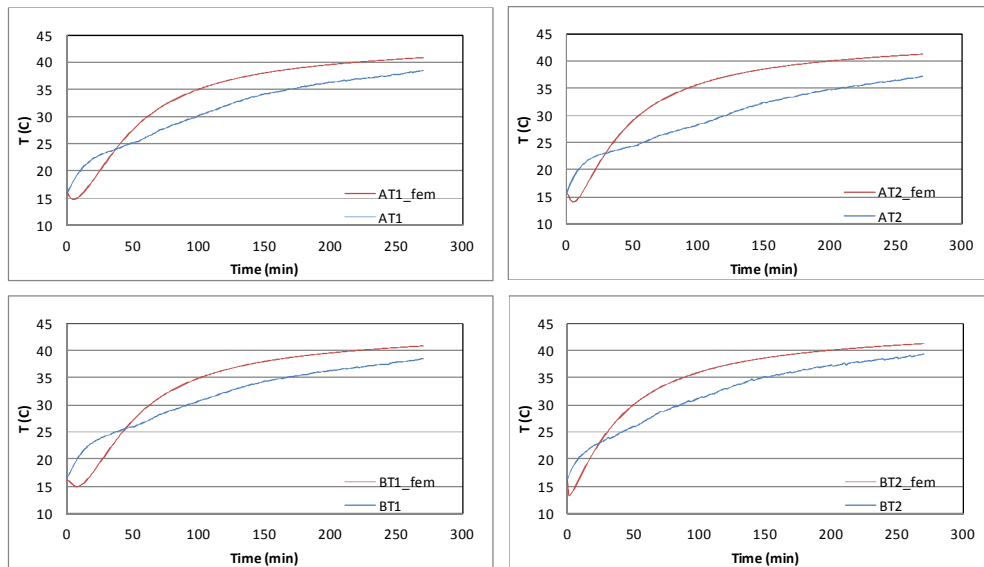


**Figure D.2c.** Temperature change at four different locations (AT1, AT2, BT1, BT2) in lean meat with flow normal to fibers, drying along the fibers ( $\nu$ ) with respect to drying time during drying at  $48\pm 1^{\circ}\text{C}$  1.0 m/s by using model 1

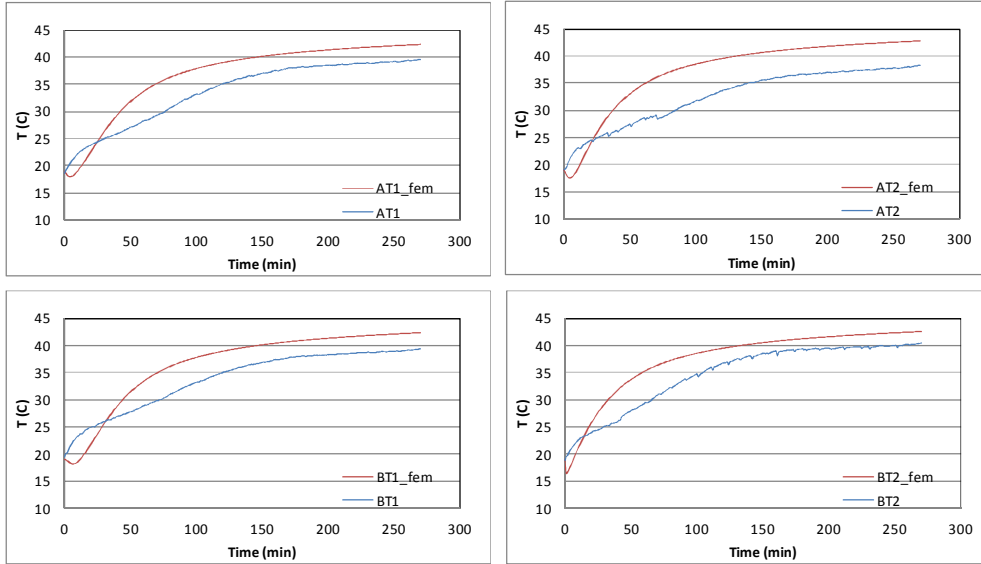


**Figure D.2d.** Temperature change at four different locations (AT1, AT2, BT1, BT2) in lean meat with flow normal to fibers, drying along the fibers (**v**) with respect to drying time during drying at  $48\pm 1^\circ\text{C}$  1.7 m/s by using model 1

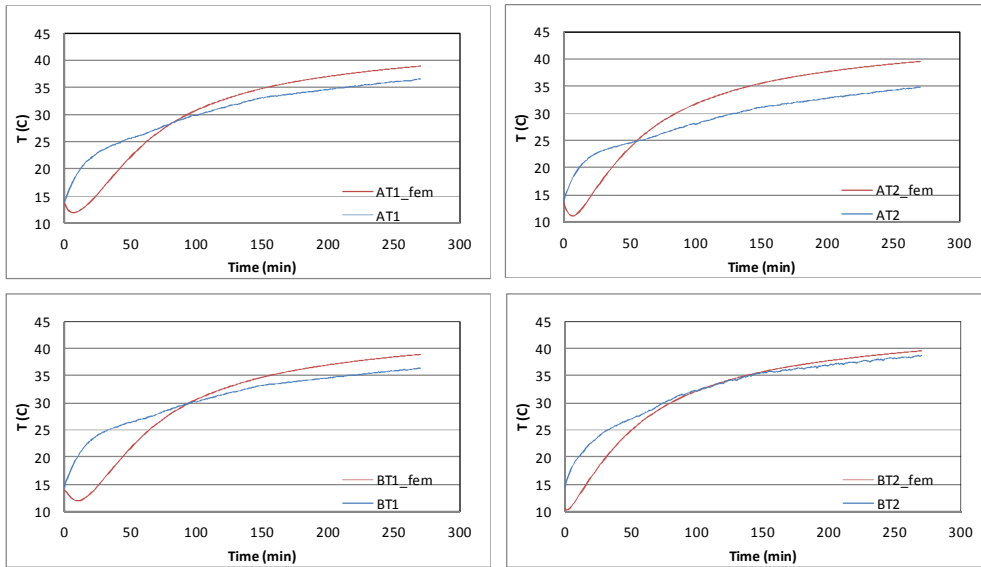


**Figure D.3a.** Temperature change at four different locations (AT1, AT2, BT1, BT2) in lean meat with flow along to fibers (**h2**) with respect to drying time during drying at  $48\pm 1^\circ\text{C}$  0.5 m/s by using model 1

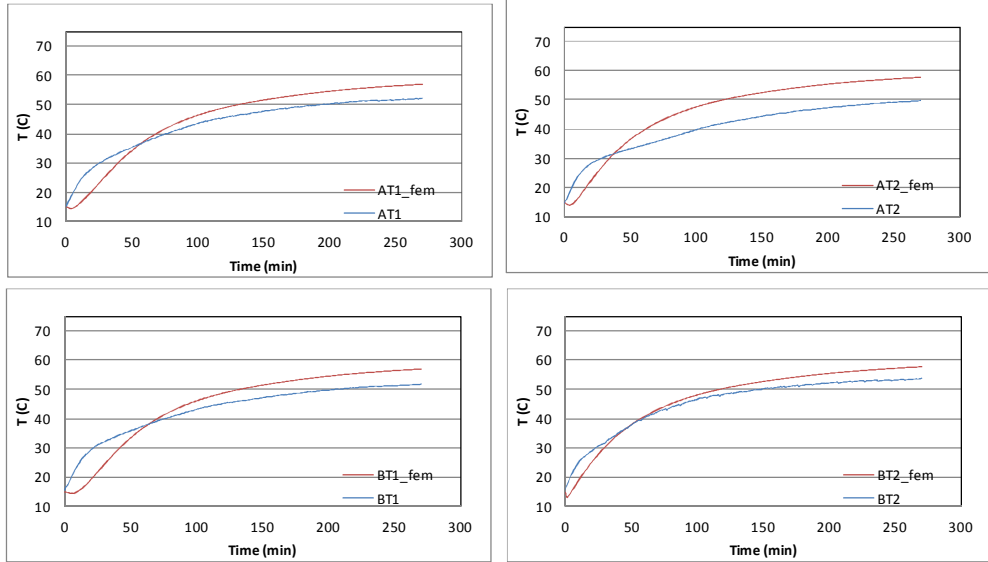


**Figure D.3b.** Temperature change at four different locations (AT1, AT2, BT1, BT2) in lean meat with flow along to fibers (**h2**) with respect to drying time during drying at  $70\pm 1^\circ\text{C}$  0.5 m/s by using model 1

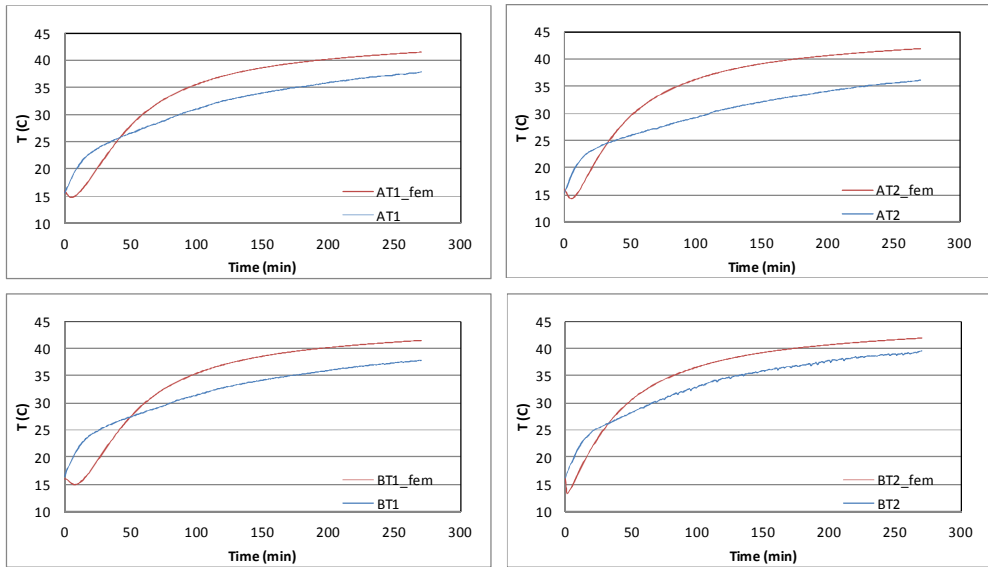


**Figure D.3c.** Temperature change at four different locations (AT1, AT2, BT1, BT2) in lean meat with flow along to fibers (**h2**) with respect to drying time during drying at  $48\pm 1^\circ\text{C}$  1.0 m/s by using model 1

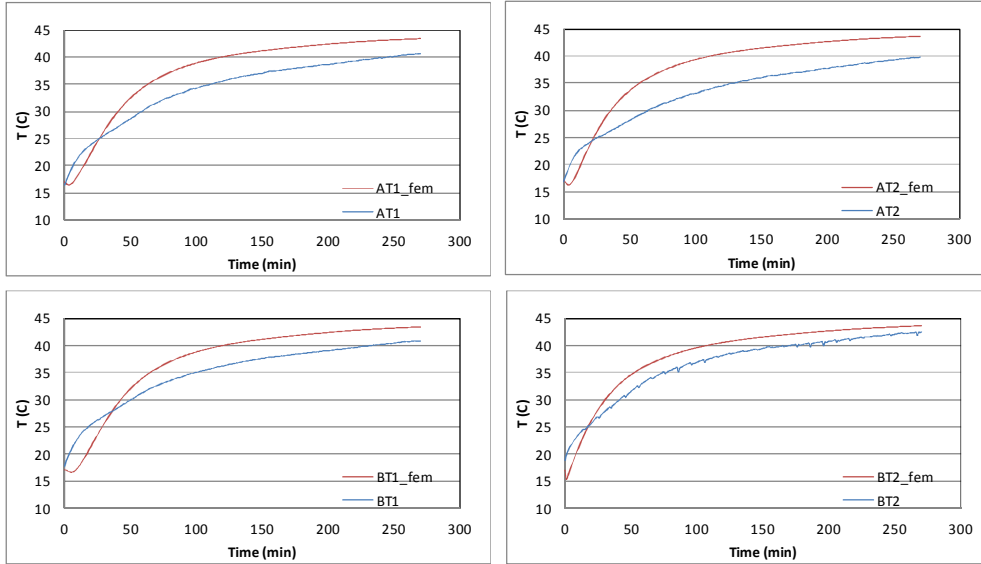


**Figure D.3d.** Temperature change at four different locations (AT1, AT2, BT1, BT2) in lean meat with flow along to fibers (**h2**) with respect to drying time during drying at  $48\pm 1^\circ\text{C}$  1.7 m/s by using model 1

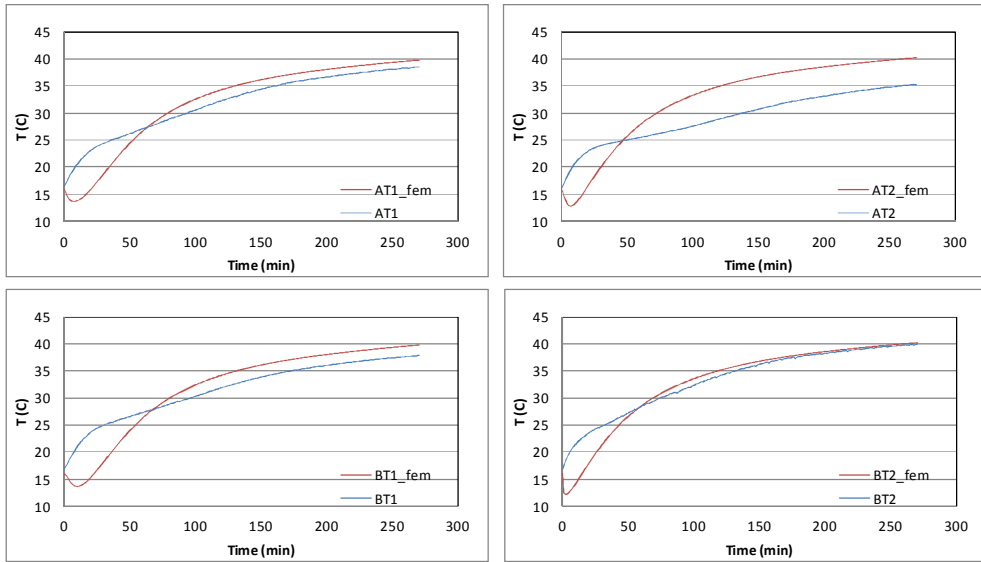


**Figure D.4a.** Temperature change at four different locations (AT1, AT2, BT1, BT2) in minced meat with respect to drying time at  $48\pm 1^\circ\text{C}$  0.5 m/s by using model 1



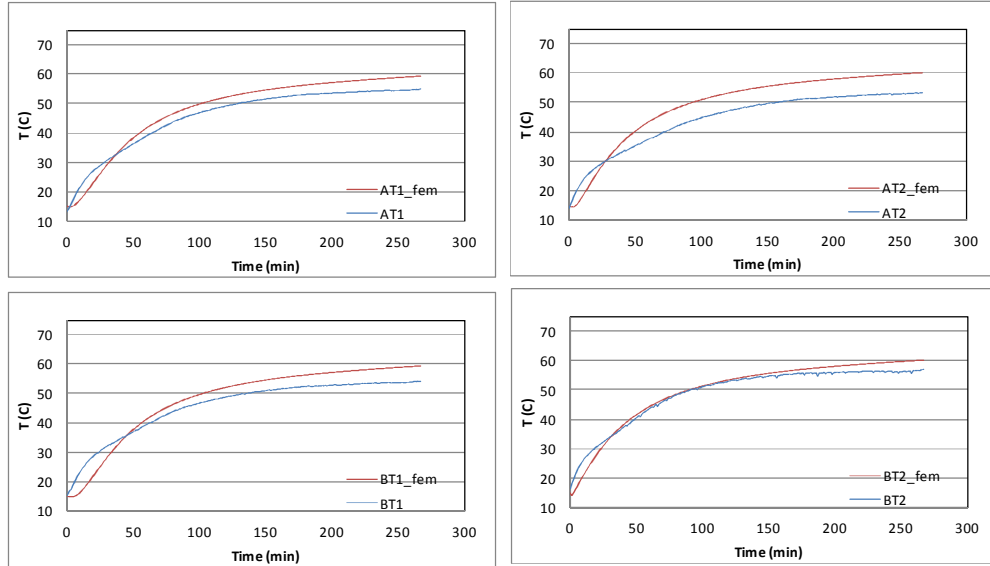


**Figure D.4b.** Temperature change at four different locations (AT1, AT2, BT1, BT2) in **minced** meat with respect to drying time at  $70\pm 1^\circ\text{C}$  0.5 m/s by using model 1

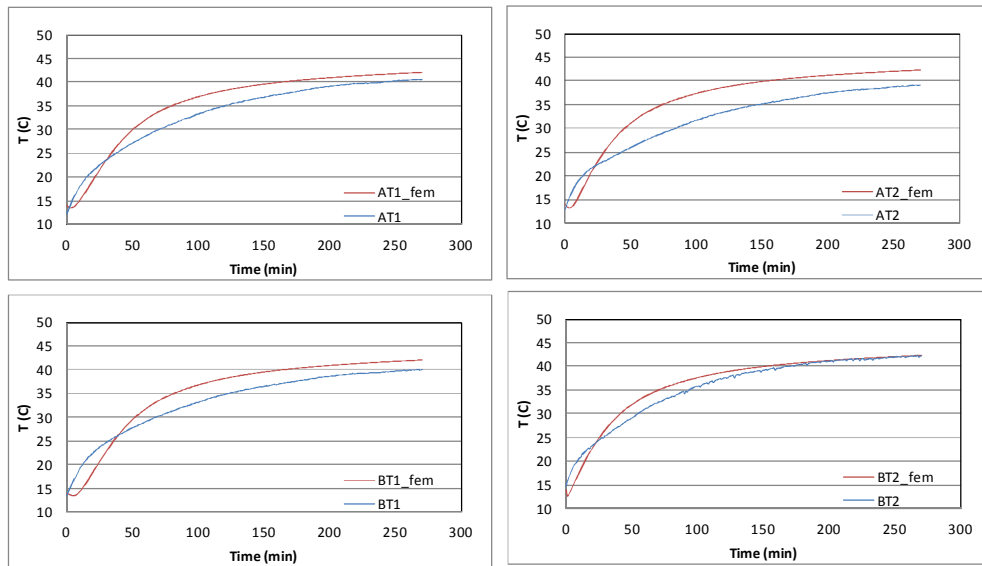


**Figure D.4c.** Temperature change at four different locations (AT1, AT2, BT1, BT2) in **minced** meat with respect to drying time at  $48\pm 1^\circ\text{C}$  1.0 m/s by using model 1

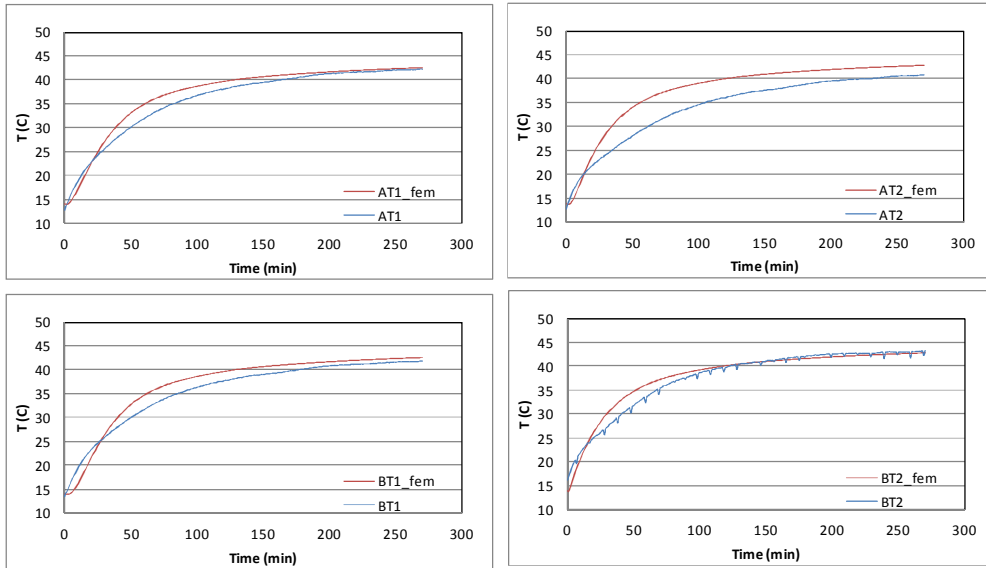


**Figure D.4d.** Temperature change at four different locations (AT1, AT2, BT1, BT2) in minced meat with respect to drying time at  $48 \pm 1^\circ\text{C}$  1.7 m/s by using model 1

### APPENDIX E

#### NONLINEAR FITTING STATEMENTS IN MATHCAD SOFTWARE PROGRAMME

**E1.** Nonlinear fitting statements for diffusivity definition as a function of only sample temperature (equation 5.3) of lean meat with flow normal to fibers (h1) during drying at 70°C and 0.5 m/s.

L := 0.01

t :=	TC :=	y :=	T :=	TC + 273 T =
------	-------	------	------	--------------

(	0	)	(	17.25	)	(	1	)
600	25.75	0.956845238	600	25.75	0.956845238	600	25.75	0.956845238
1200	30.55	0.909970238	1200	30.55	0.909970238	1200	30.55	0.909970238
1800	33.8	0.863095238	1800	33.8	0.863095238	1800	33.8	0.863095238
2400	38.15	0.821886447	2400	38.15	0.821886447	2400	38.15	0.821886447
3000	41.5	0.776900183	3000	41.5	0.776900183	3000	41.5	0.776900183
3600	43.55	0.735634158	3600	43.55	0.735634158	3600	43.55	0.735634158
4200	45.45	0.70467033	4200	45.45	0.70467033	4200	45.45	0.70467033
4800	47.25	0.671875	4800	47.25	0.671875	4800	47.25	0.671875
5400	47.7	0.641884158	5400	47.7	0.641884158	5400	47.7	0.641884158
6000	49.15	0.610977564	6000	49.15	0.610977564	6000	49.15	0.610977564
6600	50.35	0.586595696	6600	50.35	0.586595696	6600	50.35	0.586595696
7200	51.35	0.560325092	7200	51.35	0.560325092	7200	51.35	0.560325092
7800	52.05	0.536916209	7800	52.05	0.536916209	7800	52.05	0.536916209
8400	52.35	0.513450092	8400	52.35	0.513450092	8400	52.35	0.513450092
9000	52.85	0.490041209	9000	52.85	0.490041209	9000	52.85	0.490041209
9600	53.25	0.468463828	9600	53.25	0.468463828	9600	53.25	0.468463828
10200	53.45	0.446886447	10200	53.45	0.446886447	10200	53.45	0.446886447
10800	53.9	0.423477564	10800	53.9	0.423477564	10800	53.9	0.423477564
11400	54.2	0.403788919	11400	54.2	0.403788919	11400	54.2	0.403788919
12000	54.45	0.390682234	12000	54.45	0.390682234	12000	54.45	0.390682234
12600	54.7	0.369104853	12600	54.7	0.369104853	12600	54.7	0.369104853
13200	54.9	0.348500458	13200	54.9	0.348500458	13200	54.9	0.348500458
13800	55.15	0.328811813	13800	55.15	0.328811813	13800	55.15	0.328811813
14400	55.45	0.311927656	14400	55.45	0.311927656	14400	55.45	0.311927656
15000	55.7	0.297847985	15000	55.7	0.297847985	15000	55.7	0.297847985
15600	56.1	0.279132326	15600	56.1	0.279132326	15600	56.1	0.279132326
16200	56.4	0.262248168	16200	56.4	0.262248168	16200	56.4	0.262248168

	0
0	290.25
1	298.75
2	303.55
3	306.8
4	311.15
5	314.5
6	316.55
7	318.45
8	320.25
9	320.7
10	322.15
11	323.35
12	324.35
13	325.05
14	325.35
15	325.85

$$y_{\text{model}}(t, T, a, b) := \frac{8}{\pi^2} \left[ \sum_{n=0}^{20} \frac{1}{(2n+1)^2} \cdot e^{- (2n+1)^2 \cdot \pi^2 \cdot \frac{a \cdot e^{-\frac{b}{T}}}{4L^2} t} \right]$$

i := 0..27

$$\text{SSE}(a, b) := \sum_i (y_i - y_{\text{model}}(t_i, T_i, a, b))^2$$

a := 4.3

b := 6978

Given

$$\text{SSE}(a, b) = 0$$

output := MinErr(a, b)

$$\text{output} = \begin{pmatrix} 4.356 \\ 6.96 \times 10^3 \end{pmatrix}$$

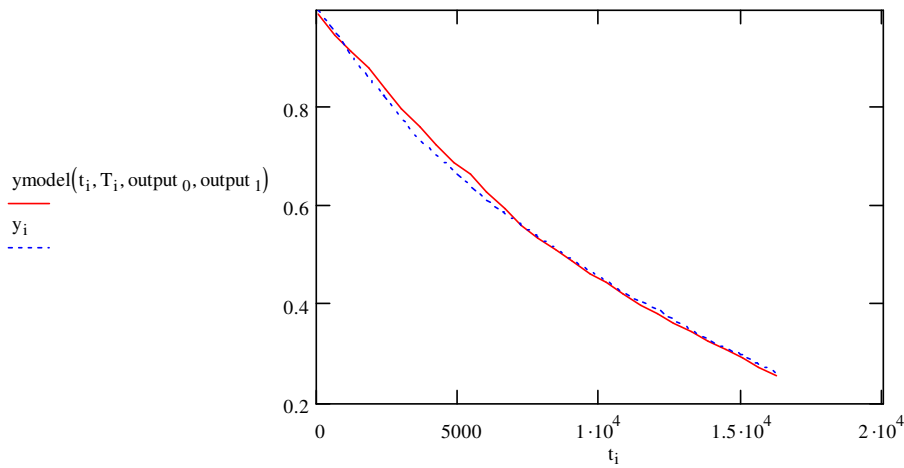
$$\text{SSE}(\text{output}_0, \text{output}_1) = 4.148 \times 10^{-3}$$

$$\text{SSE}(a, b) = 0.011$$

$$r := \text{corr}(\vec{y}, \vec{y_{\text{model}}}(t, T, \text{output}_0, \text{output}_1))$$

$$r = 0.999$$

$$r^2 = 0.998$$



$$\text{Do} := \text{output}_0 \cdot e^{-\frac{\text{output}_1}{T}}$$

	0
0	$1.679 \cdot 10^{-10}$
1	$3.321 \cdot 10^{-10}$
2	$4.801 \cdot 10^{-10}$
3	$6.121 \cdot 10^{-10}$
4	$8.405 \cdot 10^{-10}$
5	$1.067 \cdot 10^{-9}$
6	$1.231 \cdot 10^{-9}$
Do = 7	$1.404 \cdot 10^{-9}$
8	$1.587 \cdot 10^{-9}$
9	$1.636 \cdot 10^{-9}$
10	$1.804 \cdot 10^{-9}$
11	$1.955 \cdot 10^{-9}$
12	$2.089 \cdot 10^{-9}$
13	$2.188 \cdot 10^{-9}$
14	$2.231 \cdot 10^{-9}$
15	$2.306 \cdot 10^{-9}$

**E2.** Nonlinear fitting statements for diffusivity definition as a function of only sample temperature and moisture content (dry base) (equation 5.4) of lean meat with flow normal to fibers (h1) during drying at 70°C and 0.5 m/s.

$$L := 0.01T \quad \vec{L} := \vec{TC} + 27\vec{3}$$

t :=	TC :=	y :=	x :=	T =
0	17.25	1	3.1667	0
600	25.75	0.956845238	3.0913	0 290.25
1200	30.55	0.909970238	3.0094	1 298.75
1800	33.8	0.863095238	2.9275	2 303.55
2400	38.15	0.821886447	2.8555	3 306.8
3000	41.5	0.776900183	2.7769	4 311.15
3600	43.55	0.735634158	2.7048	5 314.5
4200	45.45	0.70467033	2.6507	6 316.55
4800	47.25	0.671875	2.5934	7 318.45
5400	47.7	0.641884158	2.541	8 320.25
6000	49.15	0.610977564	2.487	9 320.7
6600	50.35	0.586595696	2.4444	10 322.15
7200	51.35	0.560325092	2.3985	11 323.35
7800	52.05	0.536916209	2.3576	12 324.35
8400	52.35	0.513450092	2.3166	13 325.05
9000	52.85	0.490041209	2.2757	14 325.35
9600	53.25	0.468463828	2.238	15 325.85
10200	53.45	0.446886447	2.2003	
10800	53.9	0.423477564	2.1594	
11400	54.2	0.403788919	2.125	
12000	54.45	0.390682234	2.1021	
12600	54.7	0.369104853	2.0644	
13200	54.9	0.348500458	2.0284	
13800	55.15	0.328811813	1.994	
14400	55.45	0.311927656	1.9645	
15000	55.7	0.297847985	1.9399	
15600	56.1	0.279132326	1.9072	
16200	56.4	0.262248168	1.8777	

$$y_{\text{model}}(t, T, x, a, b, c, d) := \frac{8}{\pi^2} \sum_{n=0}^{20} \frac{1}{(2n+1)^2} \cdot e^{-\frac{(2n+1)^2 \cdot \pi^2 \cdot a \cdot e^{\frac{-b}{T}} \cdot (c \cdot e^x + d)}{4L^2} t}$$

i := 0..27

$$\text{SSE}(a, b, c, d) := \sum_i (y_i - \text{ymodel}(t_i, T_i, x_i, a, b, c, d))^2$$

$$a := 1.8$$

$$b := 6973$$

$$c := 0.07$$

$$d := 3.7$$

Given

$$\text{SSE}(a, b, c, d) = 0$$

$$\text{output} := \text{MinErr}(a, b, c, d)$$

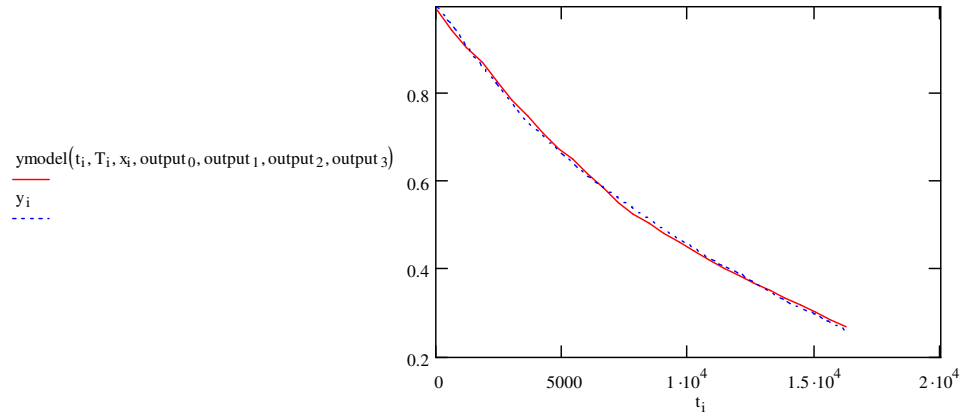
$$\text{output} = \begin{pmatrix} 1.48 \\ 7.019 \times 10^3 \\ 0.074 \\ 2.875 \end{pmatrix}$$

$$\text{SSE}(\text{output}_0, \text{output}_1, \text{output}_2, \text{output}_3) = 1.391 \times 10^{-3}$$

$$\text{SSE}(a, b, c, d) = 0.447$$

$$r := \text{corr}\left(\vec{y}, \vec{\text{ymodel}}(t, T, x, \text{output}_0, \text{output}_1, \text{output}_2, \text{output}_3)\right)$$

$$r = 0.999 \quad r^2 = 0.999$$



$$\text{Do} := \text{output}_0 \cdot e^{\frac{-\text{output}_1}{T}}$$

$$\text{Du} := \text{output}_2 \cdot e^x + \text{output}_3$$

	0
0	4.634
1	4.507
2	4.378
3	4.26
4	4.164
5	4.067
6	3.984
7	3.925
8	3.867
9	3.816
10	3.767
11	3.73
12	3.691
13	3.659
14	3.627
15	3.597

Du =

	0
0	$4.648 \cdot 10^{-11}$
1	$9.249 \cdot 10^{-11}$
2	$1.341 \cdot 10^{-10}$
3	$1.713 \cdot 10^{-10}$
4	$2.359 \cdot 10^{-10}$
5	$3 \cdot 10^{-10}$
6	$3.466 \cdot 10^{-10}$
7	$3.957 \cdot 10^{-10}$
8	$4.479 \cdot 10^{-10}$
9	$4.619 \cdot 10^{-10}$
10	$5.097 \cdot 10^{-10}$
11	$5.526 \cdot 10^{-10}$
12	$5.909 \cdot 10^{-10}$
13	$6.19 \cdot 10^{-10}$
14	$6.315 \cdot 10^{-10}$
15	$6.527 \cdot 10^{-10}$

Do =

$\longrightarrow$   
 $(Do \cdot Du) =$

	0
0	$2.154 \cdot 10^{-10}$
1	$4.168 \cdot 10^{-10}$
2	$5.872 \cdot 10^{-10}$
3	$7.299 \cdot 10^{-10}$
4	$9.824 \cdot 10^{-10}$
5	$1.22 \cdot 10^{-9}$
6	$1.381 \cdot 10^{-9}$
7	$1.553 \cdot 10^{-9}$
8	$1.732 \cdot 10^{-9}$
9	$1.763 \cdot 10^{-9}$
10	$1.92 \cdot 10^{-9}$
11	$2.061 \cdot 10^{-9}$
12	$2.181 \cdot 10^{-9}$
13	$2.265 \cdot 10^{-9}$
14	$2.291 \cdot 10^{-9}$
15	$2.348 \cdot 10^{-9}$



**APPENDIX F**

**DIFFUSIVITY VALUES AT DIFFERENT PROBE LOCATIONS**

**Table F.1.** Diffusivity values based on equation (5.3) for lean meat with h1 fiber configuration at the temperatures of AT1 and BT2 locations

<b>AT1</b>	<b>BT2</b>	<b>% difference</b>
1.77E-10	1.68E-10	-4.87
3.22E-10	3.32E-10	3.07
4.66E-10	4.80E-10	2.98
5.56E-10	6.12E-10	10.05
6.92E-10	8.41E-10	21.41
8.61E-10	1.07E-09	23.88
1.04E-09	1.23E-09	18.71
1.22E-09	1.40E-09	15.27
1.39E-09	1.59E-09	13.93
1.46E-09	1.64E-09	11.83
1.65E-09	1.80E-09	9.53
1.80E-09	1.96E-09	8.55
1.95E-09	2.09E-09	7.24
2.09E-09	2.19E-09	4.94
2.17E-09	2.23E-09	2.76
2.25E-09	2.31E-09	2.35
2.35E-09	2.37E-09	0.94
2.42E-09	2.40E-09	-0.79
2.48E-09	2.47E-09	-0.52
2.56E-09	2.52E-09	-1.56
2.61E-09	2.56E-09	-1.92
2.68E-09	2.60E-09	-2.91
2.72E-09	2.64E-09	-2.95
2.78E-09	2.68E-09	-3.60
2.84E-09	2.73E-09	-3.97
2.90E-09	2.78E-09	-4.31
2.97E-09	2.85E-09	-4.04
3.06E-09	2.90E-09	-5.04



## CURRICULUM VITAE

### MELTEMSOYDANKARABACAK

<b>Personal info</b>	<p>Nationality : TC  Date of Birth : 09.09.1980  Place of Birth : Artvin  Gender : Female  Marital Status : Married</p>
<b>Contact info</b>	<p>E-mail : meltem.soydan@tubitak.gov.tr  Tel : 0312 468 53 00/ 1172</p>
<b>Work experience</b>	<p><b>Scientific Programmes Expert-TÜBİTAK/ARDEB-TOVAG Ankara</b>  15.03.2006-</p> <ul style="list-style-type: none"> <li>• EU 7FP ICT-AGRI (Coordination of European Research within ICT and Robotics in Agriculture and related Environmental Issues) Era-Net project national contact point</li> <li>• take role in evaluating and monitoring the national and international projects funded by TUBITAK in food and agriculture related research areas.</li> <li>• Inform project researchers about TUBITAK support programmes</li> <li>• Update of TOVAG website, involved in necessary activities as unit contact point.</li> <li>• Preparation of information and statistics of TOVAG</li> <li>• take role in administrative process development and improvement studies</li> </ul> <p><b>Research Assistant – Middle East Technical University – Ankara</b>  08.10.2004-03.2006</p> <ul style="list-style-type: none"> <li>• Material and Energy Balances, Fluid Dynamics, Food Microbiology Laboratory, Food Materials Laboratory courses assistant</li> <li>• Preparation of research projects and executing financial activities for the project.</li> <li>• Preparation of activity report of Food Engineering Department</li> <li>• Other administrative activities of department</li> </ul> <p><b>Trainee(Quality Assurance Dept.)-Nestle- Karacabey/Bursa</b>  01.07.2002-01.08.2002</p> <ul style="list-style-type: none"> <li>• Preparation of project to improve HACCP system of instant soup and chocolate production line</li> <li>• Analysis to check and sustain the quality of chocolate and instant soup production line and translation of instructions for these analysis to Turkish.</li> </ul>
<b>Education info</b>	<p><b>2006- Middle East Technical University- ANKARA</b>  Graduate School of Natural and App.Sci.- Food Eng. PhD prog.</p> <p><b>2003 – 2006 Middle East Technical University- ANKARA</b>  Graduate School of Natural and App. Sci.- Food Eng. MSc prog. - 3.86/4.00</p> <p><b>1998 – 2003 Middle East Technical University – ANKARA</b>  Faculty of Eng. – Food Eng. - 3.88/4.00</p> <p><b>1994 – 1998 Konya High School – KONYA</b>  Science- Mathematics Field 5.00/5.00</p>

<b>Professional area of interests</b>	<ul style="list-style-type: none"> <li>• Food Drying</li> <li>• Food Microbiology/Biotechnology</li> <li>• Enzyme Production</li> <li>• Novel Food Processing Technologies (HHP, Ultrasound...etc)</li> <li>• Food Chemistry and Nutrition</li> </ul>
<b>Awards/ Grants/ Success</b>	<ul style="list-style-type: none"> <li>• METU Graduate School of Natural and Applied Science Course Performance Award, June 2005</li> <li>• TÜBİTAK National Master of Science Scholarship- March 2004</li> <li>• METU Food Engineering Department, graduation with first place- June, 2003</li> <li>• Konya High School graduation with first place- June,1998</li> <li>• Konya High School Alumni Association Success Scholarship (1996-1998)</li> </ul>
<b>Scientific activities participated</b>	<ul style="list-style-type: none"> <li>• <b>7. Gıda Mühendisliği Kongresi</b>, Ankara, 24-26.11.2011</li> <li>• <b>3rd International Congress on Information and Communication Technologies in Agriculture, Food, Forestry and Environment (ITAFFE'10)</b>, Samsun, 14-18.06.2010</li> <li>• Workshop on <b>ICT-AGRI Era-Net Project calls, topic selection and application procedures</b>, participated as instructor, 3rd International Congress on Information and Communication Technologies in Agriculture, Food, Forestry and Environment (ITAFFE'10)- Samsun, 14-18.06.2010</li> <li>• Workshop on <b>Mapping of current ICT research and preparation of joint transnational call</b>- Ghent/Belçika, 14-15.10.2009</li> <li>• <b>Gıda Mühendisliği 5. Kongresi</b> – Ankara, 8-10.11.2007</li> <li>• <b>2.International Food and Nutrition Congress</b> – Istanbul, 24-26.10.2007(oral presentation)</li> <li>• <b>European Technology Platforms “Food for life” 2<sup>nd</sup> stakeholders Meeting</b>, Brüksel/Belçika, September 2006</li> <li>• <b>2005 Gıda Günü Sempozyumu</b> – Ankara, 14-15.10.2005</li> <li>• <b>14. Ulusal Biyoteknoloji Kongresi</b> – Eskişehir, 31.08-02.09.2005 (Poster presentetation)</li> <li>• <b>1. International Food and Nutrition Congress</b> – Istanbul, 15-18.06.2005(Poster presentetation)</li> </ul>
<b>Publications</b>	<ul style="list-style-type: none"> <li>• Soydan Karabacak M., Esin A., Çekmecelioğlu D., 2012, Sonlu Elemanlar Yöntemi ile Yönlü Değişmeyen ve Yöne Bağımlı Besin Örneklerinin Kurutulmasının Modellenmesi, Türkiye 11. Gıda Kongresi, Hatay</li> <li>• Soydan Karabacak M., Esin A., Çekmecelioğlu D., 2011, Yöne Bağımlı ve Yönden Bağımsız Özellik Taşıyan Gıdaların Kurutulmasında ve Sıcaklık Dağılımında Hava Akış Hızı ve Sıcaklığın Etkisi, 7. Gıda Mühendisliği Kongresi, Ankara</li> </ul>

	<ul style="list-style-type: none"> <li>• Soydan Karabacak M., 2010, Coordination of European Research Within ICT and Robotics in Agriculture and Related Environmental Issues, 3<sup>rd</sup> International Congress on Information and Communication Technologies in Agriculture, Food, Forestry and Environment (ITAFFE'10)</li> <li>• Soydan M., 2007, National Food Research Support Programmes (TÜBİTAK-ARDEB), 2<sup>nd</sup> International Congress on Food and Nutrition, İstanbul</li> <li>• Soydan M., Hamamcı H., Ögel Z. B., 2005, Düşük laktozlu süt üretimi amacıyla termofilik küflerden beta-galaktozidaz üretimi ve kısmi saflaştırması, 14. Ulusal Biyoteknoloji Kongresi, Eskişehir</li> <li>• Soydan M., Hamamcı H., Ögel Z. B., 2005, Production of beta-galactosidase from thermophilic fungi for use in low lactose milk production, 1. International Congress on Food and Nutrition, İstanbul</li> </ul>
<b>Organizations</b>	<ul style="list-style-type: none"> <li>• Food Engineering Chamber</li> <li>• METU Nature Club (active memeber during 2 years of bachelor of science )</li> </ul>
<b>Hobbies</b>	Sinema, basketbol, seyahat, bowling, buz pateni
<b>Language Skills</b>	Advanced English Little German
<b>Computer Skills</b>	Microsoft Office Programmes, Mathcad